



RH-CATALYZED CARBONYLATION OF DISUBSTITUTED OLEFINS: ASYMMETRIC CATALYSIS, CONTINUOUS FLOW AND TANDEM HYDROAMINOMETHYLATION REACTION

Anton Cunillera Martin

ADVERTIMENT. L'accés als continguts d'aquesta tesi doctoral i la seva utilització ha de respectar els drets de la persona autora. Pot ser utilitzada per a consulta o estudi personal, així com en activitats o materials d'investigació i docència en els termes establerts a l'art. 32 del Text Refós de la Llei de Propietat Intel·lectual (RDL 1/1996). Per altres utilitzacions es requereix l'autorització prèvia i expressa de la persona autora. En qualsevol cas, en la utilització dels seus continguts caldrà indicar de forma clara el nom i cognoms de la persona autora i el títol de la tesi doctoral. No s'autoritza la seva reproducció o altres formes d'explotació efectuades amb finalitats de lucre ni la seva comunicació pública des d'un lloc aliè al servei TDX. Tampoc s'autoritza la presentació del seu contingut en una finestra o marc aliè a TDX (framing). Aquesta reserva de drets afecta tant als continguts de la tesi com als seus resums i índexs.

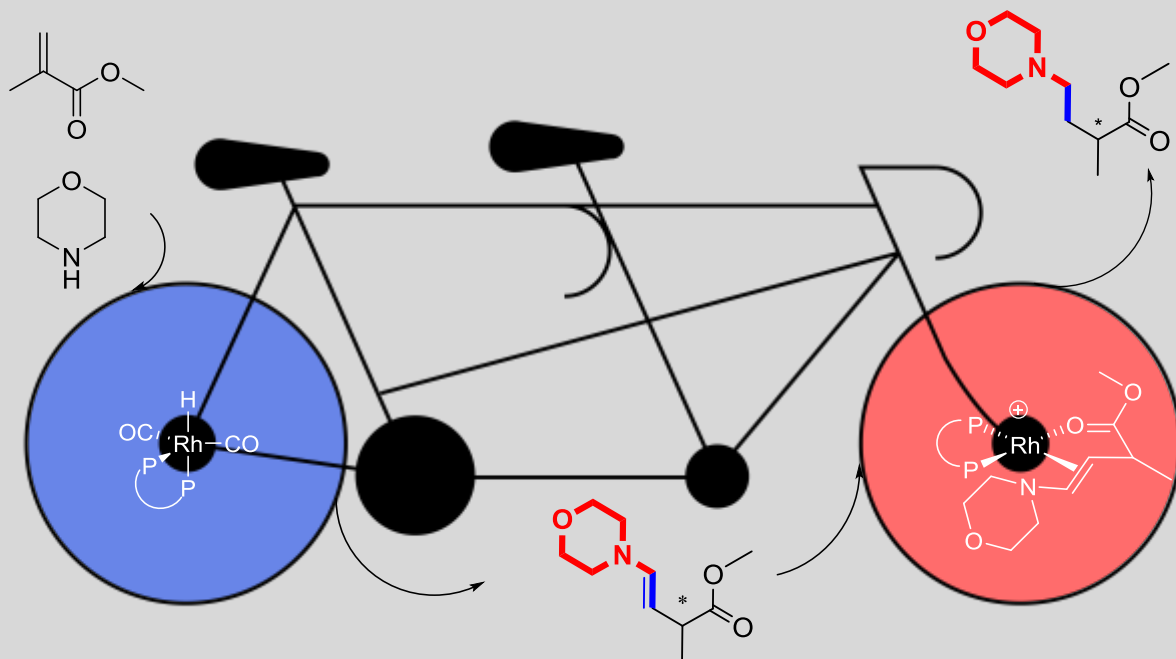
ADVERTENCIA. El acceso a los contenidos de esta tesis doctoral y su utilización debe respetar los derechos de la persona autora. Puede ser utilizada para consulta o estudio personal, así como en actividades o materiales de investigación y docencia en los términos establecidos en el art. 32 del Texto Refundido de la Ley de Propiedad Intelectual (RDL 1/1996). Para otros usos se requiere la autorización previa y expresa de la persona autora. En cualquier caso, en la utilización de sus contenidos se deberá indicar de forma clara el nombre y apellidos de la persona autora y el título de la tesis doctoral. No se autoriza su reproducción u otras formas de explotación efectuadas con fines lucrativos ni su comunicación pública desde un sitio ajeno al servicio TDR. Tampoco se autoriza la presentación de su contenido en una ventana o marco ajeno a TDR (framing). Esta reserva de derechos afecta tanto al contenido de la tesis como a sus resúmenes e índices.

WARNING. Access to the contents of this doctoral thesis and its use must respect the rights of the author. It can be used for reference or private study, as well as research and learning activities or materials in the terms established by the 32nd article of the Spanish Consolidated Copyright Act (RDL 1/1996). Express and previous authorization of the author is required for any other uses. In any case, when using its content, full name of the author and title of the thesis must be clearly indicated. Reproduction or other forms of for profit use or public communication from outside TDX service is not allowed. Presentation of its content in a window or frame external to TDX (framing) is not authorized either. These rights affect both the content of the thesis and its abstracts and indexes.



Rh-catalyzed carbonylation of disubstituted olefins: asymmetric catalysis, continuous flow and tandem hydroaminomethylation reaction

ANTON CUNILLERA MARTIN



DOCTORAL THESIS
2018

UNIVERSITAT ROVIRA I VIRGILI
RH-CATALYZED CARBOXYLATION OF DISUBSTITUTED OLEFINS: ASYMMETRIC CATALYSIS, CONTINUOUS
FLOW AND TANDEM HYDROAMINOMETHYLATION REACTION
Anton Cunillera Martin

Anton Cunillera Martín

**Rh-catalyzed carbonylation of disubstituted
olefins: asymmetric catalysis, continuous flow
and tandem hydroaminomethylation reaction**

DOCTORAL THESIS

Supervised by
Dr. Cyril Godard and Dra. Maria Aurora
Ruiz Manrique

Departament de Química Física i Inorgànica



UNIVERSITAT ROVIRA I VIRGILI

Tarragona, 2018

UNIVERSITAT ROVIRA I VIRGILI
RH-CATALYZED CARBONYLATION OF DISUBSTITUTED OLEFINS: ASYMMETRIC CATALYSIS, CONTINUOUS
FLOW AND TANDEM HYDROAMINOMETHYLATION REACTION
Anton Cunillera Martin



UNIVERSITAT ROVIRA I VIRGILI

Departament de Química Física i Inorgànica
c/ Marcel·lí Domingo s/n, Edifici N4
Campus Sescelades, 43007 Tarragona
Tel. 977 55 80 46

Els sotasignants Dr. Cyril Godard, professor agregat del Departament de Química Física i Inorgànica de la Universitat Rovira i Virgili, i Dra. María Aurora Ruiz Manrique, catedràtica del Departament de Química Física i Inorgànica de la Universitat Rovira i Virgili,

FEM CONSTAR que aquest treball, titulat "Rh-catalyzed carbonylation of disubstituted olefins: asymmetric catalysis, continuous flow and tandem hydroaminomethylation reaction", que presenta Anton Cunillera Martín per a l'obtenció del títol de Doctor i que aconsegueix els requeriments per a poder optar a Menció Internacional, ha estat realitzat sota la nostra direcció al Departament de Química Física i Inorgànica de la Universitat Rovira i Virgili.

Tarragona, 2018

Els directors de la tesi doctoral

Prof. Cyril Godard

Prof. Aurora Ruiz

UNIVERSITAT ROVIRA I VIRGILI
RH-CATALYZED CARBONYLATION OF DISUBSTITUTED OLEFINS: ASYMMETRIC CATALYSIS, CONTINUOUS
FLOW AND TANDEM HYDROAMINOMETHYLATION REACTION
Anton Cunillera Martin

La present memòria de Tesi Doctoral s'ha dut a terme gràcies al *Subprograma de Formació de Personal Investigador (FPI)* (referència: BES-2014-069199), finançat pel Ministerio de Economía y Competitividad. El treball que descriu la present tesi ha estat finançat per:

- El Ministerio de Economía, Industria y Competitividad de España (MINECO) mitjançant el projecte CTQ2013-43438-R.
- El Ministerio de Economía, Industria y Competitividad de España (MINECO) mitjançant el projecte CTQ2016-75016-R.
- L'Agència de Gestió d'Ajuts Universitaris i de Recerca mitjançant el projecte 2014 SGR 670
- L'Agència de Gestió d'Ajuts Universitaris i de Recerca mitjançant el projecte 2017 SGR 1472



UNIVERSITAT ROVIRA I VIRGILI



UNIVERSITAT ROVIRA I VIRGILI
RH-CATALYZED CARBOXYLATION OF DISUBSTITUTED OLEFINS: ASYMMETRIC CATALYSIS, CONTINUOUS
FLOW AND TANDEM HYDROAMINOMETHYLATION REACTION
Anton Cunillera Martin

Agraïments/agradecimientos

De la mateixa forma que quan et poses a escriure la tesis t'adones de la quantitat de coses que pots, i has d'explicar, és en aquest precís instant que veig la quantitat de gent a la que he d'agrair per tots aquests anys de viatge. Espero trobar les paraules adients.

Me gustaría empezar agradeciendo a mis supervisores Cyril y Aurora por la oportunidad de realizar este doctorado, por todo el apoyo recibido a lo largo de estos 4 años, y por estar siempre dispuestos cuando más lo necesitaba. Gran parte de lo que soy ahora como investigador, es gracias a vosotros.

A Carmen Claver agradezco la oportunidad de entrar en el grupo ya cuando el máster. También todas las oportunidades y facilidades para ir a congresos, charlas, seminarios, y porque no decirlo Benasque. He ido a sitios que ni imaginaba y escuchado química que ni sabía que existía. Muchas gracias.

No puedo dejarme tampoco a Sergio Castillón, siempre dispuesto para hablar y discutir de química orgánica o de cualquier tema, he disfrutado como un niño pequeño de cada discusión, consejo o comentario, gracias también de corazón.

La major part del temps d'un doctorat en química està al laboratori, on es duen a terme les reaccions, però encara més important, on es construeixen totes les amistats que t'emportes com un tresor. Començaré agraint a la gent del grup de Carmen. A Alberto, mis primeros pasos en el laboratorio fueron contigo y me alegro mucho de ello, cuanto dolor de cabeza con los pirenos, por suerte ya quedan atrás ! Eli i Jessi quin duo ! Sempre aportant somriures i caliu al laboratori, quina sort haver compartit aquests anys ! També a la gent que ha anat passant pel laboratori pels moments compartits, Laura, Aaron, Laia, Hèctor, Colavida, Claudio,

Diego, Nanette, Lluís, Olga, Alex, Olivia, a nuestra super post-doct Itziar un pilar en quien confiar dentro del grupo, y a Jorge que aunque ahora te vas, siempre has estado ahí. I would like also to thank Benedetta and Myriam, for all this time in the lab, for the good moments and for the support in the bad ones, merci e grazie mille ! A la Raquel, la nostra super tècnic per estar sempre disponible i ajudant-nos en qualsevol moment. Roger deixo la hidroaminometilació en bones mans, molta sort en el màster i al futur !

De vegades fan falta 4 anys per conèixer la gent, confiar en ella i crear una bona amistat. No és pas el teu cas Jordi Creus, ni dos dies de màster van fer falta per veure que les birres i excursions a la muntanya serien una dinàmica que encara ara portem a sobre. Ens queda l'espina del Vinyamala, que aquest any ens la traurem de sobre ! Per acabar amb el grup, al Fran. Fa uns 10 anys que vam començar la carrera, ni recordo en quin moment ens vam començar a fer tant amics, però aquí estem ara i me n'alegro de tot cor. Gràcies per fer més amenes les columnes, per les sortides a fer fotos, als riures entre vitrines, per tot i més !

Per sort (en el tema amistats), l'espai a la URV és limitat i això t'obliga a compartir lab no només amb la gent del teu grup, però també amb altres grups, i això senyors també és una gran sort. Als borilles, primer de tot dir que el metal free són els pares. Però un cop feta la broma, merci a tota la gent que ha anat passant, Xavi, Gerard, Jèssica, Enrico piripipapa ! als Ricardos², Marc G., Lorena, Elliott, Albert, i al Thierry, ja torno més content de les reunions amb Aurora ! Jana ha estat un plaer haver-te conegut, sempre aportes un somriure a aquells que t'envolten, ets una gran persona. Jordi Royes, no m'he oblidat de tu ! Quins bons riures al laboratori, disfrutant esquiant i fent birres ! Molts ànims en el que et queda de doctorat, sempre em tens aquí pel que faci falta !

A Ana Belén, si algún día llego a ser solo la mitad de buen químico y persona como lo eres tú, ya lo consideraré un éxito. Gracias por el apoyo, las horas de discusión y

las horas de laboratorio, no me imaginaba que se podía disfrutar de la química a este nivel. Siempre guardaré con cariño las tardes con Frank Sinatra cuando solo quedábamos los dos. We did it our way! También aprovecho para agradecer a Sasha la proximidad que siempre me ha mostrado. Sois una combinación perfecta. El millor, sempre pel final. Núria, costa trobar les paraules per expressar allò que sento. Ja sabia que existies durant la carrera, però no imaginava tot allò que eres com a persona i el que has arribat a ser per mi fins que no hem arribat fins aquí. Gràcies per aquests anys, m'emporto el millor tresor i és la teva amistat. Et desitjo el millor en el futur i que ho puguem seguir compartint junts !

Una porta no es mai una barrera per fer amics, i menys encara la que separa el lab 216 del 217. Gràcies a tots els oscaritos que han anat passant Mercé, Efrem, Carla, Zahra, Joan, Jordi F., Fàtima, Margalinda quin fatarrot d'experiències i bons moments, Magre un muxarrillo com deu mana i ara ja un bon alemany ! Pol ets com el flameado de Moe, tot un descobriment, gràcies per la sintonia a l'hora de dinar. A la Maria, per aquests anys i sobretot aquests últims mesos de suport, ànims, bons moments i de no tan bons, sempre és un plaer disfrutar de la teva companyia. Un bon llibre per a mi és aquell que no pots parar de llegir, que no vols que s'acabi, pot passar temps i el tornes a agafar amb ganes, i que amb el que explica t'omple d'emocions. Els bons amics poden arribar a ser iguals, i per això Carlota ets un dels meus llibres preferits ! Gràcies a l'Arnau també, pels bones estones a la muntanya i escalant, on hem de tornar !

No m'oblido dels orgànics ! Agraïr Emma, Míriam, Isma, Jordi M., Collado, Irene, Margarita, y sobretodo Macarena, siempre da mucho gusto tener un pedazo de Andalucía tan bonito cerca ! A l'Adrià que tot i ser de polímers també el compto com orgànic ! També a la Laura Abella, super triatleta, super computacional i super gran persona ! Finalment als cristal·lògrafs Josu, Nicole, Irina i Marc Medina amb

qui sempre és un plaer filosofar. Agrair a tots els tècnics i secretaries amb els que he treballat, Josep, Yolanda, Dúnia, Sílvia, Carme, Irene, Sònia, Toni de la Torre, Debora i especialment al Ramón a qui no he parat de marejar amb RMN d'alta pressió, la teva ajuda ha estat inestimable.

It's time to fly, to Copenhagen indeed. I cannot finish the chemistry part without all the people I met there. I was really lucky to live only for 3 and half months there and meet you all. Thank you Fabrizio super mario, Fabrizio Bottaro, Irene, Emilie, Cirkelne, Carola, Vanessa, Simone and Cristian. Pero especialmente a Jakob por toda su ayuda, su gran amistad y buenos momentos escalando, se te hecha de menos pendejo. Finalmente a Eduardo por todo el apoyo recibido durante estos meses, gracias de verdad, te deseo lo mejor como investigador ya que lo vales.

Agrair tots els meus amics fora de la química. Dintre dels castells als Baranerus, què fàcil és fugir dels problemes i trobar confort i riure amb vosaltres. Als meus companys de pis Lluís, Topo i Marc B. que m'han vist passar per aquest periple i m'han donat ànims i suport. Una cosa, a tu també Alba, amiga !

A la Familiy, no la que et toca, sinó aquella que pots escollir i amb qui et sents més unit que pels lligams de sang. Entre vosaltres hi trobo grans amics i les que puc dir que són les dones de la meva vida.

A mis amigos del Erasmus, Yago y Mateo, la distancia no ha sido nunca un impedimento para sentirnos cerca. Siempre nos quedará Weimar! También a Clara, eres una gran persona i con un gran corazón, prometo ponernos más al día.

Un especial agradecimiento a Álvaro, siempre has estado allí, cuánto más lo necesitaba. Eres como un hermano para mí, gracias de todo corazón.

Acabo ja agraint a la meva mare, al meu pare i al meu germà. Tot el que sóc, és gràcies a vosaltres.

Table of contents

Abbreviations and acronyms	1
Summary	5

Chapter 1 Introduction

1.1. Introduction	11
1.1.1. Rhodium catalyzed carbonylation	11
1.1.2. Rhodium catalyzed hydroformylation	13
1.1.3. Rhodium catalyzed asymmetric hydroformylation	16
1.1.3.1. Monosubstituted alkenes	16
1.1.3.2. Disubstituted alkenes	21
1.1.4. Rhodium catalyzed hydroaminomethylation	28
1.1.4.1. Monosubstituted alkenes	32
1.1.4.2. Disubstituted alkenes	38
1.1.5. Homogeneous catalyst immobilization and continuous flow chemistry	41
1.1.5.1. Homogeneous and heterogeneous catalysis	41
1.1.5.2. Homogeneous catalyst immobilization	42
1.1.5.3. Catalysis under flow conditions	45
1.2. References	47

Chapter 2 Objectives

Objectives	59
------------	----

Chapter 3

Immobilization of chiral Rh catalysts for the AHF of norbornene in flow

3.1. Introduction	63
3.1.1. Rh-catalyzed AHF of [2.2.1]-bicyclic olefins	63
3.1.2. Homogenous catalyst immobilization via π - π interactions	64
3.1.3. Immobilized catalysts for AHF in flow mode	69
3.2. Objectives of this chapter	72
3.3. Results and discussion	73
3.3.1. Synthesis of pyrene tagged chiral diphosphites	73
3.3.2. Synthesis of rhodium complexes bearing pyrene tagged diphosphite ligands	76
3.3.3. Asymmetric hydroformylation of norbornene using pyrene tagged diphosphite ligands	78
3.3.4. HP-NMR study of [RhH(CO) ₂ (3.27)]	80
3.3.5. Immobilization of complexes 3.40 and 3.41 onto carbon materials	82
3.3.6. AHF of norbornene in batch using heterogenized catalysts	85
3.3.7. Continuous AHF of norbornene in flow	88
3.4. Conclusions	96
3.5. Experimental part	98
3.6. References	112

Chapter 4

Rhodium catalyzed asymmetric HAM of α -alkyl acrylates

4.1. Introduction	117
4.1.1. Rh-catalyzed asymmetric hydroaminomethylation	117
4.1.2. γ -aminobutyric acids (GABA)	122

4.2. Objectives of this chapter	125
4.3. Results and discussion	126
4.3.1. Optimization of the reaction conditions	126
4.3.2. Rh-catalyzed asymmetric HAM of various α -alkyl acrylates	131
4.3.3. HP-NMR studies	133
4.4. Conclusions	158
4.5. Experimental part	159
4.6. References	179

Chapter 5

Synthesis of $\beta^{2,2}$ -amino esters via Rh-catalyzed regioselective HAM

5.1. Introduction	185
5.1.1. Rh-catalyzed regioselective hydroformylation for the production of quaternary carbon centers	185
5.1.2. Rh-catalyzed hydroaminovinylation of acrylates	190
5.1.3. β -amino acids	194
5.2. Objectives of this chapter	197
5.3. Results and discussion	198
5.3.1. Optimization of the reaction conditions for the regioselective HAM of methyl methacrylate	198
5.3.2. Rh-catalyzed regioselective HAM of methyl methacrylate with several amines	205
5.3.3. Optimization of the reaction conditions for the regioselective HAM of methyl methacrylate with aniline	208
5.3.4. Rh-catalyzed regioselective HAM of α -alkyl acrylates with aniline derivatives	211
5.3.5. Rh-catalyzed regioselective HAM of methyl methacrylate with benzyl amine	213
5.3.6. Rh-catalyzed AHF of ethyl benzyl acrylate	217

5.4. Conclusions	221
5.5. Experimental part	223
5.6. References	232

Chapter 6
General conclusions

General conclusions	237
---------------------	-----

Appendix	245
-----------------	-----

ABBREVIATIONS AND ACRONYMS

A	
AHF	Asymmetric HydroFormylation
atm	atmosphere
ax	axial
B	
BDP	Bis-3,4-diazaphospholane
bs	broad signal
C	
<i>ca.</i>	approximately
CBs	Carbon beads
CNTs	Carbon nanotubes
COD	Cyclooctadiene
Conv.	Conversion
D	
d	doublet
DCE	1,2-dichloroethane
DCM	Dichloromethane
dd	doublet of doublet
DDQ	2,3-dichloro-5,6-dicyano-1,4-benzoquinone
dppf	1,1'-Bis(diphenylphosphino) ferrocene
E	
ee	enantiomeric excess
eq	equatorial
equiv.	equivalents
EWG	Electron-withdrawing group

Abbreviations and Acronyms

	G
GABA	γ -amino butyric acids
	H
h	hours
HAM	HydroAminoMethylation
HEH	Hantzsch ester
HF	HydroFormylation
HMBC	Heteronuclear Multiple Bond Correlation
HP	High-Pressure
Hz	Hertz(s)
	I
ICP	Induced Coupled Plasma
IR	Infrared
	J
J	Coupling constant
	L
L	Ligand
LG	Leaving group
	M
m	multiplet
MFC	Mass Flow Controller
MS	Mass spectrometry
MWCNTs	Multi-walled carbon nanotubes
m/z	mass over charge
	N
NBS	N-Bromosuccinimide
NMDPP	Neomenthyl diphenylphosphine
NMR	Nuclear Magnetic Resonance

NOESY	Nuclear Overhauser Effect Spectroscopy
O	
OMS	Ordered Mesoporous Silica
P	
PCC	Pyridinium chlorochromate
S	
syngas	synthesis gas
SWCNTs	Single-walled carbon nanotubes
R	
RAs	Regulation agents
rGO	reduced graphene oxide
r.t	room temperature
T	
T	Temperature
t	time
t (in NMR)	triplet
tdt	triplet of doublet of triplet
TLC	Thin layer chromatography
TOF	Turnover frequency
TON	Turnover number
X	
XRD	X-Ray Diffraction
XPS	X-Ray Photoelectron Spectroscopy

UNIVERSITAT ROVIRA I VIRGILI
RH-CATALYZED CARBONYLATION OF DISUBSTITUTED OLEFINS: ASYMMETRIC CATALYSIS, CONTINUOUS
FLOW AND TANDEM HYDROAMINOMETHYLATION REACTION
Anton Cunillera Martin

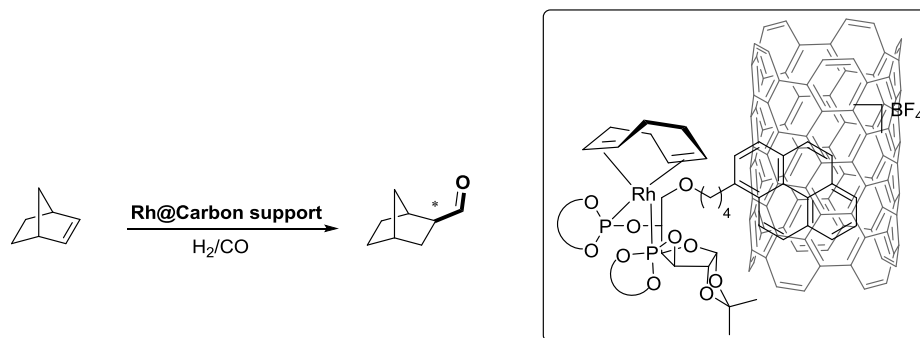
SUMMARY

The use of carbon monoxide as building block via metal catalyzed carbonylation processes has become an efficient tool for the functionalization of organic products due to the atom-economic nature of this type of reactions. In this context, the rhodium catalyzed hydroformylation of olefins reaction, discovered in 1938 by Otto Roelen, constitutes one of the most important homogeneous catalytic process applied at large scale. The rhodium catalyzed asymmetric hydroformylation of alkenes is a very attractive reaction since the chiral aldehydes obtained are versatile building blocks in the synthesis of chiral molecules such as imines, amines, alcohols or acids. Despite the variety of successful systems reported in the rhodium catalyzed asymmetric hydroformylation of alkenes, the implementation of this process at large scale is still underdeveloped, mainly due to the toxicity and high price of the metal catalyst applied. In this regard, the immobilization onto solid supports of efficient catalysts for the Rh-catalyzed AHF of alkenes for the application in continuous flow is a promising strategy. Another issue for the implementation of these catalysts at large scale is the fact that aldehydes are not usually the final molecule, but an intermediate in the synthesis of the target compound. Thus, the development of tandem hydroformylation processes are promising, since they allow the formation of versatile building block such as the aldehyde, which in the same reaction vessel is transformed in situ into more interesting molecules.

Chapter 1 describes a general introduction on the importance of the rhodium catalyzed asymmetric hydroformylation of alkenes. Furthermore, the tandem rhodium catalyzed hydroaminomethylation reaction for the production of amines is also described in detail. Finally, a brief introduction to flow chemistry is also presented.

Chapter 2 sets out the general objectives of this thesis.

Chapter 3 describes the synthesis of chiral pyrene tagged diphosphite ligands derived from glucose and of the corresponding rhodium complexes. Application of the Rh catalysts containing these chiral diphosphite ligands in the AHF of norbornene provided similar results in terms of activity, stereo- and enantioselectivity to those afforded with ligands derived from glucose previously reported in our group. The use of the rhodium complexes bearing the pyrene tagged diphosphite ligands provided higher activity, while stereo- and enantioselectivity remained unaffected in the rhodium catalyzed asymmetric hydroformylation of norbornene. It was thus concluded that the pyrene moiety does not affect the stereo- and enantioselectivity of the rhodium catalyst. This was confirmed by HP-NMR studies of the Rh hydride complex $[\text{RhH}(\text{CO})_2(\text{L})]$ (L = pyrene tagged diphosphite ligand), which demonstrated that the coordination mode of the ligand is the same than that of the previously reported chiral diphosphite derived from glucose. Then, the rhodium complexes bearing the pyrene tagged ligands were successfully immobilized onto different carbon supports using ethyl acetate as solvent (Scheme 1).

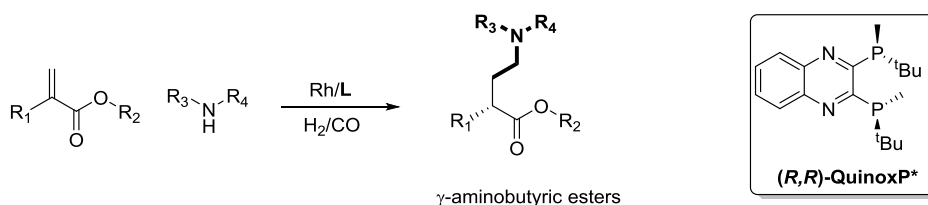


Scheme 1: Rh-catalyzed asymmetric hydroformylation of norbornene using pyrene tagged rhodium complexes immobilized onto carbon supports.

The new heterogenized catalysts were applied in the rhodium catalyzed asymmetric hydroformylation of norbornene in batch mode with lower conversions and enantioselectivities compared to the homogeneous counterpart.

Recycling experiments in batch were carried out, but a drastic decrease in the second run was observed due to catalyst leaching. Finally, the heterogenized catalysts were applied in the rhodium asymmetric hydroformylation of norbornene in flow mode with higher values in enantioselectivity compared to the homogeneous catalyst in batch mode.

The investigation carried out in [Chapter 4](#) is focused on the rhodium catalyzed asymmetric hydroaminomethylation of α -alkyl acrylates for the efficient synthesis of chiral γ -aminobutyric esters (Scheme 2). After optimization of the reaction conditions, a number of chiral γ -aminobutyric esters were synthesized in moderate to excellent yields and enantioselectivities up to 86%. This constitutes the first example of rhodium catalyzed asymmetric hydroaminomethylation of alkenes using one single rhodium precursor.

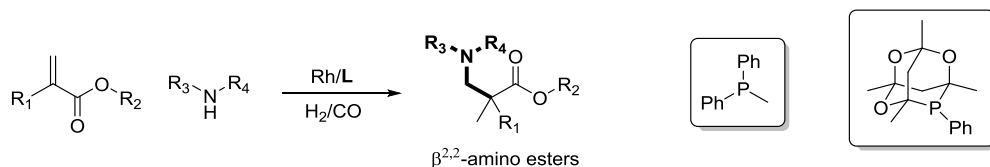


Scheme 2: Rh-catalyzed asymmetric hydroaminomethylation of α -alkyl acrylates for the synthesis of chiral γ -aminobutyric esters.

HP-NMR studies were also conducted in order to study the reactivity of the catalytic system under H_2 , CO , and H_2/CO pressure. Two new rhodium hydrides were identified using (R,R) -QuinoxP* as ligand, and their formation can be controlled by variation of the reaction conditions. It was observed that the role of the amine is crucial to promote the formation of neutral rhodium species from cationic rhodium precursor. Moreover, it was shown that the presence of neutral and cationic rhodium species is necessary to complete the reaction. For this purpose, the selection of the appropriate solvent is crucial to solubilize both types of rhodium species.

Summary

Chapter 5 describes the rhodium catalyzed regioselective hydroaminomethylation of α -alkyl acrylates for the synthesis of $\beta^{2,2}$ -amino esters (**Scheme 3**). Various ligands were tested in the Rh-catalyzed hydroaminomethylation of methyl methacrylate in the presence of morpholine, and the monodentate diphenylmethyl phosphine ligand provided the highest regioselectivity for the branched aldehyde. Nonetheless, no signals of the desired amino ester were detected. Optimization of the reaction conditions revealed that molecular sieves are necessary to afford the desired amino ester together with the neutral rhodium precursor $[\text{Rh}(\text{acac})(\text{CO})_2]$, using toluene as solvent, at 50°C , under 10 bar (H_2/CO , 1:1) when secondary amines are used.



Scheme 3: Rh-catalyzed regioselective hydroaminomethylation of α -alkyl acrylates for the synthesis of $\beta^{2,2}$ -amino esters.

Under these reaction conditions, primary amines were also tested. However, the corresponding imines were the major products. In the case of aniline, it was possible to obtain the corresponding amino ester using the cationic rhodium precursor $[\text{Rh}(\text{COD})_2]\text{BF}_4$, with a phosphine cage ligand, using toluene/DCE as solvent, at 70°C , and under 30 bar (H_2/CO , 1:1). Other primary amines such as benzyl amine were tested under various reaction conditions, but in all the cases, the imine was afforded. It was concluded that the CO pressure is poisoning the hydrogenation step of the reaction for this type of imines. Finally, the rhodium catalyzed asymmetric hydroformylation of benzyl acrylate was attempted in order to produce chiral quaternary carbon centers and ee's up to 30% could be obtained using the ligand (*R,R*)-QuinoxP*.

Chapter 1

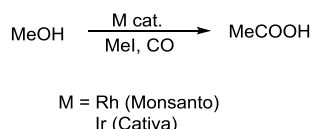
General Introduction

UNIVERSITAT ROVIRA I VIRGILI
RH-CATALYZED CARBOXYLATION OF DISUBSTITUTED OLEFINS: ASYMMETRIC CATALYSIS, CONTINUOUS
FLOW AND TANDEM HYDROAMINOMETHYLATION REACTION
Anton Cunillera Martin

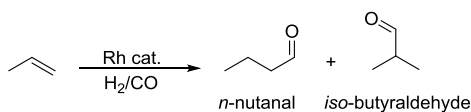
1.1. Introduction

1.1.1. Rhodium catalyzed carbonylation

The use of carbon monoxide as building block via metal catalyzed carbonylation processes has revealed an efficient tool for the functionalization of organic molecules; moreover, the atom-economy nature of this type of reactions has increased the interest for both academy and industry.¹ The production of acetic acid through methanol carbonylation (Scheme 1.1)², and the production of aldehydes by hydroformylation of propene (Scheme 1.2)³ are the two main homogeneous processes currently applied in industry. Nonetheless, metal catalyzed carbonylations are not only limited to bulk chemistry and can also be applied for the synthesis of fine chemicals.⁴



Scheme 1.1: Metal catalyzed carbonylation of methanol using rhodium (Monsanto) or iridium (Cativa) catalysts.

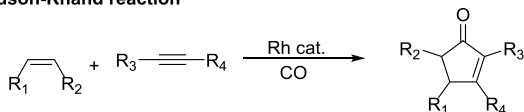


Scheme 1.2: Rh-catalyzed hydroformylation of propene for the production of *n*-butanal and *iso*-butyraldehyde.

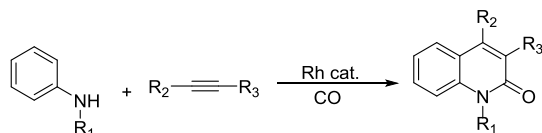
Among the metals that catalyze carbonylation reactions, rhodium has been largely studied due to its intrinsic properties that provide high activity, and selectivity for this type of reaction.⁵ Apart from the carbonylation of methanol in the Monsanto process (Scheme 1.1), the carbonylation of unsaturated compounds is where rhodium has been more extensively applied.^{2a} The Pauson-Khand reaction consists in a [2+2+1] carbonylative cyclization that provides ring-structured skeletons which are scientifically interesting and pharmaceutically attractive (Scheme 1.3).⁶

Though cobalt was the initial metal applied in this reaction, rhodium later proved to be a very successful catalyst due to its high activity, selectivity and substrate versatility.⁷

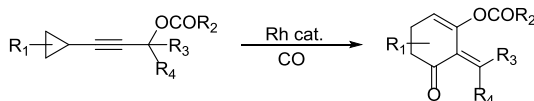
Pauson-Khand reaction



Carbonylation and annulation via C-H activation



Carbonylation of cyclopropyl propargyl esters



Scheme 1.3: Examples of rhodium catalyzed carbonylation reaction of unsaturated compounds for the synthesis of cyclic skeletons.

Recently, an attractive strategy combining the efficiency of rhodium catalysts in carbonylation and C-H activation reactions has emerged for the construction of more complex cyclic skeletons (Scheme 1.3).⁸ Other strategies involving tandem processes to access cyclohexenones from more restricted substrates containing a cyclopropyl group and an alkyne in the same structure have also been reported (Scheme 1.3).⁹

Rhodium catalyzed hydroformylation constitutes an attractive strategy for the synthesis of aldehydes from readily available starting materials such as alkenes in a high atom economy process (Scheme 1.2).¹⁰ The reaction consists in the addition of “synthesis gas” (syngas), a mixture of CO and H₂, to olefins in the presence of a catalyst. Formyl group and hydrogen are added through the π system of the alkene for the obtention of aldehydes.

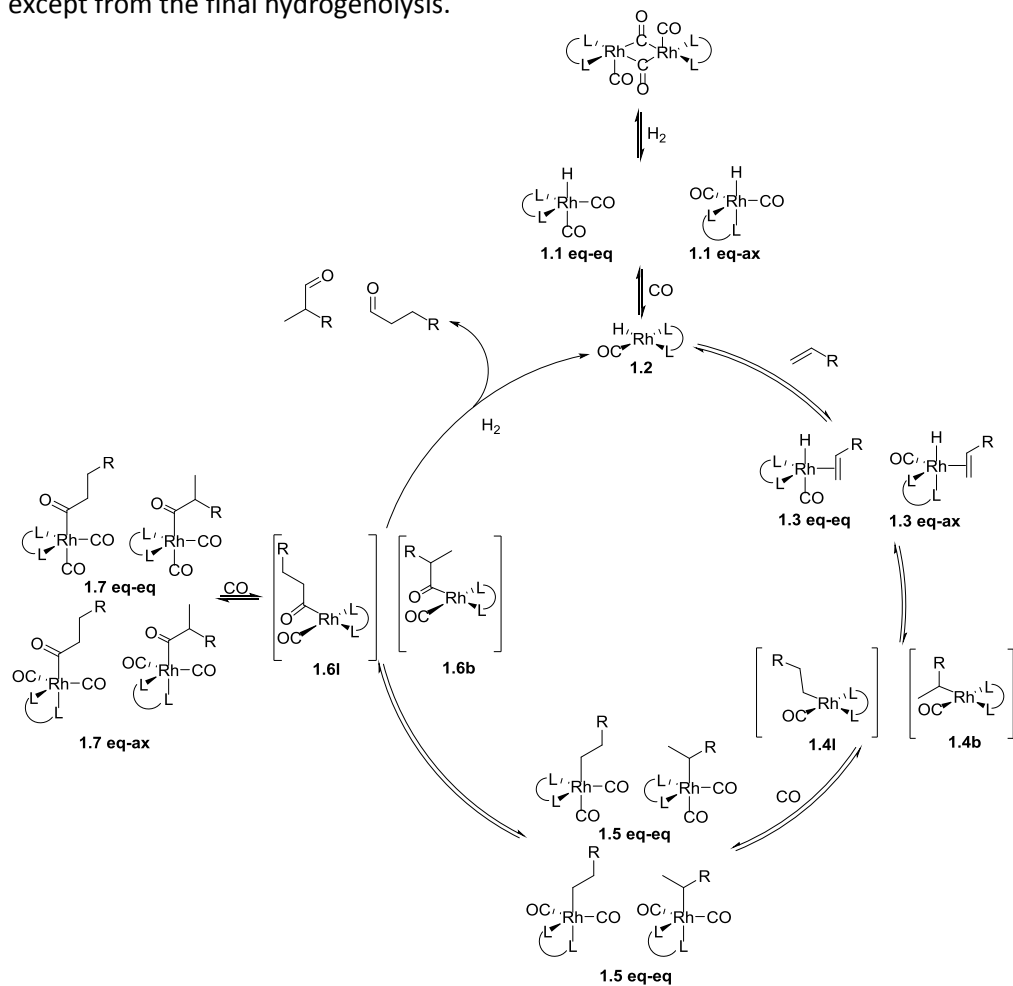
From an organic point of view, aldehydes are products of interests due to their versatile functionalization that can lead to the formation of new carbon-carbon and carbon-heteroatom bonds.¹¹ Nowadays, rhodium is the metal of choice in hydroformylation due to its high activity, and selectivity.¹²

1.1.2. Rhodium catalyzed hydroformylation

The hydroformylation (HF) reaction was discovered in 1938 by Otto Roelen while he was working on the Fischer-Tropsch process, and named it “oxo process”.¹³ In 2010, the production of so-called oxo-products was near 10.4 million tons per year proving the impact of this reaction at industrial scale.¹⁴ The hydroformylation of propene, which is a fraction of the steam-cracking process, constitutes the major application for the production of these oxo-products. The resulting *n*-butanal and *iso*-butyraldehyde represent crucial intermediates for the production of esters and acrylates (Scheme 1.2).^{3b} Heck and Breslow proposed a mechanism using a cobalt catalyst that remains accepted for the Rh-catalyzed hydroformylation¹⁵. Here, this mechanism is described for a bidentate ligand, and consists in the Wilkinson’s dissociative mechanism (Scheme 1.4). The determination and structural characterization of the resting state $[\text{Rh}(\text{L-L})(\text{CO})_2]$ **1.1** by in situ spectroscopic techniques such as High Pressure-Infrared (HP-IR) and High Pressure-Nuclear Magnetic Resonance (HP-NMR), provided great understanding of the mechanism. In the case of bidentate ligands, the species **1.1** can be observed as two different isomers where the ligand is coordinated in equatorial-axial (eq-ax) or equatorial-equatorial (eq-eq) mode.

First, fast dissociation of equatorial CO from **1.1** takes place to form the square planar intermediate **1.2** which upon coordination of the alkene in the equatorial plane, provides the complexes **1.3**. In this intermediate, the bidentate ligand can once more be coordinated in the eq-eq and/or eq-ax mode, while the hydride lies in apical position. In this step, the enantioface discrimination takes place.¹⁶

Although it has not been completely established whether the coordination of the alkenes is reversible or not, all the steps in Scheme 1.4 are described as reversible except from the final hydrogenolysis.

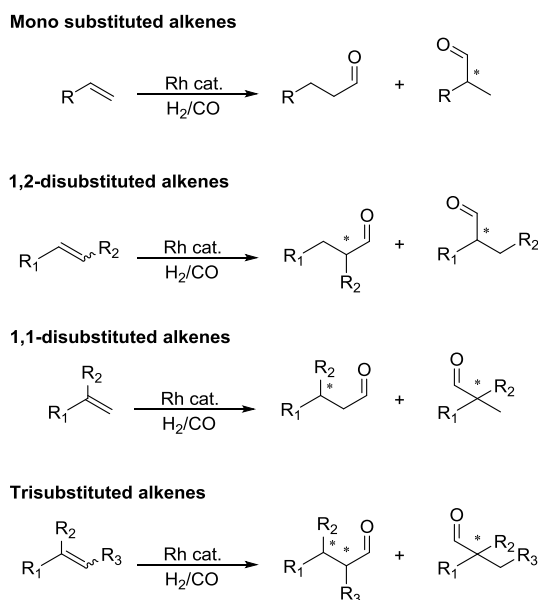


Scheme 1.4: Rh-catalyzed hydroformylation mechanism in the presence of bidentate ligand (L-L).

From **1.3**, migratory insertion of the alkene generated the square-planar alkyl complexes **1.4** followed by CO coordination to afford pentacoordinated species **1.5**. It is between species **1.3** and **1.4** where the regioselectivity is determined. The acyl square planar species **1.6** are generated by CO insertion, which finally undergo irreversible hydrogenolysis to provide the aldehyde products and regenerate the

hydride species **1.2**. The species **1.6** can also undergo CO coordination and provide acyl pentacoordinated species **1.7**. Such species have been recently observed by HP-IR and HP-NMR studies using bidentate ligands.^{16b-16d} Enantioselectivity is determined between species **1.2** and **1.6** since all these steps are in equilibrium. Depending on the reaction conditions and characteristics of the system, the rate determining step can switch between the reactions from species **1.1** to **1.6**.

The regioselectivity of this process depends on many factors, which include intrinsic substrate preferences, directing effects displayed by functional groups located close to the alkene, and the ligand. Depending on the number of substituents on the olefin, as well as the nature of the substituent, regioselectivity trends in the hydroformylation of alkenes can vary (Scheme 1.5).¹⁷



Scheme 1.5: Regioselectivity trends in rhodium catalyzed hydroformylation of various alkenes.

In the case of monosubstituted alkenes, depending on the substituent (R) the preference for the linear or branched product can change. In the case of alkyl substituents the linear product is usually favored, while when the substituent is an aryl or other electron-withdrawing group, the hydroformylation takes place in the

internal carbon producing the branched product. Similar trend is observed for 1,2-disubstituted alkenes. When 1,1-disubstituted and trisubstituted alkenes are transformed, only one regioisomer is preferentially afforded according to Keuleman's rule, which states that the formyl group is inserted in order to avoid the formation of a quaternary carbon center.¹⁸

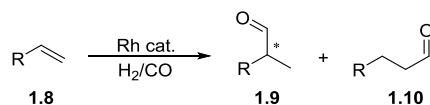
Although enantioselective hydroformylation constitutes a potentially clean, low cost, and atom-efficient method for the production of chiral aldehydes for the fine chemical industry, this reaction has not yet been applied on an industrial scale process due to several technical challenges.³ The main challenges to overcome are the low reaction rates at low temperature despite the good selectivities commonly achieved, the control of both regio- and enantioselectivity at once, and the short substrate scope for any single ligand.

1.1.3. Rhodium catalyzed asymmetric hydroformylation

The first examples of high enantioselectivity in asymmetric hydroformylation (AHF) (ee's up to 90%), were reported by Stille and Consiglio the same year using Pt diphosphite systems.¹⁹ Nonetheless, such systems provided several disadvantages such as low reaction rates, tendency to hydrogenate substrates, and low regioselectivity to branched products. Later, these issues were mainly overcome by the use of Rh-based catalysts.²⁰

1.1.3.1. Monosubstituted alkenes

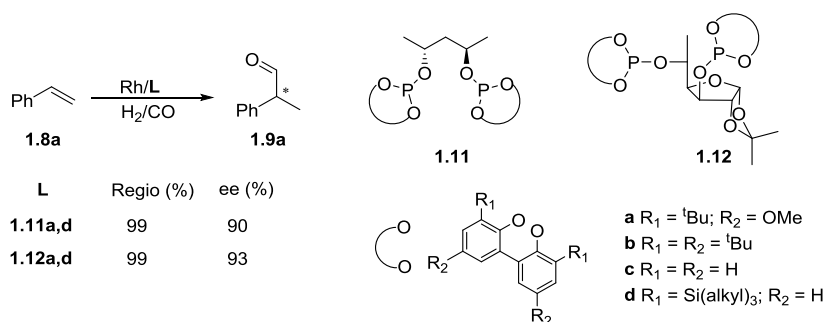
The asymmetric hydroformylation of monosubstituted olefins **1.8** has been largely studied due to the interest in the synthesis of chiral 2-substituted branched aldehydes **1.9** (Scheme 1.6). In the case of vinyl arenes, the 2-arylpropanals products are key intermediate in the synthesis of 2-arylpropanoic acids, which are the profen class of non-steroidal anti-inflammatory drugs.



Scheme 1.6: Rhodium catalyzed asymmetric hydroformylation of monosubstituted alkenes.

1,3-Diphosphite ligands

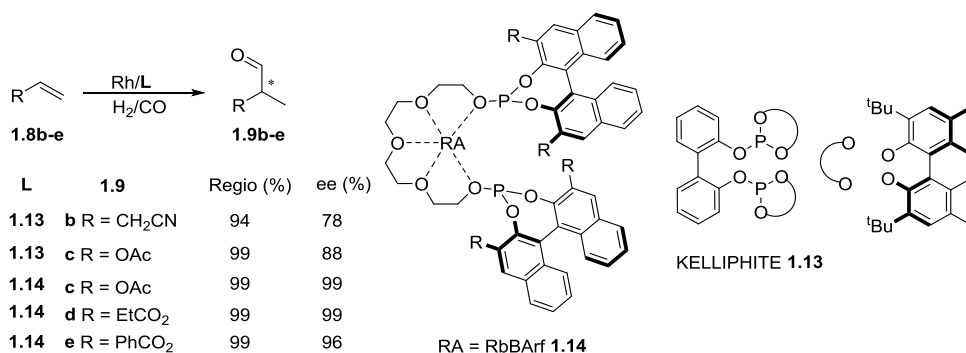
The diphosphite ligands proved to be efficient for this kind of substrates.²¹ The first successful ligand for the asymmetric hydroformylation of vinyl arenes was developed by Union Carbide and consisted in (2*R*, 4*R*)-pentane-2,4-diol diphosphite ligand **1.11**. This system provided good chemo-, regio-, and enantioselectivities (up to 90% ee).²² Apart from this structure, longer carbon chains between the oxygens were investigated but lower selectivities were obtained.²³ Furthermore, the effect of the substituents on the biaryl moiety was looked at, and showed the importance of the *ortho* and *para* substituents. The best results were obtained with ligands **1.11a** and **1.11d** (Scheme 1.7). Another example of successful ligands in asymmetric hydroformylation of vinyl arenes is the family of diphosphite ligands derived from 1,2-*O*-isopropylidene- α -D-xylofuranose and 6-deoxy-1,2-*O*-isopropylidene- α -D-glucufuranose **1.12** (Scheme 1.7).²⁴



Scheme 1.7: Rh-catalyzed asymmetric hydroformylation of monosubstituted alkene **1.8a** using ligands **1.11** and **1.12**.

In this type of ligands, the substituents on the biaryl moiety also proved to be crucial to provide high selectivities. Moreover, studies on the configuration at C5 showed that the configuration in this position is crucial to obtain high enantioselectivities.

The KELLIPHITE ligand **1.13** constitutes another example of successful chiral diphosphite ligand for AHF developed by Dow Chemical Company.²⁵ In contrast with ligands **1.11** and **1.12**, the chirality in this ligand is located in the biaryl moiety while the backbone is achiral. This ligand provided good enantioselectivities (up to 88%) in the hydroformylation of allyl cyanide **1.8b** and vinyl acetate **1.8c** (Scheme 1.8).



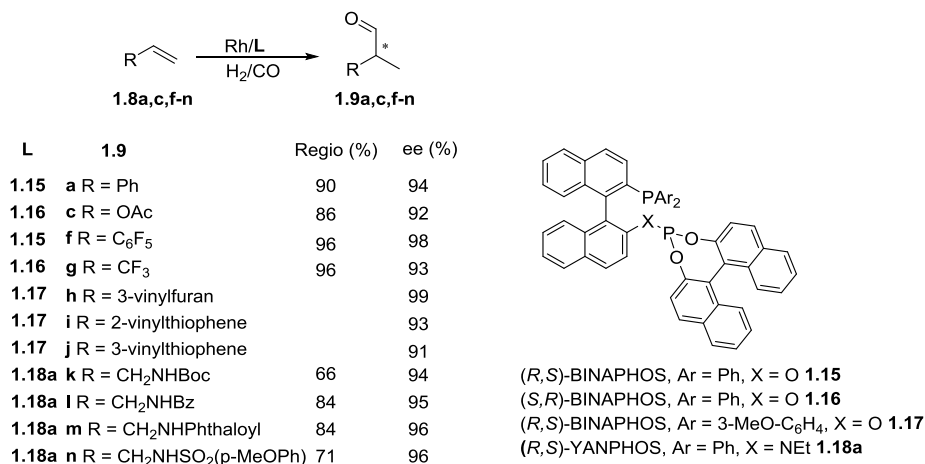
Scheme 1.8: Rh-catalyzed asymmetric hydroformylation of monosubstituted alkenes using biphosphite ligands **1.13** and **1.14**.

Vidal-Ferran *et al.* reported recently α,ω -bisphosphite-polyether ligands **1.14** containing regulation agents (RAs) that increase the activity of the corresponding rhodium complex in the asymmetric hydroformylation of vinyl benzoates (ee up to 96%) (Scheme 1.8).²⁶

Phosphine-Phosphite ligands

The (*R,S*)-BINAPHOS ligand **1.15** and (*S,R*)-BINAPHOS ligand **1.16** reported by Takaya and Nozaki were very successful ligands in the Rh-catalyzed asymmetric hydroformylation of a range of substrates (Scheme 1.9).²⁷ Apart from standard

monosubstituted alkenes for asymmetric hydroformylation such as styrene **1.8a**, allyl cyanide **1.8b**, and vinyl acetate **1.8c** for which excellent enantioselectivities were obtained (ee up to 94%), new substrates containing substituents such as –CF₃, –C₆F₅ groups, were successfully hydroformylated with high ee's.



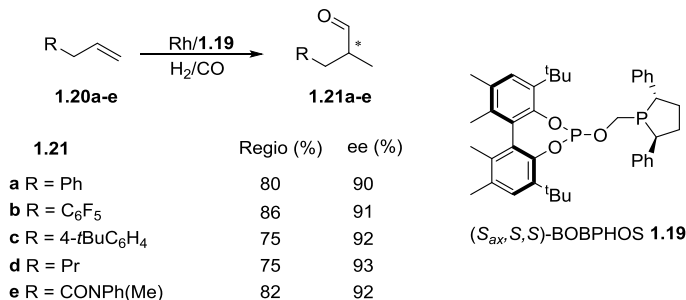
Scheme 1.9: Rh-catalyzed asymmetric hydroformylation of monosubstituted alkenes using BINAPHOS family of ligands **1.15**, **1.16**, **1.17**, **1.18**.

The BINAPHOS derivative ligand **1.17**, with only a variation on the aryl group of the phosphine moiety provided excellent selectivities for various vinyl arenes (ee's up to 97%)²⁸ while the (*R,S*)-YANPHOS ligand **1.18a**, containing a phosphoramidite moiety instead of a phosphite, afforded good regioselectivities (up to 84%), excellent ee's (up to 96%), and turnover number (TON) up to 9,700 in the asymmetric hydroformylation of *N*-allylamides **1.8k-n** (Scheme 1.9).²⁹

Though other groups developed new families of phosphine-phosphite and phosphine-phosphoramidite ligands, none of these ligands provided results comparable with those obtained with the BINAPHOS ligands or derivatives in terms of regio- and enantioselectivities, and scope of substrates.³⁰

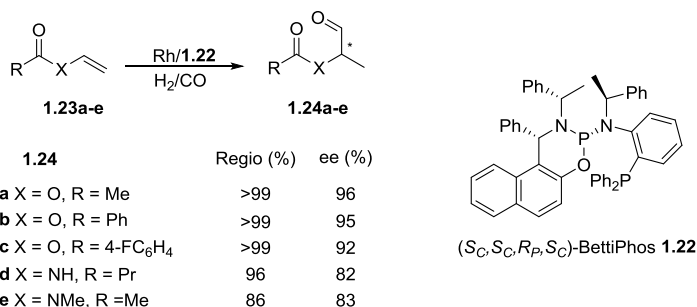
Recently, the (*S_{ox}S,S*)-BOBPPOS ligand **1.19** reported by Clarke and co-workers was applied in the AHF of alkyl alkenes **1.20**, affording unprecedented high regioselectivities (up to 89%) and excellent ee's (up to 92%) for branched aldehydes

(Scheme 1.10).³¹ Furthermore, detailed spectroscopic experiments were carried out in order to characterize Rh intermediates **1.1** and **1.6** (Scheme 1.4) to provide an explanation for this preference for the branched product.^{16b}



Scheme 1.10: Rh-catalyzed asymmetric hydroformylation of alkyl alkenes using BOBPBOS ligand **1.19**.

Leitner and co-workers recently reported the promising bidentate phosphine-phosphoramidite BettiPhos **1.22** that provided excellent ee's (up to 96%), and total regioselectivities in the Rh-catalyzed asymmetric hydroformylation of vinyl esters and amides **1.23** (Scheme 1.11).³²

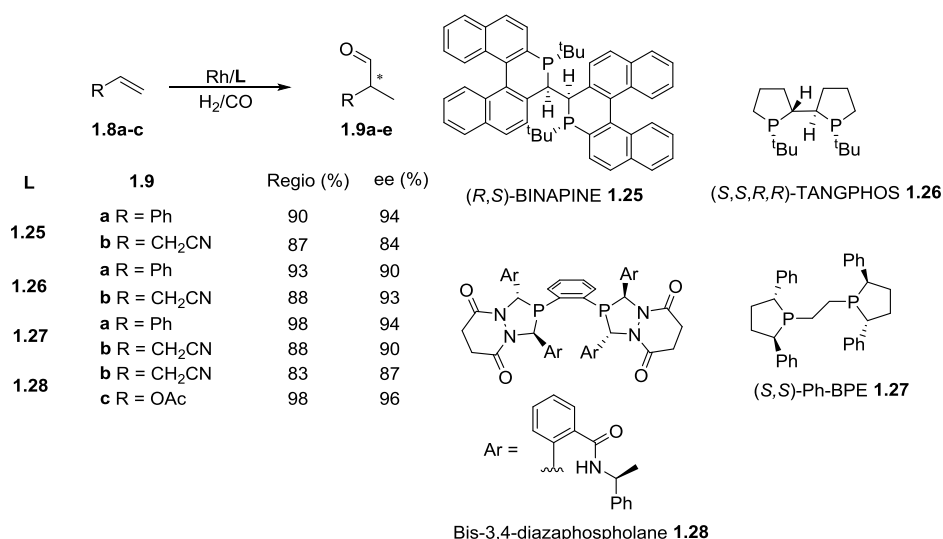


Scheme 1.11: Rh-catalyzed asymmetric hydroformylation of vinyl esters and amides using the BettiPhos ligand **1.22**.

Bisphosphacyclic ligands

The first examples of bisphospholanes structure to provide high enantioselectivities in the asymmetric hydroformylation of styrene **1.8a**, allyl cyanide **1.8b**, and vinyl acetate **1.8c** were (*S*)-BINAPINE ligand **1.25** and (*S,S,R,R*)-

TANGPHOS ligand **1.26** (Scheme 1.12).³³ Since then, efforts have been devoted to the development of novel bisphospholane scaffolds. The (*S,S*)-Ph-BPE **1.27** and the Bis-3,4-diazaphospholane (BDP) **1.28** ligands provided excellent regioselectivities and enantioselectivities in the asymmetric hydroformylation of styrene **1.8a**, allyl cyanide **1.8b** and vinyl acetate **1.8c** (Scheme 1.12). Furthermore, the BDP ligand **1.28** and derivatives provided excellent chemo-, regio- and enantioselectivities in the AHF of a wide scope of monosubstituted alkenes such as 1,3-dienes with ee's up to 97%, enamides with ee's up to 99%, and other allyl alkenes.³⁴



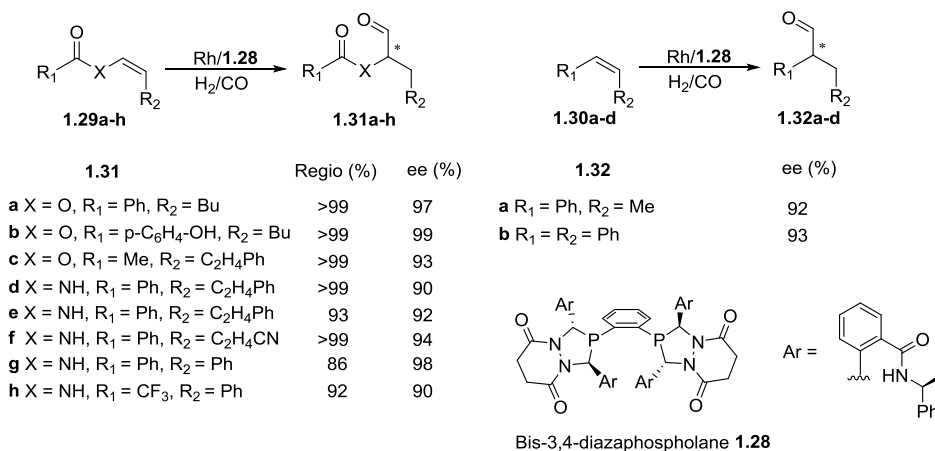
Scheme 1.12: Rh-catalyzed asymmetric hydroformylation of monosubstituted alkenes using the bisphospholane ligands **1.25**, **1.26**, **1.27**, and **1.28**.

1.1.3.2. Disubstituted alkenes

In the Rh-catalyzed asymmetric hydroformylation most of the attention has been focused on monosubstituted alkenes while only a few examples of efficient ligands have been applied successfully in the asymmetric hydroformylation of 1,2- and 1,1-disubstituted alkenes to date (Scheme 1.5). Their low reactivity due to the higher steric hindrance as well as a more complicated control of the regioselectivity makes these kinds of substrates more challenging.

Linear 1,2-disubstituted alkenes

The ligand **1.28** demonstrated its potential in the asymmetric hydroformylation of 1,2-disubstituted alkenes (Scheme 1.13). Excellent regio- and enantioselectivities were afforded in the asymmetric hydroformylation of Z-enamides and enol esters **1.29** (ee's up to 98%).³⁵ Furthermore, good results were also obtained in the asymmetric hydroformylation of vinyl arenes **1.30**, although the scope for these substrates was more restricted. In view of the success of ligand **1.28**, Burke and Risi reported the total synthesis of Patulolide C, (-)-Pyrenophorol, and (+)-Decaresstrictine L, which display antibacterial and antifungal activities.³⁶ In all the three cases, the asymmetric hydroformylation of alkenes using the ligand **1.28** was the crucial step to construct the skeleton of these complex molecules.

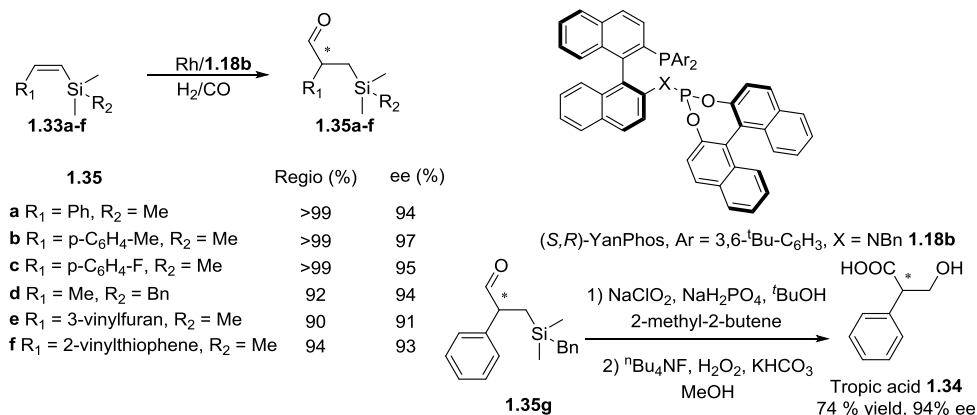


Scheme 1.13: Rh-catalyzed asymmetric hydroformylation of 1,2-disubstituted alkenes using ligand **1.28**.

Another strategy followed by Tan and Breit to hydroformylate 1,2-disubstituted alkenes was based on scaffolding ligands. Such methodology consists in a catalyst that is able to create covalent bonds with a substrate. This interaction between the ligand and the substrate facilitates the reaction and increases the selectivities, since the catalyst is specifically addressed to react with a specific part of the

substrate, the double bond in this case. Following this strategy, homoallylic alcohols were successfully hydroformylated with excellent selectivities.³⁷

More recently, Zhang and co-workers reported the asymmetric hydroformylation of 1,2-disubstituted alkenylsilanes **1.33** using the (*S,R*)-(NBn)-Yanphos ligand **1.18b** providing excellent enantioselectivities (up to 97%) and excellent regioselectivities (up to >99%) (Scheme 1.14).³⁸ In this case, the presence of a silyl group improves the regioselectivity due to its steric hindrance. Moreover, further functionalization of the silicon group into alcohol functionality via Fleming-Tamao oxidation afforded tropic acid **1.34** (Scheme 1.14).



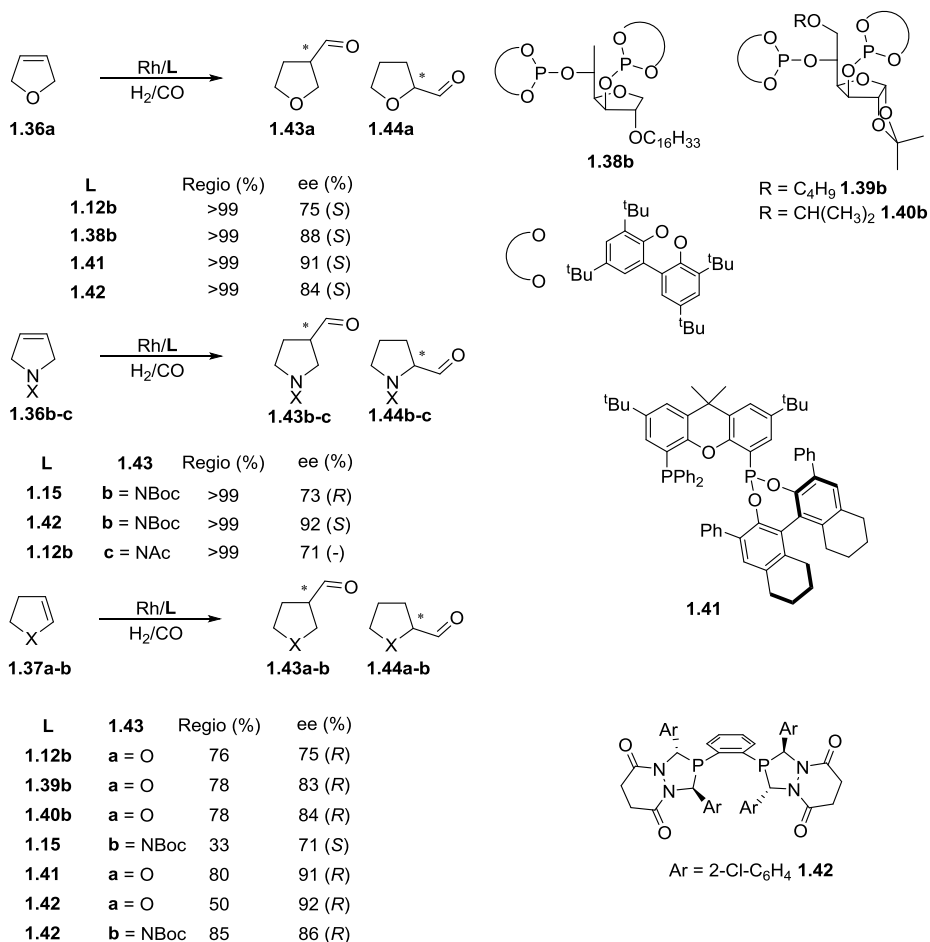
Scheme 1.14: Rh-catalyzed asymmetric hydroformylation of 1,2-disubstituted alkenylsilanes using ligand **1.18b**.

Cyclic 1,2-disubstituted alkenes

5-membered ring heterocycles such as dihydrofurans and dihydropyrroles have focused most of the attention for 1,2-disubstituted alkenes. The presence of a heteroatom in the cycle might favor isomerization when a metal-hydride species is present. It is therefore crucial to avoid the isomerization in order to obtain high regio-, chemo-, and enantioselectivities. In this context, various ligands revealed to inhibit the isomerization reaction, and provided good to excellent enantioselectivities. The BINAPHOS ligand **1.15** afforded full regioselectivity and good ee's (up to 73%) for 2,5-dihydropyrrole substrates **1.36**, although for the 2,3-

Chapter 1

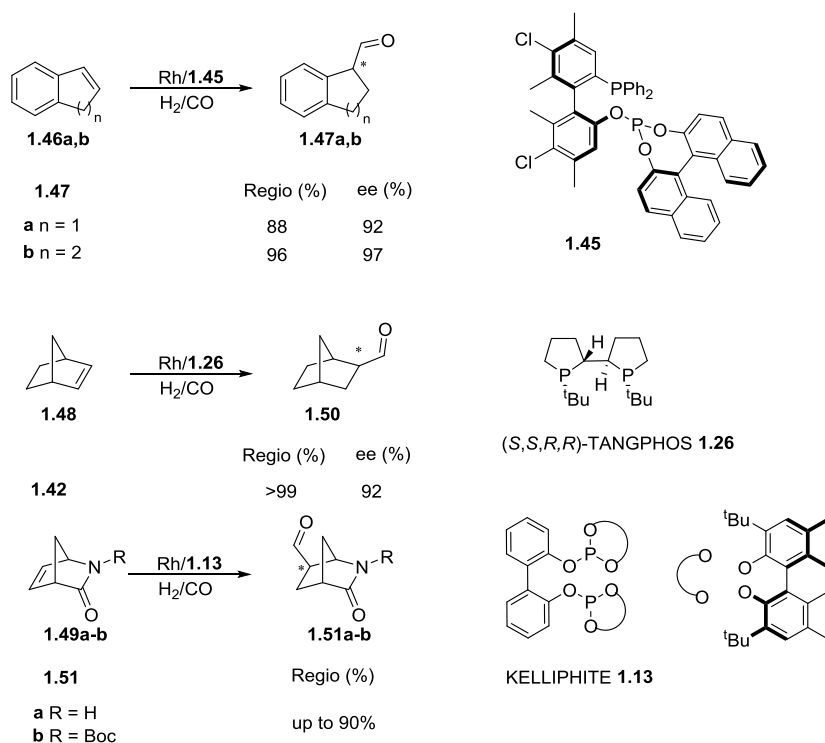
dihydropyrrole substrate **1.37**, the regioselectivities were not as high (Scheme 1.15).³⁹ In the case of 1,3-diphosphite ligands derived from carbohydrates, those containing glucose backbone (**1.38b**, **1.39b**, **1.40b**) provided full regioselectivity and high ee's (up to 88%) in the asymmetric hydroformylation of 2,5-dihydrofuran **1.36**, and ee's up to 84% were obtained in the asymmetric hydroformylation of 2,3-dihydrofurane **1.37**, although regioselectivity was lower in this case (up to 78%).⁴⁰



Scheme 1.15: Rh-catalyzed asymmetric hydroformylation of monocyclic 1,2-disubstituted olefins using ligands **1.38b**, **1.39b**, **1.40b**, **1.41**, and **1.42**.

The Xantphos derived ligand **1.41** proved very efficient for 2,3- and 2,5-dihydrofuran substrates with excellent ee's (up to 91%).⁴¹ The bis-3,4-diazophospholane ligand **1.42** afforded excellent ee's (up to 92%) and excellent regioselectivities. Moreover, with this system, the hydroformylation of both dihydropyrrole and dihydrofuran alkenes was also achieved.⁴² Other monocyclic 1,2-disubstituted alkenes like dioxapines or *N*-Boc-2,2-dimethyl-2,3-dihydrooxazole, which is a precursor for the Garner's aldehyde, were successfully hydroformylated with excellent enantioselectivities using diphosphite and bis-3,4-diazophospholane ligands.^{26b-43} Substrates containing bicyclic structures are of interest since they are present in several molecules of interest for medicinal applications.⁴⁴ Despite the attractive synthetic route that asymmetric hydroformylation offers to achieve interesting products starting from bicyclic olefins, only a few examples of chiral ligands have been able to hydroformylate bicyclic 1,2-disubstituted alkenes with high selectivities to date. Catalysts containing BINAPHOS analogous ligand **1.45** were able to hydroformylate 1,2-dihydronaphthalene **1.46a** and 1-*H*-indene **1.46b** with enantioselectivities up to 96% and excellent regioselectivities up to 97% (Scheme 1.16).

Norbornene **1.48** and its derivatives are also interesting bicyclic alkenes for asymmetric hydroformylation. Bunel et. al. reported the first successful asymmetric hydroformylation of norbornene using TANGPHOS **1.26** in 2005.⁴⁵ Full stereoselectivity to the *exo*-product and enantioselectivities up to 92% were obtained, and similar results were afforded for other derivatives (Scheme 1.16). KELLIPHITE **1.13** has been recently used in the hydroformylation of bicyclic lactams **1.49a-b** with full *exo*-selectivity and regioselectivities up to 90%.⁴⁶

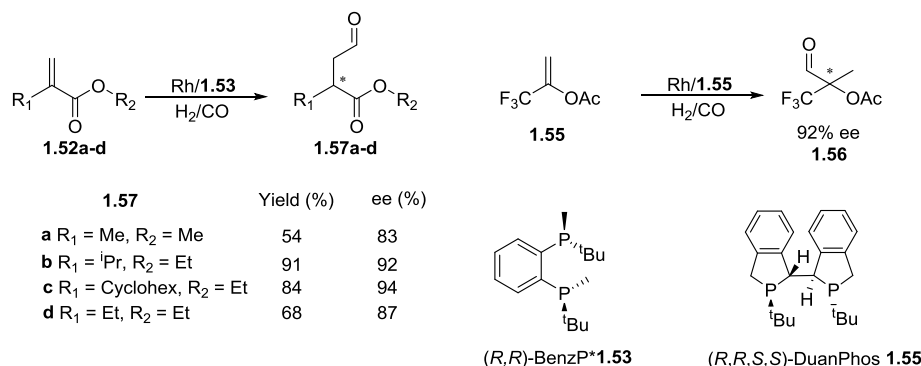


Scheme 1.16: Rh-catalyzed asymmetric hydroformylation of 1,2-bicyclic alkenes using ligand **1.45**, **1.23** and **1.13**.

1,1-Disubstituted Alkenes

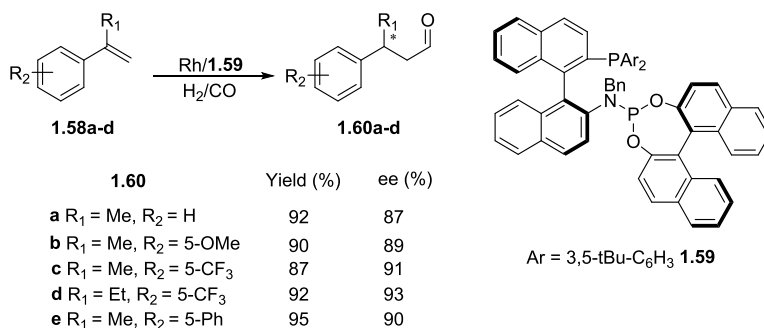
Only a few examples of successful AHF of 1,1-disubstituted alkenes have been reported to date. A number of ligands have been applied in the asymmetric hydroformylation of these substrates, nonetheless poor to moderate enantioselectivities were achieved even when the versatile ligands BINAPHOS **1.15** and BINAPINE **1.25** were applied.⁴⁷ In contrast, the successful asymmetric hydroformylation of α -alkyl acrylates **1.52** was reported by Buchwald and co-workers using the (*R,R*)-BenzP* ligand **1.53** (Scheme 1.17).⁴⁸ Excellent regioselectivities (up to 91%) and enantioselectivities (up to 94%) were obtained under very mild conditions. Later on, the same group reported the asymmetric hydroformylation of 3,3,3-trifluoroprop-1-en-2-yl acetate **1.54** using (*R,R,S,S*)-DuanPhos **1.55** with enantioselectivities up to 92%. Furthermore, the synthesis of

enantiomerically pure 2-trifluoromethylallylic acid was achieved after oxidation and subsequent hydrolysis of the resulting aldehyde **1.56** at a 10 mmol scale.⁴⁹ Chirality at the phosphorus appeared as an important feature of the ligand to afford high enantioselectivities for these kinds of substrates.



Scheme 1.17: Rh-catalyzed asymmetric hydroformylation of 1,1-functionalized olefins using ligands **1.53** and **1.55**.

Recently, Zhang and co-workers reported the asymmetric hydroformylation of α -alkylstyrene **1.58** using the hybrid phosphorus ligand **1.59** derived from YANPHOS.⁵⁰ They obtained complete regioselectivity to the linear product and high ee for this kind of substrates (up to 93%) under mild conditions (5 bar of syngas and 80°C), although long reaction times are required (48h) (Scheme 1.18).



Scheme 1.18: Rh-catalyzed asymmetric hydroformylation of α -alkyl styrene derivatives using ligand **1.59**.

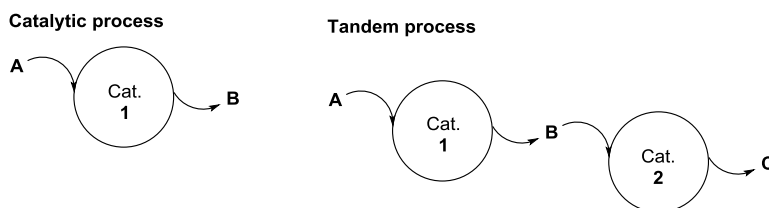
The combination of sterically hindered aryl groups in the phosphine together with the *S,S* configuration at the binaphthol group is described as key for the

enantioface differentiation in the migratory insertion, which is the enantioselectivity determining step.

Despite the clear potential of asymmetric hydroformylation for the synthesis of chiral aldehydes, the application of this process at large scale has not yet been completed. As previously mentioned, aldehydes are not usually isolated as final products, since the real products of interest are usually products derived from the aldehydes. In this context, tandem processes with HF as the initial step constitute an interesting strategy.

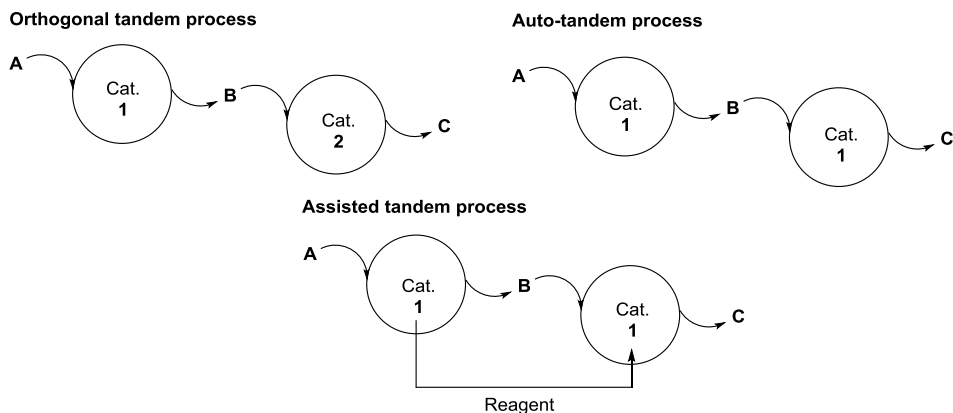
1.1.4. Rhodium catalyzed hydroaminomethylation

Metal catalyzed processes have demonstrated their efficiency to carry out various types of chemical transformations. However, the possibility to carry out several catalytic transformations in “one pot” is even more attractive from an environmental and efficiency point of view. In this context, tandem catalytic processes are described as sequential catalytic transformations of the substrate through two, or even more, mechanistic pathways (Scheme 1.19).⁵¹



Scheme 1.19: Scheme of a catalytic process from A to B, and a tandem process from A to C.

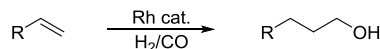
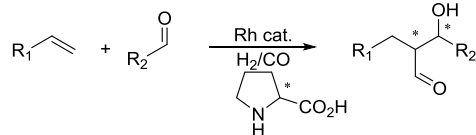
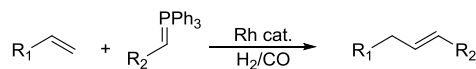
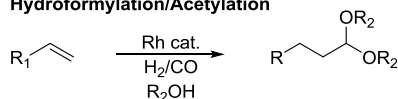
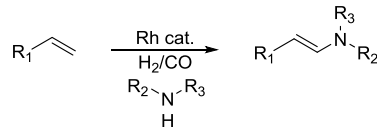
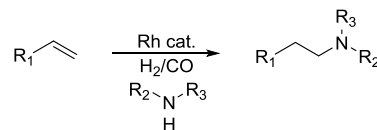
There are three main types of tandem catalytic processes: a) orthogonal tandem catalysis is when two independent catalyst precursors are used in the same reaction, b) auto-tandem catalysis is when the same catalyst precursor is able to carry out the different transformations in the process, and finally c) assisted tandem process is when a single catalyst species can be modified by addition of an external reagent to perform a change in mechanism (Scheme 1.20).^{51a}



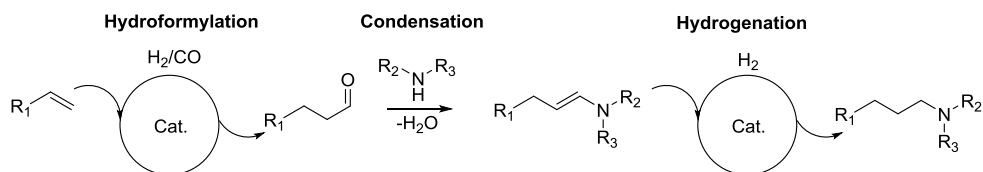
Scheme 1.20: Scheme of the three types of tandem processes.

As previously mentioned, aldehydes are very attractive building blocks in organic synthesis, but are usually not the final target molecule. For this reason, tandem hydroformylation processes are promising, since they allow the formation of versatile building blocks such as aldehydes, which in the same reaction vessel are transformed in situ into more interesting molecules (Scheme 1.21).

Alcohols can be prepared by in situ reduction of the aldehyde using the same hydrogen pressure present in the medium.⁵² In the presence of a carbonyl compound such as an aldehyde and an organocatalyst, aldol reaction takes place to expand the structure of the molecule.⁵³ It is also possible to create new C-C bonds if the aldehyde reacts with a phosphorus ylide via a Wittig reaction.⁵⁴ On the other hand, aldehydes can act as electrophiles and react with a nucleophile present in the media. If the nucleophile is an alcohol, then hemiacetals or acetals can be created.⁵⁵ In the presence of a primary or secondary amine, imines and enamines can be easily prepared.⁵⁶ When these imines or enamines are hydrogenated to create the corresponding amine, the reaction receives the name of hydroaminomethylation (HAM) (Scheme 1.21).

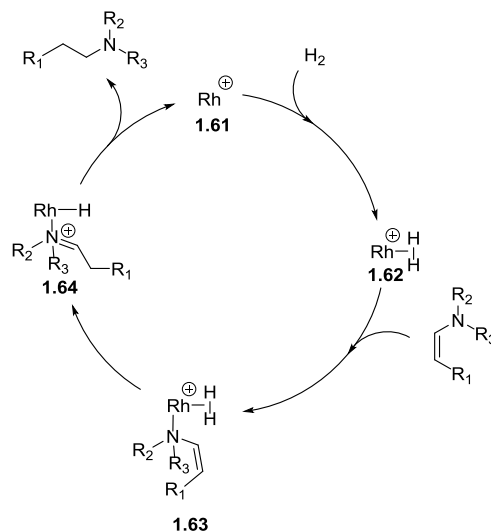
Hydroformylation/reduction for the synthesis of alcohols**Hydroformylation/Aldol reaction****Hydroformylation/Wittig olefination****Hydroformylation/Acetylation****Hydroaminovinilation reaction****Hydroaminomethylation reaction****Scheme 1.21:** Examples of hydroformylation tandem processes.

The efficient and selective synthesis of amines using easily available and abundant precursors is a long-standing goal of chemical research, since they are powerful building blocks for the synthesis of pharmaceuticals, peptides, alkaloids and agrochemical, dyes, and monomers for polymerization.⁵⁷ It has been estimated that worldwide amine demand will reach 19.9 billion \$ between 2015 and 2020.⁵⁸ In this context, the metal catalyzed hydroaminomethylation reaction constitutes an attractive alternative to the classical multistep organic synthetic routes. The reaction was discovered by Reppe and co-workers between 1928 and 1944 at BASF company when they were studying the production of acrylamide by reaction of acetylene, carbon monoxide and ammonia using nickel and iron carbonyl catalysts.⁵⁹ As a tandem reaction, several consecutive steps take place during the reaction: 1) first, the hydroformylation of the alkene affords the corresponding aldehyde; 2) the condensation of the amine with the aldehyde produces either an enamine or an imine, and 3) hydrogenation of the enamine or imine into the amine completes the reaction (Scheme 1.22).



Scheme 1.22: Tandem hydroaminomethylation for monosubstituted alkenes (only linear products are presented).

Despite that ruthenium⁶⁰ was used for this process, rhodium is in general the metal of choice for this reaction, due to its performance in hydroformylation,⁶¹ and efficiency in the hydrogenation of imines and enamines.⁶² From the mechanistic point of view, it is presumed that neutral $[\text{Rh}(\text{H})(\text{CO})_2\text{L}]$ (L = bidentate ligand) species catalyze the hydroformylation step (Scheme 1.4), while the hydrogenation of enamines and imines takes place in the presence of neutral or cationic species.⁶³ In this chapter, the catalytic cycle for enamine hydrogenation involving rhodium cationic species is described using Rh^+ for simplification (Scheme 1.23).^{63a}

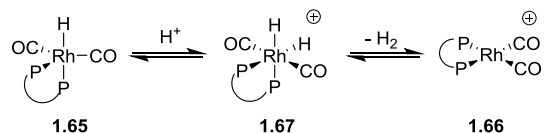


Scheme 1.23: Rh-catalyzed enamine hydrogenation mechanism via cationic species **1.61**.

First, hydrogen is coordinated to rhodium species **1.61** to generate $\text{Rh}-\eta^2$ -dihydrogen complex **1.62**. Then, enamine coordinates to rhodium complex **1.62** through the nitrogen to afford complex **1.63**. A first hydrogen transfer promotes

the formation of an iminium intermediate **1.64**, which undergoes a second hydrogen transfer to release the final amine product and regenerates the initial cationic rhodium species **1.61** (Scheme 1.23).

Phosphorus ligands are the most successful in the hydrogenation of both imines and enamines.⁶⁴ Regarding the rhodium precursor, the cationic $[\text{Rh}(\text{L})_2]\text{X}$ (L = COD or NBD, X = PF_6 , BF_4 , SbF_6 , etc.) precursors are usually applied,⁶⁵ although in some cases neutral $[\text{RhCOD}(\mu\text{-Cl})]_2$ has also proved to be successful.^{63b} Kalck and co-workers recently reported an equilibrium between neutral **1.65** and cationic **1.66** species via protonation of the neutral species **1.67** (Scheme 1.24).⁶⁶



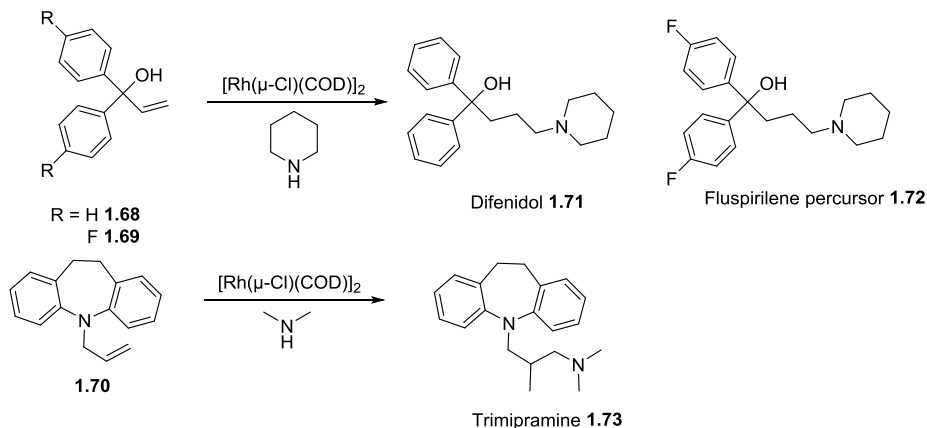
Scheme 1.24: Equilibrium between neutral and cationic rhodium species in hydroaminomethylation described by Kalck et. al.

Hydrogenation of the alkene into the alkane and hydrogenation of the aldehyde into the corresponding alcohol are non-desired side reactions that can also take place in the process. Therefore, the catalytic system should be designed to perform the hydroformylation rapidly, to allow the condensation of the aldehyde with primary or secondary amines to be sufficiently rapid to generate the imine/enamine product. In this case, the hydrogenation of these latter species would be the rate determining step in the hydroaminomethylation reaction.⁶⁷

1.1.4.1. Monosubstituted alkenes

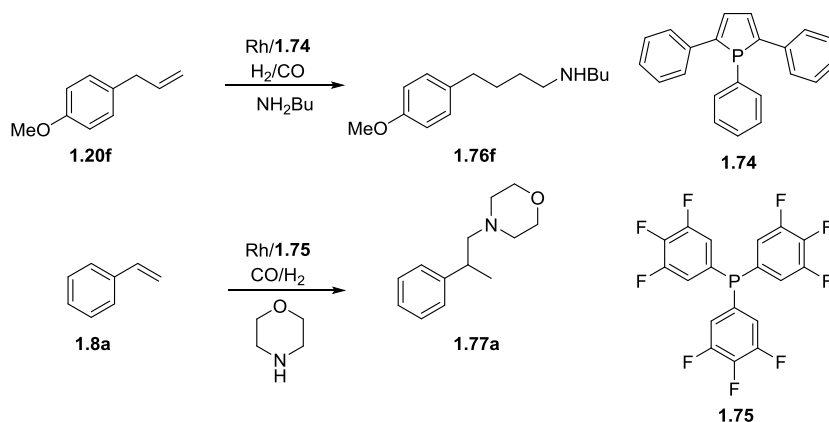
The hydroaminomethylation of monosubstituted alkenes have been reported by several groups over the last decade. Among them, the most studied substrates are the arylalkenes, especially those derived from styrene, since arylethylamines exhibit pharmacological activity.⁶⁸ Eilbracht and co-workers reported the rhodium catalyzed hydroaminomethylation of 1,1-diaryl-allyl-alcohols **1.68** and **1.69** and

vinyl benzoazepine **1.70** using a non-modified $[\text{Rh}(\mu\text{-Cl})(\text{COD})]_2$ catalyst to afford antihistaminic drugs such as Difenidol **1.71**, Fluspirilene precursor **1.72** or biological active Trimipramine **1.73** (Scheme 1.25).⁶⁹



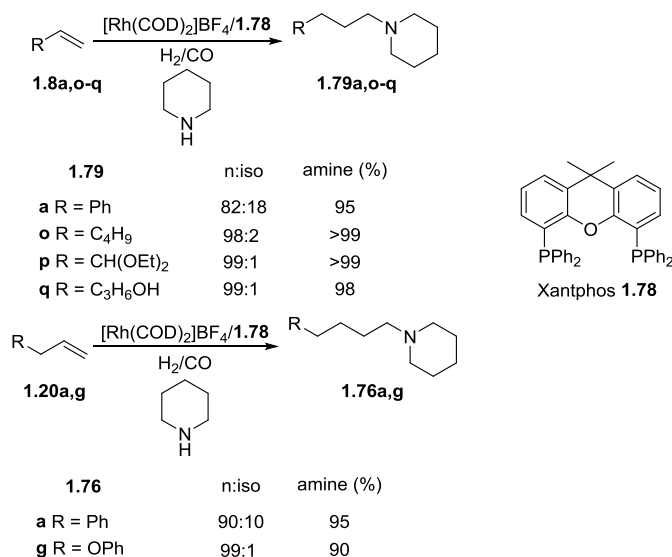
Scheme 1.25: Rh-catalyzed hydroaminomethylation of monosubstituted alkenes **1.68-1.70** using unmodified rhodium catalyst.

Despite these results with non-modified catalysts, the use of catalytic systems containing phosphorus ligands are expected to provide high activity and selectivity for both hydroformylation and hydrogenation. Urrutigoity et. al. reported the hydroaminomethylation of estragole **1.20f**, a biorenewable starting material, using different class of monodentate phosphorus ligands (Scheme 1.26).⁷⁰



Scheme 1.26: Rh-catalyzed hydroaminomethylation of monosubstituted alkenes **1.20f** and **1.8a** using monodentate phosphorus ligands **1.74** and **1.75**.

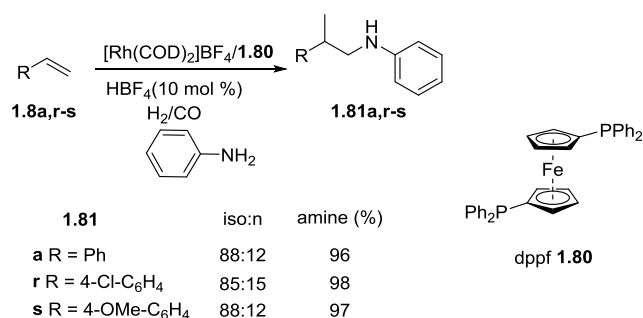
Furthermore, the electronic effect of the ligands was studied, showing that the monodentate ligand **1.74** and derivatives provide better activity and selectivity than classical systems using triphenylphosphine and monophosphites. Similar studies were performed by Clarke and co-workers using the electrodeficient phosphine **1.75** in the hydroaminomethylation of styrene **1.8a** (Scheme 1.26).^{63b-70} In contrast to monodentate ligands, bidentate phosphorus ligands offer much stronger coordination and higher steric hindrance to the metal center. In consequence, diphosphine ligands tend to provide better chemo- and regioselectivities in the rhodium catalyzed hydroaminomethylation. Beller and co-workers reported the use of Xantphos **1.78** together with the cationic precursor $[\text{Rh}(\text{COD})_2]\text{BF}_4$ for the hydroaminomethylation of several terminal alkyl alkenes, aryl alkenes, and vinyl arenes.⁷¹ Excellent chemo- and regioselectivities to linear amines **1.76** and **1.79** were obtained (Scheme 1.27).



Scheme 1.27: Rh-catalyzed hydroaminomethylation of monosubstituted alkenes for the production of linear amines using the Xantphos ligand **1.78**.

Vogt et. al. improved the results in terms of activity and regioselectivity to the linear amines using more π -acceptor diposphorus ligands based on Xanthene.⁷² Apart from linear amines, the production of branched aryethylamines through the

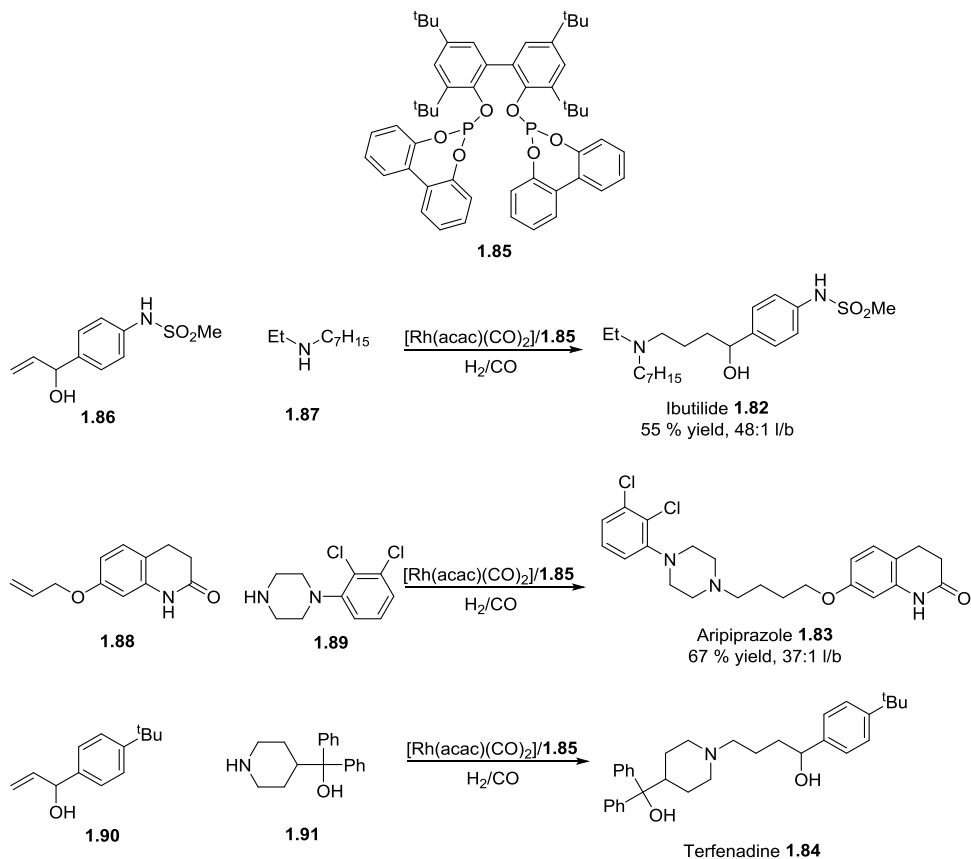
reaction of styrene with an amine is attractive due to the importance of these compounds in the pharmaceutical industry.⁷³ In this context, Beller et. al. achieved the production of branched amines from styrene and derivatives using 1,1'-bis(diphenylphosphino) ferrocene (dppf) **1.80** as ligand with excellent regio- and chemoselectivities. In this case, the use of a cationic precursor and a mixture of methanol/toluene as solvent was necessary to afford the desired products (Scheme 1.28).⁷⁴ Moreover, the use of tetrafluoroboric acid (HBF₄) was necessary to afford amines in high yields.



Scheme 1.28: Rh-catalyzed hydroaminomethylation of styrene derivatives **1.8** for the production of branched amines **1.81** using dppf **1.80** as ligand.

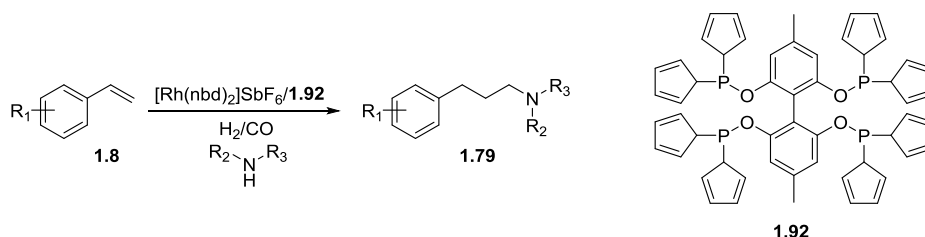
Apart from these systems, other groups successfully employed diphosphine ligands for the selective hydroaminomethylation of monosubstituted alkenes obtaining either linear or branched amines.⁷⁵

As previously mentioned, diphosphite ligands can provide excellent results in the hydroformylation of several alkenes due to their π -acceptor character. Despite their sensitivity to hydrolysis, diphosphite ligands have also been applied for the production of biological active compounds starting from monosubstituted alkenes.⁷⁶ Ibutilide **1.82**, Aripiprazole **1.83** or Tertefadine **1.84** are some examples of molecules of interests produced via hydroaminomethylation of monosubstituted alkenes using the bidentate biphephos derivative **1.85** ligand (Scheme 1.29).



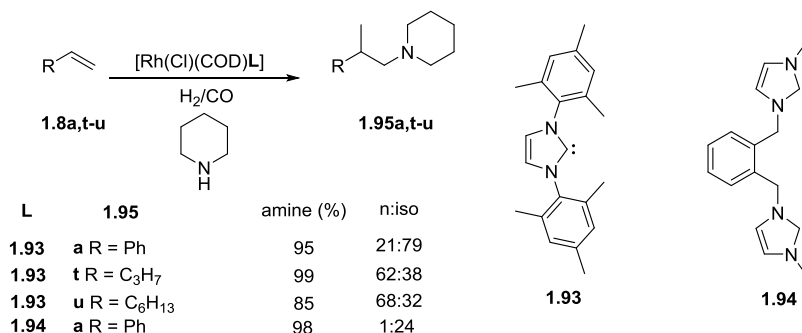
Scheme 1.29: Rh-catalyzed hydroaminomethylation of monosubstituted alkenes using ligand **1.85** for the production of biological active molecules.

In 2013, Zhang and co-workers reported that the tetraphosphorus ligand **1.92** provided outstanding linear selectivity for the hydroaminomethylation of styrene and derivatives (up to >99:1 n/iso) (Scheme 1.30).⁷⁷ The high regioselectivity was explained by the high steric hindrance provided by the ligand, together with the increased chelating effect due to the presence of four phosphorus atoms. Apart from styrene, the same group produced amines from other terminal olefins such as 1-octene and 1-hexene with high regioselectivities to the linear amine product using the ligand family **1.92** and other tetraphosphorus ligands.⁷⁸



Scheme 1.30: Regioselective Rh-catalyzed hydroaminomethylation of styrene and derivatives using ligand **1.92**.

In contrast to the large number of phosphorus ligands applied for both rhodium catalyzed hydroformylation and hydroaminomethylation, N-heterocyclic carbenes have been less applied for this reaction. In this context, Beller et. al. reported in 2003 the hydroaminomethylation of terminal olefins using N-heterocyclic monocarbene ligand **1.93** and N-heterocyclic dicarbene **1.94** for the production of linear amines with excellent activities and chemoselectivities. In the case of styrene **1.8a**, regioselectivities up to 21:79 n/iso were achieved using ligand **1.93**. Nevertheless, in the case of terminal aliphatic olefins, the system provided poor regioselectivities (Scheme 1.31).⁷⁹ Later, N-heterocyclic dicarbene ligand **1.94** was applied for the production of branched amines **1.95** from styrene **1.8a** with good regioselectivities (up to 1:24 n/iso) (Scheme 1.31).⁸⁰



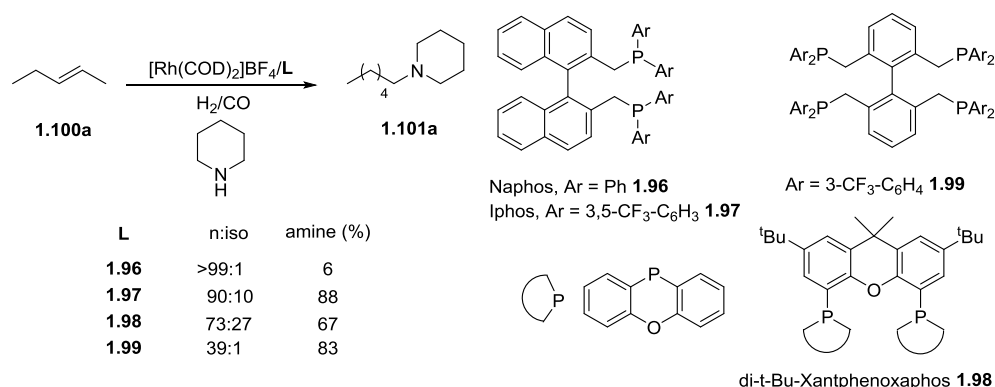
Scheme 1.31: Rh-catalyzed hydroaminomethylation of monosubstituted olefins using carbene ligands **1.93** and **1.94**.

1.1.4.2. Disubstituted alkenes

Owing to the challenges mentioned before, disubstituted olefins have been less studied than monosubstituted alkenes, and efforts have been focusing on two main types of disubstituted substrates: 1,2- and 1,1-disubstituted olefins.

1,2-Disubstituted alkenes

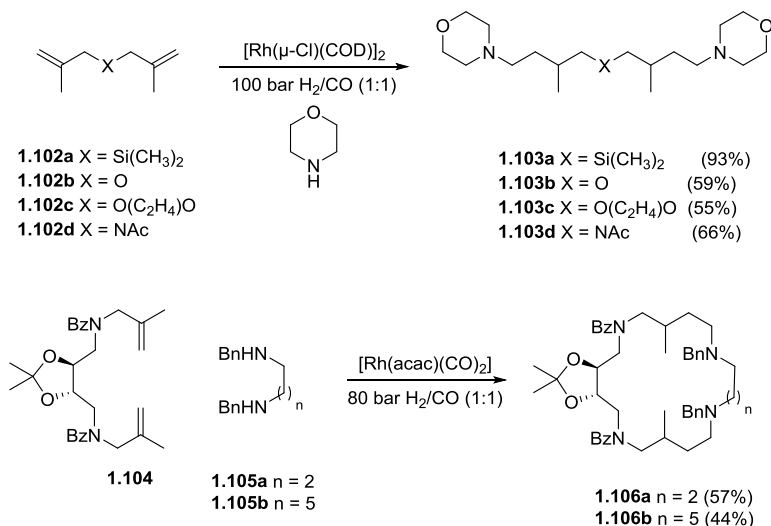
The use of bulky diphosphine ligands with a large bite angle such as Xantphos **1.78** and derivatives allowed the transformation of internal alkenes into terminal aldehydes in the hydroformylation reaction through isomerization of the double bond.⁸¹ Consecutive hydride transfer and β -H elimination allows the formation of terminal alkyl rhodium species, which are subsequently carbonylated into the linear aldehyde. Beller and co-workers applied these systems in the hydroaminomethylation of internal olefins using ligands **1.96-1.98** for the production of terminal amines with excellent regioselectivities (up to 99:1) (Scheme 1.32).^{56a-82} The same strategy was used by Zhang and co-workers using tetraphosphorus ligand **1.99**, with excellent activities and selectivities towards the linear amines (Scheme 1.32).⁸³



Scheme 1.32: Rh-catalyzed isomerization-hydroaminomethylation of internal disubstituted olefins using large bite angle diphosphine ligands **1.96-1.98** and tetraphosphorus ligand **1.99**.

1,1-Disubstituted alkenes

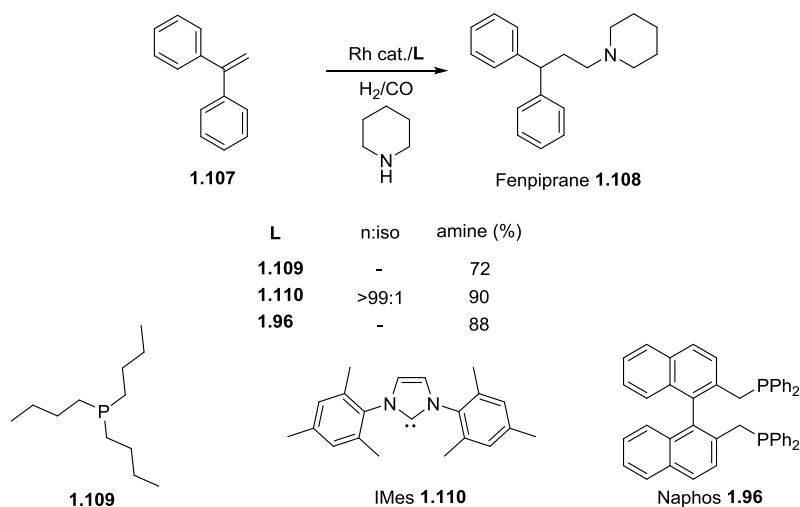
The production of linear amines from 1,1-disubstituted olefins has been studied since the intrinsic properties of the substrate usually facilitate the production of the terminal product. The hydroaminomethylation of 1,1-disubstituted olefins **1.102** containing bis(methyl)silane, ethers and amines for the production of the analogous linear amine **1.103** was achieved with good to excellent selectivities using non-modified rhodium precursor. Furthermore, molecules containing such a structure possesses potential biological activity (Scheme 1.33).⁸⁴ Other groups also used non-modified rhodium catalysts to hydroaminomethylate dialkenes **1.104** with diamines **1.105** for the production of oxo- and azamacroheterocyclic systems **1.106**, which are of interest due to their binding properties (Scheme 1.33).⁸⁵



Scheme 1.33: Rh-catalyzed hydroaminomethylation of 1,1-disubstituted olefins using non-modified rhodium catalysts.

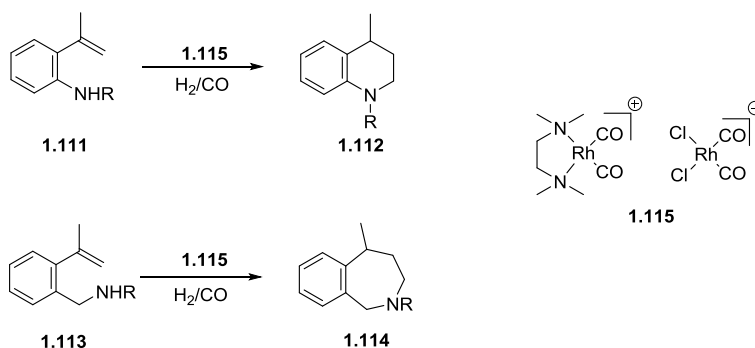
The hydroaminomethylation of 1,1-diarylethenes **1.107** gives access to 3,3-diarylpropylamines **1.108**, which are of pharmaceutical interest.⁸⁶ In this context, Eilbracht *et al.* reported the synthesis of these compounds using a catalyst bearing tributylphosphine **1.109** with good selectivities towards the desired linear amines; however, high pressures (90/20 bar CO/H_2) were necessary (Scheme 1.34).⁸⁷ Later,

Beller and co-workers reported the selective synthesis of 3,3-diarylpropylamines **1.108** via rhodium catalyzed hydroaminomethylation using the N-heterocyclic carbene **1.110** as ligand with low catalyst loading (0.1 mol%) (Scheme 1.34).^{79b} More recently, Zhang and co-workers reported the synthesis of the same compounds using the diphosphine Naphos **1.96** with excellent selectivities, low pressures (20/10 bar CO/H₂), and low catalyst loadings (0.1 mol%) (Scheme 1.34).⁸⁸



Scheme 1.34: Synthesis of Fenpiprane **1.108** through hydroaminomethylation of ethene-1,1-diyldibenzene **1.107** using **1.109**, **1.110** and **1.96** as ligands.

The hydroaminomethylation of 2-(prop-1-en-2-yl)aniline derivatives **1.111** affords tetrahydroquinolines **1.112**, which are of interest for the preparation of pharmaceuticals and agrochemicals.⁸⁹ When compounds **1.113** containing a methylene group between the nitrogen and the aryl group are submitted, 7-membered rings are produced; these compounds are known as 2-benzazepines **1.114**. For the synthesis of these compounds, the rhodium complexes containing the dinitrogen ligands **1.115** were used by Alper *et al.* obtaining good to excellent yields towards the desired amines (Scheme 1.35).⁹⁰



Scheme 1.35: Rh-catalyzed hydroaminomethylation of 2-(prop-1-en-2-yl)aniline **1.111** and compound **1.113** for the synthesis of tetraquinolines **1.112** and 2-benzazepines **1.114** using complex **1.115**.

In conclusion, the rhodium catalyzed hydroaminomethylation reaction has demonstrated its potential for the synthesis of amines. Nevertheless, several challenges remain to be tackled and a deeper understanding of the equilibrium between hydroformylation and hydrogenation catalysts is necessary.

1.1.5. Homogeneous catalyst immobilization and continuous flow chemistry

1.1.5.1. Homogeneous and heterogeneous catalysis

Nowadays, over 90% of all industrial chemicals are produced through catalytic processes.⁹¹ Homogeneous, heterogeneous or even enzymatic catalysis are primarily molecular phenomenon since they involve the chemical transformation of molecules into new compounds. Despite the advantages that homogeneous and heterogeneous catalysis provide, there are main drawbacks to overcome in both cases.⁹²

The main type of heterogeneous catalysts are oxides and metal supported particles, which are in a different phase than the reagents and the products.⁹³ Therefore, an easy recovery of the catalyst can be achieved, thus facilitating their implementation in industrial processes. Nonetheless, harsh reaction conditions such as high temperatures and pressures are usually required in order to increase

the rate of diffusion of reactants towards the catalytic core, adsorption of reactants, products desorption, etc. Moreover, heterogeneous catalysis often provides low, and difficulty to identify and modify the active site of the catalysts. Despite these disadvantages, most bulk processes in industry are carried out via heterogeneous catalysis.

Homogeneous catalysis, the catalyst and the reagents are in the same phase, usually a liquid phase. These catalysts provide high activity and selectivity, such as chemo-, regio- and enantioselectivity mainly because the performance of homogeneous catalysts can usually be tuned by variation in the structure of the ligands. Moreover, modern spectroscopic methods such as multinuclear NMR provide a deep understanding of the mechanisms at atomic level, which provide information for the design of more efficient catalysts. However, the main drawback of homogeneous catalysts is the difficulty to separate them from the reaction products, thus limiting the possibility of their recovery and re-use.^{3a}

Consequently, the research of more efficient catalytic systems that combine the advantages of both homogeneous (catalyst selectivity) and heterogeneous (catalyst recycling) catalysis is one of the challenges of modern chemistry.

1.1.5.2. Homogeneous catalysts immobilization

Several strategies have been developed for the recovery and reuse of homogeneous catalysts and for an appropriate separation of the catalyst from the products.⁹⁴ Among the different approaches, the immobilization of homogeneous catalysts onto solid supports is the predominant strategy, and the resulting catalysts are known as “heterogenized catalysts”. Such heterogenized systems can be achieved *via* different approaches (Figure 1.1).⁹⁵

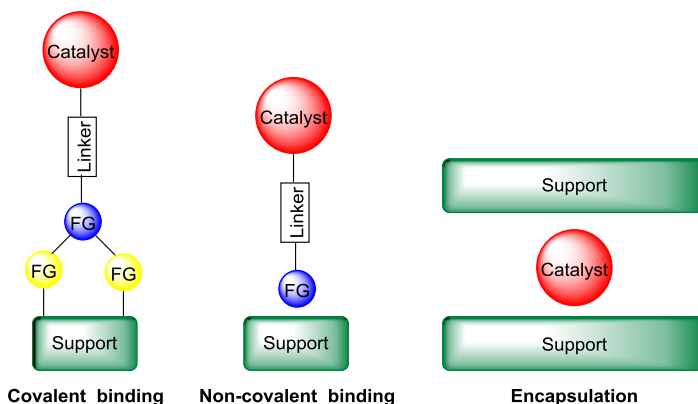


Figure 1.1: Main approaches for the immobilization of homogeneous catalysts onto solid supports.

Immobilization via covalent interactions

The catalyst can be anchored onto the surface of the support via covalent binding; therefore, a chemical reaction between the solid support and the catalyst is required to create the covalent bond. Thus, the ligand must be designed to include a functionality that can react with the solid support, and extra synthetic efforts are necessary. Apart from the anchoring strategy, the design of the system has to avoid undesired interactions between the metal center and the support or the pro-immobilizable functional groups present in the support. Despite the additional efforts necessary, the strong interaction generated provides a robust heterogenized system, which minimizes the metal leaching. Several types of supports, such as inorganic oxides⁹⁶ or polymeric supports⁹⁷ can be applied for this strategy since they can contain hydroxyl groups⁹⁸ or can be modified to contain nitrogen⁹⁹ or sulfur¹⁰⁰ groups that are suitable for covalent interactions (Figure 1.2).

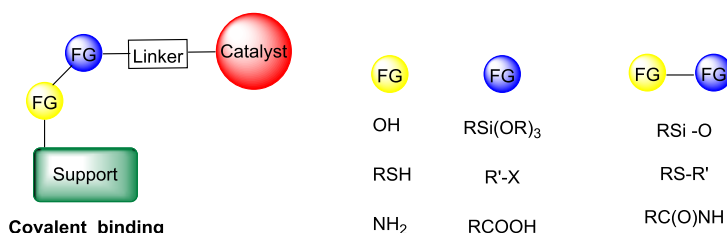


Figure 1.2: Example of different covalent interactions between catalysts and supports.

Immobilization via non-covalent interactions

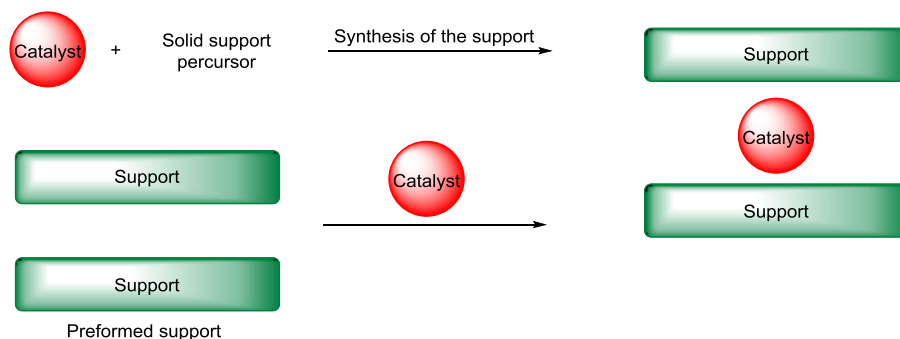
In the case of non-covalent binding strategy, the interaction between the solid support is not based on a covalent bond but on other types of interactions between the support and the ligand such as electrostatic interactions, hydrogen bonding, Van de Waals forces, π - π interactions, etc.¹⁰¹ Since no reaction is necessary between the support and the catalyst to create a covalent bond, many of the systems do not require significant modifications of either the ligand nor the support; in consequence the cost for their preparation is lower, which makes it more attractive for potential industrial applications. However, the main drawback of these systems concerns the strength of the interactions between the catalyst and the solid support, which often lead to catalyst leaching.

Immobilization via encapsulation

The encapsulation strategy is based in the confinement of a homogeneous catalyst into a solid support. While the catalyst is encapsulated in the pores of the support and cannot diffuse through it, reactants and reagents have to be able to go through the support without restriction.¹⁰¹

Since the encapsulation is primarily based on physical phenomena, no interaction between support and catalyst is required to maintain the catalyst attached. The parameters to take into account in order to minimize catalyst leaching are the pore size, the homogeneous distribution of the pore size along the support and the rigidity of the support. Zeolites¹⁰² and Ordered Mesoporous Silica (OMS)¹⁰³ are

usually the supports of choice since they combine these characteristics. The preparation of heterogenized catalysts via encapsulation is based on two main strategies: building the catalyst inside the support or building the support around a preformed catalyst (Scheme 1.36).



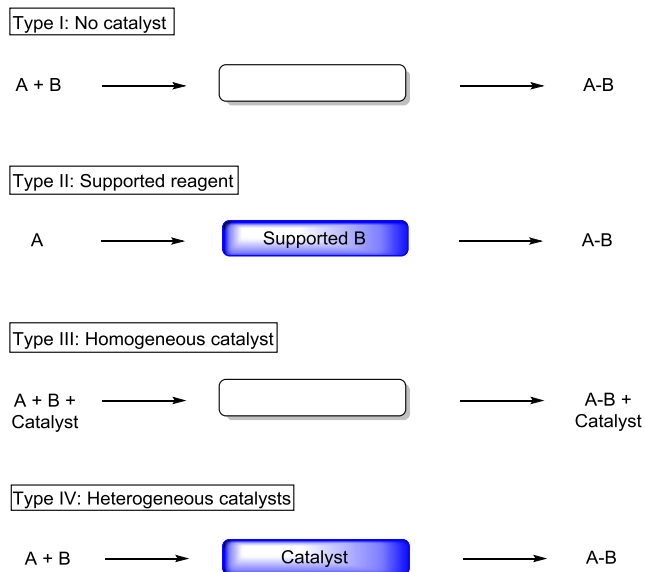
Scheme 1.36: Main strategies for catalyst entrapment into a porous solid support.

1.1.5.3. Catalysis under continuous flow condition

A continuous flow system is defined as a chemical process operating in a continuous manner.¹⁰⁴ Over the last years, continuous flow processes have gained attention as an alternative to the traditional batch-based processes for the production of fine chemicals.^{3a} Among the advantages that the flow offers, the most important are the improvement in heat and mass transfer,⁶⁷⁻¹⁰⁵ better control over residence time, enhanced energy efficiency due to improved temperature control,¹⁰⁶ better isolation of the system for sensitive reactions to air and moisture, improved safety through operation since smaller volumes are applied.¹⁰⁷ Moreover, flow chemistry can establish integrated processes, and in consequence, reduce the operation units and provide fully automated processes.¹⁰⁸

According to what Kobayashi and co-workers, the continuous flow systems can be divided in 4 types (Scheme 1.37).¹⁰⁹ In type I, the reagents (A and B) are pumped through the reactor, where the reaction takes place, and finally the product is

obtained, however unreacted A and B, and side products are also collected. In contrast, type II contains a substrate (B) immobilized in the reactor wall. If substrate B is used in excess, substrate A can be completely transformed. Nonetheless, the reactor has to be changed with all the complications implied when substrate B is consumed. In type III, a homogeneous catalyst is applied to transform reagents A and B while they pass through the reactor.



Scheme 1.37: Kobayashi's suggested type of continuous flow systems.

Therefore, even if the reagents are fully converted into the desired product, extra separation step is necessary. In type IV, the catalyst lies immobilized inside the reactor and acts as heterogeneous catalyst. In this case, an immobilization step of the catalyst prior to catalysis is necessary; however, if the reaction proceeds ideally, no separation step is necessary and the catalyst can be easily recycled and reused. In summary, type IV is the ideal system for application in flow mode since, in principle, no separation from the catalyst is required.¹¹⁰

In the following chapters, the synthesis of heterogenized chiral catalysts containing modified diphosphite ligands for the rhodium catalyzed asymmetric hydroformylation of bicyclic 1,2-disubstituted olefins in batch and flow mode will

be first described. Secondly, the rhodium catalyzed asymmetric hydroaminomethylation of 1,1-disubstituted olefins, namely α -alkyl acrylates, for the production of chiral γ -aminobutyric esters is reported. Furthermore, results on the rhodium catalyzed regioselective hydroaminomethylation of α -alkyl acrylates to produce β -amino esters are also included.

1.2. References

¹ Beller, M. *Catalytic Carbonylation Reactions*, Beller, M., Springer-Verlag Berlin Heidelberg, Berlin, Germany, **2006**.

² ^{a)} Haynes, A. *Chapter 1 - Catalytic Methanol Carbonylation in Advances in Catalysis*, Eds. Academic Press, Vol. 53, Amsterdam, The Netherlands, **2010**, pp. 1-45. ^{b)} Haynes, A.; Maitlis, P. M.; Morris, G. E.; Sunley, G. J.; Adams, H.; Badger, P. W.; Bowers, C. M.; Cook, D. B.; Elliott, P. I. P.; Ghaffar, T.; Green, H.; Griffin, T. R.; Payne, M.; Pearson, J. M.; Taylor, M. J.; Vickers, P. W.; Watt, R. J. *J. Am. Chem. Soc.* **2004**, *126*, 2847-2861.

³ ^{a)} Cornils, B.; Herrmann, W. A. *Applied Homogeneous Catalysis with Organometallic Compounds, Vol. 1*, Cornils, B.; Herrmann, W. A., Wiley-VCH, Weinheim, Germany, **2002**. ^{b)} Weissermel, K.; Arpe, H.-J. *Industrial Organic Chemistry*, Weissermel, K.; Arpe, H.-J., Wiley-VCH, Weinheim, Germany, **2008**.

⁴ ^{a)} Gehrtz, P. H.; Hirschbeck, V.; Ciszek, B.; Fleischer, I. *Synthesis* **2016**, *48*, 2679-2679. ^{b)} Wu, X.-F.; Fang, X.; Wu, L.; Jackstell, R.; Neumann, H.; Beller, M. *Acc. Chem. Res.* **2014**, *47*, 1041-1053.

⁵ *Rhodium Catalysis*, Claver, C., Springer Nature, Cham, Switzerland, **2018**.

⁶ Lee, H. W.; Kwong, F. Y. *Eur. J. Org. Chem.* **2010**, *2010*, 789-811.

⁷ Gibson, S. E.; Stevenazzi, A. *Angew. Chem. Int. Ed.* **2003**, *42*, 1800-1810.

⁸ Li, X.; Li, X.; Jiao, N. *J. Am. Chem. Soc.* **2015**, *137*, 9246-9249.

⁹ Shu, D.; Li, X.; Zhang, M.; Robichaux, P. J.; Guzei, I. A.; Tang, W. *J. Org. Chem.* **2012**, *77*, 6463-6472.

¹⁰ Bernhard, B. *Aldehydes: synthesis by hydroformylation of alkenes in Science of synthesis*, Eds. Thieme, Vol. 25, Stuttgart, Germany, **2007**.

¹¹ a) Trost, B. M. *Science* **1991**, *254*, 1471-1477. b) Breit, B. *Acc. Chem. Res.* **2003**, *36*, 264-275.

¹² *C-1 Building Blocks in Organic Synthesis 1. Additions to Alkenes, Alkynes, and Carbonyl Compounds, Vol. 1*, van Leeuwen, P. W. N. M., Thieme, Stuttgart, Germany, **2013**.

¹³ Franke, R.; Selent, D.; Börner, A. *Chem. Rev.* **2012**, *112*, 5675-5732.

¹⁴ Naqvi, S. Oxo Alcohols. Process Economics Program Report, ihsmarket.com, **2010**, 21E

¹⁵ Heck, R. F. *Acc. Chem. Res.* **1969**, *2*, 10-16.

¹⁶ a) van der Veen, L. A.; Boele, M. D. K.; Bregman, F. R.; Kamer, P. C. J.; van Leeuwen, P. W. N. M.; Goubitz, K.; Fraanje, J.; Schenk, H.; Bo, C. *J. Am. Chem. Soc.* **1998**, *120*, 11616-11626. b) Dingwall, P.; Fuentes, J. A.; Crawford, L.; Slawin, A. M. Z.; Bühl, M.; Clarke, M. L. *J. Am. Chem. Soc.* **2017**, *139*, 15921-15932. c) Nozaki, K.; Matsuo, T.; Shibahara, F.; Hiyama, T. *Organometallics* **2003**, *22*, 594-600. d) Nelsen, E. R.; Brezny, A. C.; Landis, C. R. *J. Am. Chem. Soc.* **2015**, *137*, 14208-14219.

¹⁷ van Leeuwen, P. W. N. M. *Homogeneous Catalysis: Understanding the Art*, Kluwer, Dordrecht, The Netherlands, **2004**.

¹⁸ Keulemans, A. I. M.; Kwantes, A.; van Bavel, T. *Rec. Trav. Chim. Pays Bas.* **1948**, *67*, 298-308.

¹⁹ a) Consiglio, G.; Nefkens, S. C. A.; Borer, A. *Organometallics* **1991**, *10*, 2046-2051. b) Stille, J. K.; Su, H.; Brechot, P.; Parrinello, G.; Hegedus, L. S. *Organometallics* **1991**, *10*, 1183-1189.

²⁰ a) Agbossou, F.; Carpentier, J.-F.; Mortreux, A. *Chem. Rev.* **1995**, *95*, 2485-2506.

b) Gladiali, S.; Bayón, J. C.; Claver, C. *Tetrahedron: Asymmetry* **1995**, *6*, 1453-1474.

²¹ Diéguez, M.; Pàmies, O.; Claver, C. *Tetrahedron: Asymmetry* **2004**, *15*, 2113-2122.

²² a) Babin, J. E.; Whiteker, G. T. *Chem. Abstr.* **1993**, *119*, 159. b) Whiteker, G. T.; Briggs, J. R.; Babin, J. E.; Barner, B. A. in *Catalysis of Organic Reactions*, Eds. Chemical Industries Series, Vol. 89, New York, **2003**, pp. 359-367.

²³ a) Buisman, G. J. H.; Vos, E. J.; Kamer, P. C. J.; van Leeuwen, P. W. N. M. *J. Chem. Soc., Dalton Trans.* **1995**, 409-417. b) Buisman, G. J. H.; van der Veen, L. A.;

Klootwijk, A.; de Lange, W. G. J.; Kamer, P. C. J.; van Leeuwen, P. W. N. M.; Vogt, D. *Organometallics* **1997**, *16*, 2929-2939.

²⁴ a) Diéguez, M.; Pàmies, O.; Ruiz, A.; Castellón, S.; Claver, C. *Chem. Eur. J.* **2001**, *7*, 3086-3094. ^{b)} Dieguez, M.; Pamies, O.; Ruiz, A.; Claver, C. *New J. Chem.* **2002**, *26*, 827-833.

²⁵ a) Cobley, C. J.; Klosin, J.; Qin, C.; Whiteker, G. T. *Org. Lett.* **2004**, *6*, 3277-3280. ^{b)} Cobley, C. J.; Gardner, K.; Klosin, J.; Praquin, C.; Hill, C.; Whiteker, G. T.; Zanotti-Gerosa, A.; Petersen, J. L.; Abboud, K. A. *J. Org. Chem.* **2004**, *69*, 4031-4040.

²⁶ a) Vidal-Ferran, A.; Mon, I.; Bauzá, A.; Frontera, A.; Rovira, L. *Chem. Eur. J.* **2015**, *21*, 11417-11426. ^{b)} Rovira, L.; Vaquero, M.; Vidal-Ferran, A. *J. Org. Chem.* **2015**, *80*, 10397-10403.

²⁷ a) Sakai, N.; Mano, S.; Nozaki, K.; Takaya, H. *J. Am. Chem. Soc.* **1993**, *115*, 7033-7034. ^{b)} Nozaki, K. *The Chemical Record* **2005**, *5*, 376-384.

²⁸ a) Tanaka, R.; Nakano, K.; Nozaki, K. *J. Org. Chem.* **2007**, *72*, 8671-8676. ^{b)} Nakano, K.; Tanaka, R.; Nozaki, K. *Helv. Chim. Acta* **2006**, *89*, 1681-1686.

²⁹ Xiaowei, Z.; Bonan, C.; Shichao, Y.; Xumu, Z. *Angew. Chem. Int. Ed.* **2010**, *49*, 4047-4050.

³⁰ Cunillera, A.; Godard, C.; Ruiz, A. *Asymmetric Hydroformylation Using Rhodium in Rhodium Catalysis*, Eds. Springer Nature, Cham, Switzerland, **2018**, pp. 99-143.

³¹ Noonan, G. M.; Fuentes, J. A.; Cobley, C. J.; Clarke, M. L. *Angew. Chem. Int. Ed.* **2012**, *51*, 2477-2480.

³² Schmitz, C.; Holthusen, K.; Leitner, W.; Franciò, G. *ACS Catal.* **2016**, *6*, 1584-1589.

³³ Axtell, A. T.; Klosin, J.; Abboud, K. A. *Organometallics* **2006**, *25*, 5003-5009.

³⁴ a) McDonald, R. I.; Wong, G. W.; Neupane, R. P.; Stahl, S. S.; Landis, C. R. *J. Am. Chem. Soc.* **2010**, *132*, 14027-14029. ^{b)} Watkins, A. L.; Landis, C. R. *Org. Lett.* **2011**, *13*, 164-167. ^{c)} Adint, T. T.; Wong, G. W.; Landis, C. R. *J. Org. Chem.* **2013**, *78*, 4231-4238.

³⁵ Abrams, M. L.; Foarta, F.; Landis, C. R. *J. Am. Chem. Soc.* **2014**, *136*, 14583-14588.

- ³⁶ a) Risi, R. M.; Burke, S. D. *Org. Lett.* **2012**, *14*, 1180-1182. b) Risi, R. M.; Maza, A. M.; Burke, S. D. *J. Org. Chem.* **2015**, *80*, 204-216.
- ³⁷ a) Joe, C. L.; Blaisdell, T. P.; Geoghan, A. F.; Tan, K. L. *J. Am. Chem. Soc.* **2014**, *136*, 8556-8559. b) Grünanger, C. U.; Breit, B. *Angew. Chem. Int. Ed.* **2008**, *120*, 7456-7459.
- ³⁸ You, C.; Li, X.; Yang, Y.; Yang, Y.-S.; Tan, X.; Li, S.; Wei, B.; Lv, H.; Chung, L.-W.; Zhang, X. *Nat. Commun.* **2018**, *9*, 2045.
- ³⁹ a) Nozaki, K.; Takaya, H.; Hiayama, T. *Top. Catal.* **1997**, *4*, 175. b) Sakai, N.; Nozaki, K.; Takaya, H. *J. Chem. Soc., Chem. Commun.* **1994**, 395-396.
- ⁴⁰ a) Gual, A.; Godard, C.; Castellón, S.; Claver, C. *Adv. Synth. Catal.* **2010**, *352*, 463-477. b) Dieguez, M.; Pamies, O.; Claver, C. *Chem. Commun.* **2005**, 1221-1223. c) Mazuela, J.; Coll, M.; Pàmies, O.; Diéguez, M. *J. Org. Chem.* **2009**, *74*, 5440-5445.
- ⁴¹ Chikkali, S. H.; Bellini, R.; de Bruin, B.; van der Vlugt, J. I.; Reek, J. N. H. *J. Am. Chem. Soc.* **2012**, *134*, 6607-6616.
- ⁴² Kun, X.; Xin, Z.; Zhiyong, W.; Xumu, Z. *Chem. Eur. J.* **2014**, *20*, 4357-4362.
- ⁴³ Clemens, A. J. L.; Burke, S. D. *J. Org. Chem.* **2012**, *77*, 2983-2985.
- ⁴⁴ Botteghi, C.; Paganelli, S.; Schionato, A.; Marchetti, M. *Chirality* **1991**, *3*, 355-369.
- ⁴⁵ Huang, J.; Bunel, E.; Allgeier, A.; Tedrow, J.; Storz, T.; Preston, J.; Correll, T.; Manley, D.; Soukup, T.; Jensen, R.; Syed, R.; Moniz, G.; Larsen, R.; Martinelli, M.; Reider, P. J. *Tetrahedron Lett.* **2005**, *46*, 7831-7834.
- ⁴⁶ Noonan, G. M.; Copley, C. J.; Lebl, T.; Clarke, M. L. *Chem. Eur. J.* **2010**, *16*, 12788-12791.
- ⁴⁷ Deng, Y.; Wang, H.; Sun, Y.; Wang, X. *ACS Catal.* **2015**, *5*, 6828-6837.
- ⁴⁸ Wang, X.; Buchwald, S. L. *J. Am. Chem. Soc.* **2011**, *133*, 19080-19083.
- ⁴⁹ Wang, X.; Buchwald, S. L. *J. Org. Chem.* **2013**, *78*, 3429-3433.
- ⁵⁰ You, C.; Li, S.; Li, X.; Lan, J.; Yang, Y.; Chung, L. W.; Lv, H.; Zhang, X. *J. Am. Chem. Soc.* **2018**, *140*, 4977-4981.

- ⁵¹ a) Fogg, D. E.; dos Santos, E. N. *Coord. Chem. Rev.* **2004**, *248*, 2365-2379. b) Wasilke, J.-C.; Obrey, S. J.; Baker, R. T.; Bazan, G. C. *Chem. Rev.* **2005**, *105*, 1001-1020.
- ⁵² Eilbracht, P.; Bärfacker, L.; Buss, C.; Hollmann, C.; Kitsos-Rzychon, B. E.; Kranemann, C. L.; Rische, T.; Roggenbuck, R.; Schmidt, A. *Chem. Rev.* **1999**, *99*, 3329-3366.
- ⁵³ a) Chercheja, S.; Nadakudity, S. K.; Eilbracht, P. *Adv. Synth. Catal.* **2010**, *352*, 637-643. b) Abillard, O.; Breit, B. *Adv. Synth. Catal.* **2007**, *349*, 1891-1895.
- ⁵⁴ a) Breit, B.; Zahn, S. K. *Angew. Chem. Int. Ed.* **1999**, *38*, 969-971. b) Wong, G. W.; Landis, C. R. *Angew. Chem. Int. Ed.* **2013**, *52*, 1564-1567.
- ⁵⁵ Diebolt, O.; Cruzeuil, C.; Müller, C.; Vogt, D. *Adv. Synth. Catal.* **2012**, *354*, 670-677.
- ⁵⁶ a) Ahmed, M.; Bronger, R. P. J.; Jackstell, R.; Kamer, P. C. J.; van Leeuwen, P. W. N. M.; Beller, M. *Chem. Eur. J.* **2006**, *12*, 8979-8988. b) Moballigh, A.; Majeed, S. A.; Ralf, J.; Matthias, B. *Angew. Chem. Int. Ed.* **2003**, *42*, 5615-5619.
- ⁵⁷ Blunt, J. W.; Copp, B. R.; Keyzers, R. A.; Munro, M. H. G.; Prinsep, M. R. *Natural Product Reports* **2012**, *29*, 144-222.
- ⁵⁸ Amines Market by Amine Type-Global Trends and Forecast to 2020, marketsandmarkets.com, **2015**, CH 2431
- ⁵⁹ Reppe, W. *Carbonylierung, I. Über die Umsetzung von Acetylen mit Kohlenoxyd und Verbindungen mit reaktionsfähigen Wasserstoffatomen Synthesen alfa,beta-ungersättigter Carbonsäuren und ihrer Derivate.* in *J. Liebigs Ann. Chem.*, Eds. WILEY-VCH, Vol. 582, Weinheim, Germany, **1953**, pp. 243-308.
- ⁶⁰ a) Wu, L.; Fleischer, I.; Jackstell, R.; Beller, M. *J. Am. Chem. Soc.* **2013**, *135*, 3989-3996. b) Srivastava, V. K.; Eilbracht, P. *Catal. Commun.* **2009**, *10*, 1791-1795.
- ⁶¹ *Rhodium Catalyzed Hydroformylation*, van Leeuwen, P. W. N. M.; Claver, C., Kluwer Academics Publishers, Dordrecht, The Netherlands, **2002**.
- ⁶² *Handbook of Homogeneous Hydrogenation, Vol. 1*, De Vries, J. G.; Elsevier, C. J., WILEY-VHC Verlag GmbH & Co., Weinheim, Germany, **2007**.
- ⁶³ a) Tin, S.; Fanjul, T.; Clarke, M. L. *Catal. Sci. Technol.* **2016**, *6*, 677-680. b) Fuentes, J. A.; Wawrzyniak, P.; Roff, G. J.; Buhl, M.; Clarke, M. L. *Catal. Sci. Technol.*

2011, *1*, 431-436. ^{c)} Marcazzan, P.; Abu-Gnim, C.; Seneviratne, K. N.; James, B. R. *Inorg. Chem.* **2004**, *43*, 4820-4824. ^{d)} Fabrello, A.; Bachelier, A.; Urrutigoity, M.; Kalck, P. *Coord. Chem. Rev.* **2010**, *254*, 273-287.

^{64 a)} Tararov, V. I.; Kadyrov, R.; Riermeier, T. H.; Holz, J.; Börner, A. *Tetrahedron Lett.* **2000**, *41*, 2351-2355. ^{b)} Hou, G.-H.; Xie, J.-H.; Wang, L.-X.; Zhou, Q.-L. *J. Am. Chem. Soc.* **2006**, *128*, 11774-11775.

⁶⁵ Xie, J.-H.; Zhu, S.-F.; Zhou, Q.-L. *Chem. Rev.* **2011**, *111*, 1713-1760.

⁶⁶ Crozet, D.; Gual, A.; McKay, D.; Dinoi, C.; Godard, C.; Urrutigoity, M.; Daran, J.-C.; Maron, L.; Claver, C.; Kalck, P. *Chem. Eur. J.* **2012**, *18*, 7128-7140.

⁶⁷ Kalck, P.; Urrutigoity, M. *Chem. Rev.* **2018**, *118*, 3833-3861.

⁶⁸ Chen, G.; Xia, H.; Cai, Y.; Ma, D.; Yuan, J.; Yuan, C. *Bioorg. Med. Chem. Lett.* **2011**, *21*, 234-239.

^{69 a)} Rische, T.; Müller, K.-S.; Eilbracht, P. *Tetrahedron* **1999**, *55*, 9801-9816. ^{b)} Schmidt, A.; Marchetti, M.; Eilbracht, P. *Tetrahedron* **2004**, *60*, 11487-11492.

⁷⁰ Oliveira, K. C. B.; Carvalho, S. N.; Duarte, M. F.; Gusevskaya, E. V.; dos Santos, E. N.; Karroumi, J. E.; Gouygou, M.; Urrutigoity, M. *Appl. Catal. A: Gen.* **2015**, *497*, 10-16.

⁷¹ Ahmed, M.; Seayad, A. M.; Jackstell, R.; Beller, M. *J. Am. Chem. Soc.* **2003**, *125*, 10311-10318.

⁷² Hamers, B.; Kosciusko-Morizet, E.; Müller, C.; Vogt, D. *ChemCatChem* **2009**, *1*, 103-106.

^{73 a)} Seayad, J.; Tillack, A.; Hartung, C. G.; Beller, M. *Adv. Synth. Catal.* **2002**, *344*, 795-813. ^{b)} Kumar, K.; Michalik, D.; Garcia Castro, I.; Tillack, A.; Zapf, A.; Arlt, M.; Heinrich, T.; Böttcher, H.; Beller, M. *Chem. Eur. J.* **2004**, *10*, 746-757.

⁷⁴ Routaboul, L.; Buch, C.; Klein, H.; Jackstell, R.; Beller, M. *Tetrahedron Lett.* **2005**, *46*, 7401-7405.

⁷⁵ Chen, C.; Dong, X.-Q.; Zhang, X. *Org. Chem. Front.* **2016**, *3*, 1359-1370.

^{76 a)} Briggs, J. R.; Klosin, J.; Whiteker, G. T. *Org. Lett.* **2005**, *7*, 4795-4798. ^{b)} Whiteker, G. T. *Top. Catal.* **2010**, *53*, 1025-1030.

⁷⁷ Li, S.; Huang, K.; Zhang, J.; Wu, W.; Zhang, X. *Org. Lett.* **2013**, *15*, 3078-3081.

⁷⁸ Yan, Y.; Zhang, X.; Zhang, X. *Adv. Synth. Catal.* **2007**, *349*, 1582-1586.

⁷⁹ a) Seayad, A. M.; Selvakumar, K.; Ahmed, M.; Beller, M. *Tetrahedron Lett.* **2003**, *44*, 1679-1683. b) Moballigh, A.; Cathleen, B.; Lucie, R.; Ralf, J.; Holger, K.; Anke, S.; Matthias, B. *Chem. Eur. J.* **2007**, *13*, 1594-1601.

⁸⁰ Dutta, B.; Schwarz, R.; Omar, S.; Natour, S.; Abu-Reziq, R. *Eur. J. Org. Chem.* **2015**, *2015*, 1961-1969.

⁸¹ a) Holger, K.; Ralf, J.; Klaus-Diether, W.; Cornelia, B.; Matthias, B. *Angew. Chem. Int. Ed.* **2001**, *40*, 3408-3411. b) Kranenburg, M.; van der Burgt, Y. E. M.; Kamer, P. C. J.; van Leeuwen, P. W. N. M.; Goubitz, K.; Fraanje, J. *Organometallics* **1995**, *14*, 3081-3089. c) Bronger, R. P. J.; Kamer, P. C. J.; van Leeuwen, P. W. N. M. *Organometallics* **2003**, *22*, 5358-5369.

⁸² Seayad, A.; Ahmed, M.; Klein, H.; Jackstell, R.; Gross, T.; Beller, M. *Science* **2002**, *297*, 1676-1678.

⁸³ Liu, G.; Huang, K.; Cao, B.; Chang, M.; Li, S.; Yu, S.; Zhou, L.; Wu, W.; Zhang, X. *Org. Lett.* **2012**, *14*, 102-105.

⁸⁴ Eilbracht, P.; Ludger Kranemann, C.; Bärfacker, L. *Eur. J. Org. Chem.* **1999**, *1999*, 1907-1914.

⁸⁵ a) Angelovski, G.; Keränen, M. D.; Eilbracht, P. *Tetrahedron: Asymmetry* **2005**, *16*, 1919-1926. b) Kranemann, Christian L.; Eilbracht, P. *Eur. J. Org. Chem.* **2000**, *2000*, 2367-2377.

⁸⁶ Billinghamurst, J. W. *Nature* **1960**, *188*, 972.

⁸⁷ Rische, T.; Eilbracht, P. *Tetrahedron* **1999**, *55*, 1915-1920.

⁸⁸ Li, S.; Huang, K.; Zhang, J.; Wu, W.; Zhang, X. *Org. Lett.* **2013**, *15*, 1036-1039.

⁸⁹ Kouznetsov, V.; Palma, A.; Ewert, C. *Curr. Org. Chem.* **2001**, *5*, 519-551.

⁹⁰ a) Vieira, T. O.; Alper, H. *Chem. Commun.* **2007**, 2710-2711. b) Vieira, T. O.; Alper, H. *Org. Lett.* **2008**, *10*, 485-487.

⁹¹ Armor, J. N. *Catal. Today* **2011**, *163*, 3-9.

⁹² Coperet, C.; Chabanas, M.; Petroff, S.-A. R.; Basset, J.-M. *Angew. Chem. Int. Ed.* **2003**, *42*, 156-181.

⁹³ Bailie, J. E.; Hutchings, G. J.; O'Leary, S. *Supported Catalysts A2 - Buschow, K.H. Jürgen in Encyclopedia of Materials: Science and Technology (Second Edition)*, Eds. Elsevier, Oxford, **2001**, pp. 8986-8990.

⁹⁴ a) *Catalyst separation, recovery and recycling; chemistry and process design*, Cole-Hamilton, D. J.; Tooze, R. P., Springer, Dordrecht, **2006**. b) *Recoverable and recyclable catalysts*, Bengalia, M., Wiley-Blackwell, Chichester, **2009**.

⁹⁵ a) McMorn, P.; Hutchings, G. J. *Chem. Soc. Rev.* **2004**, *33*, 108-122. b) Corma, A.; Garcia, H. *Top. Catal.* **2008**, *48*, 8-31.

⁹⁶ Song, C. E.; Lee, S. *Chem. Rev.* **2002**, *102*, 3495-3524.

⁹⁷ Dioos, B. M. L.; Vankelecom, I. F. J.; Jacobs, P. A. *Adv. Synth. Catal.* **2006**, *348*, 1413-1446.

⁹⁸ Corma, A.; Garcia, H. *Adv. Synth. Catal.* **2006**, *348*, 1391-1412.

⁹⁹ Hagiwara, H.; Ko, K. H.; Hoshi, T.; Suzuki, T. *Synlett* **2008**, *2008*, 611-613.

¹⁰⁰ Al-Hashimi, M.; Qazi, A.; Sullivan, A. C.; Wilson, J. R. H. *J. Mol. Catal. A: Chem.* **2007**, *278*, 160-164.

¹⁰¹ Fraile, J. M.; García, J. I.; Mayoral, J. A. *Chem. Rev.* **2009**, *109*, 360-417.

¹⁰² Gigante, B.; Corma, A.; García, H.; Sabater, M. J. *Catal. Lett.* **2000**, *68*, 113-119.

¹⁰³ Inagaki, S.; Guan, S.; Fukushima, Y.; Ohsuna, T.; Terasaki, O. *J. Am. Chem. Soc.* **1999**, *121*, 9611-9614.

¹⁰⁴ Britton, J.; Jamison, T. F. *Nature Protocols* **2017**, *12*, 2423-2446.

¹⁰⁵ Anastas, P. T.; Kirchoff, M. M. *Acc. Chem. Res.* **2002**, *35*, 686-694.

¹⁰⁶ Vile, G.; Perez-Ramirez, J. *Nanoscale* **2014**, *6*, 13476-13482.

¹⁰⁷ Noel, T.; Buchwald, S. L. *Chem. Soc. Rev.* **2011**, *40*, 5010-5029.

¹⁰⁸ Wiles, C.; Watts, P. *Green Chem.* **2012**, *14*, 38-54.

¹⁰⁹ Tsubogo, T.; Oyamada, H.; Kobayashi, S. *Nature* **2015**, *520*, 329.

¹¹⁰ a) Porta, R.; Benaglia, M.; Puglisi, A. *Org. Process Res. Dev.* **2016**, *20*, 2-25. ^{b)}
Shen, G.; Osako, T.; Nagaosa, M.; Uozumi, Y. *J. Org. Chem.* **2018**. ^{c)} Sarmiento, J. T.;
Suárez-Pantiga, S.; Olmos, A.; Varea, T.; Asensio, G. *ACS Catal.* **2017**, *7*, 7146-7155.

UNIVERSITAT ROVIRA I VIRGILI
RH-CATALYZED CARBOXYLATION OF DISUBSTITUTED OLEFINS: ASYMMETRIC CATALYSIS, CONTINUOUS
FLOW AND TANDEM HYDROAMINOMETHYLATION REACTION
Anton Cunillera Martin

Chapter 2

Objectives

UNIVERSITAT ROVIRA I VIRGILI
RH-CATALYZED CARBONYLATION OF DISUBSTITUTED OLEFINS: ASYMMETRIC CATALYSIS, CONTINUOUS
FLOW AND TANDEM HYDROAMINOMETHYLATION REACTION
Anton Cunillera Martin

The main objective of this Ph.D. thesis deals with the development of efficient catalysts for rhodium catalyzed carbonylation of disubstituted olefins. For this purpose, the present work includes two main strategies: the immobilization of highly efficient rhodium complexes bearing diphosphite ligands onto carbon supports for the application of the rhodium catalyzed hydroformylation of norbornene in flow mode, and the application of the tandem rhodium catalyzed hydroaminomethylation reaction for the production of amines.

The investigation detailed in [Chapter 3](#) aims at the application of heterogenized rhodium catalysts for the asymmetric hydroformylation of norbornene under batch and flow conditions. The specific objectives of this chapter are:

- To synthesize and characterize a set of new pyrene tagged chiral diphosphite ligands derived from glucose, and the preparation and characterization of the corresponding rhodium complexes.
- To immobilize the rhodium complexes onto carbon supports in order to prepare new heterogenized catalysts for the asymmetric hydroformylation of norbornene.
- To study the catalytic performance and recyclability of the heterogenized catalysts in the Rh-catalyzed asymmetric hydroformylation of norbornene in batch.
- To study the catalytic performance of the heterogenized catalysts in the Rh-catalyzed asymmetric hydroformylation of norbornene under flow conditions.

The work described in [Chapter 4](#) deals with the rhodium catalyzed asymmetric hydroaminomethylation of α -alkyl acrylates for the synthesis of chiral γ -aminobutyric esters. The specific objectives of this chapter are:

- To develop an efficient system for the synthesis of chiral γ -aminobutyric esters via rhodium catalyzed asymmetric hydroaminomethylation of α -alkyl acrylates using one single catalyst.
- To study the versatility of the system in the synthesis of γ -aminobutyric esters by testing various α -alkyl acrylates and amines.
- To study the reactivity of the system via High-Pressure NMR and Infrared spectroscopy.

The research described in [Chapter 5](#) deals with the rhodium catalyzed regioselective hydroaminomethylation of α -alkyl acrylates for the synthesis of $\beta^{2,2}$ -amino esters. The specific objectives of this chapter are:

- To perform a screening of phosphorus ligands in the rhodium catalyzed regioselective hydroaminomethylation of methyl methacrylate with morpholine to afford branched products with high efficiency.
- To develop an efficient system for the synthesis of $\beta^{2,2}$ -amino esters via rhodium catalyzed regioselective hydroaminomethylation of α -alkyl acrylates with secondary amines.
- To develop an efficient system for the synthesis of $\beta^{2,2}$ -amino esters via rhodium catalyzed regioselective hydroaminomethylation of α -alkyl acrylates with primary amines.
- To test various chiral phosphorus ligands in the rhodium catalyzed asymmetric hydroformylation of benzyl ethylacrylate to produce chiral products containing quaternary carbon centers.

Chapter 3

Immobilisation of chiral Rh catalysts for the AHF of norbornene in flow

UNIVERSITAT ROVIRA I VIRGILI
RH-CATALYZED CARBONYLATION OF DISUBSTITUTED OLEFINS: ASYMMETRIC CATALYSIS, CONTINUOUS
FLOW AND TANDEM HYDROAMINOMETHYLATION REACTION
Anton Cunillera Martin

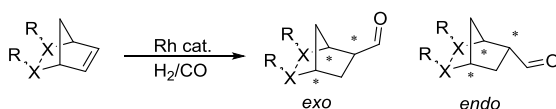
3.1. Introduction

3.1.1. Rhodium catalyzed AHF of [2.2.1]-bicyclic olefins

As mentioned in chapter 1, the rhodium catalyzed asymmetric hydroformylation of olefins constitutes an efficient strategy to access enantioenriched aldehydes. The selective hydroformylation of [2.2.1]-bicyclic olefins is a challenging area due to the following features (Scheme 3.1):

1. Three chiral centers are generated upon desymmetrization of the olefin through one C-C bond favored.¹
2. The symmetry of the molecule prevents regio-selectivity issues; nonetheless, *endo*- and *exo*-selectivities are important.² Although in general *exo*-selectivity is preferred.
3. Derivatives containing functional groups located opposite to the C=C bond might lead to interesting building blocks.³

To the best of our knowledge, only a few successful reports have been described success on the rhodium catalyzed asymmetric hydroformylation of [2.2.1]-bicyclic olefins.⁴



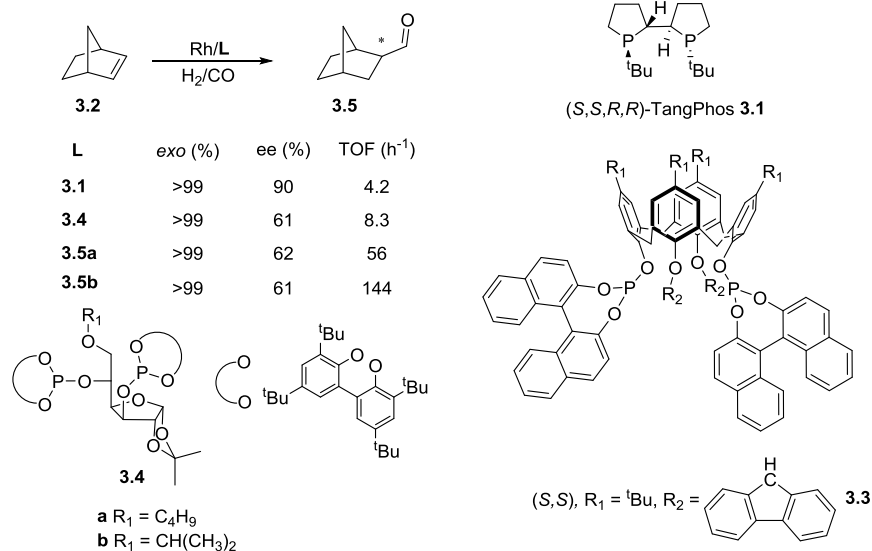
Scheme 3.1: Rh-catalyzed asymmetric hydroformylation of [2.2.1]-bicyclic olefins.

Using the C₂-symmetric diphosphine TangPhos ligand **3.1**, Bunel *et al.* obtained exclusively the *exo*-product and ee up to 92% in the asymmetric hydroformylation of norbornene **3.2** (Scheme 3.2).^{4a} However, long reaction times were required.

In this context, various groups reported the use of diphosphite ligands in the asymmetric hydroformylation of [2.2.1]-bicyclic olefins.^{2a-4b} Indeed, since they possess a strong π -acceptor character, they provided much higher activities with

full stereoselectivity towards the *exo*-product, and good enantioselectivities. In the specific case of norbornene, the hemi-spherical diphosphite ligands **3.3** were applied with good activity, full *exo*-selectivity, and good *ee*'s (Scheme 3.2).

Recently, our group investigated the asymmetric hydroformylation of norbornene using the C_1 -symmetric diphosphite ligand **3.4** derived from *D*-glucofuranose with outstanding activity, high *exo*-selectivity, and good enantioselectivities (Scheme 3.2).⁵



Scheme 3.2: Rh-catalyzed asymmetric hydroformylation of norbornene using ligands **3.1**, **3.3**, and **3.4**.

3.1.2. Homogeneous catalyst immobilization via π - π interactions

The carbon nanotubes (CNTs) and other graphitic materials are of interest as supports to immobilize homogeneous catalysts via π - π interactions since they provide a stable anchoring for metal complexes (Figure 3.1).⁶

π - π forces are non-covalent interactions that take place between the π electron densities of stacked aromatic systems.⁷ Benzene immediately comes to mind as model for aromatic interactions, nevertheless it was demonstrated that larger

aromatic systems, such as pyrene and coronene, form stronger interactions with CNTs through π - π stacking interactions.⁸

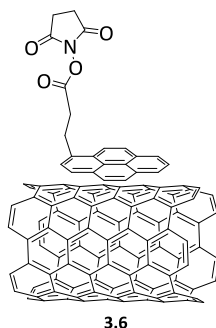
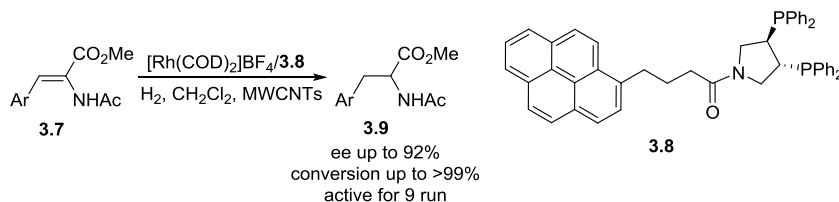


Figure 3.1: Functionalization of CNT via non-covalent interactions (π - π interactions).

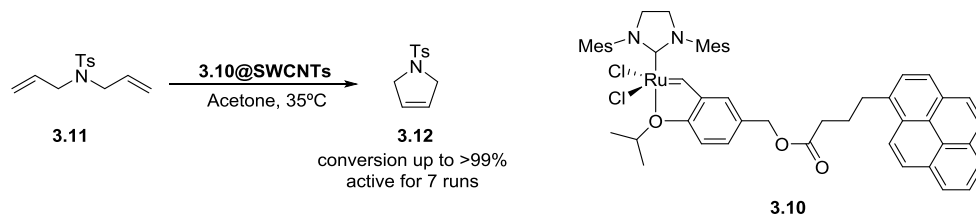
Indeed, a study of π -interactions between organic molecules, such as benzene, 2,3-dichloro-5,6-dicyano-1,4-benzoquinone (DDQ), azulene, and pyrene with CNTs demonstrated that the stacking interactions between the pyrene (9.69 kcal/mol) moiety is *ca.* twice stronger than with benzene (4.61 kcal/mol).⁹ These reports therefore indicated that in order to obtain a stable heterogenized catalyst via such interactions, the presence of either a pyrene or coronene moiety within the structure of the catalyst/ligand is required.

Within the last years, several groups reported the immobilization of homogeneous catalysts via π - π interactions onto different carbon materials. Qi-Lin and co-workers reported the asymmetric hydrogenation of olefin **3.7** using the pyrene tagged diphosphine ligand **3.8** (Scheme 3.3).¹⁰ The pyrene moiety was easily introduced in the structure of the ligand and the corresponding complex, which were subsequently immobilized onto multi-walled carbon nanotubes (MWCNTs). In this reaction, the immobilized system provided the same enantioselectivities than those obtained with the homogeneous system. Moreover, the catalyst was recycled up to 9 times, although it was necessary to increase the reaction time from the third run due to a loss of activity, but the enantioselectivity remained unaffected.



Scheme 3.3: Rh-catalyzed asymmetric hydrogenation of olefins **3.7** using pyrene tagged chiral diphosphine **3.8** for 9 runs.

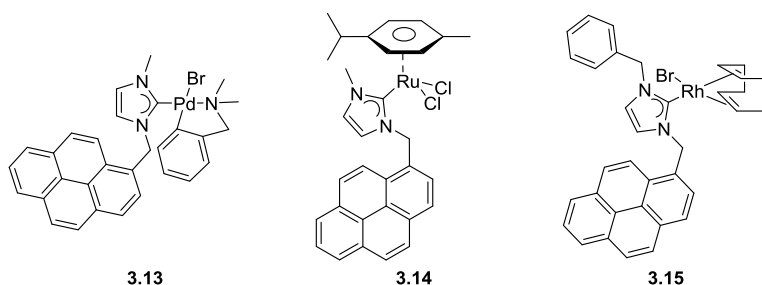
Later, Wang and co-workers reported the immobilization of the ruthenium catalyst **3.10** for alkene metathesis onto single-walled carbon nanotubes (SWCNTs) via the introduction of a pyrene moiety in the backbone of the carbene ligand (Scheme 3.4).¹¹ The catalyst was recycled up to 7 cycles in the metathesis of various alkenes, although in this case, the increase of the reaction time was necessary after the third cycle in order to maintain similar conversions. Interestingly, the effect of the solvent was studied for the immobilization of the complexes, and it was concluded that polar solvents such as acetone or ethyl acetate are the most efficient to maintain the catalyst attached to the support, while non polar solvents such as benzene or toluene immediately detached the catalyst from the support.



Scheme 3.4: Ru-catalyzed ring closing metathesis using complex **3.10@SWCNTs** for 7 runs.

Ouali et. al. modified a palladium dendritic catalyst for Suzuki coupling with a pyrene moiety to immobilize it onto the surface of carbon coated magnetic cobalt nanoparticles.¹² This design did not only allow recycling the catalyst up to 10 times, but also facilitate the recovery of the catalyst, since cobalt nanoparticles are magnetic and can be easily trapped at the bottom of the flask using a magnet.

More recently, Peris and co-workers immobilized the carbene complexes **3.13-3.15** onto reduced graphene oxide as an alternative to carbon nanotubes (Scheme 3.5).¹³ The modified N-heterocyclic carbenes containing a pyrene moiety were easily synthesized, and coordinated to the corresponding metals for alkene and ketone hydrogenation, nitro reduction into amines, dehydrofluorination, alkyne hydrosilylation and 1,4-addition to α,β -unsaturated ketones with high activity and selectivity for the target molecule.

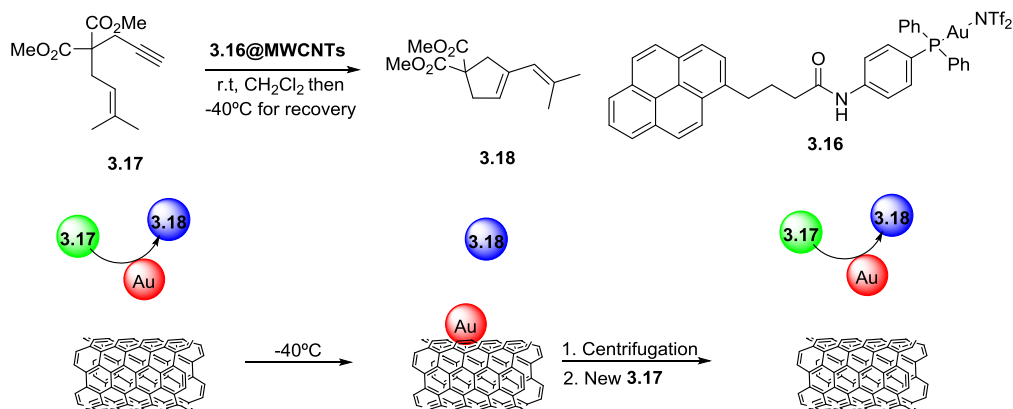


Scheme 3.5: Pyrene tagged carbene complexes reported by Peris and co-workers.

Despite the use of more apolar solvents such as toluene and the application of high temperatures (up to 100°C) the catalysts could be recycled up to 10 times without loss of either activity or selectivity. Along their studies, it was demonstrated that when the complexes contained two pyrene moieties instead of one, the catalyst leaching was reduced.

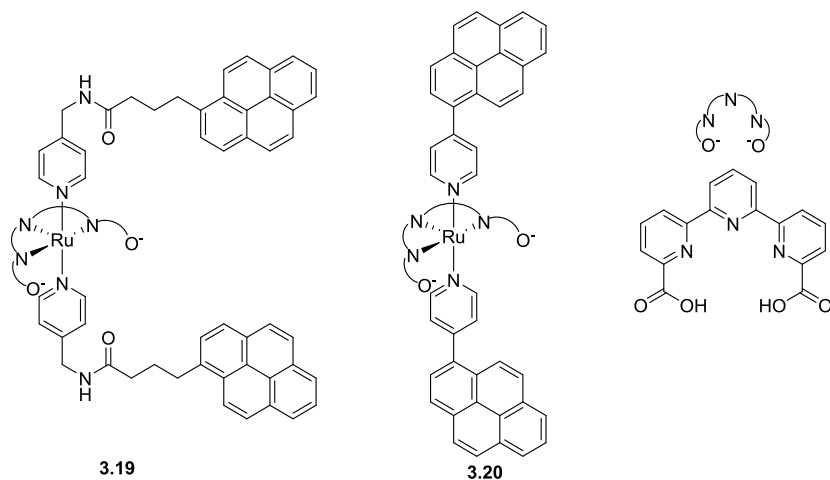
Hermans and co-workers reported a pyrene tagged gold catalyst **3.16** for enyne-cyclization (Scheme 3.6).¹⁴ In this work, they demonstrated the so called “boomerang effect”, which consists in the detachment of the catalyst from the support during the catalysis using the appropriate solvent and temperature; at the end of the reaction the catalyst was again immobilized onto the carbon material by cooling the reaction mixture to -40°C (Scheme 3.6). Following this approach, they were able to perform the reaction for 4 runs with the same conversion and selectivity.

Chapter 3



Scheme 3.6: Top: Gold pyrene catalyst **3.16** developed by Hermans and co-workers for enyne **3.17** cyclization. Bottom: Boomerang effect.

Sun and co-workers reported the pyrene modified ruthenium catalyst **3.19** immobilized onto MWCNTs for water splitting.¹⁵ Following the same strategy, Llobet et. al. reported the ruthenium catalyst **3.20** immobilized onto glassy carbon for water oxidation (Scheme 3.7).¹⁶ The catalyst provided an outstanding TON (up to 1 million).



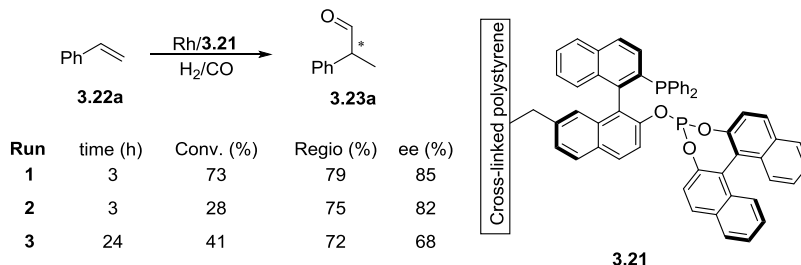
Scheme 3.7: Pyrene tagged ruthenium catalyst **3.19** and **3.20** for water oxidation.

3.1.3. Immobilized AHF catalysts in flow mode

Despite the interest of hydroformylation, safety issues due to the use of explosive hydrogen and toxic carbon monoxide makes complicated the scale up and industrial application of hydroformylation. Moreover, the use of rhodium as precious metal makes necessary the recovery of such expensive metal. The implementation of rhodium catalyzed hydroformylation in flow processes is therefore an attractive strategy. In this context, rhodium catalyzed hydroformylation has recently been performed under flow conditions using different covalent immobilization strategies for the production of nonanal.¹⁷

In the case of asymmetric hydroformylation, only a few examples were reported to date. To the best of our knowledge only two types of ligands have been immobilized onto solid supports for Rh-catalyzed asymmetric hydroformylation so far. The first work was reported by Nozaki and co-workers, who described the immobilization of the BINAPHOS ligand onto a cross-linked polymer matrix.¹⁸ To do so, the BINAPHOS ligand had to be modified via the introduction of a vinyl moiety in the naphthalenic backbone. This ligand was submitted to radical polymerization with a commercially available mixture of divinylbenzene that contains 1,2-, 1,3- and 1,4- divinylbenzene to finally afford the PS-BINAPHOS **3.21** ligand in a mixture 3:97 (BINAPHOS : divinylbenzenes). As reported by the authors, the well distributed catalyst over the polymeric structure avoided the formation of dimeric species, which would be inactive in catalysis. Interestingly, when the immobilized catalyst was applied in the asymmetric hydroformylation of different alkenes such as styrene, vinyl acetate, (Z)-2-butene, and 3,3,3-trifluoropropene, the results obtained were similar in terms of activity and selectivity to those afforded in the homogeneous version.^{18c} However, when recycling experiments were carried out in batch mode for the asymmetric hydroformylation of styrene, the activity dropped in the second run, and it was necessary to increase the time in the third

run in order to maintain the activity (Scheme 3.8). The loss of activity was attributed to the polymer-crushing during the reaction due to the mechanical stirring.



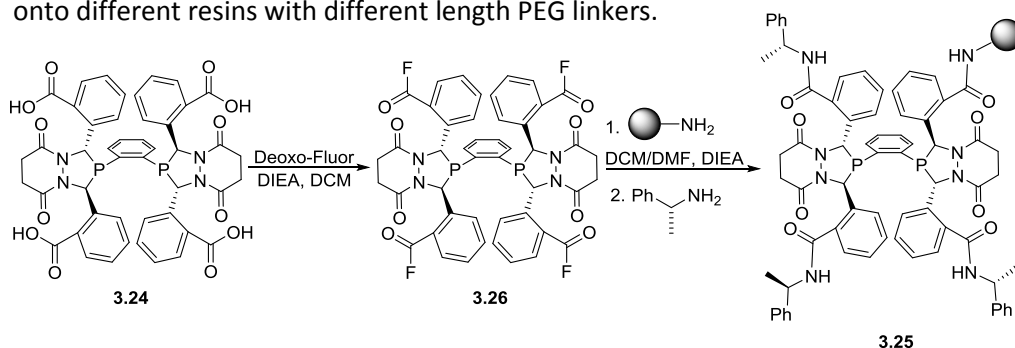
Scheme 3.8: Rh-catalyzed asymmetric hydroformylation of styrene **3.22a** recycling in batch mode using **3.21** immobilized ligand.

Later, the same group reported the asymmetric hydroformylation of alkenes in flow mode using the same ligand **3.21** and supercritical CO₂ as solvent for the reaction.¹⁹ In order to carry out the catalysis, different injections of styrene solution mixed with the syngas were passed through the catalyst bed. With this system in hands, it was possible to carry out up to 7 cycles in flow without significant loss of either activity (up to 90%) or selectivity. However, high pressures (120 atm) were necessary in order to maintain the activity around 90%. If the pressure was reduced to 88 atm, then the activity dramatically dropped to less than 20 %. On the other hand, the same system was used to hydroformylate various alkenes in different injections (cycles), and in all the cases good to excellent selectivities were afforded. It was possible to use the same catalyst to hydroformylate up to 6 different alkenes and in between, styrene was used in order to check if the activity was maintained.

More recently, Landis and co-workers immobilized the bisdiazophospholane (BDP) ligand **3.24** onto different amine resins.²⁰ To do so, extra synthetic steps were necessary to functionalize the homogeneous ligand with tetraacyl fluoride groups, which was reacted with amine groups present on the resins to attach the ligand.

Immobilisation of chiral Rh catalysts for the AHF of norbornene in flow

Later, the unattached acyl fluoride groups were treated with (*S*)-methylbenzylamine to generate tetracarboxamides. Finally, the synthesis of ligand **3.25** was completed by capping with the resin-based primary amine sites with acetic anhydride that did not react with the tetraacyl fluoride BDP **3.26** (Scheme 3.9), since free amine groups could serve as coordination points for $[\text{Rh}(\text{acac})(\text{CO})_2]$, and their presence can induce the racemization of the chiral aldehydes. Furthermore, Landis and co-workers immobilized the BDP ligand **3.24** onto different resins with different length PEG linkers.



Scheme 3.9: Synthesis of BPD immobilized ligand **3.25** onto resins.

The immobilized ligands **3.25** were tested in the Rh-catalyzed asymmetric hydroformylation of styrene and vinyl acetate. They observed that the separation between the support and the metal center is important since the longer the separation, the better the selectivities afforded. Nonetheless, lower regioselectivities and enantioselectivities were obtained in all cases when compared with the homogeneous catalyst. The ligand **3.25** was applied in batch mode and up to 9 cycles were performed in the Rh-catalyzed asymmetric hydroformylation of styrene with some variations in pressure in cycles 5, 7 and 9 that demonstrated a negative effect on the enantioselectivity and positive effect on the b:l ratio using higher pressures. Catalyst leaching was measured after each cycle, and showed that the largest loss of catalyst takes place in the first cycles.

Moreover, the effect of the solvent was tested in cycle 7, in which toluene was substituted by THF and provided a higher metal loss.

Finally, a racemic version of the immobilized **3.25** was applied in a plug flow reactor to conduct the hydroformylation of vinyl acetate. The system was active for 6 runs (*ca.* 39 hours) with good regioselectivities for the branched product and full conversion. The largest loss of catalyst was in the first cycle (up to 6,1%) and later remain at 0.5 % per cycle.

3.2. Objectives of this chapter

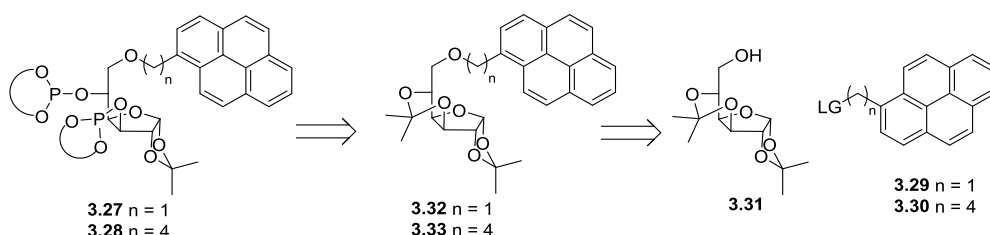
In view of the results described, the immobilization of chiral rhodium complexes bearing C₁-diphosphite ligands derived from sugars could provide an interesting heterogenized system for the asymmetric hydroformylation of norbornene in flow.

The specific objectives of this chapter are:

- The synthesis and characterization of pyrene tagged C₁-diphosphite ligands with spacer of different length between the sugar backbone and the pyrene.
- The synthesis and characterization of the corresponding Rh (I) complexes.
- The application of the pyrene tagged rhodium complexes in the AHF of norbornene.
- The spectroscopic study of [RhH(CO)₂(L)] (L = diphosphite pyrene tagged ligand) via HP-NMR spectroscopy.
- The immobilisation of the Rh (I) complexes onto carbon supports.
- The application of the heterogenized catalysts in the AHF of norbornene in batch and flow modes.

3.3. Results and discussion

After retrosynthetic analysis of the pyrene tagged chiral diphosphite ligands **3.27** and **3.28**, the introduction of the pyrene moiety into the sugar backbone was proposed via condensation of pyrene containing groups **3.29** and **3.30**, which contain a good leaving group (LG), with the alcohol **3.31** to afford **3.32** and **3.33**. The following steps for the synthesis of ligands **3.27** and **3.28** proceeded as reported in the literature (Scheme 3.10).²¹

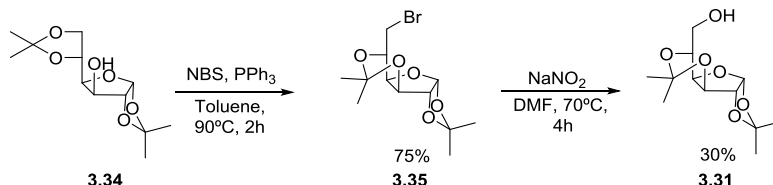


Scheme 3.10: Retrosynthesis for the introduction of the pyrene moiety into the sugar structure.

The alcohol **3.31** can be prepared from commercially available D-glucofuranose in two steps.²²

3.3.1. Synthesis of pyrene tagged chiral diphosphites

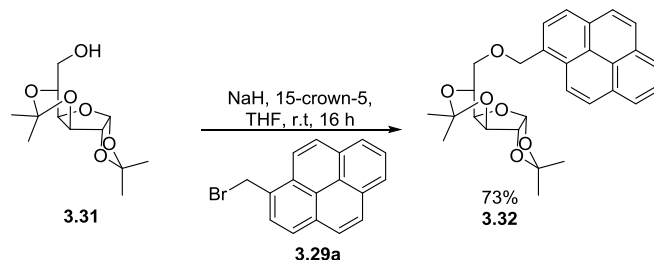
The first step in the synthesis of the pyrene tagged chiral diphosphites ligands involves the reaction of D-glucofuranose **3.34** with N-bromosuccinimide (NBS) and triphenylphosphine.²² The reaction proceeds smoothly and the corresponding bromo derivative **3.35** was obtained in 75 % yield. Subsequent treatment of **3.35** with sodium nitrite afforded the alcohol **3.31** in 30% yield (Scheme 3.11).



Scheme 3.11: Synthesis of alcohol **3.31**.

Chapter 3

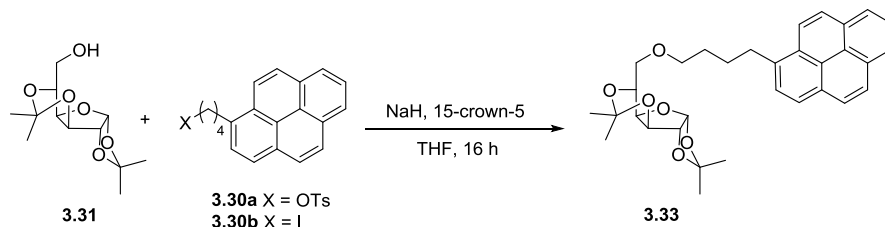
In the next step, **3.31** was deprotonated using sodium hydride as a base and reacted with the commercially available 1-(bromomethyl)pyrene **3.29a** to afford **3.32** in 73% yield (Scheme 3.12).



Scheme 3.12: Synthesis of **3.32**.

In order to increase the length between the sugar backbone and the pyrene moiety, the synthesis of **3.33** was attempted. Different electrophiles bearing tosyl **3.30a** and iodo **3.30b** leaving groups were tested as electrophiles. However, even when higher temperatures were applied, the desired product **3.33** was not detected (Table 3.1).

Table 3.1: Attempted alkylation of **3.31** with pyrene derivatives **3.30a** and **3.30b**.

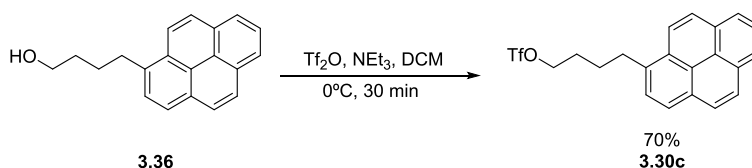


Entry	X	3.30 (equiv.)	T(°C)	Time	3.33 ^a
1	OTs	2	r.t	16h	n.d.
2	OTs	2	60	48h	n.d.
3	I	2	r.t	16h	n.d.
4	I	2	60	48	n.d.

^aYield was evaluated by preparative TLC, and by ¹H NMR spectroscopy.

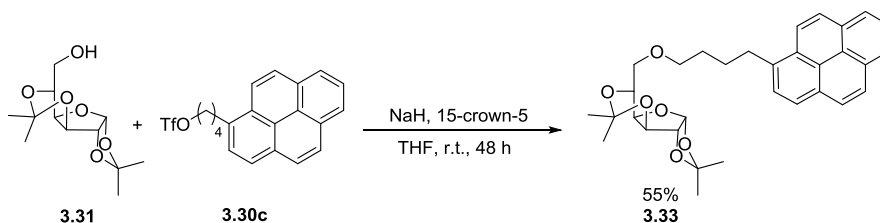
The reaction was followed by thin layer chromatography (TLC) and ^1H NMR spectroscopy, however in all the cases only signals corresponding to the starting material were observed (entry 1-4, Table 3.1). When **3.30b** was used at 60°C (entry 4, Table 3.1), decomposition of the pyrene derivative was observed, but **3.33** was not detected.

In view of these complications, the synthesis of a more electrophilic pyrene derivative **3.30c** bearing a triflate group was performed by reaction of commercially available pyrenebutanol **3.36**, triflic anhydride and triethylamine at room temperature in dichloromethane (Scheme 3.13).



Scheme 3.13: Synthesis of **3.30c**.

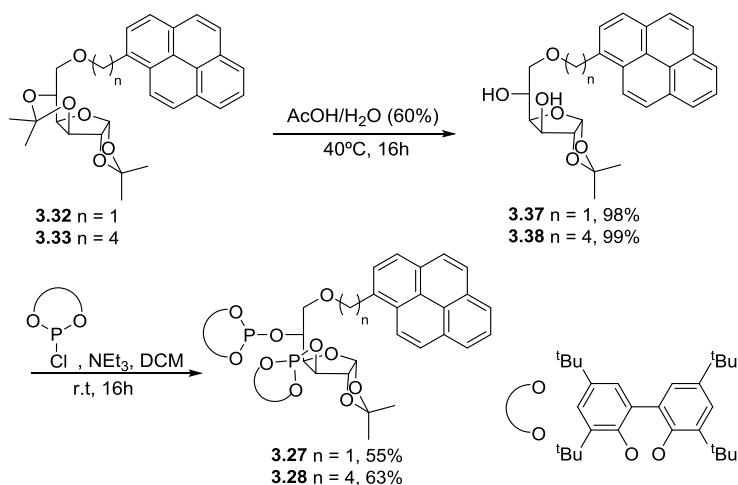
Alkylation of alcohol **3.31** with triflate **3.30c** was performed under the same conditions than for the synthesis of **3.32**. Under these conditions, the desired **3.33** was afforded in good yield (55%) (Scheme 3.14).



Scheme 3.14: Synthesis of **3.33**.

The next step was the deprotection of the 3,5-acetal using acetic acid (AcOH) in water (60%) which provided diols **3.37** and **3.38** in excellent yields (up to 99%) (Scheme 3.15). These diols reacted with the freshly synthesized phosphochloridites with triethylamine to give the diphosphites **3.27** and **3.28** in

good yields (55-63%) (Scheme 3.15). The new compounds bearing pyrene moiety were fully characterized by NMR spectroscopy and mass-spectrometry (MS). Both ligands presented signals at 144-146 ppm as two doublets (*ca.* $J_{P,P} = 32-35$ Hz) by ^{31}P NMR spectroscopy due to through space coupling between the two non-equivalent phosphorus.



Scheme 3.15: Synthesis of diphosphites **3.27** and **3.28**.

In conclusion, the pyrene tagged diphosphite ligands **3.27** and **3.28** were easily synthesized in a few synthetic steps. The synthesis of the ligand **3.27** did not require any synthetic extra effort compared to the analogous sugar derivative ligands. In contrast, the synthesis of ligand **3.28** required the synthesis of triflate derivative **3.30c** to introduce the pyrene moiety.

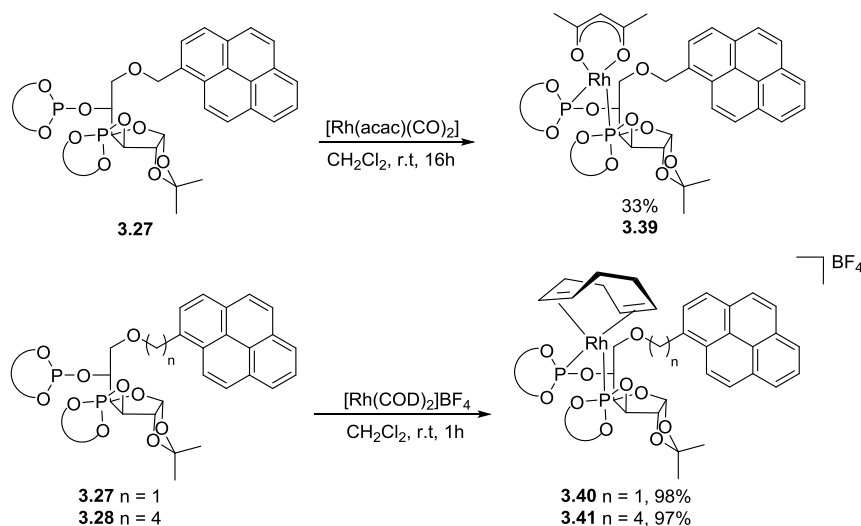
3.3.2. Synthesis of rhodium complexes bearing pyrene tagged diphosphite ligands

In the previous reports on the immobilization of chiral ligands for asymmetric hydroformylation, the ligands were first immobilized onto the structure of the support, and subsequently corresponding complexes by adding $[\text{Rh}(\text{acac})(\text{CO})_2]$.^{18c-}

²⁰ Using this strategy, issues related to the presence of unreacted metal precursors

Immobilisation of chiral Rh catalysts for the AHF of norbornene in flow

and/or ligand can be predicted. Therefore, in this study, the coordination of the ligand at the rhodium center was completed prior to the immobilization. The rhodium complexes were prepared by mixing ligand **3.27** and **3.28** with neutral $[\text{Rh}(\text{acac})(\text{CO})_2]$ and cationic $[\text{Rh}(\text{COD})_2]\text{BF}_4$ precursors (Scheme 3.16). The neutral complex $[\text{Rh}(\text{acac})(\mathbf{3.27})]$ **3.39** was afforded in moderate yield (33%), since it was necessary to purify the complex by column chromatography.



Scheme 3.16: Synthesis of rhodium complexes **3.39**, **3.40** and **3.41**.

In contrast, the cationic complexes $[\text{Rh}(\text{COD})(\mathbf{3.27})]\text{BF}_4$ **3.40** and $[\text{Rh}(\text{COD})(\mathbf{3.28})]\text{BF}_4$ **3.41** were readily prepared in excellent yields (up to 98%) since their purification was carried out by precipitation with pentane. All complexes were characterized by NMR spectroscopy and MS.

When the complex **3.40** was analyzed in details by ^1H NMR, signals from the pyrene moiety, coordinated cyclooctadiene (COD) and sugar backbone signals could be observed (Figure 3.2). In the $^{31}\text{P}\{^1\text{H}\}$ NMR spectra, the phosphorus were observed as second order signals at *ca.* 123 ppm (Figure 3.3).

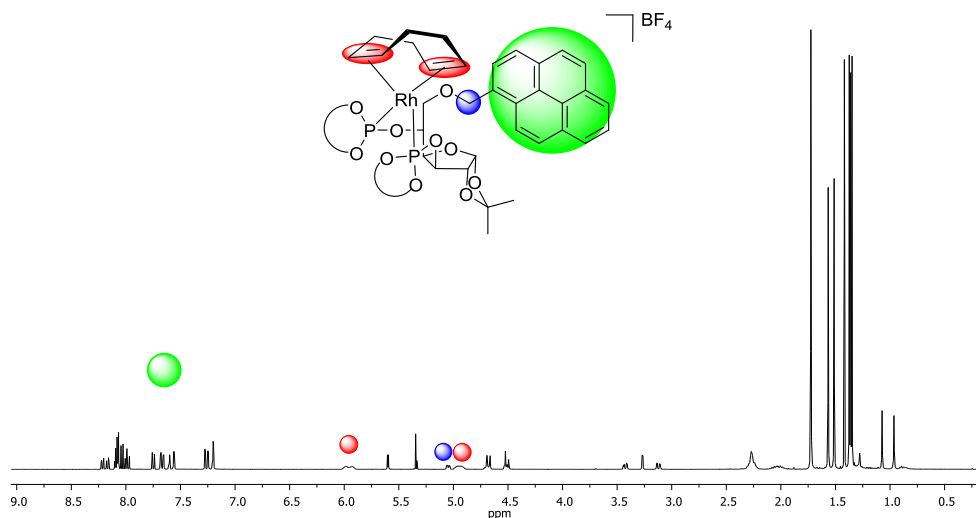


Figure 3.2: ^1H NMR spectra from complex **3.40**. Signals from cyclooctadiene, benzylic proton, and pyrene emphasized.

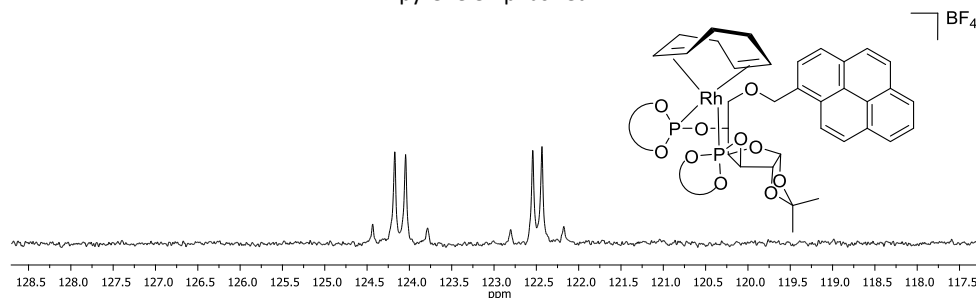


Figure 3.3: $^{31}\text{P}\{^1\text{H}\}$ NMR spectra from complex **3.40**.

3.3.3. Asymmetric hydroformylation of norbornene using the pyrene tagged ligands

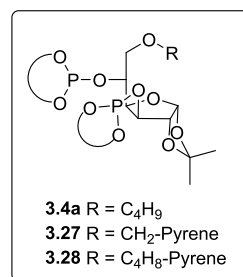
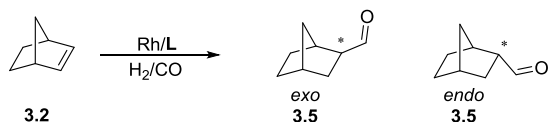
The new pyrene tagged ligands were tested in the asymmetric hydroformylation of norbornene to verify any possible effect that could be induced by the introduction of the pyrene tag (Table 3.2).

First, the reaction was performed using the $[\text{Rh}(\text{acac})(\text{CO})_2]$ and $[\text{Rh}(\text{COD})_2]\text{BF}_4$ rhodium precursors under catalytic conditions; however no conversion of norbornene was observed (entry 1-2, Table 3.2). In contrast, when the system

Immobilisation of chiral Rh catalysts for the AHF of norbornene in flow

[Rh(acac)(CO)₂]/**3.27** and [Rh(acac)(CO)₂]/**3.28** were applied, 15% conversion, full *exo*-selectivity and 62% ee were afforded (entry 3-4, Table 3.2). The ligand **3.5a** bearing a butyl group instead of a pyrene was applied under the same reaction conditions, and provided similar results compared to diphosphites **3.27** and **3.28** (entry 5, Table 3.2).⁵

Table 3.2: Rh-catalyzed asymmetric hydroformylation of **3.2** using ligand **3.4a**, pyrene tagged ligands **3.27**, **3.28** and complexes **3.40** and **3.41**.



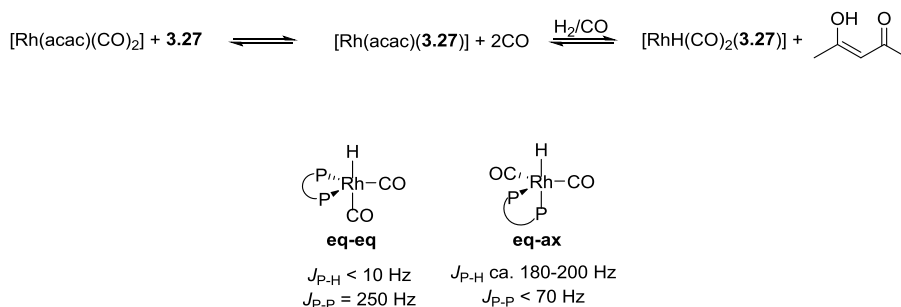
Entry ^a	Catalyst	Yield (%) ^b	<i>exo</i> (%) ^b	ee (%) ^c	TOF (h ⁻¹)
1	[Rh(acac)(CO) ₂]	-	-	-	-
2	[Rh(COD) ₂]BF ₄	-	-	-	-
3	[Rh(acac)(CO) ₂]/ 3.27	15	>99	62	60
4	[Rh(acac)(CO) ₂]/ 3.28	15	>99	62	60
5	[Rh(acac)(CO) ₂]/ 3.4a	15	>99	62	56
6	[Rh(COD)(3.27)]BF ₄ 3.40	24	>99	63	96
7	[Rh(COD)(3.28)]BF ₄ 3.41	25	>99	63	96

^aReaction conditions: Rh = 0.012 mmol, Rh/L = 1:1.1, Substrate/Rh = 1600:1, P = 18 bar (H₂/CO, 1: 1), solvent = 5 mL toluene, T = 20°C, t = 4h. ^bYield and *exo*-selectivity determined by ¹H NMR spectroscopy and GC-MS using naphthalene as internal standard. Enantioselectivity of *exo*-product measured by chiral GC analysis after reduction into the alcohol.

Finally, the use of the rhodium complexes **3.40** and **3.41** provided higher conversion (up to 25%), full stereoselectivity towards the *exo*-product, and the same enantioselectivity (entry 5-6, Table 3.2). Thus, it was concluded that the pyrene moiety does not affect the catalytic performance of the Rh catalysts in this reaction.

3.3.4. HP-NMR study of $[\text{RhH}(\text{CO})_2(\mathbf{3.27})]$

In order to gain information into the coordination mode of the new chiral diphosphites at rhodium under H_2/CO atmosphere, HP NMR experiments were performed using diphosphite **3.27** (Scheme 3.17).



Scheme 3.17: General mechanism for the formation of $[\text{RhH}(\text{CO})_2(\mathbf{3.27})]$ species.

The ligand **3.27** (1 equiv.) was added to a solution of $[\text{Rh}(\text{acac})(\text{CO})_2]$ (1 equiv.) in toluene- d_8 at room temperature and left stirring for 10 minutes. Upon the addition of the ligand, a rapid change in the color of the solution was observed from green to yellow. Next, the solution was introduced in a 5 mm HP-NMR tube, pressurized at 18 bar (H_2/CO , 1:1), heated at 45°C and left shaking for 16 hours. Then, the HP-NMR tube was placed into the spectrometer and the ^1H and $^{31}\text{P}\{^1\text{H}\}$ NMR spectra were recorded at room temperature (Figure 3.4).

In the ^1H NMR spectrum at 25°C , a broad doublet corresponding to the hydride signal of the $[\text{RhH}(\text{CO})_2(\mathbf{3.27})]$ species was detected at -9.85 ppm ($J_{\text{Rh,H}} = 1.3 \text{ Hz}$). Such small coupling constant was attributed to an **eq-eq** coordination mode.²³ In the $^{31}\text{P}\{^1\text{H}\}$ NMR spectrum, a broad signal at 151 ppm was observed. The detection of such broad signal suggested that a fluxional process was taking place at room temperature. Thus, ^1H and $^{31}\text{P}\{^1\text{H}\}$ NMR spectra were recorded at lower temperatures (Figure 3.4). When temperature reached -50°C , the broad signal observed at 151 ppm turned into two 2nd order signals that were assigned to two inequivalent phosphorus atoms bonded to rhodium.

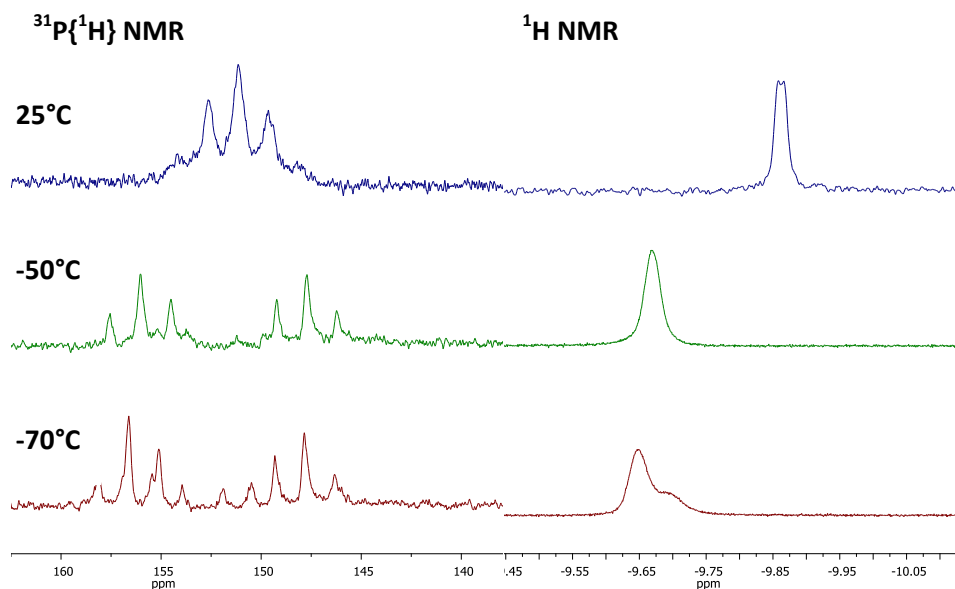
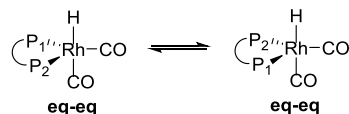


Figure 3.4: ^1H and $^{31}\text{P}\{^1\text{H}\}$ NMR spectra of complex $[\text{RhH}(\text{CO})_2(\mathbf{3.27})]$ in toluene- d_8 recorded at variable temperature.

The coordination mode of analogous ligands that contain alkyl groups was previously reported under the same conditions and provided similar results.²¹ Simulations of the $^{31}\text{P}\{^1\text{H}\}$ NMR spectra using *gNMR V4.0* software confirmed an exchange of the inequivalent phosphorus atoms in the **eq-eq** mode was taking place (Scheme 3.18).



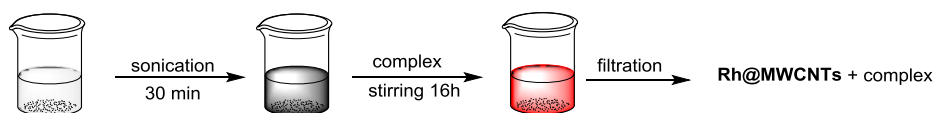
Scheme 3.18: Equilibrium between species bearing C_1 -symmetric diphosphite ligands.

Finally, ^1H - ^1H Nuclear Overhauser Effect Spectroscopy (NOESY) experiment was performed to detect any through space interaction between the hydride and the pyrene moiety. However, only interactions with the sugar backbone were observed. With these results in hand, it was concluded that ligand **3.27** coordinates in an **eq-eq** coordination mode with an exchange between

phosphorus atoms, similarly to ligands **3.4**. On the other hand, NOESY experiments confirmed that the pyrene moiety is far from the Rh-H center. Therefore, the pyrene moiety has no effect in the coordination of the ligand in the studied $[\text{RhH}(\text{CO})_2(\mathbf{3.27})]$ species, which is in agreement with the catalytic results that showed that the stereo- and enantioselectivity remained unaffected.

3.3.5. Immobilization of complexes **3.40** and **3.41** onto carbon materials

To complete the synthesis of the corresponding heterogenized catalysts, the rhodium complexes **3.40**, and **3.41** were reacted with several carbon supports following the procedure described in Scheme 3.19.



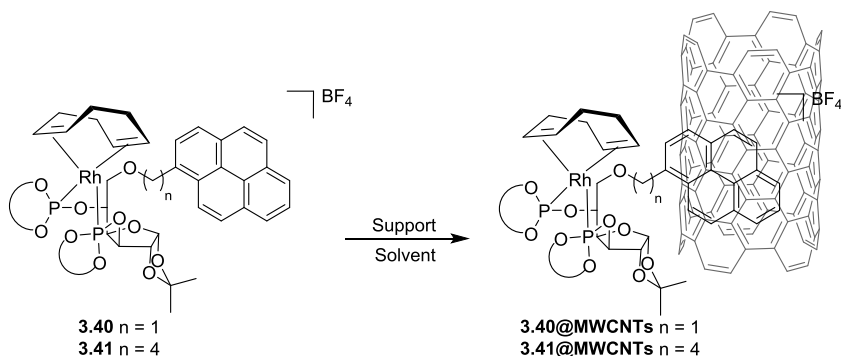
Scheme 3.19: Procedure for the immobilization process of pyrene tagged complexes onto MWCNTs.

The optimization of the conditions for the immobilization was carried out using MWCNTs as carbon support (Table 3.3). The solvents used for the immobilization were dichloromethane and ethyl acetate (EtOAc), since polar solvents favor the π - π interactions between the pyrene and the support.¹¹ The procedure for the immobilization was the following: first, the carbon support was dispersed by sonication in the solvent of choice for 30 minutes. Then, the complex was added as a solid to the solution, and the mixture was left stirring at room temperature for 16 hours. It is worth mentioning that the amount of solvent, and therefore the concentration, is important. When MWCNTs are dispersed into the solvent, a sufficient amount of solvent is necessary to avoid the formation of a muddy solution. Finally, the heterogenized catalyst is filtrated and washed three times with the solvent used for the immobilization. The amount of complex immobilized onto the MWCNTs was analyzed by Induced Coupled Plasma (ICP) of the solid after

Immobilisation of chiral Rh catalysts for the AHF of norbornene in flow

filtration. Interestingly, the rhodium complex that is not immobilized can be easily recovered after the filtration and subsequently reused.

Table 3.3: Optimization of reaction conditions for the immobilization of rhodium complexes **3.40** and **3.41** onto carbon supports.



Entry	Complex	Support	Support/Complex ^a	Solvent	Rh (wt %) ^b
1	3.40	MWCNTs	10	CH ₂ Cl ₂	0.17
2	3.41	MWCNTs	10	CH ₂ Cl ₂	0.15
3	3.40	MWCNTs	5	CH ₂ Cl ₂	0.19
4	3.40	MWCNTs	10	EtOAc	0.25
5	3.40	MWCNTs	3	EtOAc	0.45
6	3.41	MWCNTs	3	EtOAc	0.41
7	3.41	rGO	3	EtOAc	0.48
8	3.41	CBs	3	EtOAc	0.56
9	3.41	N-CNTs	3	EtOAc	1.13
10	3.41	S-CNTs	3	EtOAc	2.21

^a Support/Complex ratio = weight Support/ weight Complex. ^b Determined by ICP analysis of the solid after filtration.

A ratio 10:1 of MWCNTs/complex (wt/wt) was first tested to immobilize complexes **3.40** and **3.41**, with dichloromethane as solvent (entries 1-2, Table 3.3). Under these conditions, a similar amount of Rh was measured for both complexes (ca. 0.15wt %). When a lower MWCNTs/Complex ratio was used (entry 3, Table 3.3), a slight increase in Rh loading was observed. In view of these results, EtOAc was used as solvent for the immobilization reaction (entries 4-6, Table 3.3).

Using this solvent, the Rh loading could be increased up to 0.45 wt % for both complexes. Moreover, the complex **3.41** was immobilized onto commercially available reduced graphene oxide (rGO) and commercially available mesoporous carbon beads (CBs), that were treated at 2000°C for one hour.²⁴ In both cases, the complex **3.41** was successfully immobilized onto the carbon supports with an Rh content of 0.48% in the case of the **3.41@rGO**, and 0.56% in the case of the **3.41@CBs** (entries 7-8, Table 3.3). Interestingly, CBs are easy to handle due to their large size (0.5-1 mm), which facilitates the filtration and recovery of the material.

Finally, in collaboration with the group of Prof. Philippe Serp from Toulouse, the immobilization of complex **3.41** was attempted onto nitrogen (N) and sulfur (S) doped CNTs under optimized conditions (entries 9-10, Table 3.3). To our delight, the presence of heteroatoms at the surface of the carbon material increased the immobilization up to 2.21 wt% (entries 9-10, Table 3.3).

The new heterogenized catalysts **3.40@MWCNTs** and **3.41@MWCTNs** were analyzed by X-ray photoelectron spectroscopy (XPS) (Figure 3.5). The analysis showed two signals at 308.9 and 312.9 eV which correspond to Rh (I) ions at the surface of the solid.

In conclusion, the rhodium complexes **3.40** and **3.41** were successfully immobilized onto MWCTNs using EtOAc as solvent. XPS analysis confirmed that the oxidation state of the rhodium center did not change through the immobilization. Finally, complex **3.41** was successfully immobilized onto rGO and CBs with similar results than those obtained with MWCNTs. Interestingly, the use of doped CNTs provided material with higher Rh content.

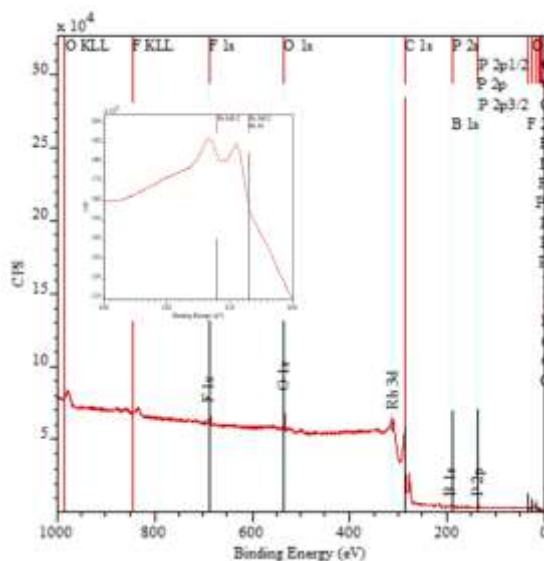


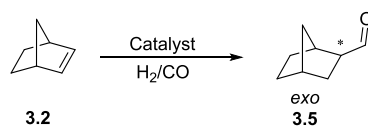
Figure 3.5: XPS spectra of **3.40@MWCNTs**. Inset: Rh narrow scan.

3.3.6. AHF of norbornene in batch using heterogenized catalysts

At this stage, the heterogenized catalysts **3.40@MWCNTs** and **3.41@MWCNTs** were tested in the asymmetric hydroformylation of norbornene **3.2** under batch conditions. In this case, the solvent was switched to ethyl acetate to maximize the interaction between the support and the catalyst (Table 3.4). Using the catalyst **3.40@MWCNTs**, no conversion was observed at 20°C (entry 1, Table 3.4). However, when the reaction was set at 40°C, the aldehyde **3.5** was obtained in moderate yield (48 %, entry 2, Table 3.4). When the temperature was increased to 60°C, full conversion towards the desired product was obtained. Although the *exo*-selectivity was excellent in all cases, the enantioselectivity was only 30% (entry 2-3, Table 3.4). In contrast, the catalyst **3.41@MWCNTs** showed some activity at 20°C (entry 4, Table 3.4), indicating a clear effect of the length of the linker between the pyrene moiety and the ligand. Under these conditions, 37% ee was obtained. This value is lower than that afforded with the catalyst **3.41** prior to its

immobilization (up to 63%) (entry 6, Table 3.2). These results clearly indicate that the support has a negative effect in batch mode. Finally, when the Rh loading and the reaction time were increased, higher yield (up to 40%) was obtained; however the enantioselectivity remained lower than at the previously obtained with the homogeneous catalyst (entry 5, Table 3.4). In order to study the effect of the support in the different heterogenized catalysts, **3.41@CBs** was tested in the AHF in batch of **3.2** and provided **3.5** in 40% yield and 40% ee (entry 6, Table 3.4).

Table 3.4: Rh-catalyzed asymmetric hydroformylation of **3.2** using heterogenized catalyst.



Entry ^a	Catalyst	T (°C)	NMR Yield (%) ^b	ee (%) ^c	TOF(h ⁻¹)
1	3.40@MWCNTs	20	-	-	-
2	3.40@MWCNTs	40	48	30	60
3	3.40@MWCNTs	60	>99	30	125
4	3.41@MWCNTs	20	7	37	9
5 ^d	3.41@MWCNTs	20	40	38	16
6 ^d	3.41@CBs	20	40	40	16
7 ^d	3.41@N-CNTs	20	15	40	6
8 ^d	3.41@S-CNTs	20	13	39	6

^a Reaction conditions: Catalyst: 0.00036 mmol, Substrate/Rh = 500, P = 18 bar (H₂/CO, 1:1), solvent = 1 mL EtOAc, T = 20°C, t = 4h. ^b Yield and *exo*-selectivity determined by ¹H NMR spectroscopy and GC-MS using naphthalene as internal standard. ^c Enantioselectivity of the *exo*-product measured by chiral GC analysis after reduction into the alcohol. ^d Substrate/Rh = 1000, t = 24h.

When **3.41@N-CNTs** and **3.41@S-CNTs** were used, the yield obtained was up to 15% and enantioselectivity afforded was up to 40% (entries 7-8, Table 3.4). Therefore, it can be concluded that independently from the support used, the enantioselectivity is negatively affected. Moreover, the lower yields afforded using N- and S-doped CNTs might be due to coordination of the Rh center to these heteroatoms, thus inhibiting the coordination of norbornene **3.2**.

Such negative effects of supports on both the activity and selectivity of heterogenized catalysts were previously reported.²⁵

At this point, recycling experiments were performed to probe the robustness of the catalyst **3.41@MWCNTs** (Table 3.5). However, a drop in activity was observed upon recycling of the catalyst and in the 3rd run, no conversion was observed. ICP values of the solid after each run demonstrated that almost 78% of the rhodium content is lost in the first run, and the rest is removed in the second. This result then explains the lack of conversion obtained in the third run.

Table 3.5: Recycling experiments in batch in the asymmetric hydroformylation of **3.2**.

C1=CC2CCC1C2 $\xrightarrow[\text{H}_2/\text{CO}]{\mathbf{3.41@MWCNTs}}$ C1=CC2CCC1C2C=O
3.2 **3.5**
exo

Run ^a	Catalyst	T (°C)	NMR Yield (%) ^b	ee (%) ^c	Rh lost % ^d
1	3.41@MWCNTs	20	40	38	78
2	3.41@MWCNTs	20	5	38	20
3	3.41@MWCNTs	20	-	-	n.d.

^a Reaction conditions: Catalyst: 0.00036 mmol, Substrate/Rh = 1000, P = 18 bar, H₂/CO = 1, solvent = 1 mL EtOAc, t = 24h. ^b Yield and *exo*-selectivity determined by ¹H NMR spectroscopy and GC-MS using naphthalene as internal standard. ^c Enantioselectivity of the *exo*-product measured by chiral GC analysis after reduction into the alcohol. ^d Measured by ICP from the solid after filtration.

These results therefore clearly indicate that catalyst leaching from the support takes place during the AHF reaction. This could be due to the removal of rhodium species **3.41** from the support during the reaction. However a negative effect of the magnetic stirring couldn't be discarded. Nozaki and co-workers previously reported such issues during the recycling of their catalyst attached on cross-linked polystyrene and concluded that the magnetic stirring could crush the polymer during the reaction.^{18b} Similar issues might therefore explain the results obtained with the systems developed in this study.

3.3.7. Continuous AHF of norbornene in flow

In view of the results obtained in batch, the catalyst **3.41@MWCNTs** was tested in the asymmetric hydroformylation of norbornene **3.2** under flow conditions. The continuous flow experiments were carried out at the Technical University of Denmark (DTU) in collaboration with the group of Prof. Anders Riisager.

Reactor flow design and standard procedure

The stock solution of norbornene **3.2** was fed into the flow reactor by means of a HPLC pump. The nitrogen and the H₂/CO syngas mixture (1:1) were fed into the reactor by means of mass flow controllers (MFC). The mixed flow was then introduced into a U-shape reactor tube where the fixed bed was situated on the left side containing the solid catalyst diluted in silica, while the right side was filled with glass beads in order to favor the mixing between the gas and liquid phase (Figure 3.6). If glass beads were not used, clogging of the reactor was observed. The reaction took place in the packed bed and the products flew out of the reactor to be collected in a cold trap at -77°C using isopropanol (iPrOH) and dry ice.

Once the catalyst was charged, the procedure to carry out the catalysis was the following: first, the reactor was filled with nitrogen in order to have the system under inert atmosphere. Once the desired pressure was reached, the system was filled with syngas, and left at this pressure for 30 minutes in order to detect any possible leaking in the system, and to activate the catalyst. With the system stable at the desired pressure of syngas, the stock solution of norbornene **3.2** was pumped into the system at the desired flow. At this moment, the reaction started. However, *ca.* 30-50 minutes were necessary prior to the collection of the first samples to analyze. In Table 3.6, the standard parameters for the flow experiments are described. The effects of other parameters such as solvent and pressure were varied and the results will be described in the following sections.

Immobilisation of chiral Rh catalysts for the AHF of norbornene in flow

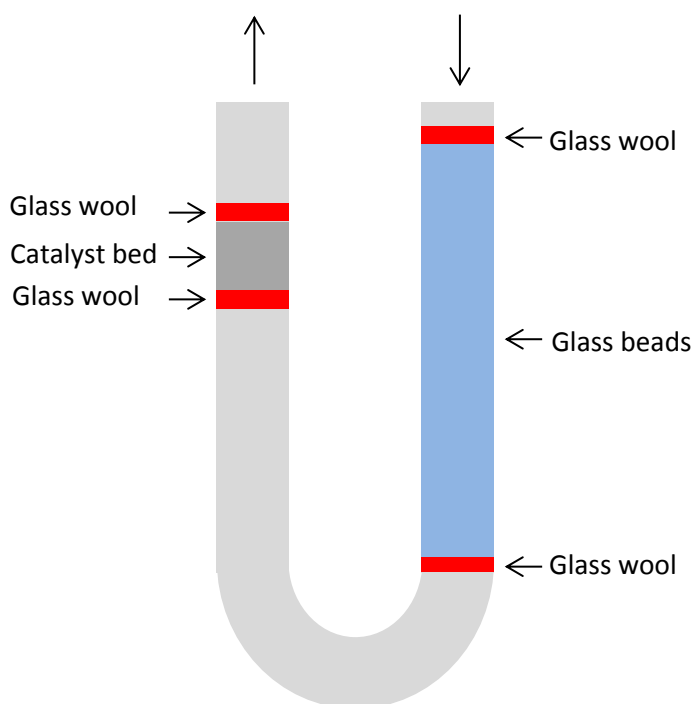
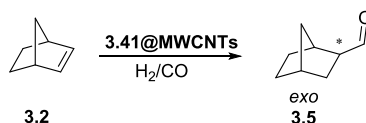


Figure 3.6: U-shape reactor design. Right: glass wool and glass beads. Left: Catalyst bed and glass wool.

Table 3.6: Reaction conditions for the asymmetric hydroformylation of **3.2** under continuous flow conditions.



[3.2] (M)	$\mu_{3.2}$ (mL/min)	μ_{CO} (mL/min)	μ_{H_2} (mL/min)	T (°C)	Rh μmol
0.75	0.66	22	22	20	3.5

Effect of the solvent

Two solvents (EtOAc and acetone) were tested to compare the performance of **3.41@MWCNTs** under these conditions. The syngas pressure was 10 bar (H_2/CO , 1:1) (Figure 3.7). When ethyl acetate was used as solvent, a peak in activity was

observed after 60 minutes of reaction with 9 % of conversion. Later, the activity started to slowly drop. In the case of acetone, similar activity was observed (up to 11%) at 40 minutes; however, the drop in activity was stronger than in the case of EtOAc. In both cases, yellowish solutions were observed probably due to catalyst leaching from the support. Since EtOAc showed a lower decay in activity, it was selected as solvent for the following experiments.

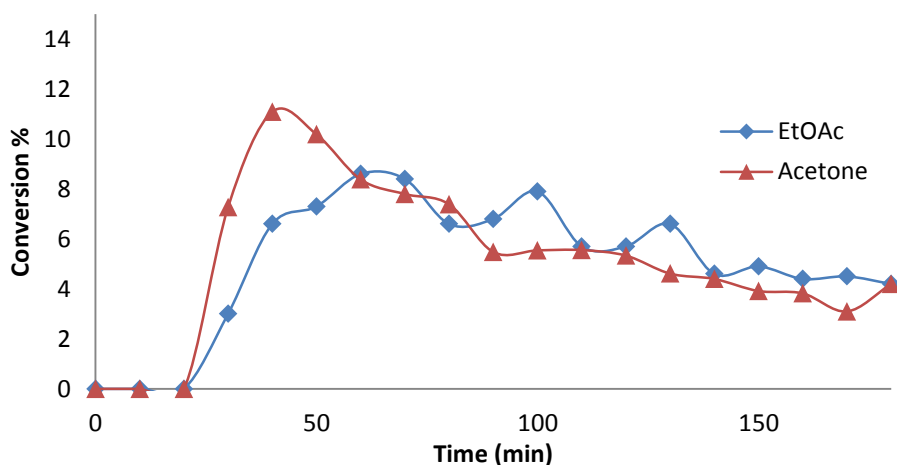


Figure 3.7: Conversion vs. time on stream for asymmetric hydroformylation of **3.2** using **3.41@MWCNTs** under continuous flow; reaction conditions are displayed in Table 3.6.

Effect of the total pressure

Next, the effect of the total syngas pressure was investigated. Three pressures were studied: 5, 10 and 14 bar. Since the activity afforded in the previous experiment was low (Figure 3.7), the substrate solution flow was decreased to 0.33 mL/min in order to enhance the contact time and therefore obtain higher conversions. First, the reaction was carried out under 5 bar (H_2/CO , 1:1) of pressure for 240 min (Top, Figure 3.8). During the first minutes, conversions up to 14% were measured, and decreased after 100 min of reaction. It then remained constant at *ca.* 5% until 240 min. Interestingly, enantioselectivity started at similar values than the homogeneous reaction (*ca.* 62%) and increased up to 72% where it

Immobilisation of chiral Rh catalysts for the AHF of norbornene in flow

remained constant until the end of the experiment (Bottom, Figure 3.8). Under 10 bar of syngas, higher conversions (up to 18%) (Top, Figure 3.8) and similar enantioselectivities (up to 73%) were afforded (Bottom, Figure 3.8).

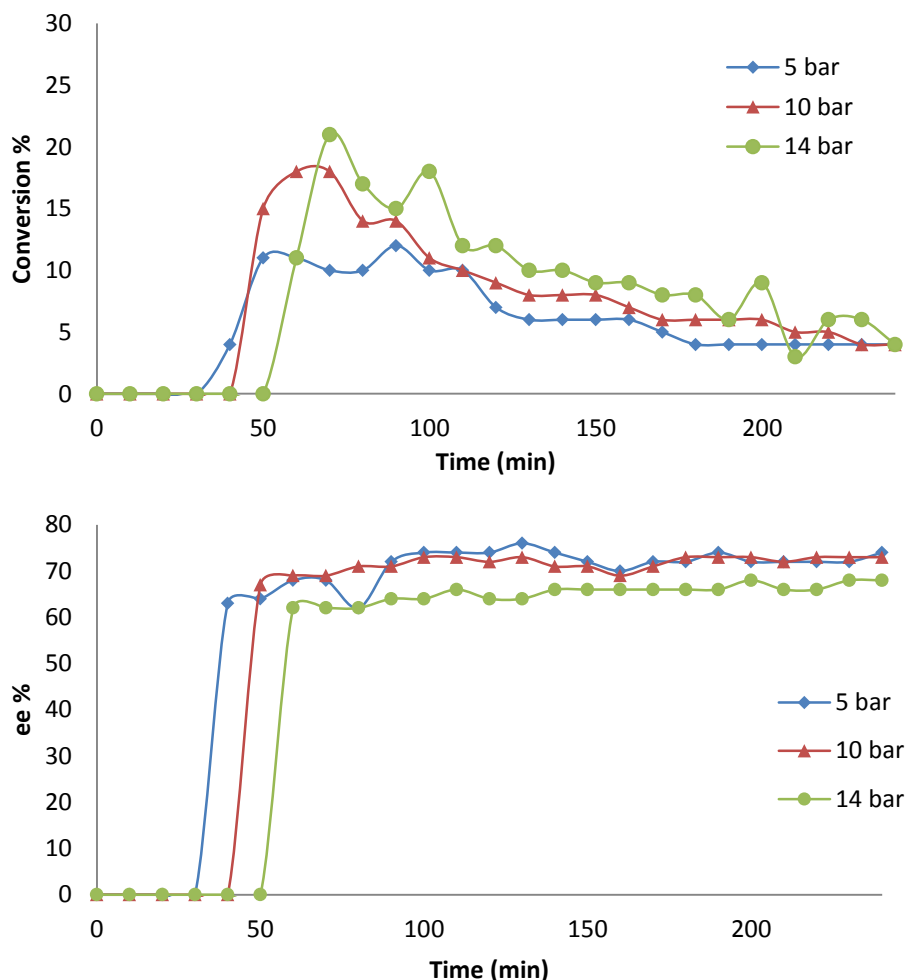


Figure 3.8: Rh-catalyzed asymmetric hydroformylation of **3.2** using **3.41@MWCNTs** at three different pressures under flow conditions. Top: effect of the pressure on the conversion. Bottom: effect of the pressure on the enantioselectivity. Conversion determined by GC-analysis. Enantioselectivity determined by chiral GC analysis after the reduction into the alcohol.

When the pressure was further increased to 14 bar, conversions up to 21% were measured (Top, Figure 3.8), although a slight decrease in enantioselectivity was

detected (up to 68%) (Bottom, Figure 3.8). In all cases, full stereoselectivity to the *exo*-product was obtained, as in the homogeneous case. Under these conditions, the activity of the catalyst reached its highest value after *ca.* 100 min and then started to drop. Furthermore, during the collection of the first samples (between 50 and 120 min), the solution was colored as in the previous experiments. In view of this results, 10 bar (H_2/CO , 1:1) of pressure was selected since it provided the best compromise for activity and enantioselectivity.

The increase in ee observed when comparing batch and flow results were attributed to an improved gas-liquid mass transfer under continuous conditions. Indeed, it has been previously reported that the enantioselectivity is highly dependent on the concentration of the gases in solution, especially CO ,²⁶ and that in flow reactors, the solubility of the gases can be improved due to the better gas-liquid mass transfer.²⁷

Effect of the carbon support

Motivated by these results, we decided to study the effect of the carbon support was studied using two of the heterogenized **3.41@rGO** and **3.41@CBs** previously synthesized at 10 bar of syngas pressure (Figure 3.9). When **3.41@rGO** was used, the conversion first reached 13% after 70 min, and then dropped to 7% after 240 min. During the reaction, total stereoselectivity for the *exo*-product was again obtained, and the enantioselectivity obtained was *ca.* 64%. In the case of **3.41@CBs**, the maximum of conversion (up to 14%) was afforded after *ca.* 60 min of reaction, to finally drop until 10% after 240 min of reaction. Throughout the reaction, total stereoselectivity for the *exo*-product was again observed, and interestingly, the enantioselectivity obtained was up to 75%.

In conclusion, both heterogenized complexes provided slightly lower initial conversions compared to **3.41@MWCNTs**, nonetheless the decay in conversion was less pronounced, which suggests a more stable immobilization of the catalyst.

Immobilisation of chiral Rh catalysts for the AHF of norbornene in flow

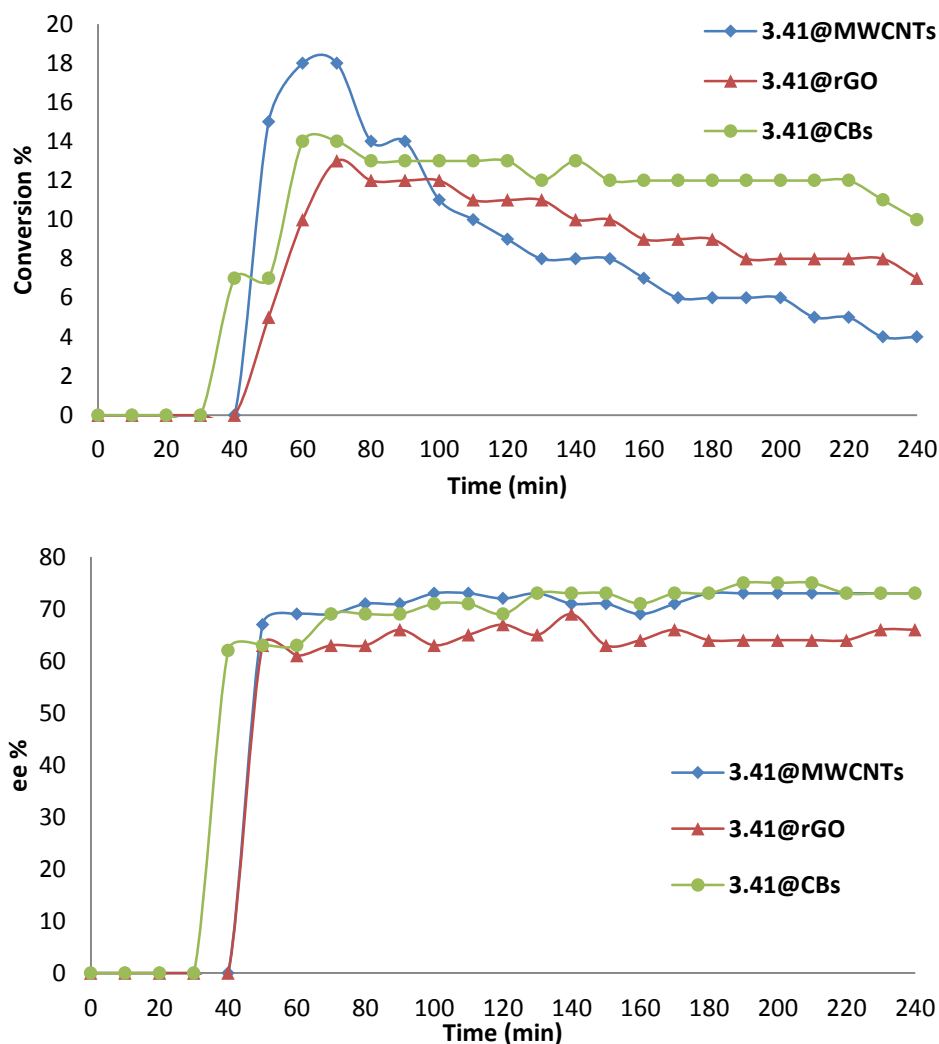


Figure 3.9: Rh-catalyzed hydroformylation of **3.2** using **3.41@support** in continuous flow. Top: Effect of the support in the conversion. Bottom: effect of the support in the enantioselectivity. Conversion was determined by GC-analysis. Enantioselectivity determined by chiral GC analysis after the reduction into the alcohol.

The explanation for this behaviour might be related to the larger surface area of rGO (500-400 m²/g) and CBs (211 m²/g) compared to MWCNTs (80 m²/g), and the strength of the ligand interactions with the support. While rGO contains hydroxyl and carboxylic groups that might interact with the catalyst, CBs are mesoporous

and might contain catalyst entrapped inside the structure, which might hinder its detachment from the support.

In terms of stereoselectivity all the heterogenized complexes maintained the full selectivity for the *exo*-product. Regarding the enantioselectivity, **3.41@rGO** provided lower enantioselectivity than the other heterogenized catalysts, while **3.41@CBs** afforded similar results than **3.41@MWCNTs**. The decrease in enantioselectivity for the **3.41@rGO** might be due to the presence of hydroxyl and carbonyl groups at the surface of the supports which may affect the phosphite ligand or the catalyst. Thus, **3.41@CBs** provided the best results in terms of conversion and enantioselectivity.

In view of the results afforded by **3.41@CBs**, the robustness of the system was probed with two experiments. First, the catalyst **3.41@CBs** was left overnight under 10 bar of syngas after the experiment previously described. At this point, a new reaction was started (Figure 3.10). During the first minutes high activity was observed (up to 37%), which is probably due to the presence of aldehyde product **3.3** remaining from the previous experiment. However, when activity went back to 10%, it decayed only until 8% after 240 min of experiment. Furthermore, the enantioselectivity was 73%. This experiment indicated that our catalyst remained active and selective even when left under pressure for several hours. The slight decay in activity observed might again be due to catalyst detachment or to a catalyst deactivation.

Immobilisation of chiral Rh catalysts for the AHF of norbornene in flow

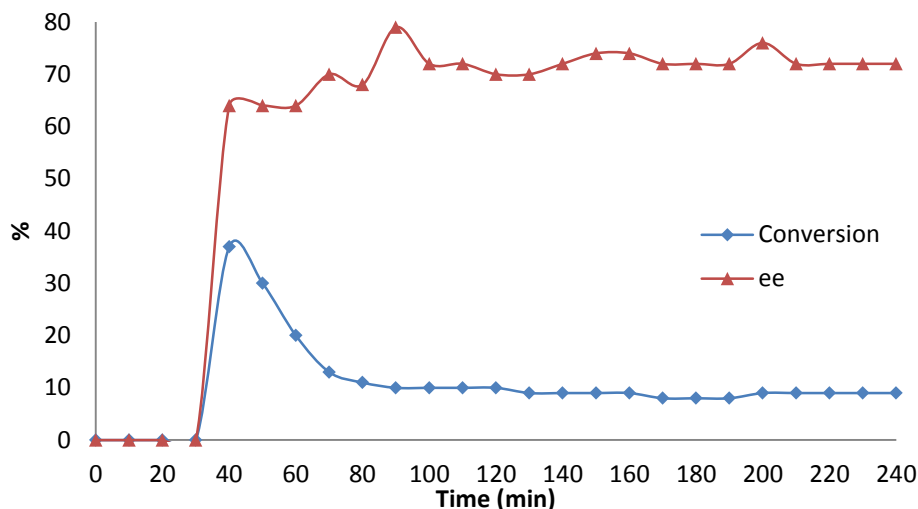


Figure 3.10: Rh-catalyzed asymmetric hydroformylation of **3.2** using **3.41@CBs** after 16h under H₂/CO pressure. Conversion determined by GC-analysis. Enantioselectivity determined by chiral GC analysis after the reduction into the alcohol.

For the second experiment, the amount of rhodium was increased to 11 μmol (Figure 3.11). As expected, when more catalyst was used, the conversion increased (up to 35%) compared to previous experiments, and enantioselectivity remained unaffected (up to 74%). After 360 min of experiment, the activity was 28% and the enantioselectivity remained unaltered.

In conclusion, the three heterogenized catalysts **3.41@MWCNTs**, **3.41@rGO** and **3.41@CBs** were successfully applied in the asymmetric hydroformylation of norbornene **3.2** in flow. The rGO and CBs provided a lower decay in conversion compared to MWCNTs, possibly due to the larger surface area of this support. On the other hand, the catalyst supported on rGO provided lower enantioselectivity than the other supported catalysts. Thus, CBs constituted the best support of the series in terms of conversion and enantioselectivity. When the **3.41@CBs** was tested after 16h under syngas pressure, the same activity and enantioselectivity was obtained, proving that the catalyst remains stable after this time. When larger

amounts of rhodium were used, the conversions obtained were higher and the enantioselectivity remained high (up to 75%).

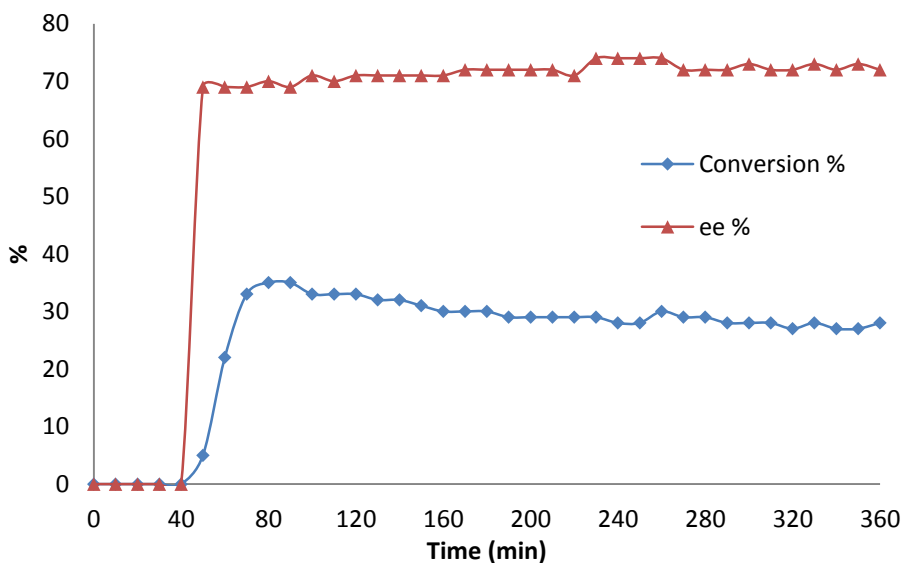


Figure 3.11: Rh-catalyzed asymmetric hydroformylation of **3.2** using **3.41@CBs** in continuous flow. Rh = 11 μ mol. Conversion determined by GC-analysis. Enantioselectivity determined by chiral GC analysis after the reduction into the alcohol.

3.4. Conclusions

From the study described in this chapter, the following conclusions can be extracted:

- i) The chiral pyrene tagged diphosphite ligands **3.27** and **3.28** were synthesized in good yield (55-63%) and fully characterized by NMR spectroscopy and MS.
- ii) The cationic complexes $[\text{Rh}(\text{COD})(\mathbf{3.27})]\text{BF}_4$ **3.40** and $[\text{Rh}(\text{COD})(\mathbf{3.28})]\text{BF}_4$ **3.41** were synthesized in excellent yields, and fully characterized by NMR spectroscopy and MS.

- iii) The pyrene tagged catalysts were applied in the homogeneous asymmetric hydroformylation of norbornene **3.2** with similar results to analogous alkyl diphosphites in terms of activity and selectivity. Therefore, the pyrene moiety does not affect the activity or selectivity of the resulting catalyst.
- iv) HP-NMR studies revealed an **eq-eq** coordination mode of the ligand **3.27** in the $[\text{RhH}(\text{CO})_2(\mathbf{3.27})]$ species with a fast exchange between phosphorus atoms, similarly to analogous diphosphite ligands.
- v) The rhodium complexes **3.40** and **3.41** were successfully immobilized onto MWCNTs using EtOAc as solvent under very mild conditions to afford the heterogenized catalysts **3.40@MWCNTs** and **3.41@MWCNTs**. The complex **3.41** was also immobilized onto rGO and CBs with similar catalyst loading and onto N-CNTs and S-CNTs with higher Rh content.
- vi) Both **3.40@MWCNTs** and **3.41@MWCNTs** were used in the AHF of norbornene **3.2** in batch. The catalyst **3.41@MWCNTs** provided the best result proving that the separation between the pyrene and the ligand was important. However, the immobilization proved to have negative effects on both the activity and enantioselectivity of the catalyst. The other heterogenized catalysts were also used in the AHF of norbornene **3.2** and all provided the same enantioselectivity. Lower yield was obtained in the case of the catalyst immobilized at the N- and S-CNTs.
- vii) Recycling experiments with **3.41@MWCNTs** were performed in the AHF of norbornene **3.2** in batch mode. However, the catalyst activity drastically dropped in the second run due to catalyst leaching.
- viii) The catalyst **3.41@MWCNTs** was successfully applied in the AHF of norbornene **3.2** under flow conditions. After optimization, the catalyst was active for 240 min., but loss of activity was observed over time due to catalyst detachment. Nonetheless, the enantioselectivity obtained was slightly higher than in the homogeneous case.

- ix) The heterogenized catalysts **3.41@rGO** and **3.41@CBs** were also applied in the AHF of norbornene **3.2** under flow conditions. Interestingly, a lower decay in activity compared to **3.41@MWCNTs** was observed. Regarding to the enantioselectivity, **3.41@rGO** displayed lower values while **3.41@CBs** provided similar results than **3.41@MWCNTs**.
- x) Among the heterogenized catalysts, **3.41@CBs** provided the best performance in terms of activity, selectivity and robustness, and it was possible to increase the catalyst loading without affecting the stereo- and enantioselectivity.

3.5. Experimental part

3.5.1. General considerations

All the reactions were carried out using Schlenk-line or glovebox techniques. Anhydrous solvents were collected from the system Braun MB SPS-800 except from EtOAc, which was dried with CaH₂, and stored under inert atmosphere.

Commercially available reagents were purchased from Sigma Aldrich, Alfa Aesar and Acros Organics and were used as received, without further purification, unless otherwise stated. MWCNTs were purchased to HeJi, rGO to Graphenea, and CBs to MAST Carbon International.

The ligand **3.4a**, compounds **3.35**, **3.31** and phosphochloridite used in the synthesis of the diphosphite ligands were synthesized according to the literature.²²

¹H, ¹³C{¹H} and ³¹P{¹H} NMR spectra were recorded using a Varian Mercury VX 400 (400, 100.6, and 161.97 MHz respectively). Chemical shift values (δ) are reported in ppm relative to TMS (¹H and ¹³C{¹H}) or H₃PO₄ (³¹P{¹H}), and coupling constants are reported in Hertz. The following abbreviations are used to indicate the

multiplicity: s, singlet; d, doublet; t, triplet; q, quartet; m, multiplet; bs, broad signal. High-resolution mass spectra (HRMS) were recorded on an Agilent Time-of-Flight 6210 using ESI-TOF (electrospray ionization-time of flight). Samples were introduced in the mass spectrometer ion source by direct injection using a syringe pump and were externally calibrated using sodium formate. The instrument was operating in the positive ion mode. Reactions were monitored by TLC carried out on 0.25 mm E. Merck silica gel 60 F₂₅₄ glass or aluminum plates. Developed TLC plates were visualized under a short-wave UV lamp (254 nm) and by heating the TLC plates that were previously dipped in potassium permanganate. Flash column chromatography was carried out using forced flow of the indicated solvent on Merck silica gel 60 (230-400 mesh). Hydroformylation reactions in batch were carried out in a 5-positions 10 mL Parr stainless steel autoclave reactor. Gas chromatographic analysis was carried out using a HP 6890 gas chromatograph instrument (J&W Scientific split/splitless injector, HP-5 column 25 m × 0.25 × 0.33 mm, carrier gas: 150 kPa He, FID detector) equipped with a HP3396 series integrator. The enantiomeric ratios were determined by chiral GC analysis after the reduction into the corresponding alcohol in a Hewlett-Packard HP 6890 gas chromatograph (split/splitless injector, J&W Scientific, CP Chirasil-Dex chiral, 25 m column, internal diameter: 0.25 mm, film thickness: 0.25 µm, carrier gas: 50 kPa He, FID detector).

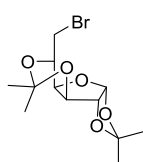
ICP-OES analyses were carried out using a Spectro Arcos FHS-16 spectrometer at the Servei Científicotècnics at the Universitat Rovira I Virgili in Tarragona.

XPS analyses were conducted on a PHI 5500 Multitechnique System (from Physical Electronics) with a monochromatic X-ray source (Aluminium Kalfa line of 1486.6 eV energy and 350 W), placed perpendicular to the analyzer axis and calibrated using the 3d_{5/2} line of Ag with a full width at half maximum (FWHM) of 0.8 eV. The

analyzed area was a circle of 0.8 mm diameter, and the selected resolution for the spectra was 187.5 eV of Pass Energy and 0.8 eV/step for the general spectra and 23.5 eV of Pass Energy and 0.1 eV/step for the spectra of the different elements in the depth profile spectra. A low energy electron gun (less than 10 eV) was used in order to discharge the surface when necessary. All Measurements were made in an ultra-high vacuum (UHV) chamber pressure between 5×10^{-9} and 2×10^{-8} torr.

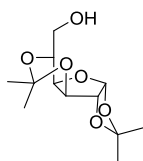
3.5.2. Synthetic procedures

6-Bromo-6-deoxy-1,2:3,5-di-*O*-isopropylidene- α -D-glucofuranoside (**3.35**)²²



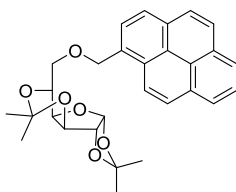
1,2:5,6-Di-*O*-isopropylidene- α -D-glucofuranose **3.36** (5g, 19.2 mmol), Ph_3P (8.32g, 31.7 mmol), and *N*-bromosuccinimide (5.23g, 29.4 mmol) were dissolved in toluene (50 mL). The solution was heated at 90°C and left stirring for 2 h. Then the solution was cooled, washed with NaHCO_3 sat. (20 mL), and the aqueous layer was extracted with toluene (3 x 10 mL). The combined organic layers were dried with MgSO_4 , filtrated and concentrated. The resulting residue was purified by flash chromatography (EtOAc/Hexane, 1:16) and afforded **3.35** (4.66 g, 75 %) as a colorless oil.

$^1\text{H NMR}$ (400 MHz, CDCl_3) δ : 1.32 (s, 3H), 1.36 (s, 3H), 1.37 (s, 3H), 1.48 (s, 3H), 3.43 (dd, $J_{\text{H,H}} = 11.2, 7.6$ Hz, 1H), 3.60 (dd, $J_{\text{H,H}} = 11.0, 3.4$ Hz, 1H), 3.73 (td, $J_{\text{H,H}} = 7.2, 3.2$ Hz, 1H), 4.22 (d, $J_{\text{H,H}} = 4.4$ Hz, 1H), 4.31 (dd, $J_{\text{H,H}} = 7.2, 4.0$ Hz, 1H), 4.58 (d, $J_{\text{H,H}} = 3.6$ Hz, 1H), 5.98 (d, $J_{\text{H,H}} = 3.6$ Hz, 1H); $^{13}\text{C NMR}$ (100.6 MHz, CDCl_3) δ : 23.9 (1C), 24.0 (1C), 26.6 (1C), 27.3 (1C), 33.1 (1C), 72.0 (1C), 75.2 (1C), 81.7 (1C), 84.0 (1C), 101.5 (1C), 106.5 (1C), 112.5 (1C). These peaks are in agreement with those reported in the literature.

6-hydroxy-1,2:3,5-di-*O*-isopropylidene- α -*D*-glucofuranoside (3.31)²²

NaNO_2 (1.992g, 28.9 mmol) was added to a solution of compound **3.35** (4.66g, 14.4 mmol) in DMF (30 mL), and the mixture was stirred at 70°C for 4h. The reaction was monitored by TLC (EtOAc/Hexane, 1:1). The reaction was stopped and the residue was evaporated to dryness. Purification by flash chromatography (EtOAc/Hexane, 1:2) afforded **3.31** (1.21g, 30%) as colorless oil.

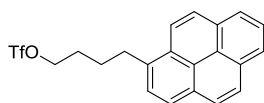
$^1\text{H NMR}$ (400 MHz, CDCl_3) δ : 1.29 (s, 3H), 1.33 (s, 6H), 1.45 (s, 3H), 3.63 (m, 2H), 3.79 (dd, $J_{\text{H,H}} = 11.6, 2.8\text{Hz}$, 1H), 4.15 (d, $J_{\text{H,H}} = 3.6\text{ Hz}$, 1H), 4.33 (dd, $J_{\text{H,H}} = 6.8, 3.6\text{ Hz}$, 1H), 4.54 (d, $J_{\text{H,H}} = 4.0\text{ Hz}$, 1H), 5.95 (d, $J_{\text{H,H}} = 4.0\text{ Hz}$, 1H); $^{13}\text{C NMR}$ (100.6 MHz, CDCl_3) δ : 24.1 (1C), 24.2 (1C), 26.6 (1C), 27.2 (1C), 63.4 (1C), 72.6 (1C), 75.1 (1C), 79.1 (1C), 84.0 (1C), 101.0 (1C), 106.5 (1C), 112.3 (1C). These peaks are in agreement with those reported in the literature.

1,2:3,5-di-*O*-isopropylidene-6-*O*-methylpyrene- α -*D*-glucofuranoside (3.32)

Compound **3.31** (540 mg, 2.1 mmol) was dissolved in dry THF (4 mL) and added to a solution of previously washed NaH (171.6 mg, 4.3 mmol) in THF (4 mL) at 0°C. The solution was stirred at this temperature for 1h, 15-crown-5 ether (125 μL , 0.6 mmol) was then added, and the solution was left stirring for 15 min. Finally, 1-(bromomethyl)pyrene **3.29** (741.3 mg, 2.5 mmol) was added and the reaction mixture was left stirring for 16h at room temperature. The solvent was evaporated under reduced pressure, and the residue dissolved in CH_2Cl_2 (15 mL). The resulting solution was washed with NH_4Cl sat. (10 ml), and the aqueous layer was extracted with CH_2Cl_2 (3 x 4 mL). The combined organic phases were dried (MgSO_4), filtrated, and evaporated to dryness. Purification by flash chromatography (EtOAc/Hexane, 1:8) afforded **3.32** (984 mg, 73 %) as a white solid.

$^1\text{H NMR}$ (400 MHz, CDCl_3) δ : 1.30 (s, 3H), 1.38 (s, 3H), 1.39 (s, 3H), 1.41 (s, 3H), 3.80 (m, 3H), 4.20 (d, $J_{\text{H,H}} = 3.6$ Hz, 1H), 4.36 (dd, $J_{\text{H,H}} = 6.6, 3.6$ Hz, 1H), 4.56 (d, $J_{\text{H,H}} = 4$ Hz, 1H), 5.31 (m, 2H), 5.97 (d, $J_{\text{H,H}} = 3.6$ Hz, 1H), 7.99-8.43 (m, 9H, Ar); **$^{13}\text{C NMR}$** (100.6 MHz, CDCl_3) δ : 24.1 (1C), 24.3 (1C), 26.7 (1C), 27.2 (1C), 70.7 (1C), 71.7 (1C), 72.3 (1C), 75.1 (1C), 79.7 (1C), 84.1 (1C), 101.1 (1C), 106.5 (1C), 112.3 (1C), 123.7-131.5 (16C, Ar). **ESI-HRMS**: Calculated for $\text{C}_{29}\text{H}_{30}\text{O}_6$. Exact: (M: 474.204, $\text{M}+\text{NH}_4^+$: 492.238); Experimental (M: 474.204, $\text{M}+\text{NH}_4^+$: 492.237).

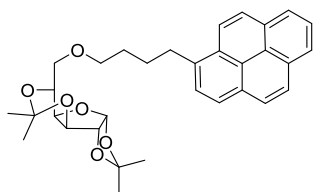
4-(pyrene-1-yl)butyl triflate (**3.30c**)²⁸



1-pyrenebutanol **3.36** (400 mg, 1.46 mmol) and triethylamine (0.3 mL, 2.18 mmol) were dissolved in CH_2Cl_2 (6 mL) at 0°C . To this solution, trifluoromethanesulphonic anhydride (0.36 mL, 2.18 mmol) was added dropwise. The resulting mixture was stirred for 30 min at 0°C , quenched with NaHCO_3 sat. (5 mL), and extracted with Et_2O (3 x 6 mL). The organic phases were combined, washed with brine, dried over MgSO_4 , filtrated and concentrated under vacuum. The resulting residue was filtrated through a plug of silica eluting with CH_2Cl_2 , and dried under vacuum to afford **3.30c** (413 mg, 70 %) as light brown oil.

$^1\text{H NMR}$ (400 MHz, CDCl_3) δ : 1.99 (m, 4H), 3.41 (t, $J_{\text{H,H}} = 7.2$ Hz, 2H), 4.57 (t, $J_{\text{H,H}} = 5.9$ Hz, 2H), 7.85-8.23 (m, 9H, Ar). **$^{13}\text{C NMR}$** (100.6 MHz, CDCl_3) δ : 27.2 (1C), 29.2 (1C), 32.7 (1C), 53.6 (1C), 123.1-135.3 (17C, Ar, $-\text{CF}_3$). These peaks are in agreement with those reported in the literature.

1,2:3,5-di-*O*-isopropylidene-6-*O*-butylpyrene- α -*D*-glucofuranoside (**3.33**)

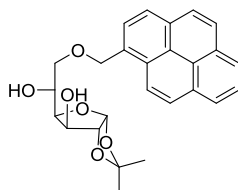


Compound **3.31** (192 mg, 0.74 mmol) was dissolved in dry THF (2 mL) and added to a solution of previously washed NaH (60.0 mg, 1.47 mmol) in THF (1 mL) at

0°C. The solution was stirred at this temperature for 1h, 15-crown-5 ether (75 μ L, 0.4 mmol) was then added, and the solution was left stirring for 15 min. Finally, freshly synthesized **3.30c** (451.1 mg, 1.11 mmol) was added and the reaction mixture was left stirring for 48 h at room temperature. The solvent was evaporated under reduced pressure, and the residue dissolved in CH₂Cl₂ (10 mL). The resulting solution was washed with NH₄Cl sat. (5 mL), and the aqueous layer was extracted with CH₂Cl₂ (3 x 5 mL). The combined organic phases were dried (MgSO₄), filtrated, and evaporated to dryness. Purification by flash chromatography (EtOAc/Hexane, 1:8) afforded **3.33** (210 mg, 55 %) as white solid.

¹H NMR (400 MHz, CDCl₃) δ : 1.32 (s, 3H), 1.35 (s, 3H), 1.37 (s, 3H), 1.45 (s, 3H), 1.80 (m, 2H), 1.93 (m, 2H), 3.37 (t, $J_{H,H}$ = 8 Hz, 2H), 3.57 (t, $J_{H,H}$ = 8Hz, 2H), 3.60 (dd, $J_{H,H}$ = 10.8 Hz, 2.8 Hz, 1H), 3.63 (dd, $J_{H,H}$ = 10.8 Hz, 2.8 Hz, 1H), 3.73 (td, $J_{H,H}$ = 6, 2.8 Hz, 1H), 4.21 (d, $J_{H,H}$ = 3.6 Hz, 1H), 4.34 (dd, $J_{H,H}$ = 7.2, 4 Hz, 1H), 4.58 (d, $J_{H,H}$ = 3.6 Hz, 1H, 1H), 6.0 (d, $J_{H,H}$ = 3.6 Hz, 1H), 7.86-8.29 (m, 9H, Ar); **¹³C NMR** (100.6 MHz, CDCl₃) δ : 23.9 (1C), 24.1 (1C), 26.5 (1C), 27.1 (1C), 28.3 (1C), 29.5 (1C), 33.2 (1C), 71.2 (1C), 71.5 (1C), 74.9 (1C), 79.5 (1C), 84.0(1C), 100.9 (1C), 106.4 (1C), 112.1 (1C), 122.3-133.2 (16C, Ar). **ESI-HRMS**: Calculated for C₃₂H₃₆O₆ Exact: (M: 516.2512, M+Na: 539.2410); Experimental (M+Na: 539.2410).

1,2-O-isopropylidene-6-O-methylpyrene- α -D-glucofuranoside (**3.37**)

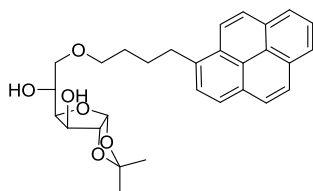


Compound **3.32** (400 mg, 0.84 mmol) was added to a AcOH/H₂O (65%, 10 mL) solution, and the suspension was left stirring at 40°C overnight. After cooling to room temperature, the solution was co-evaporated with EtOH, and toluene to afford **3.37** (356 mg, 98 % yield) as a white powder.

¹H NMR (400 MHz, CDCl₃) δ : 1.28 (s, 3H), 1.43 (s, 3H), 3.76 (dd, $J_{H,H}$ = 10, 6 Hz, 1H), 3.88 (dd, $J_{H,H}$ = 9.8, 3.2 Hz, 1H), 4.10 (dd, $J_{H,H}$ = 6.4, 2.8 Hz, 1H), 4.23 (m, 1H), 4.31 (d, $J_{H,H}$ = 2.4 Hz), 4.46 (d, $J_{H,H}$ = 3.6 Hz, 1H), 5.25 (s, 2H), 5.94 (d, $J_{H,H}$ = 3.6 Hz, 1H),

7.96-8.31 (m, 9H, Ar); $^{13}\text{C NMR}$ (100.6 MHz, CDCl_3) δ : 26.2 (1C), 26.9 (1C), 69.6 (1C), 71.5 (1C), 72.4 (1C), 75.8 (1C), 79.9 (1C), 85.1(1C), 106.0 (1C), 112.2 (1C), 122.3-133.2 (16C, Ar). **ESI-HRMS**: Calculated for $\text{C}_{26}\text{H}_{26}\text{O}_6$. Exact: (M: 434.1729, M+Na: 457.1627); Experimental (M+Na: 457.1622).

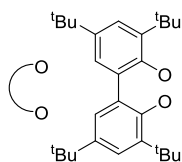
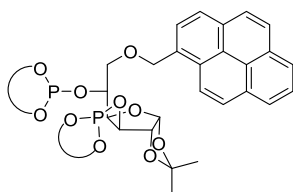
1,2-O-isopropylidene-6-O-butylpyrene- α -D-glucofuranoside (3.38)



Compound **3.33** (210 mg, 0.41 mmol) was added to a $\text{AcOH}/\text{H}_2\text{O}$ (65%, 10 mL) solution, and the suspension was left stirring at 40°C overnight. After cooling to room temperature, the solution was co-evaporated with EtOH, and toluene to afford **3.38** (192 mg, 99 % yield) as a white powder.

$^1\text{H NMR}$ (400 MHz, CDCl_3) δ : 1.30 (s, 3H), 1.44 (s, 3H), 1.88 (m, 2H), 1.92 (m, 2H), 3.37 (t, $J_{\text{H,H}} = 7.6$ Hz, 2H), 3.57 (m, 3H), 3.71 (dd, $J_{\text{H,H}} = 10, 3.2$ Hz, 1H), 4.07 (dd, $J_{\text{H,H}} = 6, 2.8$ Hz, 1H), 4.23 (m, 1H), 4.31 (d, $J_{\text{H,H}} = 2.8$ Hz, 1H), 4.46 (d, $J_{\text{H,H}} = 3.6$ Hz, 1H), 5.96 (d, $J_{\text{H,H}} = 3.6$ Hz, 1H), 7.85-8.28 (m, 9H, Ar); $^{13}\text{C NMR}$ (100.6 MHz, CDCl_3) δ : 26.3 (1C), 26.9 (1C), 28.4 (1C), 29.7 (1C), 33.4 (1C), 69.7 (1C), 71.6 (1C), 71.7 (1C), 71.7 (1C), 76.1 (1C), 79.9 (1C), 85.2(1C), 104.9 (1C), 111.8 (1C), 122.3-133.2 (16C, Ar). **ESI-HRMS**: Calculated for $\text{C}_{29}\text{H}_{32}\text{O}_6$. Exact: (M: 476.2199, M+Na: 499.2097); Experimental (M+Na: 499.2104).

3,5-Bis-O-[3,3'-5,5'-tetra-tert-butyl-1,1'-biphenyl-2,2'-diyl]-6-O-methylpyrene-1,2-O-isopropyliden- α -D-glucofuranoside (3.27)



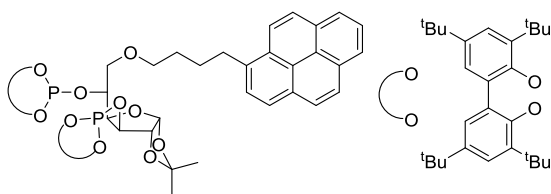
Compound **3.37** (200 mg, 0.46 mmol) was azeotropically dried with toluene (3 x 2 mL), and dissolved in dry CH_2Cl_2 (3 mL), and NEt_3 (200 μL). Freshly

synthesised phosphochloridite in dry CH_2Cl_2 (3 mL), and NEt_3 (200 μL) was slowly added to the **3.37** solution at 0°C via syringe. The reaction was left to reach room

temperature, and left stirring for 16h. Then, the solvent was evaporated, and the resulting residue was purified by flash chromatography (Toluene, 1% NEt₃) to afford compound **3.27** (324 mg, 55 %) as a white solid.

¹H NMR (400 MHz, C₆D₆) δ: 0.93 (s, 3H), 1.18 (s, 9H), 1.24 (s, 18H), 1.29 (s, 9H), 1.32 (s, 3H), 1.56 (s, 9H), 1.59 (s, 9H), 1.63 (s, 9H), 1.70 (s, 9H), 4.19 (d, J_{H,H} = 3.2 Hz, 2H), 4.49 (d, J_{H,H} = 3.6 Hz, 1H), 4.98 (dd, J_{H,H} = 2.4 Hz, 8.6 Hz), 5.03 (s, 2H), 5.24 (m, 1H), 5.32 (d, J_{H,H} = 5.2 Hz, 1H), 5.59 (d, J_{H,H} = 3.6 Hz, 1H), 7.34-8.35 (m, 17H, Ar); ¹³C NMR (100.6 MHz, C₆D₆) δ: 26.1 (1C), 26.6 (1C), 29.6 (1C), 29.6-35.5 (32C), 70.6 (1C), 71.7 (1C), 72.4 (d, J_{P,C} = 11.5 Hz, 1C), 76.6 (1C), 79.0 (1C), 84.4(1C), 105.2 (1C), 111.7 (1C), 124.0-146.9 (40C, Ar); ³¹P NMR (161.97 MHz, C₆D₆) δ: 144.3 (d, J_{P,P} = 32.8 Hz, 1P), 146.9 (d, J_{P,P} = 32.8 Hz, 1P). ESI-HRMS: Calculated for C₈₂H₁₀₄O₁₀P₂. Exact: (M: 1310.71047, M+Na: 1311.7183); Experimental (M+H: 1311.7180).

3,5-Bis-O-[3,3'-5,5'-tetra-tert-butyl-1,1'-biphenyl-2,2'-diyl]-6-O-butylpyrene-1,2-O-isopropyliden-α-D-glucofuranoside (3.28)



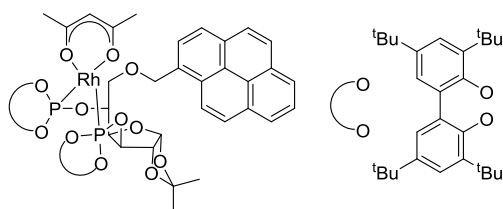
Compound **3.38** (333 mg, 0.7 mmol) was azeotropically dried with toluene (3 x 2 mL), and dissolved in dry CH₂Cl₂ (5 mL), and

NET₃ (200 μL). Freshly synthesized phosphochloridite in dry CH₂Cl₂ (5 mL), and NET₃ (680 μL) was slowly added to the **3.38** solution at 0°C via syringe. The reaction was left to reach room temperature, and left stirring for 20 h. Then, the solvent was evaporated, and the resulting residue was purified by flash chromatography (Toluene, 1% NEt₃) to afford compound **3.28** (600 mg, 63 %) as a white solid.

¹H NMR (400 MHz, C₆D₅CD₃) δ: 0.91 (s, 3H), 1.20 (s, 9H), 1.24 (s, 9H), 1.26 (s, 9H), 1.28 (s, 9H), 1.31 (s, 3H), 1.51 (s, 9H), 1.59 (s, 12H), 1.65 (s, 20H), 1.88 (m, 2H), 3.17 (t, J_{H,H} = 8 Hz, 2H), 3.31 (m, 3H), 3.93 (m, 3H), 4.37 (d, J_{H,H} = 3.6 Hz, 1H), 4.77 (dd, J_{H,H} = 8.8, 2.4 Hz, 1H), 5.02 (bs, 1H), 5.20 (m, 2H), 5.57 (d, J_{H,H} = 3.6 Hz, 1H), 7.29-

8.18 (m, 17H, Ar); ^{13}C NMR (100.6 MHz, $\text{C}_6\text{D}_5\text{CD}_3$) δ : 26.9 (1C), 27.4 (1C), 29.3 (1C), 30.5 (1C), 30.8 (1C), 32.0-32.4 (24C), 34.1 (1C), 35.1-36.4 (8C), 71.8 (1C), 72.1 (1C), 73.4 (d, $J_{\text{P,C}} = 9.4$ Hz, 1C), 77.8 (1C), 79.8 (1C), 85.3 (1C), 106.1 (1C), 112.4 (1C), 124.5-147.7 (40C, Ar); ^{31}P NMR (161.97 MHz, $\text{C}_6\text{D}_5\text{CD}_3$) δ : 144.1 (d, $J_{\text{P,P}} = 35.1$ Hz, 1P), 146.4 (d, $J_{\text{P,P}} = 35.3$ Hz, 1P). **ESI-HRMS**: Calculated for $\text{C}_{85}\text{H}_{110}\text{O}_{10}\text{P}_2$. Exact: (M: 1352,7574, M+Na: 1375,7472); Experimental (M+Na: 1375.7457).

[Rh(acac)(3.27)] (3.39)



Compound **3.27** (96.4 mg, 0.07 mmol) in CH_2Cl_2 (3 mL) was added to a $[\text{Rh}(\text{acac})(\text{CO})_2]$ (15.8 mg, 0.06 mmol) solution in CH_2Cl_2 (2 mL), and the reaction was left stirring for 16h.

Then, the solvent was evaporated and the resulting residue purified by flash chromatography (Toluene, 1% NE_3) to afford compound **3.39** (30 mg, 33%) as yellow solid.

^1H NMR (400 MHz, CD_2Cl_2) δ : 1.04 (s, 9H), 1.06 (s, 3H), 1.25 (s, 3H), 1.29 (s, 3H), 1.40 (s, 9H), 1.41 (s, 9H), 1.43 (s, 9H), 1.59 (s, 9H), 1.72 (s, 9H), 1.73 (s, 9H), 1.79 (s, 9H), 3.32 (d, $J_{\text{H,H}} = 3.6$ Hz, 1H), 3.64 (m, 2H), 4.25 (d, $J_{\text{H,H}} = 12$ Hz, 1H), 4.47 (m, 1H), 4.63 (m, 1H), 4.66 (d, $J_{\text{H,H}} = 12$ Hz, 1H), 4.83 (m, 1H), 5.23 (s, 1H), 5.37 (d, $J_{\text{H,H}} = 2.4$ Hz, 1H), 7.18-8.20 (m, 17H, Ar); ^{13}C NMR (100.6 MHz, CD_2Cl_2) δ : 26.6 (1C), 27.4 (1C), 34.6-36.3 (32C), 70.29 (1C), 71.9 (1C), 74.3 (1C), 76.9 (1C), 77.8 (1C), 77.8 (1C), 99.7 (1C), 106.4 (1C), 112.7 (1C), 123.3-147.2 (40C, Ar), 185.2 (1C), 185.3 (1C); ^{31}P NMR (161.97 MHz, CD_2Cl_2) δ : 142.9 (m, 1P), 144.8 (m, 1P). **ESI-HRMS**: Calculated for $\text{C}_{87}\text{H}_{111}\text{O}_{12}\text{P}_2\text{Rh}$. Exact: (M: 1512.6606, M+Na: 1535.6504); Experimental (M+Na: 1535.6486).

(2 mL), and the reaction was left stirring for 1h. Then, the complex was precipitated with pentane, and washed with pentane several times to afford **3.41** (160 mg, 97%) as an orange solid.

¹H NMR (400 MHz, CD₂Cl₂) δ: 0.98 (s, 3H), 1.10 (s, 3H), 1.30 (s, 9H), 1.39 (s, 9H), 1.40 (s, 9H), 1.42 (s, 9H), 1.43 (s, 9H), 1.55 (s, 9H), 1.73 (bs, 9H), 1.76 (s, 9H), 1.81 (m, 4H), 2.02 (m, 2H), 2.28 (m, 6H), 2.75 (m, 1H), 2.93(m, 2H), 3.31 (m, 4H), 4.61 (m, 2H), 4.89 (m, 1H), 4.99 (m, 1H) , 5.05 (m, 1H), 5.67 (d, $J_{H,H} = 3.6$ Hz, 1H), 5.98 (m, 2H), 7.16-8.20 (m, 17H, Ar); **¹³C NMR** (100.6 MHz, CD₂Cl₂) δ: 26.4 (1C), 26.8 (1C), 28.9-36.3 (40C), 70.7 (1C), 76.2 (1C), 77.6 (1C), 81.8 (1C), 84.1 (d, $J_{P,C} = 3.4$ Hz, 1C), 102.7 (1C), 103.5 (1C), 105.6 (1C), 112.8 (1C), 113.1 (1C), 114.7 (1C), 123.6-149.9 (40C, Ar); **³¹P NMR** (161.97 MHz, CD₂Cl₂) δ: 123.8 (m, 1P), 125.4 (m, 1P). **ESI-HRMS**: Calculated for C₉₃H₁₂₂O₁₀P₂Rh. Exact: (M⁺: 1563.7568); Experimental (M⁺: 1563.7561).

3.5.3. AHF Experiments in batch

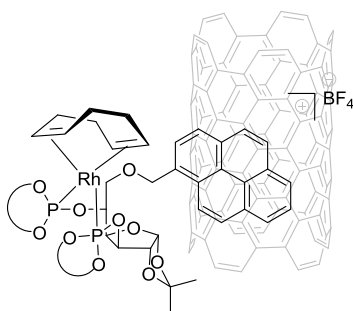
General procedure: In a typical experiment, the autoclave was filled in the glovebox with a solution of rhodium catalyst, the corresponding quantities of diphosphite and norbornene **3.2** in toluene. Then, the autoclave was purged 3 times with CO, and finally pressurised to the appropriate pressure of CO/H₂, heated at the desired pressure and left stirring. After the desired time the autoclave was cooled using in ice bath for 20 min and depressurised. Conversion and stereoselectivity were determined immediately after catalysis by ¹H NMR spectroscopy and GC-MS analysis of the crude of the reaction without evaporation of the solvent.

AHF in batch using homogeneous catalysts: General procedure was followed using rhodium catalyst (0.012 mmol), the corresponding quantities of diphosphite (0.013 mmol) if necessary, and norbornene **3.2** (19.2 mmol) in toluene (5 mL).

AHF in batch using heterogenized catalyst: General procedure was followed using rhodium catalyst (0.36 μmol) and norbornene **3.2** (0.36 mmol) in toluene (1 mL).

3.5.4. Immobilization of Rh complexes onto carbon materials

The experimental procedure describes the immobilization of rhodium complexes onto MWCNTs. The same procedure was applied for the other carbon materials.



In a Schlenck flask, 150 mg of MWCNTs were added to a solution of EtOAc (15 mL). The mixture was sonicated in an ultrasound bath for 30 min in order to disperse the MWCNTs. After that, complex **3.40** (50 mg) was added to the previous suspension, and the reaction was left stirring at

room temperature for 16h. Then, the solid was filtrated, and washed with EtOAc (3 x 5 mL), and dried under vacuum to yield the heterogenized catalyst (80 mg, Rh content by ICP = 0.45 wt %).

Entry	Catalyst	Support (mg)	Complex (mg)	Rh (wt %) ^a
1	3.40@MWCNTs	150	50	0.45
2	3.41@MWCNTs	730	240	0.41
3	3.41@N-MWCNTs	45	15	1.13
4	3.41@S-MWCNTs	45	15	2.21
5	3.41@rGO	150	50	0.48
6	3.41@CBs	150	50	0.56

^a Determined by ICP analysis of the solid.

3.5.5. In situ HP NMR spectroscopy

In a typical HP-NMR experiment, a sapphire tube ($\varnothing = 5$ mm) was filled in the glovebox with a solution of $[\text{Rh}(\text{acac})(\text{CO})_2]$ (2.1-2 mM) and ligand (molar ratio PP/Rh = 1.1) in toluene- d_8 (0.5 mL). The solution was analysed by ^1H and ^{31}P NMR spectroscopy. Next the HP-NMR tube was purged 3 times with CO and pressurised to the appropriate pressure of H_2/CO . After 24h at 45°C , the solution was analysed by multinuclear NMR spectroscopy.

3.5.6. Determination of the enantiomeric excess

0.1 mL from the crude of the reaction was dissolved in MeOH (1 mL) in a vial with a magnetic stirrer, and then cooled to 0°C with an ice bath. To the previous solution, NaBH_4 (1 eq.) was added and left stirring for 12 h. The reaction was quenched with H_2O (1 mL), extracted with Et_2O (3 x 1 mL), dried with MgSO_4 and filtrated. The enantiomeric excess of the resulting alcohol was measured by GC.

Gas chromatography method: CP Chirasil-Dex CB, 25 m column, internal diameter: 0.25 mm, film thickness: $0.25\ \mu\text{m}$, carrier gas 50 kPa He, temperature: 100°C for 5 min, rate $6^\circ\text{C}/\text{min}$ to 130°C and hold for 2 min, rate $2^\circ\text{C}/\text{min}$ to 150°C and hold for 5 min, $t_{r\ \text{major}} = 17.1$ min, $t_{r\ \text{minor}} = 16.8$ min.

3.5.7. Set-up for the continuous asymmetric hydroformylation of norbornene using the U-Shape reactor

Preparation of the substrate stock solution

In a 500 mL flask under inert atmosphere, a concentration of 0.75 M of norbornene was built up by exactly weighing the added amount of substrate, and then adding the corresponding amount of EtOAc. After complete dissolution of norbornene, the flask was connected to the HPLC pump and a balloon filled with argon was connected to the flask.

Packing of the supported catalyst in the U-Shape reactor

Under inert atmosphere, the desired amount of catalyst was weighted in a GC vial and diluted with silica to a total volume of 0.8 mL. Glass wool was added on the left side of the U-Shape reactor tube, then the mixture of heterogenized catalyst with silica, and finally packed with glass wool on the top. On the right side, glass wool was added, then glass beads until a total height of 30 cm, and finally packed with glass wool. Then, the U-Shape reactor tube was connected to the flow system under inert atmosphere to run the AHF experiments.

Setting reaction parameters, sample collection and sample analysis

First, nitrogen was added by means of MFC into the system for 30 min. Secondly, the U-Shape reactor was connected to the system. After that, the pressure of the system was increased with a pressure valve regulator until the desired total pressure. Then, the nitrogen flow was stopped and the syngas mixture was introduced to the system by means of MFC. When the pressure was stable for 30 min, the substrate solution was pumped into the system via HPLC pump. The solution was collected at the end of the system in a cold trap, which was cooled using isopropanol and dry ice. The samples were collected every 10 min, 0.1 mL of each sample was diluted in 1 mL and analyzed by GC-MS to determine the conversion, and *exo*-selectivity. Another sample of 0.1 mL was reduced into the alcohol in order to determine the enantiomeric excess via chiral GC analysis.

3.6. References

- ¹ a) Bournaud, C.; Lecourt, T.; Micouin, L.; Méliet, C.; Agbossou-Niedercorn, F. *Eur. J. Org. Chem.* **2008**, *2008*, 2298-2302. b) Parrinello, G.; Stille, J. K. *J. Am. Chem. Soc.* **1987**, *109*, 7122-7127.
- ² a) Sémeril, D.; Matt, D.; Toupet, L. *Chem. Eur. J.* **2008**, *14*, 7144-7155. b) Monnereau, L.; Sémeril, D.; Matt, D.; Toupet, L. *Adv. Synth. Catal.* **2009**, *351*, 1629-1636.
- ³ V. Gusevskaya, E.; Jiménez-Pinto, J.; Börner, A. *ChemCatChem* **2014**, *6*, 382-411.
- ⁴ a) Huang, J.; Bunel, E.; Allgeier, A.; Tedrow, J.; Storz, T.; Preston, J.; Correll, T.; Manley, D.; Soukup, T.; Jensen, R.; Syed, R.; Moniz, G.; Larsen, R.; Martinelli, M.; Reider, P. J. *Tetrahedron Lett.* **2005**, *46*, 7831-7834. b) Noonan, G. M.; Cobley, C. J.; Lebl, T.; Clarke, M. L. *Chem. Eur. J.* **2010**, *16*, 12788-12791.
- ⁵ Blanco, C., *Norbornene functionalization through asymmetric Pd- and Rh-catalyzed carbonylation processes*, PhD thesis, Universitat Rovira i Virgili, Tarragona, Spain, **2010**.
- ⁶ a) Chen, R. J.; Zhang, Y.; Wang, D.; Dai, H. *J. Am. Chem. Soc.* **2001**, *123*, 3838-3839. b) Chen, J.; Chen, W.; Zhu, D. *Environ. Sci. Technol.* **2008**, *42*, 7225-7230.
- ⁷ a) Martinez, C. R.; Iverson, B. L. *Chem. Sci.* **2012**, *3*, 2191-2201. b) Estarellas, C., *Theoretical and experimental study of cooperative effects in noncovalent interactions*, PhD thesis, Illes Balears University, Spain, **2012**.
- ⁸ Janiak, C. *J. Chem. Soc., Dalton Trans.* **2000**, 3885-3896.
- ⁹ Tournus, F.; Latil, S.; Heggie, M. I.; Charlier, J. C. *Phys. Rev. B* **2005**, *72*, 075431.
- ¹⁰ Liang, X.; Jian-Hua, X.; Yong-Sheng, C.; Li-Xin, W.; Qi-Lin, Z. *Adv. Synth. Catal.* **2008**, *350*, 1013-1016.
- ¹¹ Liu, G.; Wu, B.; Zhang, J.; Wang, X.; Shao, M.; Wang, J. *Inorg. Chem.* **2009**, *48*, 2383-2390.
- ¹² Keller, M.; Collière, V.; Reiser, O.; Caminade, A. M.; Majoral, J. P.; Ouali, A. *Angew. Chem. Int. Ed.* **2013**, *52*, 3626-3629.

- ¹³ a) Sabater, S.; Mata, J. A.; Peris, E. *ACS Catal.* **2014**, *4*, 2038-2047. b) Sabater, S.; Mata, J. A.; Peris, E. *Organometallics* **2015**, *34*, 1186-1190. c) Ruiz-Botella, S.; Peris, E. *ChemCatChem* **2018**, *10*, 1874-1881.
- ¹⁴ Vriamont, C.; Devillers, M.; Riant, O.; Hermans, S. *Chem. Eur. J.* **2013**, *19*, 12009-12017.
- ¹⁵ Li, F.; Zhang, B.; Li, X.; Jiang, Y.; Chen, L.; Li, Y.; Sun, L. *Angew. Chem. Int. Ed.* **2011**, *50*, 12276-12279.
- ¹⁶ Creus, J.; Matheu, R.; Peñafiel, I.; Moonshiram, D.; Blondeau, P.; Benet-Buchholz, J.; García-Antón, J.; Sala, X.; Godard, C.; Llobet, A. *Angew. Chem. Int. Ed.* **2016**, *55*, 15382-15386.
- ¹⁷ a) Janssen, M.; Wilting, J.; Müller, C.; Vogt, D. *Angew. Chem. Int. Ed.* **2010**, *49*, 7738-7741. b) Webb, P. B.; Kunene, T. E.; Cole-Hamilton, D. J. *Green Chem.* **2005**, *7*, 373-379. c) Fang, J.; Jana, R.; Tunge, J. A.; Subramaniam, B. *Appl. Catal., A* **2011**, *393*, 294-301.
- ¹⁸ a) Nozaki, K.; Itoi, Y.; Shibahara, F.; Shirakawa, E.; Ohta, T.; Takaya, H.; Hiyama, T. *J. Am. Chem. Soc.* **1998**, *120*, 4051-4052. b) Nozaki, K.; Shibahara, F.; Itoi, Y.; Shirakawa, E.; Ohta, T.; Takaya, H.; Hiyama, T. *Bull. Chem. Soc. Jpn.* **1999**, *72*, 1911-1918. c) Shibahara, F.; Nozaki, K.; Matsuo, T.; Hiyama, T. *Bioorg. Med. Chem. Lett.* **2002**, *12*, 1825-1827.
- ¹⁹ Shibahara, F.; Nozaki, K.; Hiyama, T. *J. Am. Chem. Soc.* **2003**, *125*, 8555-8560.
- ²⁰ Adint, T. T.; Landis, C. R. *J. Am. Chem. Soc.* **2014**, *136*, 7943-7953.
- ²¹ Gual, A.; Godard, C.; Castillón, S.; Claver, C. *Adv. Synth. Catal.* **2010**, *352*, 463-477.
- ²² Gual, A.; Godard, C.; Claver, C.; Castillón, S. *Eur. J. Org. Chem.* **2009**, *2009*, 1191-1201.
- ²³ *Mechanisms in Homogeneous Catalysis*, Eds. Heaton, B. Wiley-VCH, Darmstadt, Germany, **2005**.
- ²⁴ García-Suárez, E. J.; Menéndez-Vázquez, C.; García, A. B. *J. Mol. Liq.* **2012**, *169*, 37-42.
- ²⁵ Hübner, S.; de Vries, J. G.; Farina, V. *Adv. Synth. Catal.* **2016**, *358*, 3-25.

Chapter 3

²⁶ Watkins, A. L.; Landis, C. R. *J. Am. Chem. Soc.* **2010**, *132*, 10306-10317.

²⁷ Abrams, M. L.; Buser, J. Y.; Calvin, J. R.; Johnson, M. D.; Jones, B. R.; Lambertus, G.; Landis, C. R.; Martinelli, J. R.; May, S. A.; McFarland, A. D.; Stout, J. R. *Org. Process Res. Dev.* **2016**, *20*, 901-910.

²⁸ Cabré, A., *Supported and non-supported palladium and ruthenium complexes bearing chiral NHC-ligands for selective oxidative transformations*, Master thesis, Universitat Autònoma de Barcelona, Universitat Rovira i Virgili, **2015**.

Chapter 4

Rhodium catalyzed asymmetric HAM of α -alkyl acrylates

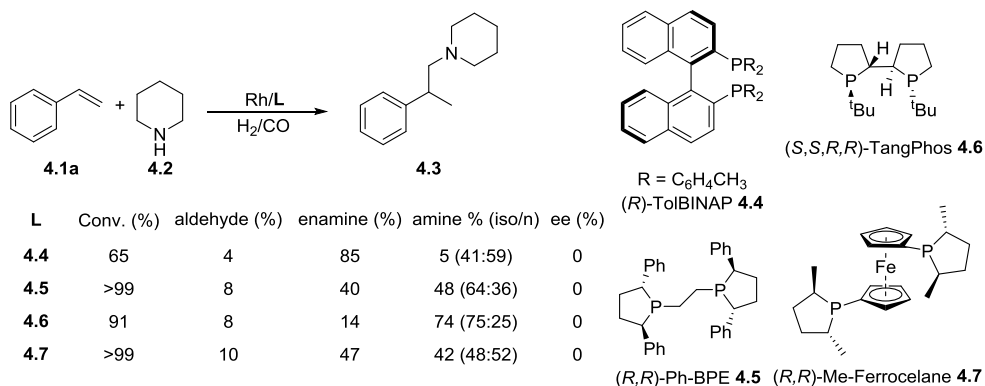
UNIVERSITAT ROVIRA I VIRGILI
RH-CATALYZED CARBOXYLATION OF DISUBSTITUTED OLEFINS: ASYMMETRIC CATALYSIS, CONTINUOUS
FLOW AND TANDEM HYDROAMINOMETHYLATION REACTION
Anton Cunillera Martin

4.1. Introduction

4.1.1. Rh-catalyzed asymmetric hydroaminomethylation

The rhodium catalyzed hydroaminomethylation of alkenes revealed a promising strategy for the production of amines.¹ Moreover, the possibility to obtain chiral amines via asymmetric hydroaminomethylation constitutes an interesting strategy. Nonetheless, to the best of our knowledge, there are no reports on the asymmetric version of this reaction using a single catalyst.

Kalck and co-workers performed a thorough study on the asymmetric hydroaminomethylation of styrene **4.1a** with piperidine **4.2** using a broad scope of chiral diphosphine ligands, which are very efficient in asymmetric hydroformylation and asymmetric hydrogenation (Scheme 4.1).² Moreover, the study was completed by HP-NMR investigations and DFT calculations.



Scheme 4.1: Rh-catalyzed hydroaminomethylation of **4.1** with **4.2** using ligands **4.4**, **4.5**, **4.6** and **4.7**.

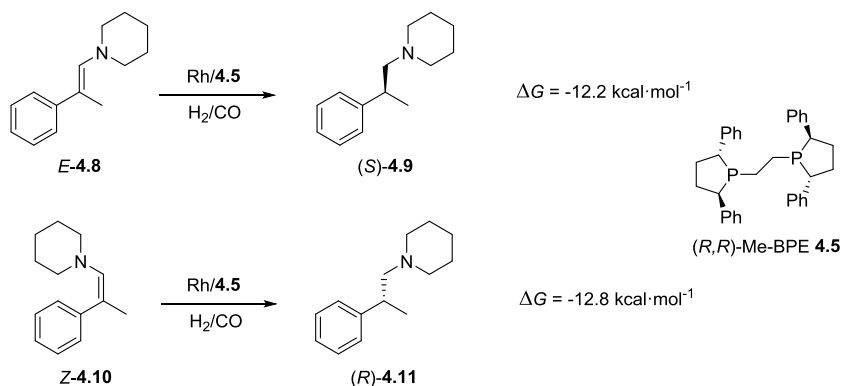
These are only some examples of ligands applied by Kalck *et al.*

In this case, it was observed that the hydroformylation and condensation proceed rapidly; however, the hydrogenation step is more complicated since the branched enamine is conjugated to the aryl ring. Therefore, the hydrogenation of the enamine is the rate determining step. The enantioselectivity is induced in the

hydrogenation step, since the chiral information obtained in the hydroformylation step is lost after the condensation of the amine with the chiral aldehyde.

High to full conversion were afforded, good chemo- and regioselectivity towards the branched intermediates was also obtained, but only diphospholane ligand **4.6** provided the amine with high selectivity (Scheme 4.1). Despite the successful results obtained and the study of various reaction conditions, in all the cases no enantiomeric excess was afforded.

As observed by NMR spectroscopy, upon condensation of the amine, two enamines **4** can be generated, (*E*)- and (*Z*)-enamine. The asymmetric hydrogenation of these enamines will lead to the (*S*)- or (*R*)-product respectively. At this point of the study, DFT calculations demonstrated that the hydrogenation of both enamines is equivalent in energy (Scheme 4.2). Thus, no enantiomeric excess can be obtained with this system.



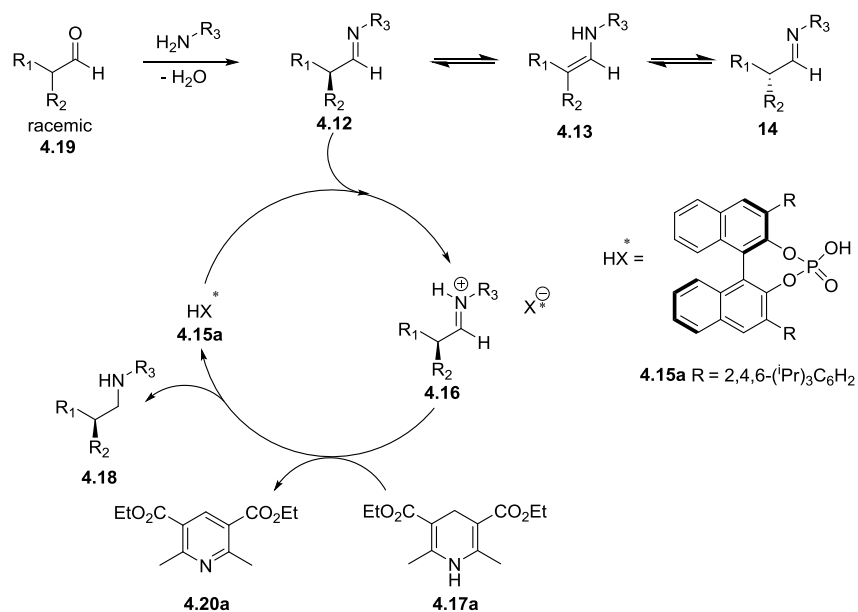
Scheme 4.2: Energy values for the hydrogenation of *E*-enamine **4.8** and *Z*-enamine **4.10**.

In view of this issue, several groups attempted to overcome this issue using alternative approaches to conventional HAM.

List and co-workers reported the catalytic asymmetric amination of aldehydes via dynamic kinetic resolution.³ Such strategy takes profit of the imine-enamine equilibrium (**4.12-4.13-4.14**), in which racemization produces both enantiomers (**4.12** and **4.14**), by the use of a chiral phosphoric acid **4.15a** that promotes the

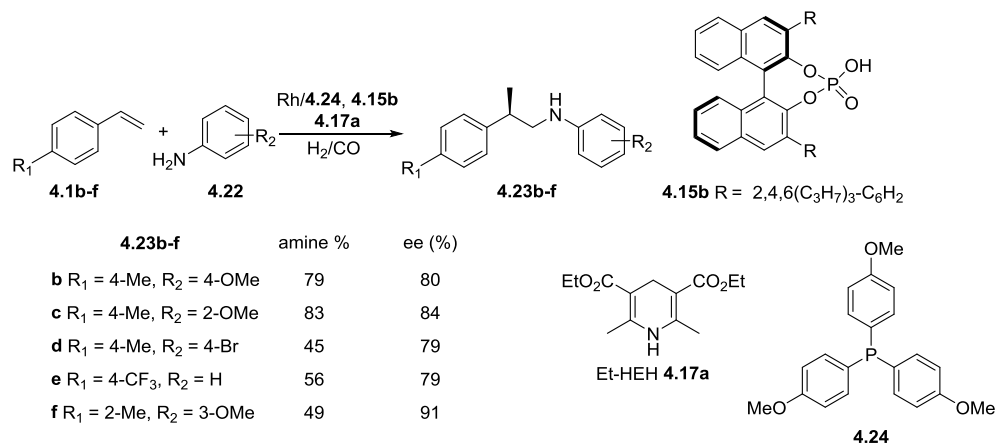
Rhodium catalyzed asymmetric HAM of α -alkyl acrylates

formation of an iminium **4.16** of only one enantiomer, which is later reduced with a Hantzsch ester (HEH) **4.17a** to afford the chiral amine **4.18** (Scheme 4.3).



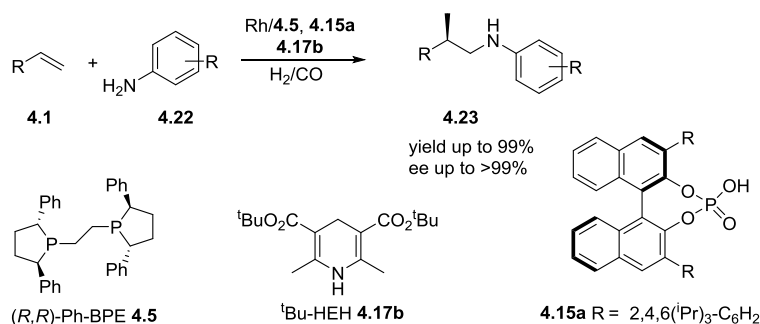
Scheme 4.3: Dynamic kinetic reductive amination of aldehydes developed by List *et al.*

Xiao and co-workers adapted this methodology to the rhodium catalyzed HAM in a metal and organo-catalyzed asymmetric hydroaminomethylation (Scheme 4.4).⁴ Instead of aldehydes as starting materials, the system works as a conventional HAM of styrene derivatives **4.1b-f** to produce the corresponding branched aldehyde via rhodium catalyzed hydroformylation, subsequently, the condensation takes place to produce the corresponding imine, which is reduced via the same strategy depicted in Scheme 4.3 to produce the final amine **4.21** in moderate to good yield, and moderate to excellent enantioselectivities (Scheme 4.4). The system required stoichiometric amounts of Et-HEH **4.17a**, the use of a chiral phosphoric acid **4.15b** in catalytic amounts, long reaction times (up to 72h), and the system is limited to aniline derivatives.



Scheme 4.4: Rh- and organocatalyzed asymmetric hydroaminomethylation of **4.1** with **4.22**.

Recently, Han et al. improved the system by using (*R,R*)-Ph-BPE ligand **4.5** in the hydroformylation, phosphoric acid **4.15b** and *t*Bu-HEH **4.17b**.⁵ These changes allowed reducing the total pressure to 1 bar, use lower temperatures, and provide amines **4.23** in higher yields and enantioselectivities compared with the system used by Xiao and co-workers (Scheme 4.5). Moreover, the scope of alkenes was expanded to other aromatic groups such as thiophene, and other olefins such as acrylamides and acrylates. However, the reaction still requires long reaction times (up to 72h), additional reagents, and the system is still limited to aniline derivatives.

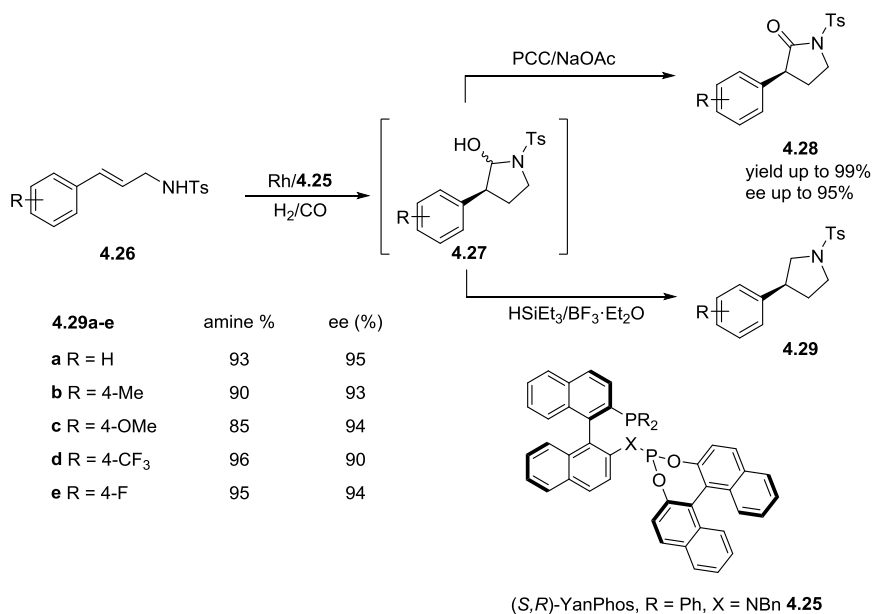


Scheme 4.5: Improved system in the metal and organocatalyzed asymmetric HAM of **4.1** with **4.22** reported by Han and co-workers.

Rhodium catalyzed asymmetric HAM of α -alkyl acrylates

In contrast to the previous strategy, Zhang et. al. recently reported the so called interrupted hydroaminomethylation of *trans*-1,2-disubstituted olefins (Scheme 4.6).⁶ In order to avoid the problems produced in the equilibrium between imines and enamines, Zhang and co-workers interrupted the formation of these species by the use of external oxidants or reducing agents.

The system used (*S,R*)-YanPhos **4.25** as ligand in the asymmetric hydroformylation of 3-substituted allyl amines **4.26**, then intramolecular condensation provided a stable hemiacetal **4.27** that was either oxidized to the chiral pyrrolidinones **4.28** using pyridinium chlorochromate (PCC) or reduced to the chiral pyrrolidines **4.29** using triethylsilane and boron trifluoride diethyl etherate.



Scheme 4.6: Rh-catalyzed asymmetric interrupted hydroaminomethylation of **4.26** using **4.25** as ligand for the obtention of **4.28** or **4.29**.

Both **4.28** and **4.29** were afforded in excellent yields (up to 99%) and excellent enantioselectivities (up to 95%). Interestingly, the enantioselectivity is determined in the hydroformylation step in contrast to the classical approach where the enantioselectivity is induced in the hydrogenation step.

Moreover, the system is tolerant to different heteroaryl groups, substituent with different electronic properties on the aromatic ring, and the possibility to expand the new ring from 5 to 6 members. However, the system suffered from drawbacks such as long reaction times (up to 70h), the requirement of additional reagents in stoichiometric amount, some of them very toxic such as PCC, and the restriction to tosyl group in the amine moiety. Despite these disadvantages, the molecules afforded were envisioned as possible intermediates for the synthesis Vernakalant⁷ and Enablex⁸.

In conclusion, there are no examples of rhodium catalyzed asymmetric hydroaminomethylation of olefins using one single metal catalyst. Therefore, the development of a system capable to induce enantioselectivity using a single catalyst would be a more efficient system to the production of chiral nitrogen containing molecules.

4.1.2. γ -amino butyric acids (GABA)

Among amine containing molecules, amino acids are the most crucial molecules in human life, since they do not only have relevant biological activity, but also act as precursors for the synthesis of hormones and low-molecular weight nitrogenous substances with each having biological importance.⁹

γ -amino acids act as major inhibitory transmitters in the mammalian central nervous system.¹⁰ Furthermore, GABA derivatives with substituents in the carbon chain have been applied in the treatment of diseases and disorders including anxiety, depression, epilepsy, autism spectrum disorder, stroke, drug and neurodegenerative disorders: Huntington's disease, Parkinson's disease and Alzheimer's disease.¹¹ Some examples of medicines containing γ -amino acid motif commercialized by pharmaceutical agents are Baclofen **4.30**,¹² Pregabalin **4.31**,¹³ Vigabatrin **4.32**,¹⁴ and Phenibut **4.33**.¹⁵ (Figure 4.1).

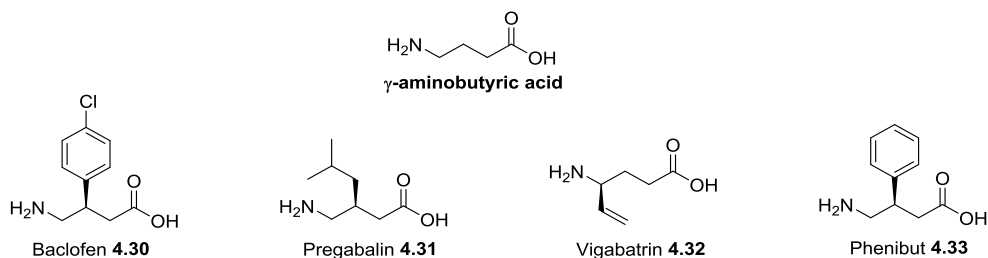
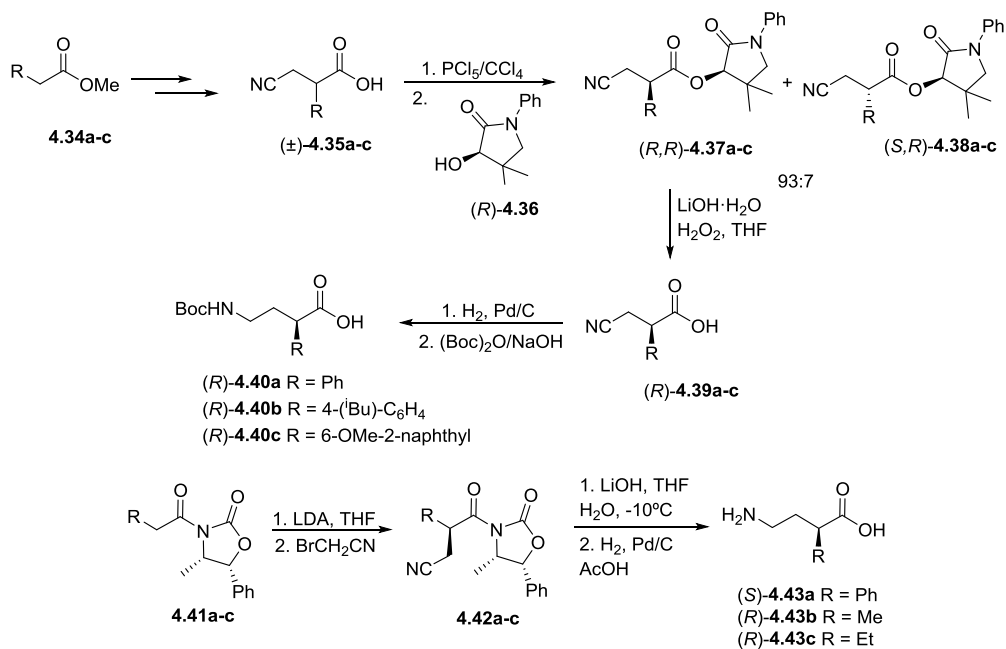
Rhodium catalyzed asymmetric HAM of α -alkyl acrylates

Figure 4.1: Biological active molecules containing γ -aminobutyric acids.

The development of efficient synthetic routes towards chiral GABA has been of interest throughout the recent years.¹⁶ For instance, α -substituted- γ -aminobutyric acids have been synthesized via different strategies (Scheme 4.7). The product is obtained enantiomerically pure after a final enantioresolution step.

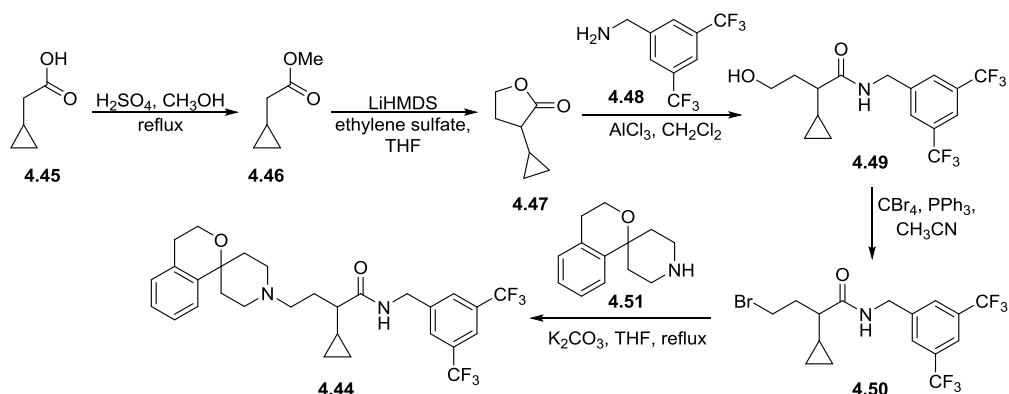


Scheme 4.7: Two examples of synthetic strategies reported for the synthesis of α -substituted- γ -aminobutyric acids.

Apart from the interest for GABA, derivatives containing amides or esters groups can also display biological activity. For example, GABA motif containing amide groups **4.44** has recently been evaluated as CCR2 antagonists for chronic inflammatory processes, such as atherosclerosis, multiple sclerosis and

Chapter 4

rheumatoid arthritis.¹⁷ However, the synthesis of these molecules also requires huge synthetic efforts (Scheme 4.8).



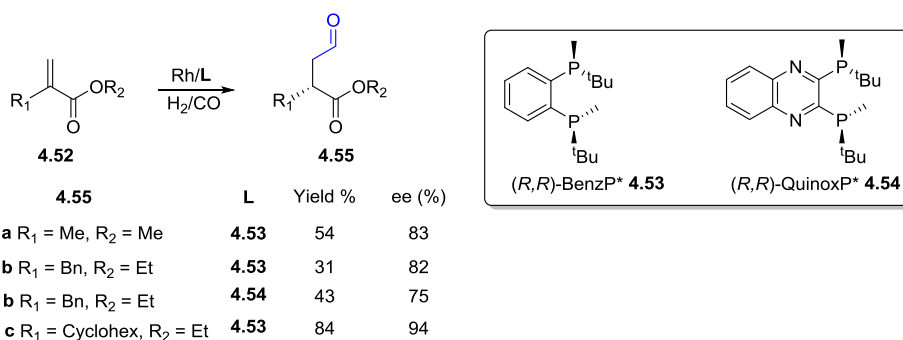
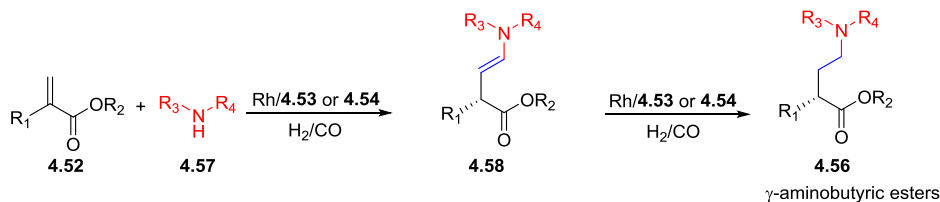
Scheme 4.8: Synthesis of CCR2 antagonist 4.44.

The possibility to access chiral GABA and derivatives through a more direct approach to reduce the number of synthetic steps would thus be interesting. In this context, the rhodium catalyzed asymmetric hydroaminomethylation would be an attractive and simple approach to access the α -substituted- γ -aminobutyric acid scaffold. On one hand, the number of synthetic steps would be reduced, and on the other hand, the production of enantio-enriched GABA motifs would not require the use of chiral auxiliaries to induce enantioselectivity, and would avoid an enantioresolution process to separate the enantiomers.

As described in chapter 1, the rhodium catalyzed asymmetric hydroformylation can provide chiral aldehydes with high enantioselectivity. Thus, induction of the chirality in the HAM through the asymmetric hydroformylation of the appropriate substrate would provide chiral amines. The Rh-catalyzed asymmetric hydroformylation of α -alkyl acrylates 4.52 was reported by Buchwald and co-workers using (R,R) -BenzP* 4.53 and (R,R) -QuinoxP* 4.54 with for the production of lineal aldehyde 4.55 in excellent yields and enantioselectivities (Scheme 4.9).¹⁸ If the rhodium catalyzed asymmetric hydroaminomethylation using one of these P-chirogenic ligands is carried out on α -alkyl acrylates 4.52, the enantioselectivity would be induced in the hydroformylation step (Scheme 4.9). Then, the

Rhodium catalyzed asymmetric HAM of α -alkyl acrylates

condensation and equilibrium imine/enamine would not affect the chiral information. Finally, the catalytic system containing ligands (*R,R*)-BenzP* **4.53** or (*R,R*)-QuinoxP* **4.54** should smoothly hydrogenate the enamine or imine, since they proved to be efficient for the hydrogenation of a large number of unsaturated compounds.¹⁹ This strategy could provide access to chiral γ -aminobutyric esters **4.56** in a simple and elegant approach (Scheme 4.9).

Buchwald asymmetric hydroformylation of α -alkyl acrylates:Proposed strategy in this work to access chiral γ -aminobutyric esters:

Scheme 4.9: Top: Rh-catalyzed AHF acrylates **4.52** using ligands **4.53** or **4.54**. Bottom: Strategy for the synthesis of γ -aminobutyric esters **4.56** via Rh-catalyzed asymmetric HAM using **4.53** or **4.54**.

4.2. Objectives of this chapter

The main objective of this chapter is the development of an asymmetric version of the rhodium catalyzed hydroaminomethylation of alkenes for the production of chiral amines.

The specific objectives of this chapter are:

- The synthesis of γ -aminobutyric esters via rhodium catalyzed asymmetric hydroaminomethylation of α -alkyl acrylates **4.52** using P-chirogenic ligands (*R,R*)-BenzP* **4.53** and (*R,R*)-QuinoxP* **4.54**.
- The study of the effect of syngas pressure, rhodium precursors and solvent in the HAM reaction of α -alkyl acrylates **4.52**
- The study of the effect of different substituents on α -position of α -alkyl acrylates **4.52**.
- The study of the effect of secondary and primary amines on the reaction outcome.
- The study of the reactivity towards CO, H₂ and H₂/CO pressures of the rhodium precursors in the presence of amines, and in the presence of the α -alkyl acrylates **4.52** using HP NMR spectroscopy.

4.3. Results and discussion

4.3.1. Optimization of the reaction conditions

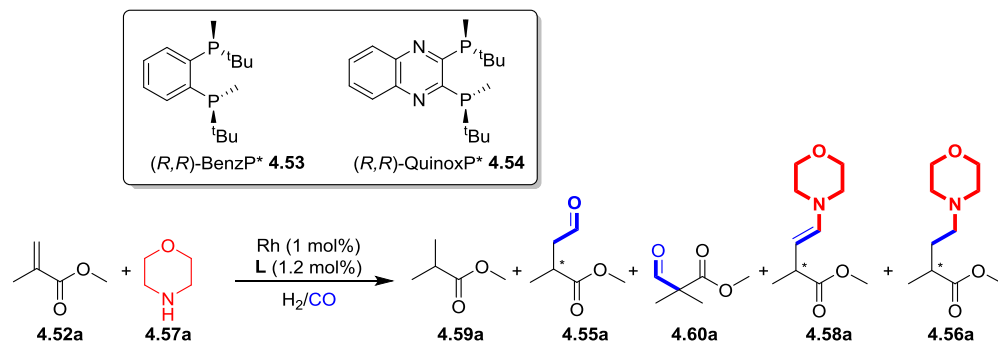
To conduct the rhodium catalyzed asymmetric hydroaminomethylation of α -alkyl acrylates **4.52** with amines, a short optimization of the reaction conditions was carried out using methyl methacrylate **4.52a**, morpholine **4.57a**, and (*R,R*)-QuinoxP* **4.54** as ligand (Table 4.1).

First, the reaction conditions reported for the asymmetric hydroformylation of **4.52a** were tested using the [Rh(acac)(CO)₂] precursor, toluene as solvent, 10 bar H₂/CO (4:1), and 90°C in the presence of morpholine **4.57a** (entry 1, Table 4.1).¹⁸ Under these conditions, complete conversion of the methyl methacrylate **4.52a** was observed, but the final amino ester **4.56a** was not detected. Instead, the main reaction product was the linear enamine **4.58a**. Moreover, 40 % of hydrogenated alkene **4.59a**, 5 % of linear aldehyde **4.55a**, and 9 % of branched aldehyde **4.60a** were also detected. When the partial CO pressure was increased, a major amount of branched aldehyde **4.60a** (52%) and less linear enamine **4.58a** (28%) were

Rhodium catalyzed asymmetric HAM of α -alkyl acrylates

obtained; however the amino ester **4.56a** was still not detected (entry 2, Table 4.1). When the total pressure was increased to 20 bar (entry 3, Table 4.1), no hydrogenation of the linear enamine **4.58a** was observed. However, the selectivity towards the alkene hydrogenation product **4.59a** (up to 60%) increased.

Table 4.1: Optimization of the reaction conditions for the asymmetric hydroaminomethylation of **4.52a** with **4.57a**.



Entry ^a	Conv. (%) ^b	L	4.59a ^b	4.55a ^b	4.60a ^b	4.58a ^b	4.56a [Y] ^b	ee (%) ^c
1	>99	4.53	40	5	9	45	-	-
2 ^d	>99	4.53	18	2	52	28	-	-
3 ^e	>99	4.53	60	12	8	20	-	-
4 ^f	96	4.53	33	10	11	4	38 [30]	72
5 ^g	>99	4.53	31	-	6	-	63 [60]	73
6 ^g	91	4.54	59	-	4	-	28 [20]	70

^a Reaction conditions: **4.52a** (0.5 mmol), **4.57a** (0.5 mmol), [Rh(acac)(CO)₂] (1 mol%), L (1.2 mol %), P = 10 bar (H₂/CO, 4:1), toluene (0.4 ml), T = 90°C, t = 16 h. ^b % Conversion and yield determined by ¹H NMR spectroscopy using naphthalene as internal standard, values in brackets refer to isolated yields. ^c ee of **4.56a** determined by HPLC. ^d P = 10 bar (H₂/CO, 1:1). ^e P = 20 bar (H₂/CO, 4:1). ^f tol./DCE (1:1, 0.4 ml). ^g [Rh(COD)₂]₂BF₄ (1 mol%), tol./DCE (1:1, 0.4 ml).

Interestingly, when a mixture of toluene/1,2-dichloroethane (DCE) was used as solvent, the amino ester **4.56a** was the major product (38% by ¹H NMR) isolated in 30% yield and with ee of 72% (entry 4, Table 4.1). This result confirmed that the

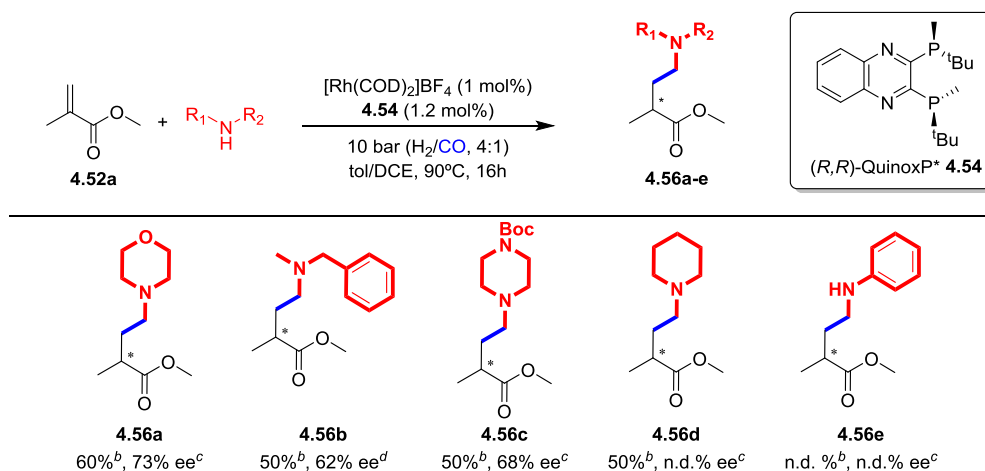
chirality was induced in the hydroformylation step and was maintained through the reaction. It is expected that DCE facilitates the solubility of cationic species involved in the hydrogenation of the enamine **4.58a**. At this point, the cationic precursor $[\text{Rh}(\text{COD})_2]\text{BF}_4$ (entry 5, Table 4.1) was tested and provided the chiral amino ester **4.56a** in 60% isolated yield (63% by ^1H NMR) and 73% of enantiomeric excess. Moreover, neither the enamine **4.58a** nor the linear aldehyde **4.55a** were detected. Finally, the ligand (*R,R*)-BenzP* **4.53** was tested under optimized conditions (entry 5, Table 4.1). Nevertheless, the amino ester **4.56a** was isolated in 20% yield (28% by ^1H NMR) and 70% ee (entry 6, Table 4.1). Furthermore, higher amount of the alkene hydrogenation product **4.59a** (59%) was afforded compared to the ligand (*R,R*)-QuinoxP* **4.54** (up to 31%) under these conditions (entry 5, Table 4.1). Therefore, it was concluded that the system containing the ligand (*R,R*)-QuinoxP* **4.54**, a cationic rhodium precursor and a mixture of toluene/DCE as solvents was convenient to perform the asymmetric hydroaminomethylation of methyl methacrylate **4.52a** with morpholine **4.57a** at 10 bar H_2/CO (4:1) and 90°C. Moreover, it was observed that the solvent has an important role, since neutral precursor is only able to complete the reaction when used with toluene/DCE, while using toluene, the reaction stops at the enamine **4.58a**. Similar effect of the solvent was already observed by Clarke and co-workers in the HAM of styrene **4.1a** with morpholine **4.57a**, in which reaction was not completed in toluene and using neutral $[\text{Rh}(\text{acac})(\text{CO})_2]$.²⁰ These results suggested that the presence of a polar medium is necessary to achieve hydrogenation of the enamine intermediate, which could be due to the low solubility of cationic Rh species that are active in this reduction step.

With these conditions in hand (entry 5, Table 4.1), the scope of amines used in the HAM of methyl methacrylate **4.52a** was extended (Table 4.2). The secondary amines in general provided similar yields (up to 50%), and similar enantioselectivities (up to 68%) than morpholine **4.57a**. Moreover, the reaction was tolerant to different protecting groups such as benzyl or Boc of amino esters

Rhodium catalyzed asymmetric HAM of α -alkyl acrylates

4.56b and **4.56c**, in which the protecting group is maintained and allow further functionalization of the molecule. In the case of the amino ester **4.56d**, the enantiomeric excess could not be measured either by chiral HPLC of the ester or the corresponding alcohol, nor by ^1H NMR spectroscopy using $\text{Eu}(\text{hcf})_3$. Nonetheless, similar ee to the other secondary amines would be expected.

Table 4.2: Rh-catalyzed asymmetric hydrominomethylation of **4.56a** with different amines.



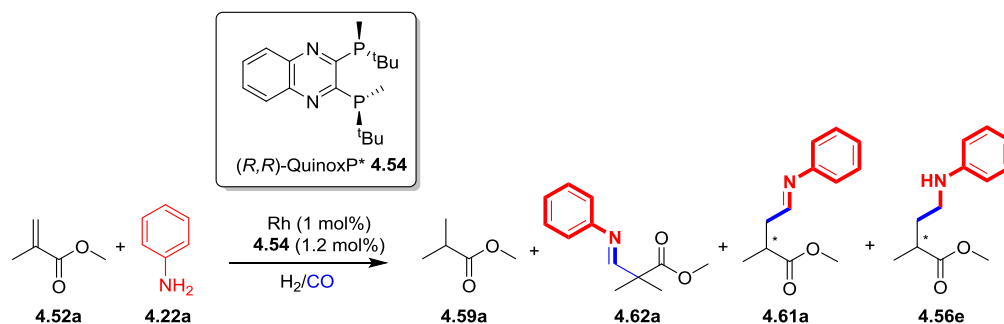
^a Reaction conditions: **4.52a** (0.5 mmol), amine (0.5 mmol), Rh (1 mol%), **4.54** (1.2 mol %), P = 10 bar (H_2/CO , 4:1), tol/DCE (1:1, 0.4 ml), T = 90°C , t = 16h. ^b Isolated yields obtained from two independent runs. ^c ee determined by HPLC. ^d ee determined by HPLC after reduction into the alcohol.

When the reaction was performed with aniline **4.22a**, very low conversion of methyl methacrylate **4.52a** was detected, and only the alkene hydrogenation product **4.59a** and linear imine **4.61a** were observed in low yields by ^1H NMR spectroscopy (entry 1, Table 4.3).

The use of (R,R) -QuinoxP* **4.54** as ligand and $[\text{Rh}(\text{acac})(\text{CO})_2]$ as precursor in toluene (entry 2, Table 4.3), provided full conversion of methyl methacrylate **4.52a**, and the imine intermediates **4.61a** and **4.62a** in poor yields (11 and 18% respectively by ^1H NMR). Furthermore, high amounts of the alkene hydrogenation product **4.59a** (up to 69%) were detected by ^1H NMR spectroscopy. Changing the

solvent from toluene to toluene/DCE mixture provided amino ester **4.56e** in 12% yield and 60% of enantiomeric excess (entry 3, Table 4.3). The increase of the catalyst loading up to 2 mol % afforded amino ester **4.56e** in higher amounts (26% by ^1H NMR spectroscopy) and the enantioselectivity was maintained to 60%; however, hydrogenation of the alkene remained an important issue (entry 4, Table 4.3).

Table 4.3: Optimization of reaction conditions for the asymmetric hydroaminomethylation of **4.52a** with **4.22a**.



Entry ^a	Rh	Conv. (%) ^b	4.59a ^b	4.62e ^b	4.61a ^b	4.56e [Y] ^b	ee (%) ^c
1 ^d	[Rh(COD) ₂]BF ₄	22	16	-	6	-	-
2	[Rh(acac)(CO) ₂]	>99	69	11	18	-	-
3 ^d	[Rh(acac)(CO) ₂]	>99	66	6	16	12 [11]	60
4 ^e	[Rh(acac)(CO) ₂]	>99	51	6	16	26 [19]	60
5 ^f	[Rh(COD) ₂]BF ₄	77	28	16	17	16 [15]	40

^a Reaction conditions: **4.52a** (0.5 mmol), **4.22a** (0.5 mmol), Rh (1 mol%), **4.54** (1.2 mol %), P = 10 bar (H₂/CO, 4:1), toluene (0.4 ml), T = 90°C, t = 16h. ^b % conversion and yield determined by ^1H NMR using naphthalene as internal standard, values in bracket refer to isolated yields. ^c ee determined by HPLC. ^d to/DCE (1:1, 0.4 ml). ^e Rh (2 mol%), **4.54** (2.4 mol%), to/DCE (1:1, 0.4 ml). ^f NEt₃ (0.5 mol%), to/DCE (1:1, 0.4 ml).

In previous reports, the amine was described as a base to facilitate the formation of mono-hydride species when cationic precursors are used.²¹ Therefore, triethylamine (NEt₃) was tested as external base with the cationic rhodium precursor (entry 5, Table 4.3). Interestingly, the conversion increased to 77%.

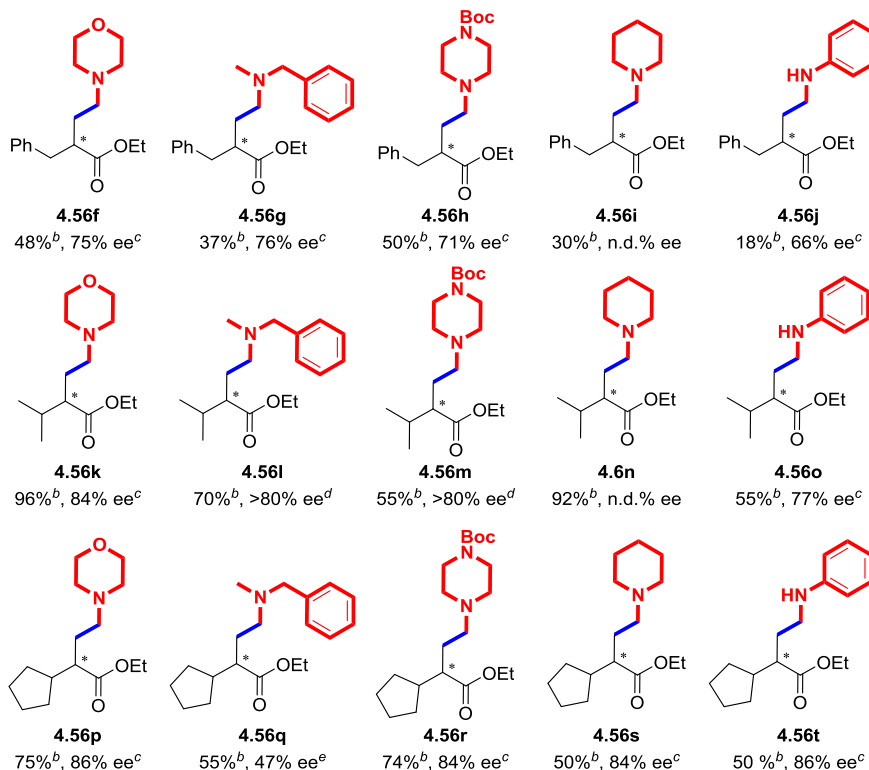
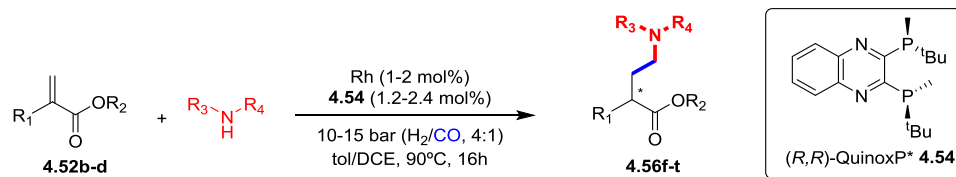
Moreover, the imines **4.61a** and **4.62a** were detected in 17 and 16% yield respectively, and the amino ester **4.56e** was observed in 16% yield by ^1H NMR spectroscopy and 40% of ee. Thus, it is clear that triethylamine had an effect in the activity when a cationic precursor was used, but the enantioselectivity was reduced.

In conclusion, it was decided to use the conditions described in entry 4 (Table 4.3) for the subsequent experiments using aniline **4.22a** as amine. As expected, the use of the neutral precursor favored the hydroformylation (entry 2, Table 4.3); however, the higher amount of alkene hydrogenated compared to the case of morpholine **4.57a**, suggests that aniline **4.22a** plays a role in catalysis. Moreover, the basicity of the amine was important to achieve activity and chemoselectivity when the cationic precursor is used, since the use of NEt_3 increased the conversion from 22% (entry 1, Table 4.3) to 77% (entry 5, Table 4.3), and more hydroformylation products were obtained.

4.3.2. Rh-catalyzed asymmetric HAM of various α -alkyl acrylates

At this stage, various α -alkyl acrylates **4.52** bearing distinct alkyl substituents at the α -position were tested as substrates (Table 4.4). A broad scope chiral of γ -aminobutyric esters was afforded in moderate to excellent yields (up to 96%), and good to high enantioselectivities (up to 86%). For GABA derivative **4.56f-j** bearing a benzyl group, slightly lower yields were obtained compared those bearing a methyl group, but the enantiomeric excess increased (up to 76%). The GABA derivatives **4.56s-t** containing isopropyl and cyclopentyl groups provided the best results in terms of yield (up to 96%) and enantioselectivity (up to 86%). Nonetheless, the increase in steric hindrance also required small modifications of the reaction conditions. For instance, in the case of isopropyl, an increase of the total pressure to 15 bar was required to achieve full conversion.

Chapter 4

Table 4.4: Substrate scope of α -alkyl acrylates **4.52** for the Rh-catalyzed asymmetric hydroaminomethylation with various amines.

^a Reaction conditions: **4.52** (0.5 mmol), amine (0.5 mmol), [Rh(COD)₂]BF₄ (1 mol%), **4.54** (1.2 mol%), P = 10 bar (H₂/CO, 4:1), toluene/DCE (1:1, 0.4 ml), T = 90°C, t = 16h. For **4.56k-o** P = 15 bar. For **4.56p-s** Rh (1.5 mol%) and **4.54** (1.8 mol%). For **4.56j, o, t** Rh = [Rh(acac)(CO)₂] (2 mol%). ^b Isolated yields obtained from two independent runs. ^c ee determined by HPLC. ^d ee determined by ¹H NMR spectroscopy using Eu(hcf)₃. ^e ee determined by HPLC after reduction to the alcohol.

In the case of α -alkyl acrylates containing a cyclopentyl group, a slight increase of the catalyst loading (up to 1.5 mol %) was necessary to afford full conversion. The reaction proved to be tolerant to benzyl and Boc groups independently of the acrylate used. Interestingly, in the case of amino ester **4.56s** it was possible to

determine the enantiomeric excess, and it was confirmed that when piperidine is used as amine, the enantioinduction is maintained. For amino ester **4.56q** the enantiomeric excess was determined by HPLC after reduction of the product into the analogous alcohol. The lower ee value obtained (47%) indicated the possibility of a racemization process during the reduction.

In conclusion, a broad scope of chiral γ -aminobutyric esters **4.56** was obtained via rhodium catalyzed asymmetric hydroaminomethylation using a single catalyst. Furthermore, this reaction constitutes the first report of Rh-catalyzed asymmetric hydroaminomethylation using one single catalyst. An explanation for the lower yield obtained with the substrate bearing a benzyl substituent is the isomerization of the alkene to form a more stable trisubstituted olefin, which is more difficult to hydroformylate. Such isomerization was already observed by other groups using this substrate.¹⁸⁻²²

4.3.3. HP-NMR studies

In order to gain understanding about the species present during catalysis, various HP-NMR experiments were conducted under different reaction conditions. It was decided to work under the optimized reaction conditions previously described (entry 5, Table 4.1) using the cationic precursor $[\text{Rh}(\text{COD})_2]\text{BF}_4$, (*R,R*)-QuinoxP* **4.54**, a mixture of solvents (toluene- d^8 /DCE, 1:1) in a total volume of 0.4 ml.

The reactivity of $[\text{Rh}(\text{COD})_2]\text{BF}_4$ with (*R,R*)-QuinoxP* **4.54** was studied by mixing them at room temperature inside a 5 mm HP-NMR tube for 1 hour. When the solution was analyzed by ^{31}P NMR spectroscopy, two phosphorus signals were detected as doublets at 38.9 ($J_{\text{Rh,P}} = 130$ Hz) and 41.6 ppm ($J_{\text{Rh,P}} = 148$ Hz) (Figure 4.2). The multiplicity and coupling constants of these signals suggested the coordination of the phosphorus at the rhodium center. These resonances were therefore attributed to $[\text{Rh}(\text{COD})(\mathbf{4.54})]\text{BF}_4$ **4.63** species where only one COD ligand has been displaced by the ligand **4.54**, while the other corresponds to

$[\text{Rh}(\mathbf{4.54})_2]\text{BF}_4$ **4.64** species bearing two (R,R) -QuinoxP* **4.54** coordinated molecules.

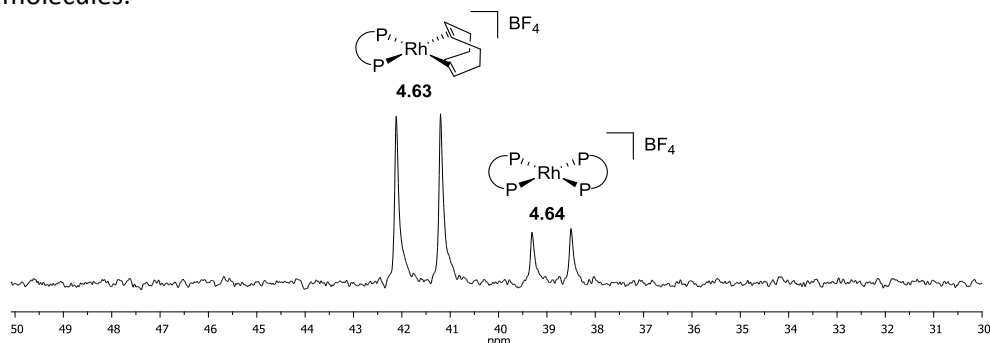


Figure 4.2: $^{31}\text{P}\{^1\text{H}\}$ NMR spectrum of $[\text{Rh}(\text{COD})_2]\text{BF}_4$ in the presence of **4.54** in $\text{tol-d}^8/\text{DCE}$.

In order to corroborate this hypothesis, both rhodium complexes **4.63** and **4.64** were isolated and characterized by NMR spectroscopy and MS spectrometry. Moreover, crystals suitable for X-ray diffraction (XRD) were obtained by vapor diffusion of pentane into a CH_2Cl_2 solution containing the complex $[\text{Rh}(\text{COD})(\mathbf{4.54})]\text{BF}_4$ **4.63** (Figure 4.3) and complex $[\text{Rh}(\mathbf{4.54})_2]\text{BF}_4$ **4.64** (Figure 4.4).

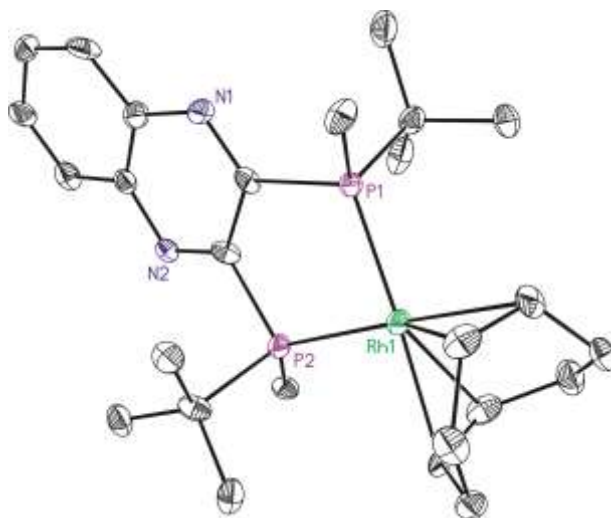


Figure 4.3: ORTEP drawing of the complex $[\text{Rh}(\text{COD})(\mathbf{4.54})]\text{BF}_4$ **4.63** (with ellipsoid at 50% probability). Solvent molecules, H, B and F atoms are omitted for clarity and only partial labelling scheme is illustrated.

Rhodium catalyzed asymmetric HAM of α -alkyl acrylates**Table 4.5:** Selected bond lengths (Å) and angles (°) for complex **4.63**.

Bond lengths			
Rh-P(1)	2.258 (3)	Rh-C(20)	2.304 (11)
Rh-P(2)	2.267 (3)	Rh-C(23)	2.236 (10)
Rh-C(19)	2.204 (13)	Rh-C(24)	2.292 (10)
Angles			
P(1)-Rh-P(2)	85.43 (10)	C(20)-Rh-(C24)	86.8 (4)
C(19)-Rh-(C23)	95.9 (4)		

In the case of complex $[\text{Rh}(\text{COD})(\mathbf{4.54})]\text{BF}_4$ **4.63**, the coordination sphere around the rhodium atom was found to correspond to a distorted square planar geometry, with P(1)-Rh-P(2) bond *cis*-angle of 85.43 (10) °, together with C(19)-Rh-(C23) and C(20)-Rh-C(24) bond *cis*-angle of 95.9 (4) ° and 86.8 (4) ° respectively (Table 4.5). The Rh-P(1) and Rh-P(2) distances were found to be 2.258 (3) and 2.267 (3) Å respectively. All these values agree with those reported for similar cationic rhodium (I) complexes bearing (*R,R*)-QuinoxP* **4.54** and COD as ligands and hexafluoro antimonate as counter ion.¹⁹

The molecular structure of complex $[\text{Rh}(\mathbf{4.54})_2]\text{BF}_4$ **4.64** presents a square planar geometry (Figure 4.4) with a small distortion presumably due to (*R,R*)-QuinoxP* **4.54** bite *cis*-angle of *ca.* 85° (Table 4.6).

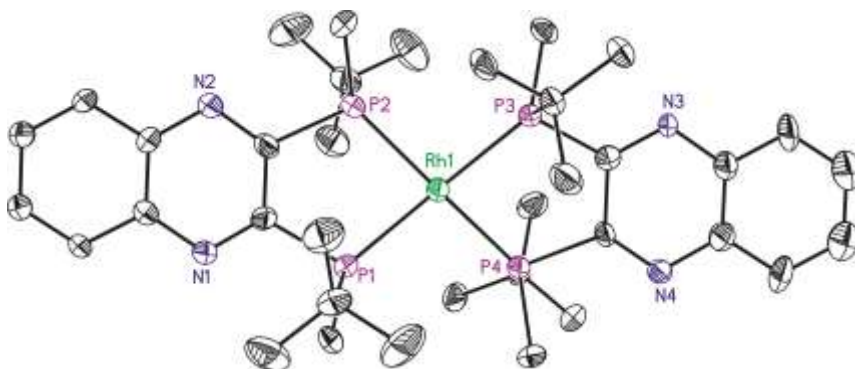


Figure 4.4: ORTEP drawing of the complex $[\text{Rh}(\mathbf{4.54})_2]\text{BF}_4$ **4.64** (with ellipsoid at 50% probability). Solvent molecules, H, B and F atoms are omitted for clarity and only partial labelling scheme is illustrated.

The Rh-P(1) and Rh-P(2) distances were found to be 2.317 (3) and 2.316 (3) Å respectively, while Rh-P(3) and Rh-P(4) present slightly shorter distances (2.305 (9) and 2.294 (9) Å respectively (Table 4.6). All these values agree with those reported for similar cationic rhodium (I) complexes bearing (*R,R*)-DuPhos.²³

Table 4.6: Selected bond lengths (Å) and angles (°) for complex **4.64**.

Bond lengths			
Rh-P(1)	2.317 (17)	Rh-P(3)	2.305(9)
Rh-P(2)	2.316 (17)	Rh-P(4)	2.294(9)
Angles			
P(1)-Rh-P(2)	84.79(6)	P(2)-Rh-P(4)	160.79(19)
P(1)-Rh-P(3)	163.5(2)	P(3)-Rh-P(4)	85.5(3)
P(1)-Rh-P(4)	98.15(19)		
P(2)-Rh-P(3)	97.02(2)		

Reactivity of [Rh(COD)₂]BF₄ in the presence of (*R,R*)-QuinoxP* under CO pressure

Next, HP-NMR studies were performed with the cationic complex [Rh(COD)₂]BF₄ in the presence of the (*R,R*)-QuinoxP* ligand **4.54** under variable CO pressure in a mixture of toluene-d⁸/DCE. First, the solution was pressurized at 10 bar of CO and stirred for 24h at room temperature. Under these conditions, the previously detected species [Rh(COD)(**4.54**)]BF₄ **4.63** was not observed and a new signal at 47.2 ppm was detected as a doublet (*J*_{Rh,P} = 115 Hz) by ³¹P NMR spectroscopy ((a), Figure 4.5). It is noteworthy that the resonance corresponding to species [Rh(**4.54**)₂]BF₄ **4.64** was still present in the mixture. Progressively increasing the CO pressure and reaction time (up to 30 bar and 96 hours) promoted almost full consumption of [Rh(**4.54**)₂]BF₄ **4.64** ((b), Figure 4.5). The resulting solution was analyzed by IR after depressurizing the HP-NMR tube, and two carbonyl characteristic bands at 2097 and 2051 cm⁻¹.

These results indicated that the corresponding species was [Rh(**4.54**)(CO)₂]BF₄ **4.65**, bearing two CO ligands in *cis* with ligand **4.54** in a square planar geometry.²¹

Rhodium catalyzed asymmetric HAM of α -alkyl acrylates

Furthermore, the species $[\text{Rh}(\mathbf{4.54})(\text{CO})_2]\text{BF}_4$ **4.65** was synthesized by bubbling CO into a solution of $[\text{Rh}(\text{COD})(\mathbf{4.54})]\text{BF}_4$ **4.63** in DCM, and characterized by NMR and IR spectroscopy.

Finally, when the HP-NMR tube was heated at 90°C for 16h ((c), Figure 4.5), a new signal was detected at 48.7 ppm as a doublet ($J_{\text{Rh,P}} = 116$ Hz) by ^{31}P NMR spectroscopy. The nature of this signal was attributed to a $[\text{Rh}(\mathbf{4.54})(\text{CO})_3]\text{BF}_4$ **4.66** species bearing three CO ligands, which was confirmed by IR spectrometry of the solution with the presence of three characteristic bands at 2120, 2086 and 2041 cm^{-1} .²¹

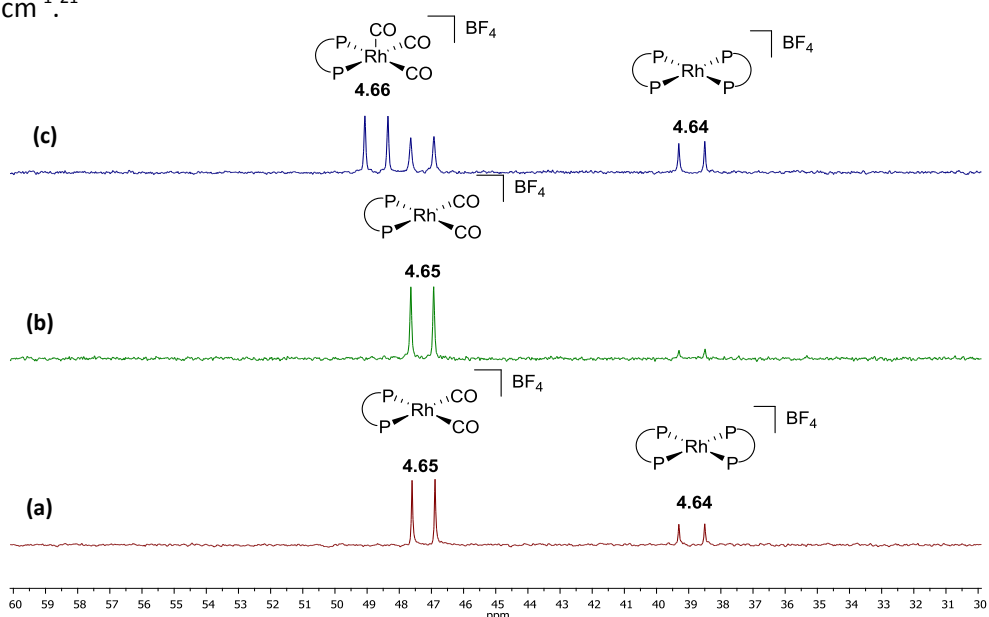
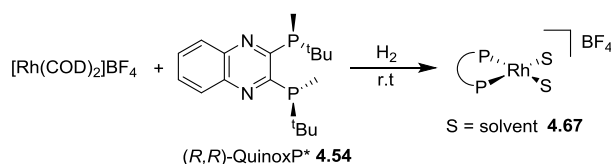


Figure 4.5: $^{31}\text{P}\{^1\text{H}\}$ NMR spectra of $[\text{Rh}(\text{COD})_2]\text{BF}_4$ and **4.54** in $\text{tol-d}^8/\text{DCE}$ at variable CO pressures and temperatures: a) 10 bar of CO for 16h at room temperature, b) 30 bar CO for 96h at room temperature, c) 10 bar at room temperature for 16h, then 10 bar of CO at 90°C for 16 h.

In conclusion, the rhodium species **4.63** rapidly reacted with CO to generate the complex $[\text{Rh}(\mathbf{4.54})(\text{CO})_2]\text{BF}_4$ **4.65** at room temperature, and species $[\text{Rh}(\mathbf{4.54})(\text{CO})_3]\text{BF}_4$ **4.66** at 90°C (Scheme 4.10). On the other hand, the species $[\text{Rh}(\mathbf{4.54})_2]\text{BF}_4$ **4.64** proved to be more robust and required longer reaction time, and higher pressures (up to 30 bar CO) to be converted into $[\text{Rh}(\mathbf{4.54})(\text{CO})_2]\text{BF}_4$ **4.65**. These observations are in agreement with previous reports.²¹

Rhodium catalyzed asymmetric HAM of α -alkyl acrylates

complex and the remaining ligands are speculated to be solvent. Imamoto *et al.* reported rhodium dihydride species with two molecules of solvents coordinated to the rhodium center using diphosphine ligands.²⁴ In this report, the signals corresponding to the hydride and the phosphorus were detected at low temperature (-90°C). Furthermore, the stability of this species is highly dependent on the counter ion, for instance, cationic rhodium species bearing BF_4^- as anion are less stable than those bearing BAr_f^- .²⁵ Despite the weak coordination ability of DCE as solvent, there are reports in the literature of cationic diphosphine rhodium complexes with DCM coordinated to the metal center.²⁶ Taking into account all this information, the identity of this species was attributed to $[\text{Rh}(\text{S})_2(\mathbf{4.54})]\text{BF}_4$ **4.67** with two solvent molecules coordinated to the Rh center.



Scheme 4.11: Reactivity of $[\text{Rh}(\text{COD})_2]\text{BF}_4$ in the presence of **4.54** under H_2 pressure.

Reactivity of $[\text{Rh}(\text{COD})_2]\text{BF}_4$ in the presence of (R,R)-QuinoxP* under H_2/CO pressure

The system $[\text{Rh}(\text{COD})_2]\text{BF}_4/\mathbf{4.54}$ was submitted to 10 bar (H_2/CO , 4:1) of syngas at 90°C for 24h as the catalytic conditions ((a), Figure 4.7). Under these conditions, the signals corresponding to the previously identified species $[\text{Rh}(\mathbf{4.54})(\text{CO})_2]\text{BF}_4$ **4.65** and $[\text{Rh}(\mathbf{4.54})(\text{CO})_3]\text{BF}_4$ **4.66** (Figure 4.5) were detected by ^{31}P NMR spectroscopy. Moreover, the species $[\text{Rh}(\mathbf{4.54})_2]\text{BF}_4$ **4.64** was also identified. When the pressure was increased to 20 bar (H_2/CO , 4:1) at 90°C for another 24h, the signal corresponding to dicarbonyl species **4.65** completely disappeared and the signal corresponding to $[\text{Rh}(\mathbf{4.54})]\text{BF}_4$ **4.64** was almost consumed, while tricarbonyl complex **4.66** was the major species in solution. No hydride signal was detected in the corresponding ^1H NMR spectra ((b), Figure 4.7).

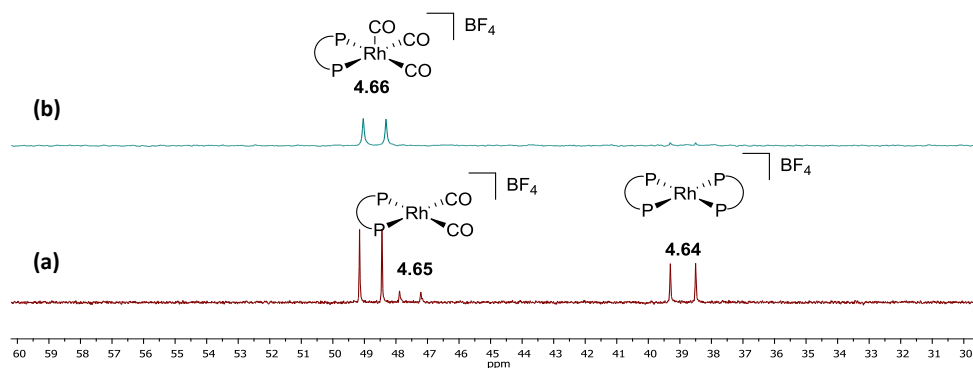
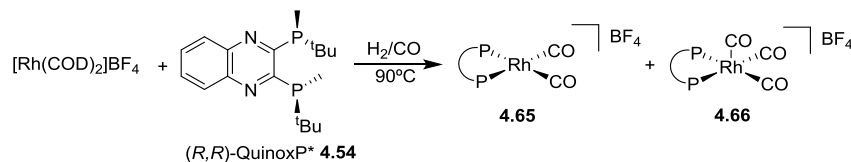


Figure 4.7: $^{31}\text{P}\{^1\text{H}\}$ NMR spectra of $[\text{Rh}(\text{COD})_2]\text{BF}_4$ and **4.54** in $\text{tol-d}^8/\text{DCE}$ at various H_2/CO pressures and at 90°C : a) 10 bar (H_2/CO , 4:1) for 24h, b) 20 bar (H_2/CO , 4:1) for 48 h.

It was therefore concluded that no rhodium hydride species was generated using the cationic rhodium precursor and ligand **4.54** under H_2/CO pressure. Instead, signals corresponding to species dicarbonyl **4.65** and tricarbonyl **4.66** rhodium species were detected (Scheme 4.12). However, this result was not consistent with the results afforded in catalysis (entry 5, Table 4.1) where the hydroformylation of the alkene takes place. At this stage, it was thus decided to study the role of the amine in the catalysis via HP-NMR spectroscopy.



Scheme 4.12: Reactivity of $[\text{Rh}(\text{COD})_2]\text{BF}_4$ in the presence of ligand **4.54** under H_2/CO pressure.

Reactivity of $[\text{Rh}(\text{COD})_2]\text{BF}_4$ in the presence of (R,R) -QuinoxP* and morpholine under H_2/CO pressure

The subsequent experiments were carried out in the presence of morpholine **4.57a**. 100 equivalents (referred to 1 equivalent of $[\text{Rh}(\text{COD})_2]\text{BF}_4$) were added to the 5 mm HP-NMR tube together with the $[\text{Rh}(\text{COD})_2]\text{BF}_4$ complex, ligand **4.54**, pressurized at 20 bar H_2/CO (4:1) and heated at 90°C for 16h. Under these conditions, two signals were detected as doublets by ^{31}P NMR spectroscopy at 48.9 ($J_{\text{Rh,P}} = 115.5$ Hz) and 51.6 ($J_{\text{Rh,P}} = 114.7$ Hz) ppm respectively (Figure 4.8). When

Rhodium catalyzed asymmetric HAM of α -alkyl acrylates

the solution was analyzed by ^1H NMR spectroscopy, two hydride signals were detected as triplet of doublet at -8.5 ($J_{\text{Rh,H}} = 10.4$ Hz, $J_{\text{P,H}} = 57.6$ Hz) and -9.0 ($J_{\text{Rh,H}} = 12.4$ Hz, $J_{\text{P,H}} = 62.8$ Hz) ppm (Figure 4.8). Furthermore, terminal carbonyls coordinated to rhodium were also detected by ^{13}C NMR spectroscopy as doublet of triplets at 199.3 ($J_{\text{P,C}} = 11.6$ Hz, $J_{\text{Rh,C}} = 69.7$ Hz) and 199.1 ppm ($J_{\text{P,C}} = 10.8$ Hz, $J_{\text{Rh,C}} = 68.8$ Hz). When the same experiments was carried out using neutral precursor $[\text{Rh}(\text{acac})(\text{CO})_2]$, under syngas but in the absence of morpholine, both signals corresponding to rhodium species **4.68** and **4.69** were again detected by ^1H NMR spectroscopy under these conditions. Thus, it was concluded that these 2 species did not contain any amine ligand.

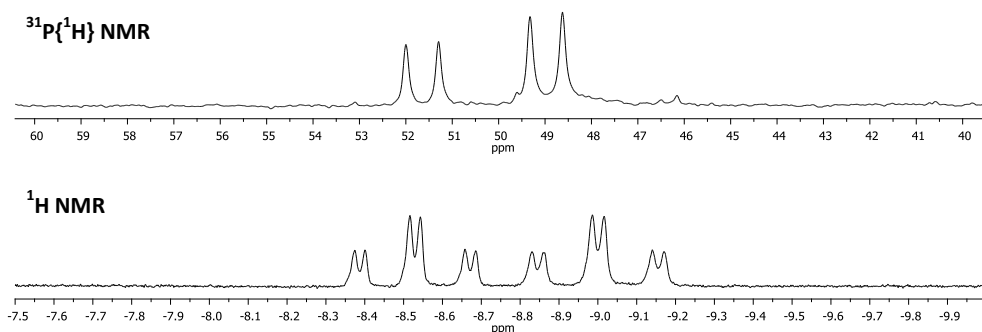


Figure 4.8: NMR spectra from of $[\text{Rh}(\text{COD})_2]\text{BF}_4$ in the presence of **4.54** and morpholine **4.57a** under H_2/CO pressure Top: $^{31}\text{P}\{^1\text{H}\}$ NMR spectra. Bottom: ^1H NMR spectra.

Analysis of the ^1H NMR spectrum revealed the presence of two set of signals: two doublet of doublets at 7.3 ppm and 8.0 ppm, corresponding to the expected resonance of a quinoxaline backbone, while the second set of signals included two doublet of doublets at 6.4 ppm and 5.7 ppm and the broad singlet at 4.0 ppm. In the alkylic region of the spectrum, several signals corresponding to protonated acetylacetonate and several methyl and tert-butyl groups were also detected (Figure 4.9). ^1H - ^{31}P Heteronuclear Multiple Bond Correlation (HMBC) exhibited correlation between the hydride signal at -8.5 ppm corresponding and the phosphorus signal at 51.6 ppm in $^{31}\text{P}\{^1\text{H}\}$ NMR spectrum.

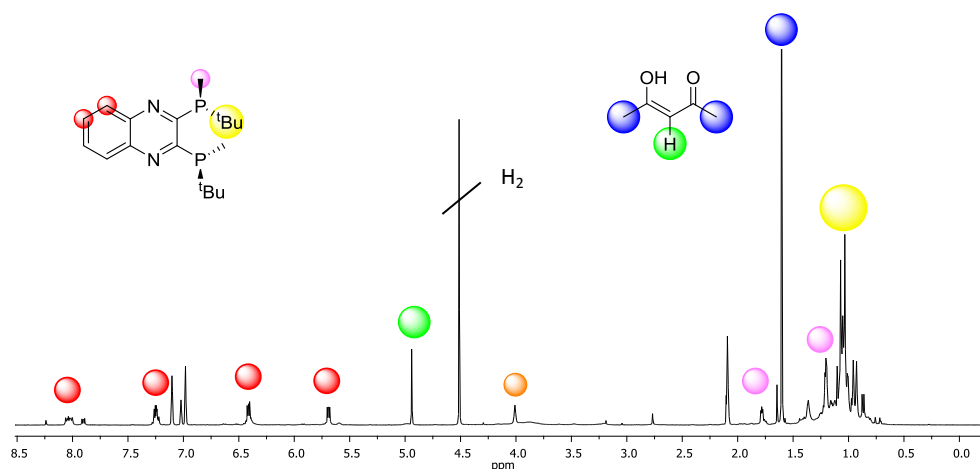


Figure 4.9: ^1H NMR spectra of $[\text{Rh}(\text{acac})(\text{CO})_2]$ in the presence of ligand **4.54** in tol-d^8 under 20 bar (H_2/CO , 4:1), at 90°C , for 16h. Red: quinaxoline backbone; green and blue: protonated acac; purple: methyl groups from quinaxoline; yellow: ^tBu groups quinaxoline; orange: new signal at 4 ppm.

The second hydride signal at -9.0 ppm in ^1H NMR spectra and the resonance at 4.0 ppm showed correlation with the phosphorus signal at 48.9 ppm. This experiment indicated the formation of two Rh-H species: species **4.68** containing a (*R,R*)-QuinoxP* **4.54** ligand unaltered while the 2nd species **4.69** contained a “modified” (*R,R*)-QuinoxP* **4.54** ligand. In this latter species, the ^1H NMR signal at 4.0 ppm revealed close in space to the proton at 5.7 ppm by ^1H - ^1H NOESY technique. 1D and 2D ^{13}C NMR spectroscopy experiments were also carried out. The data obtained are summary in Figure 4.10 and Table 4.7 and Table 4.8.

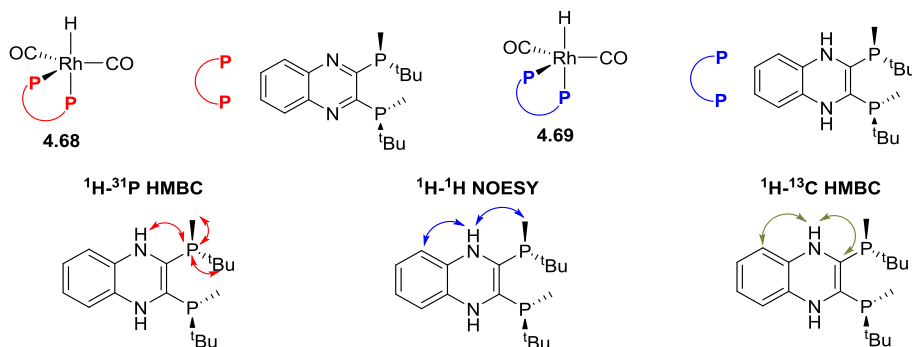


Figure 4.10: Top: Proposed structure for species **4.68** and **4.69**. Bottom: Correlations observed via 2D NMR experiments between signal at 4 ppm and the rest of quinaxoline backbone from species **4.69**.

Rhodium catalyzed asymmetric HAM of α -alkyl acrylates

Table 4.7: Selected spectroscopic data of the rhodium coordination sphere from rhodium complexes **4.68** and **4.69**.

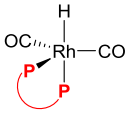
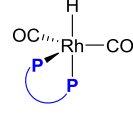
			
	$\delta^{31}\text{P}$ ppm	$\delta^1\text{H}$ ppm	$\delta^{13}\text{C}$ ppm
4.68	51.6 (d, $J_{\text{Rh,P}} = 114.7$ Hz)	- 8.5 (td, $J_{\text{Rh,H}} = 10.4$ Hz, $J_{\text{P,H}} = 57.6$ Hz)	199 (dt, $J_{\text{P,C}} = 10.8$ Hz, $J_{\text{Rh,C}} = 68.8$ Hz)
4.69	48.9 (d, $J_{\text{Rh,P}} = 115.5$ Hz)	- 9.0 (td, $J_{\text{Rh,H}} = 12.4$ Hz, $J_{\text{P,H}} = 62.8$ Hz)	199 (dt, $J_{\text{P,C}} = 11.6$ Hz, $J_{\text{Rh,C}} = 69.7$ Hz)

Table 4.8: Selected spectroscopic data corresponding to the quinaxoline backbone of rhodium complexes **4.68** and **4.69**.

4.68		4.69	
$\delta^1\text{H}$ ppm	$\delta^{13}\text{C}$ ppm	$\delta^1\text{H}$ ppm	$\delta^{13}\text{C}$ ppm
1.05 ($\text{C}(\underline{\text{CH}}_3)_3$)	28 ($\text{C}(\underline{\text{CH}}_3)_3$), 31.9 (t, $J_{\text{P,C}} = 9.4$ Hz, $\underline{\text{C}}(\text{CH}_3)_3$)	1.05 ($\text{C}(\underline{\text{CH}}_3)_3$)	28 ($\text{C}(\underline{\text{CH}}_3)_3$), 31.3 (t, $J_{\text{P,C}} = 9.9$ Hz, $\underline{\text{C}}(\text{CH}_3)_3$)
1.79 ($\underline{\text{CH}}_3$)	14.9 ($\underline{\text{CH}}_3$)	1.20 ($\underline{\text{CH}}_3$)	11.6 ($\underline{\text{CH}}_3$)
-	162.5 (t, $J_{\text{P,C}} = 47.9$ Hz, C)	-	132.2 (t, $J_{\text{P,C}} = 48.1$ Hz, C)
-	-	4 ($\underline{\text{NH}}$)	-
-	141.2 (C)	-	133.8 (C)
7.3 ($\underline{\text{CH}}$)	131.3 ($\underline{\text{CH}}$)	5.7 ($\underline{\text{CH}}$)	113.1 ($\underline{\text{CH}}$)
7.9 ($\underline{\text{CH}}$)	129.9 ($\underline{\text{CH}}$)	6.4 ($\underline{\text{CH}}$)	123.0 ($\underline{\text{CH}}$)

In the same experiment, the temperature was progressively reduced and the behavior of the signals was analyzed by ^1H NMR spectroscopy (Figure 4.11). The multiplicity of both signals changed from a clear triple of doublet to a pseudo-doublet of doublet when the temperature progressively decreased (Figure 4.11). Moreover, it was also observed that the ratio between the signals corresponding to species **4.68** and **4.69** did not change.

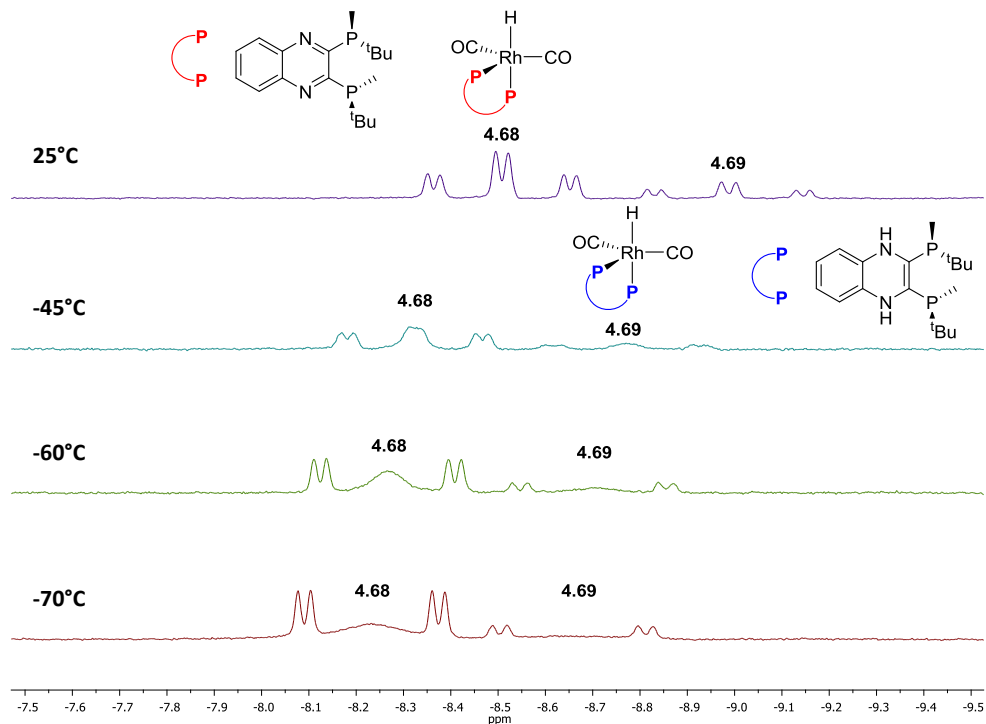


Figure 4.11: ^1H NMR spectra of $[\text{Rh}(\text{acac})(\text{CO})_2]$ in the presence of ligand **4.54** under syngas pressure in tol-d^8 recorded at variable temperature.

It was therefore concluded that under these conditions, the formation of $[\text{RhH}(\text{CO})_2(\text{PP})]$ species, usually reported as resting state of the HF catalytic cycle, was observed either by reaction under syngas of the neutral complex $[\text{Rh}(\text{acac})(\text{CO})_2]$ with ligand (R,R) -QuinoxP* **4.54**, or with the cationic complex $[\text{Rh}(\text{COD})_2]\text{BF}_4$ with ligand (R,R) -QuinoxP* **4.54** in the presence of morpholine **4.57a**. In the latter case, the amine was necessary for the formation of RhH

species. The promotion of H_2 heterolytic cleavage to form neutral RhH species from cationic precursors was previously reported.^{21-25b} The multiplicity (triplet of doublet) and coupling constants ($J_{P,H} < 70$ Hz) of these signals corresponding to rhodium monohydride species **4.68** and **4.69** are in agreement with an **eq-ax** coordination mode of the bidentate ligand in which the hydride is exchanging between axial and equatorial position at NMR time scale.²⁷ The decrease in temperature slows down the equilibrium previously mentioned, and the large coupling constants of the phosphorus in *trans* ($J_{P,H}$ ca. 120 Hz) to the hydride can be observed, while the small coupling constants of the phosphorus in *cis* to the hydride cannot be detected.²⁷ These results demonstrated that partial reduction of the quinaxoline backbone takes place under H_2/CO , providing rhodium hydride species **4.68** bearing either unaltered (*R,R*)-QuinoxP* ligand **4.54** or the rhodium hydride species **4.69** bearing the partially reduced ligand. The exact role of these species in the catalytic reaction is not clear to date.

Experiments to monitor the formation of rhodium monohydrides **4.68** and **4.69**

With these results in hand, the effect of the reaction conditions on the formation of rhodium hydride species **4.68** and **4.69** was investigated. First, the effect of the concentration of the species in solution was studied by increasing it from 0.0125M to 0.0375M (Figure 4.12).

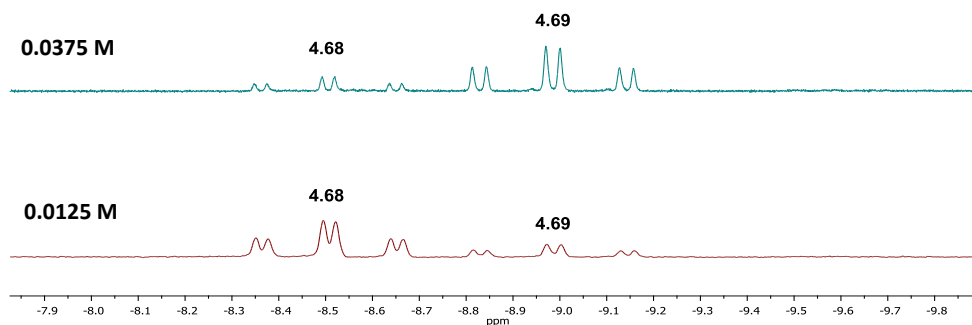


Figure 4.12: 1H NMR spectra of $[Rh(acac)(CO)_2]$ in the presence of ligand **4.54** in $tol-d^8$ under 20 bar (H_2/CO , 4:1), at $90^\circ C$, for 16h.

At 0.0125 M concentration, rhodium hydride species **4.68** is the major one (**4.68/4.69** = 60:40), while at higher concentration (0.0375 M), the rhodium hydride species **4.69** containing the reduced quinaxoline backbone turns into the major species in solution (**4.68/4.69** = 42:58). Then, the effect of the temperature was studied. When the reaction was performed with a concentration of 0.0375M, at 25°C, under 10 bar (H₂/CO, 4:1) of syngas pressure for 16h by ¹H NMR spectroscopy, the signal corresponding to rhodium hydride species **4.68** was detected together with a new signal at -10.8 ppm as a triplet doublet of triplet (tdt) ($J_{P,H} = 32, 4$ Hz, $J_{Rh,H} = 12$ Hz, $J_{P,H} = 4$ Hz). However, the signals corresponding to the RhH species **4.69** were not detected under these conditions. By ³¹P NMR spectroscopy, two doublet of triplets at 32.5 ppm ($J_{Rh,P} = 124.7$ Hz, $J_{P,P} = 10.7$ Hz) and 55 ppm ($J_{Rh,P} = 138.6$ Hz, $J_{P,P} = 10.7$ Hz) were detected observed (Figure 4.13).

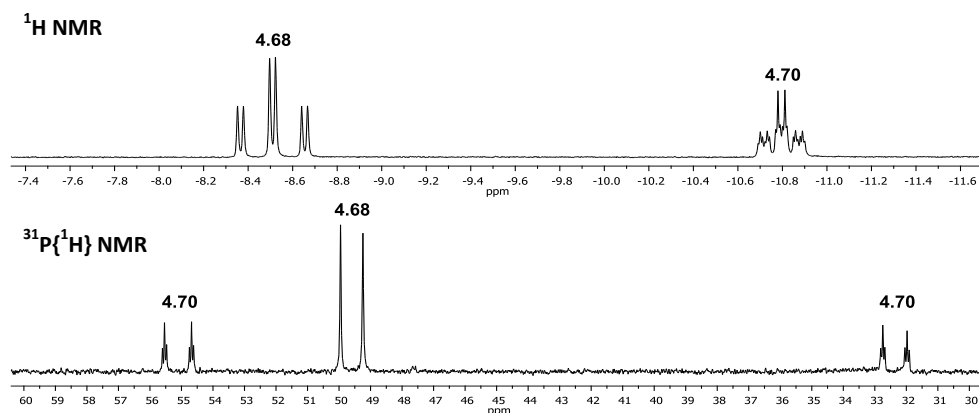


Figure 4.13: Top: ¹H NMR spectra of rhodium hydride **4.68** and species **4.70**. Bottom: ³¹P{¹H} NMR spectra of rhodium hydride **4.68** and species **4.70**.

¹H-³¹P HMBC experiment exhibited correlation between the new signal hydride signal at -10.8 ppm and the two phosphorus signals at 32.5 and 55 ppm. Furthermore, selective decoupling experiments allowed us to attribute the large P,H coupling constant ($J_{P,H} = 32$ Hz) is due to the phosphorus with signal at 32.5 ppm, and the small P,H coupling constant ($J_{P,H} = 4$ Hz) to the phosphorus with signal at 50 ppm. When the solution was analyzed by ¹³C NMR spectroscopy, only

Rhodium catalyzed asymmetric HAM of α -alkyl acrylates

the carbonyl signals corresponding to rhodium hydride **4.68** were detected, even when the experiment was carried out using labeled ^{13}C O. These signals were tentatively attributed to fluxional $[\text{RhH}(\mathbf{4.54})_2]$ **4.70** species.²⁸ After 96h of reaction, the signals corresponding to species **4.70** was not detected anymore and only signals corresponding to rhodium hydride species **4.68** could be detected at this temperature. Interestingly, upon raising the temperature to 90°C , resonances corresponding to rhodium hydride species **4.69** were detected, clearly indicating that this rhodium hydride species **4.69** is formed by reaction of rhodium hydride species **4.68** under these conditions (Figure 4.14).

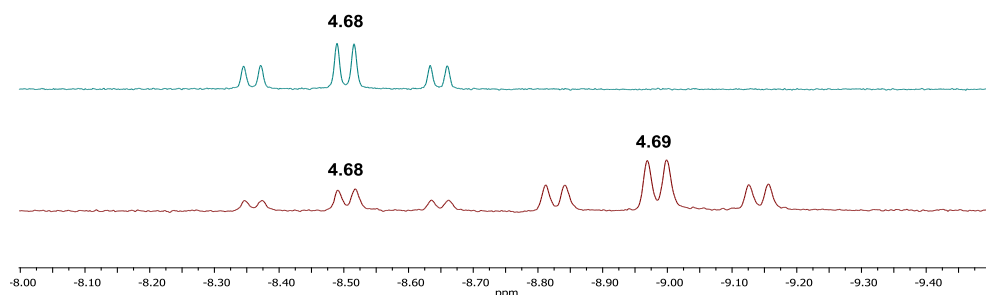
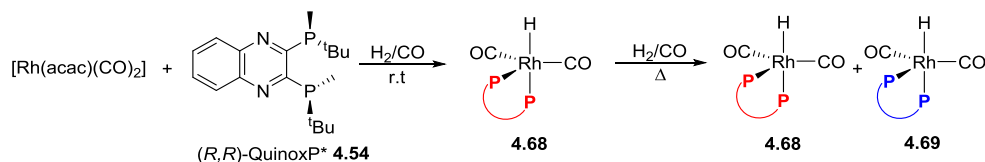


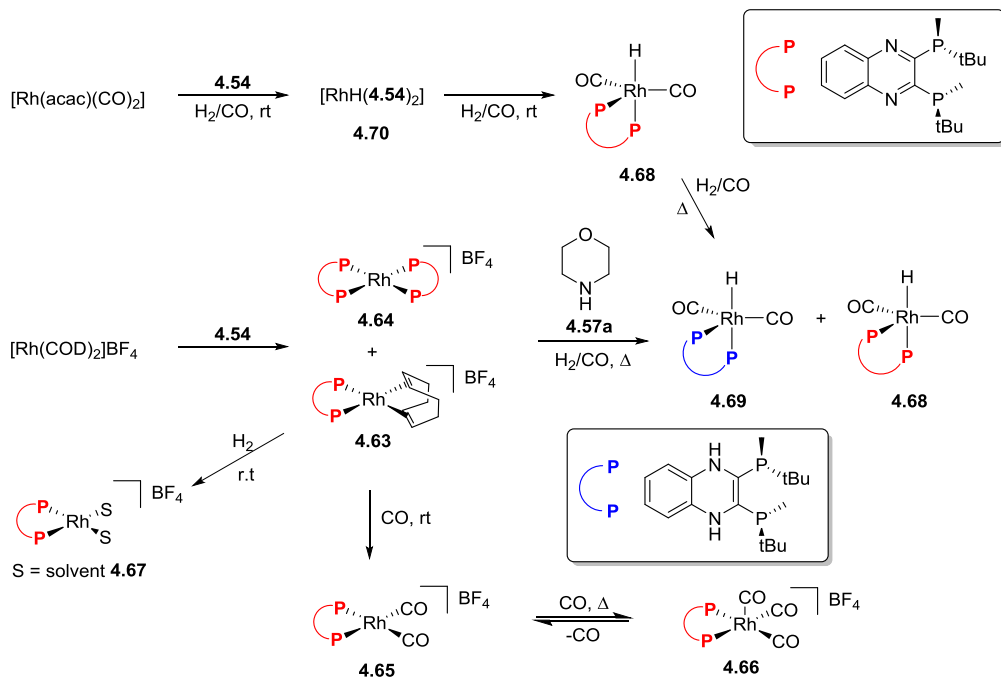
Figure 4.14: Top: ^1H NMR spectra of $[\text{Rh}(\text{acac})(\text{CO})_2]$ in the presence of ligand **4.54** in told- d^8 at room temperature under 10 bar (H_2/CO , 4:1) for 96h. Bottom: ^1H NMR spectra after the previous solution was heated at 90°C for 16h.

It was therefore concluded that rhodium hydride species **4.68** containing an unaltered quinoxaline backbone can be generated at room temperature under syngas pressure even at 0.0375 M concentration (Scheme 4.13). Moreover, the rhodium hydride species **4.69** containing the partially reduced quinoxaline backbone is generated from the rhodium hydride species **4.68** at 90°C under syngas pressure (Figure 4.14 and Scheme 4.13).



Scheme 4.13: Reactivity of $[\text{Rh}(\text{acac})(\text{CO})_2]$ in the presence of ligand **4.54** under syngas pressure at room temperature and 90°C .

All the experiments performed before are summarized in Scheme 4.14.



Scheme 4.14: Reactivity of ligand **4.54** with different rhodium precursors and morpholine **4.57a** under CO, H₂ or H₂/CO pressure, and temperature.

Reactivity of [Rh(COD)₂]BF₄ in the presence of (*R,R*)-QuinoxP* and aniline under H₂/CO pressure

In the catalytic experiments, aniline **4.22a** did not provide reactivity when it was used as amine in the HAM of α -alkyl acrylates **4.52** using a cationic rhodium precursor. Indeed, it was necessary to use a neutral rhodium precursor in order to conduct the hydroformylation step. Therefore, it was decided to study the effect of aniline in the formation of the different species via HP-NMR spectroscopy (Figure 4.15). When the cationic rhodium precursor was mixed with (*R,R*)-QuinoxP* **4.54** and aniline **4.22a**, the signals corresponding to species [Rh(COD)(**4.54**)]BF₄ **4.63** and [Rh(**4.54**)₂]BF₄ **4.64** were detected by ³¹P NMR spectroscopy as in previous experiments. Interestingly, two signals were detected as doublets at 59.7 (*J*_{Rh,P} = 97.5 Hz) ppm and 60.9 (*J*_{Rh,P} = 79 Hz) (Figure 4.15). These

Rhodium catalyzed asymmetric HAM of α -alkyl acrylates

signals were attributed to rhodium species **4.71** and **4.72** bearing (*R,R*)-QuinoxP* ligand **4.54** and aniline **4.22a** as ligands. After that, 20 bar of H₂/CO (4:1) were added to the tube and heated to 90°C for 16 hours. However, under these conditions, no hydride signals were detected by ¹H NMR spectroscopy and it was concluded that, in contrast to morpholine **4.57a**, aniline **4.22a** has not been able to promote the formation of rhodium hydride species **4.68** or **4.69**. Instead, the signal corresponding to rhodium tricarbonyl species **4.66** was detected again by ³¹P NMR spectroscopy (Figure 4.15).

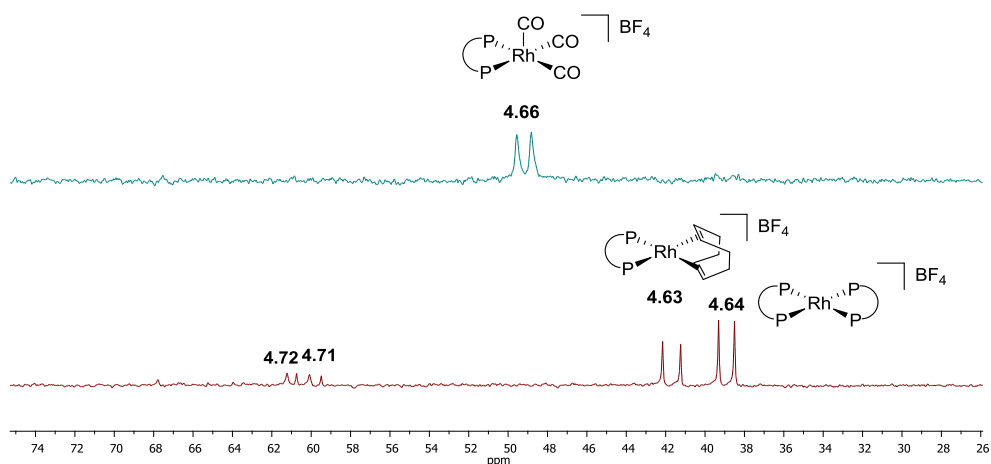


Figure 4.15: ³¹P{¹H} NMR spectra of [Rh(COD)₂]₂BF₄ in the presence of **4.54** and aniline **4.22a** in toluene-d₈/DCE. Top: 20 bar (H₂/CO, 4:1) at 90°C for 16 h. Bottom: no pressure

Reactivity of [Rh(acac)(CO)₂] and [Rh(COD)₂]₂BF₄ in the presence of (*R,R*)-QuinoxP*, morpholine, and methyl methacrylate under H₂/CO pressure

Finally, the reactivity of the two rhodium precursor previously applied was studied in the presence of (*R,R*)-QuinoxP* **4.54**, methyl methacrylate **4.52a** (100 equiv.) and morpholine **4.57a** (100 equiv.), in the solvents of choice (0.4 mL), under 10 bar (H₂/CO, 4:1) of syngas, and at 90°C.

First, when the neutral [Rh(acac)(CO)₂] precursor was used in toluene as solvent (entry 1, Table 4.1) the signal corresponding to free ligand **4.54** was detected at

Chapter 4

-17 ppm by ^{31}P NMR spectroscopy together the signal corresponding species $[\text{Rh}(\text{acac})(\mathbf{4.54})]$ **4.73** as a doublet at 62.0 ppm ($J_{\text{Rh,P}} = 187.6$ Hz) (Figure 4.16). Then, the tube was pressurized, heated at 90°C , and the reaction was monitored by ^{31}P NMR spectroscopy. After 30 min of reaction the signal corresponding to rhodium hydride species **4.68** was detected together with the signal of $[\text{Rh}(\text{acac})(\mathbf{4.54})]$ **4.73** (Figure 4.16). Upon 60 min of reaction, the signal corresponding to species **4.68** was not detected anymore. Through all the rest of the experiment, only species $[\text{Rh}(\text{acac})(\mathbf{4.54})]$ **4.73** was detected by ^{31}P NMR spectroscopy (Figure 4.16).

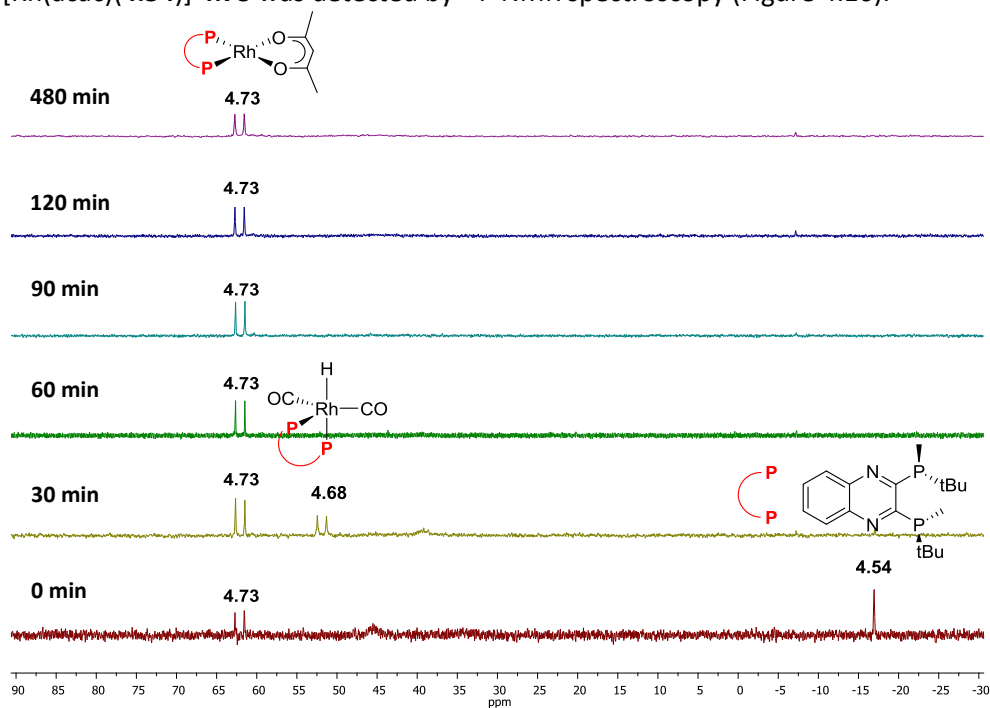
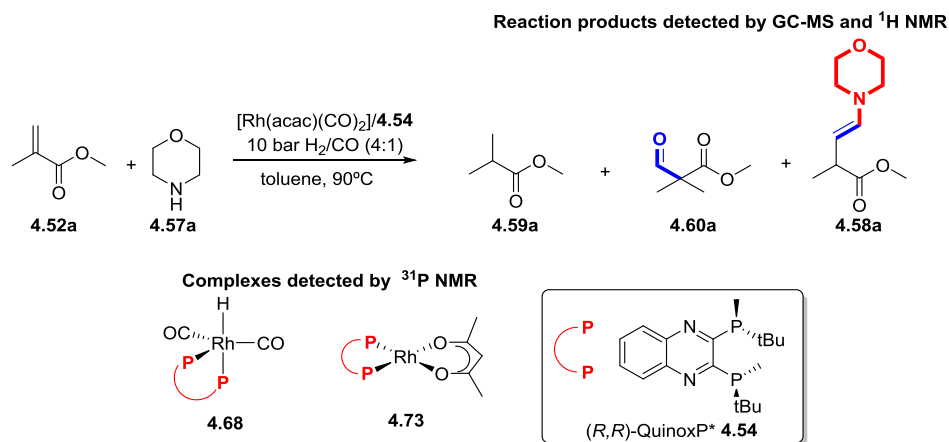


Figure 4.16: $^{31}\text{P}\{^1\text{H}\}$ NMR spectra recorded at various time in the Rh-catalyzed HAM of methyl methacrylate **4.52a** with morpholine **4.57a** using conditions from entry 1, Table 4.1

When the reaction was monitored by ^1H NMR spectroscopy, the signals from the linear enamine **4.58a** were observed at early reaction time. However, no signals corresponding to linear aldehyde **4.55a** were observed, indicating that the hydroformylation and condensation step proceed very fast. At the end of the experiment after 16h, the solution was analyzed by GC-MS and the alkene

Rhodium catalyzed asymmetric HAM of α -alkyl acrylates

hydrogenation product **4.59a**, the branched aldehyde **4.60a**, and linear enamine **4.58a** were detected, which is in agreement with the results afforded in catalysis (entry 1, Table 4.1). In conclusion, the use of a neutral precursor $[\text{Rh}(\text{acac})(\text{CO})_2]$ and ligand **4.54** in toluene promoted the formation of monohydride species that perform the asymmetric hydroformylation (Scheme 4.15). However, no cationic species responsible of the hydrogenation of the enamine was observed.



Scheme 4.15: Reactivity of $[\text{Rh}(\text{acac})(\text{CO})_2]$ and ligand **4.54** in toluene under 10 bar (H_2/CO , 4:1) at 90°C .

The next experiment was carried out using the cationic $[\text{Rh}(\text{COD})_2]\text{BF}_4$ precursor and the mixture of solvents toluene/DCE (1:1) (Figure 4.17). When the reagents were mixed without pressure, resonances corresponding to species $[\text{Rh}(\text{COD})(\mathbf{4.54})]\text{BF}_4$ **4.63** and $[\text{Rh}(\mathbf{4.54})_2]\text{BF}_4$ **4.64** were detected together with a new signal as a doublet ($J_{\text{Rh,P}} = 181.5$ Hz) at 55 ppm by ^{31}P NMR spectroscopy (Figure 4.17). The nature of this species **4.74** was attributed to a rhodium species with two morpholine **4.57a** coordinated to the rhodium instead of COD (Figure 4.17). Next, the tube was submitted to the syngas pressure, heated to 90°C and the reaction was monitored by ^{31}P NMR spectroscopy. After 30 min, the signal corresponding to species $[\text{Rh}(\text{COD})(\mathbf{4.54})]\text{BF}_4$ **4.63** disappeared and the signal attributed rhodium hydride **4.68** was detected. Furthermore, the species $[\text{Rh}(\mathbf{4.54})_2]\text{BF}_4$ **4.64** remains in solution (Figure 4.17). When the reaction was

analyzed after 60 min, the rhodium hydride **4.68** was not detected anymore. In addition, two new signals were detected as doublets of doublets at 38 ppm ($J_{\text{Rh,P}} = 123.5$ Hz, $J_{\text{P,P}} = 38.7$ Hz) and 61.5 ppm ($J_{\text{Rh,P}} = 151.7$ Hz, $J_{\text{P,P}} = 38.5$ Hz).

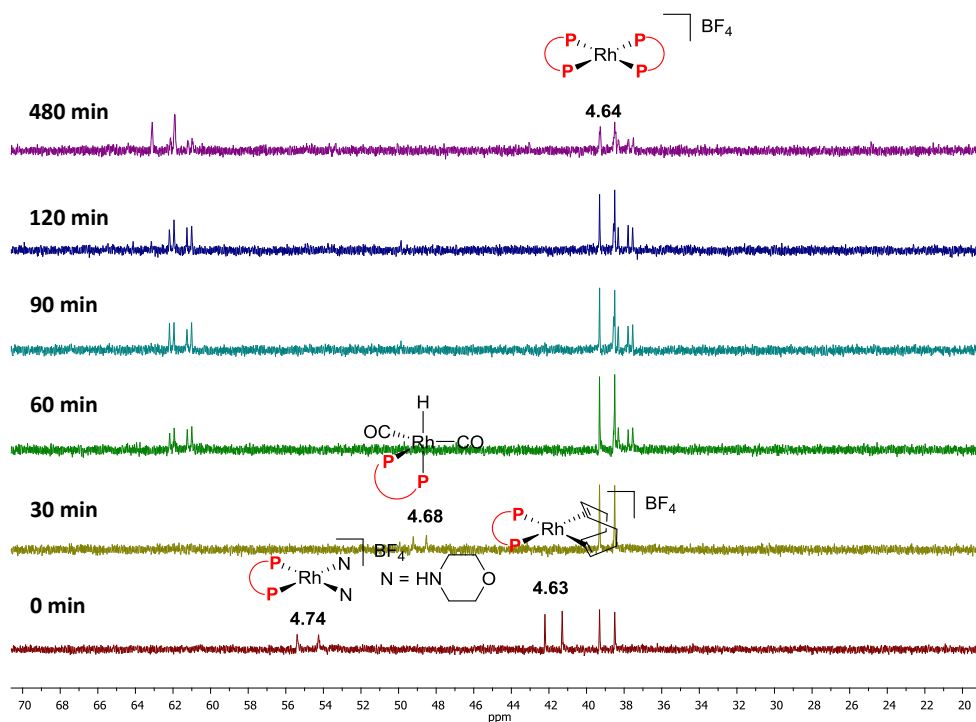


Figure 4.17: $^{31}\text{P}\{^1\text{H}\}$ NMR spectra recorded at various time in the Rh-catalyzed HAM of methyl methacrylate **4.52a** with morpholine **4.57a** using conditions from entry 5, Table 4.1.

Previous reports on mechanistic studies in the rhodium catalyzed hydrogenation of enamides using C_2 -Symmetry diphosphine ligands (*R,R*)-Dipamp **4.75** and (*R,R*)-BenzP* **4.53** described intermediate rhodium species bearing the diphosphine ligand and the enamide coordinated through a carbonyl group and the double bond (Figure 4.18).²⁴⁻²⁹ The NMR features reported for these species are in agreement with those observed in this study. The new signals were thus attributed to the new rhodium species **4.76** containing the enamine **4.58a** coordinated to the rhodium center through the carbonyl of the ester moiety and the double bond. Such a species consequently contains two non-equivalent phosphorus, one *trans*

Rhodium catalyzed asymmetric HAM of α -alkyl acrylates

to the carbonyl, and another *trans* to the double bond (Figure 4.18). Finally, when the reaction was left, a new signal was detected as a doublet ($J_{\text{Rh,P}} = 191.5$ Hz) at 62.5 ppm by ^{31}P NMR spectroscopy. The multiplicity and constant coupling suggest a symmetric Rh (I) species. This signal was tentatively attributed to a rhodium (I) species bearing (*R,R*)-QuinoxP* ligand **4.54** and two molecules of the amino ester product **4.56a** coordinated.

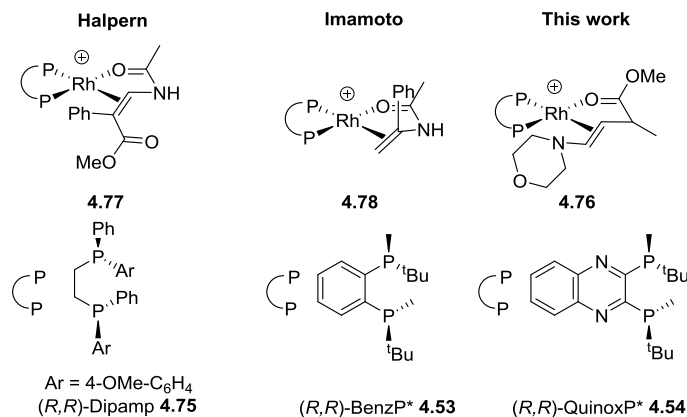
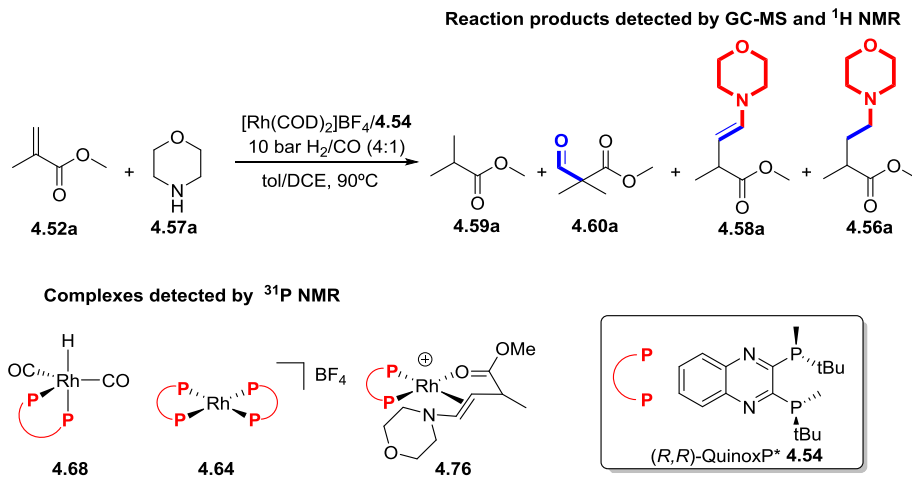


Figure 4.18: Examples of intermediates **4.77** and **4.78** detected in the rhodium catalyzed hydrogenation of enamides reported in the literature, and the proposed species **4.76** in this work.

When the reaction was monitored by ^1H NMR spectroscopy, the alkene hydrogenation product **4.59a**, the branched aldehyde **4.60a**, the linear enamine **4.58a** and linear amino ester **4.56a** were detected after 30 min of reaction. Nonetheless, the linear aldehyde **4.55a** was not observed in any case. Further analysis of the solution by GC-MS, confirmed the presence of all the reaction products mentioned before.

Thus, it was confirmed again by ^1H NMR spectroscopy that the hydroformylation of the methyl methacrylate **4.52a** and the condensation of linear aldehyde **4.55a** take place very fast. Moreover, the neutral rhodium hydride **4.68** and the cationic rhodium $[\text{Rh}(\mathbf{4.54})_2]\text{BF}_4$ **4.64** were detected by ^{31}P NMR spectroscopy. In contrast to the previous experiment (Figure 4.16), a new set of signals was detected by ^{31}P NMR spectroscopy and attributed to rhodium species **4.76** (Figure 4.18). This

species could be an intermediate during the enamine hydrogenation. The reactivity observed is illustrated in Scheme 4.16 with all the reaction products and species detected.



Scheme 4.16: Reactivity of $[\text{Rh}(\text{COD})_2]\text{BF}_4$ and ligand **4.54** in toluene/DCE under 10 bar (H_2/CO , 4:1) at 90°C .

The last HP-NMR experiment was performed using the reaction conditions used in catalysis (entry 4, Table 4.1) using the neutral precursor $[\text{Rh}(\text{acac})(\text{CO})_2]$, the ligand **4.54** and the mixture of toluene/DCE as solvent (Figure 4.19). After mixing the reagents and analyzing the solution by ^{31}P NMR spectroscopy, only a broad signal at 45.5 ppm was detected. After 30 min of reaction, a complex mixture of signals was observed by ^{31}P NMR spectroscopy at *ca.* 39 and 62 ppm. Upon 120 min of reaction, a clearer $^{31}\text{P}\{^1\text{H}\}$ NMR spectrum was obtained in which the signal corresponding to species $[\text{Rh}(\text{acac})(\text{4.54})]$ **4.73** was detected together with a new doublet signal at 38.9 ppm ($J_{\text{Rh,P}} = 133.9$ Hz). Such species presents a similar chemical shift and coupling constant to $[\text{Rh}(\text{4.54})_2]\text{BF}_4$ **4.64** (38.9 ppm and $J_{\text{Rh,P}} = 133$ Hz). Therefore, this new signal was attributed to species $[\text{Rh}(\text{4.54})_2]\text{acac}$ **4.79** analogous to $[\text{Rh}(\text{4.54})_2]\text{BF}_4$ **4.64** but containing acetylacetonate as counter ion instead of tetrafluoroborate. Such species has been previously reported in the hydrogenation unsaturated ketones.³⁰ Moreover, two signals were observed by ^{31}P

Rhodium catalyzed asymmetric HAM of α -alkyl acrylates

NMR spectroscopy as doublets of doublets at 38.1 ppm ($J_{\text{Rh,P}} = 122.9$ Hz, $J_{\text{P,P}} = 41.6$ Hz) and 59.8 ppm ($J_{\text{Rh,P}} = 153.6$ Hz, $J_{\text{P,P}} = 41.4$ Hz), and were attributed to a new rhodium species **4.80**.

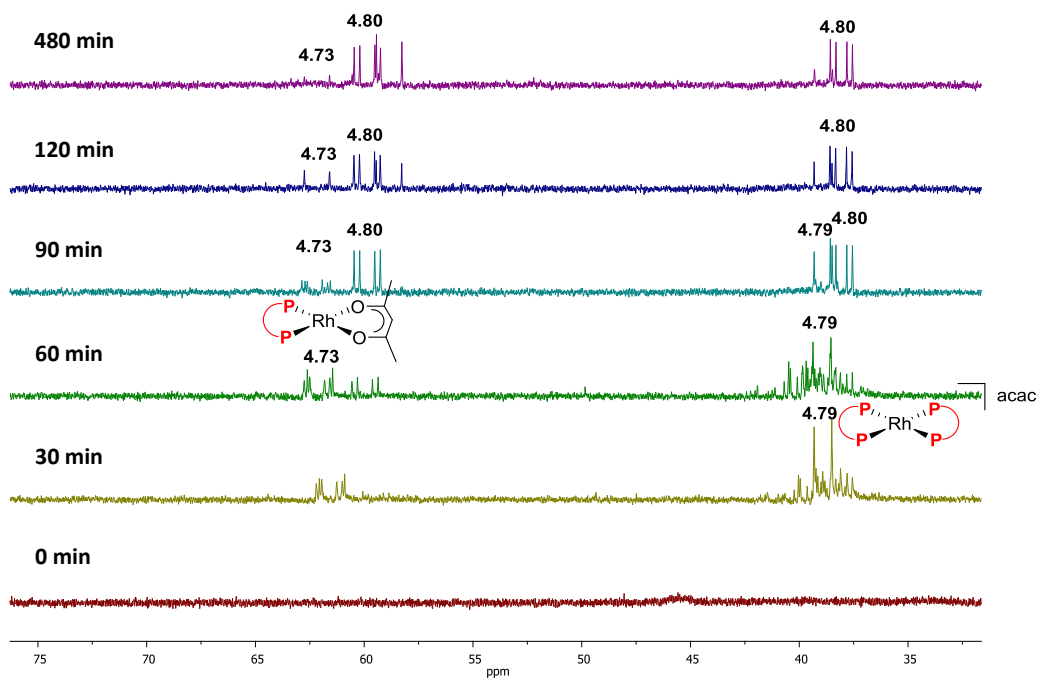


Figure 4.19: $^{31}\text{P}\{^1\text{H}\}$ NMR spectra recorded at various time in the Rh-catalyzed HAM of methyl methacrylate **4.52a** with morpholine **4.57a** using conditions from entry 4, Table 4.1.

Taking into account previous results (Figure 4.17 and Figure 4.18), the new species **4.80** presents signals with the same multiplicity to the cationic rhodium species **4.76** with the enamine **4.58a** coordinated to the rhodium center. Nonetheless, the coupling constant of the signals corresponding to species **4.80** slightly differ from those of **4.76**. Since, the only difference in the reaction conditions between this experiment (Figure 4.19) and the previous one (Figure 4.17) is the use of the neutral $[\text{Rh}(\text{acac})(\text{CO})_2]$ precursor instead of cationic $[\text{Rh}(\text{COD})_2]\text{BF}_4$ precursor, the acetylacetonate might be “involved” in the cationic species **4.80** either as counter ion, or the protonated acetylacetonate interacts somehow with the enamine **4.58a**

(Figure 4.20). Similar results were described by Imamoto and co-workers who reported the interaction of methanol with the enamide via hydrogen bonding.³¹

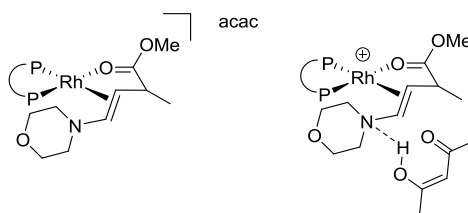
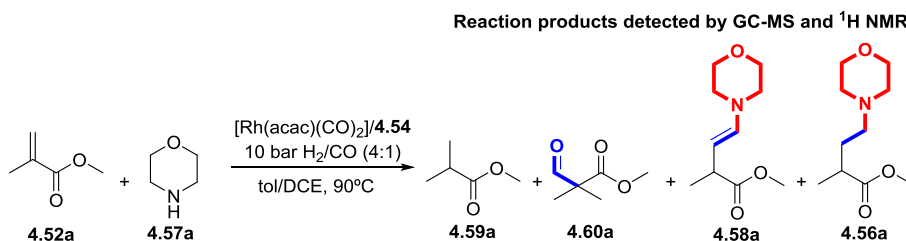
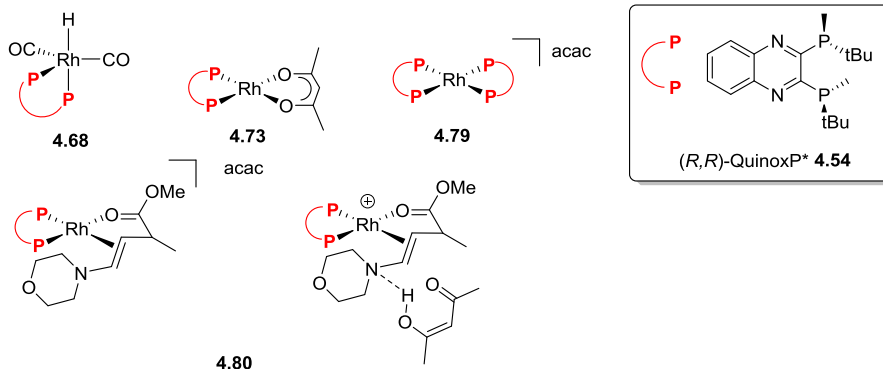


Figure 4.20: Proposed structures for the rhodium species **4.80**.

When the reaction was monitored by ¹H NMR spectroscopy, the alkene hydrogenation product **4.59a**, the branched aldehyde **4.60a**, the linear enamine **4.58a** and linear amino ester **4.56a** were detected, while no signal of linear aldehyde **4.55a** was observed. The reactivity observed is illustrated Scheme 4.17.



Complexes detected by ³¹P NMR

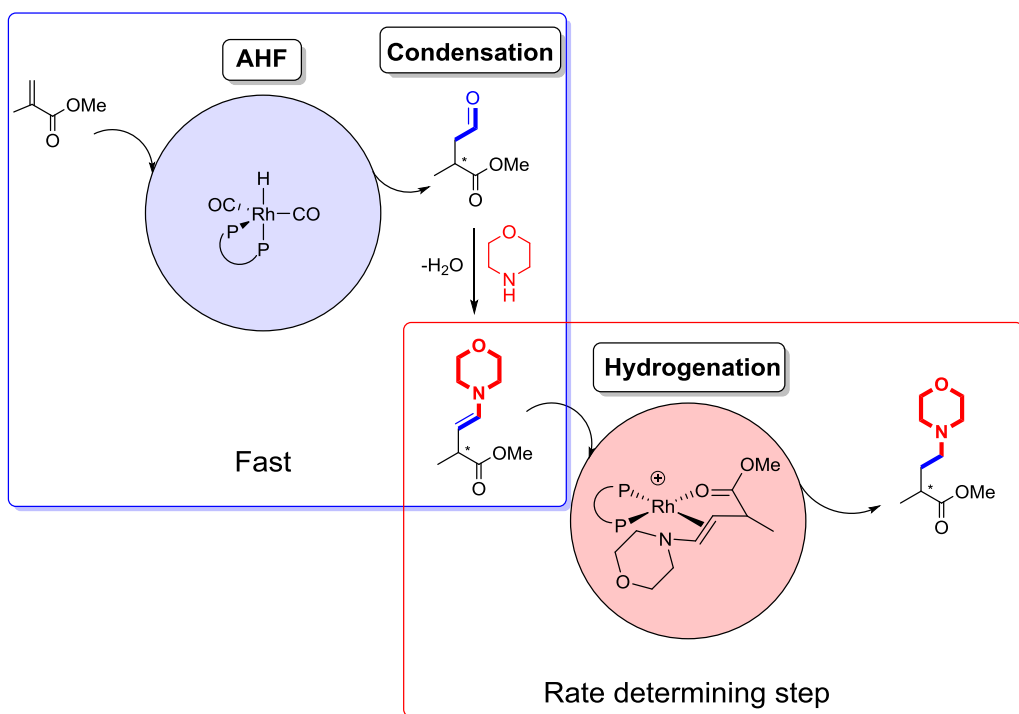


Scheme 4.17: Reactivity of $[\text{Rh}(\text{acac})(\text{CO})_2]$ and **4.54** in toluene/DCE under 10 bar (H_2/CO , 4:1) at 90°C.

In conclusion, this experiment provides evidence that both neutral species and cationic species can coexist throughout. Moreover, it demonstrates that a neutral

Rhodium catalyzed asymmetric HAM of α -alkyl acrylates

species can be transformed into a cationic species under these reaction conditions. The role of DCE as solvent in this equilibrium is still unclear, and further experiments would be required to elucidate its role in catalysis. Nonetheless, it is proposed that DCE is able to solubilize cationic species, and therefore allow the equilibrium between neutral and cationic species to be displaced. The summary of the reactivity observed through the monitoring experiments is summarized in Scheme 4.18.



Scheme 4.18: Summary of the reactivity observed in the HAM of methyl methacrylate **4.52a** with morpholine **4.57a** when the reaction was monitored using various rhodium precursors with ligand **4.54** and various mixtures of solvents.

In view of the results obtained it was concluded that the enantioselectivity is induced in the asymmetric hydroformylation of the alkene, in which neutral species are involved. Subsequent condensation of the amine generates the corresponding enamine that is hydrogenated via cationic species. The absence of

signals corresponding to the linear aldehyde via ^1H NMR spectroscopy suggests that the alkene hydroformylation and the linear aldehyde condensation take place fast, while the hydrogenation of the enamine is the rate determining step.

4.4. Conclusions

From the study described in this chapter, the following conclusions can be extracted:

- i) The synthesis of chiral α -alkyl- γ -aminobutyric esters **4.56** have been achieved via rhodium catalyzed hydroaminomethylation of α -alkyl acrylates **4.52** using (*R,R*)-QuinoxP* **4.54** as ligand.
- ii) The optimized conditions included the use of the cationic rhodium precursor $[\text{Rh}(\text{COD})_2]\text{BF}_4$, a mixture of solvents toluene/DCE, 10 bar (H_2/CO , 4:1), and 90°C for secondary amines.
- iii) When the aniline **4.22a** was used, it was necessary to use a neutral rhodium precursor and to/DCE mixture as solvent in order to obtain the target molecules.
- iv) The reaction is tolerant to protecting groups at the amine, and to various alkyl groups at the olefin.
- v) To the best of our knowledge this process constitutes the first asymmetric hydroaminomethylation process carried out using one single catalyst to the best of our knowledge.
- vi) The basicity of the amine was shown to be crucial in order to form the Rh-H species $[\text{RhH}(\text{CO})_2(\text{PP})]$ that is involved in the HF of the substrate.
- vii) Several new species were detected and characterized under CO , H_2 and H_2/CO via NMR and IR spectroscopy.
- viii) Two rhodium hydride species **4.68** and **4.69** with the ligand in **eq-ax** coordination mode have been detected and characterized. The rhodium hydride species **4.69** contains a partially reduced quinaxoline backbone.

- ix) The rhodium monohydride species **4.68** can be selectively generated at room temperature, and evolve into the rhodium monohydride **4.69** when heated. Throughout the formation of rhodium hydride **4.68**, the new rhodium hydride species **4.70** has been detected.
- x) The neutral precursor in toluene is not able to complete the hydrogenation of enamine **4.58a** since no cationic species are generated.
- xi) The cationic rhodium species **4.76** containing the enamine **4.58a** coordinated to the rhodium center was detected via ^{31}P NMR spectroscopy when optimized conditions (entry 5, Table 4.1) were applied.
- xii) The use toluene/DCE as solvent mixture facilitates the formation of cationic species $[\text{Rh}(\mathbf{4.54})_2]\text{acac}$ **4.79** and rhodium species **4.76** with the enamine **4.58a** coordinated from the neutral precursor in the mixture of toluene/DCE. Furthermore, species $[\text{Rh}(\text{acac})(\mathbf{4.54})]$ **4.73** was also observed in the media. Thus, the coexistence of neutral and cationic species during the HAM reaction was confirmed by HP-NMR spectroscopy.

4.5. Experimental

4.5.1. General considerations

All the reactions were carried out using Schlenk-line inert atmosphere techniques or glovebox techniques. Anhydrous solvents were collected from the system Braun MB SPS-800 except from 1,2-dichloroethane, which was dried over CaH_2 , and stored under inert atmosphere.

Commercially available reagents and solvents were purchased at the highest commercial quality from Sigma-Aldrich, Fluka, Alfa Aesar, Fluorochem, Strem and were used as received, without further purification, unless otherwise stated.

Chapter 4

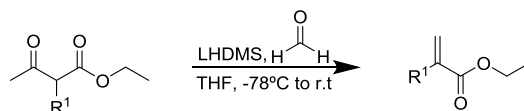
^1H , $^{13}\text{C}\{^1\text{H}\}$ and $^{31}\text{P}\{^1\text{H}\}$ NMR spectra were recorded using a Varian Mercury VX 400 (400, 100.6, and 161.97 MHz respectively). Chemical shift values (δ) are reported in ppm relative to TMS (^1H and $^{13}\text{C}\{^1\text{H}\}$) or H_3PO_4 ($^{31}\text{P}\{^1\text{H}\}$), and coupling constants are reported in Hertz. The following abbreviations are used to indicate the multiplicity: s, singlet; d, doublet; t, triplet; q, quartet; m, multiplet; bs, broad signal. High-resolution mass spectra (HRMS) were recorded on an Agilent Time-of-Flight 6210 using ESI-TOF (electrospray ionization-time of flight). Samples were introduced to the mass spectrometer ion source by direct injection using a syringe pump and were externally calibrated using sodium formate. The instrument was operating in the positive ion mode. Reactions were monitored by TLC carried out on 0.25 mm E. Merck silica gel 60 F_{254} glass or aluminum plates. Developed TLC plates were visualized under a short-wave UV lamp (254 nm) and by heating plates that were dipped in potassium permanganate. Flash column chromatography was carried out using forced flow of the indicated solvent on Merck silica gel 60 (230-400 mesh).

The Rh-catalyzed HAM reaction and Rh-catalyzed AHF reaction were set up in a CAT24 autoclave from HEL Inc. and were stirred with a teflon-coated magnetic stir bar.

The enantiomeric excess of γ -aminobutyric esters **4.52** or analogous aminoalcohols **4.81** was determined by ^1H NMR spectroscopy using $\text{Eu}(\text{hcf})_3$, and HPLC analysis on chiral stationary phase performed on a Waters ACQUITY[®] UPC² instrument, employing Daicel Chiralpak IA, IG, IC or OD-H chiral columns, and Trefoil CEL2 chiral column. The exact conditions for the analyses are specified within the supporting information section. HPLC traces were compared to racemic samples prepared performing the reactions in the presence of di-*tert*-butylphenylphosphine.

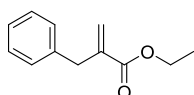
4.5.2. Synthesis of α -alkyl acrylates 4.52

General Procedure A: Synthesis of α -alkyl acrylates (4.52b-d)



The reaction was carried out in an oven dried, argon purged, schlenck fitted with a argon inlet and septum and following a modified literature procedure.¹⁸ To a stirred solution of ethyl 2-alkylacetoacetate (17 mmol, 1.0 eq) in THF (136 mL) was added LiHMDS 1.0 M in THF (19 mL, 19 mmol, 1.1 eq) at -78°C. The solution was left stirring for 30 min then paraformaldehyde (3g, excess) was added as a solid in one portion. The suspension was allowed to reach room temperature and left stirring for 16h. The mixture was filtrated through a pad of Celite to remove the excess of paraformaldehyde. The filtrate was concentrated *in vacuo* and purified by flash chromatography to afford the α -alkyl acrylate **4.52**.

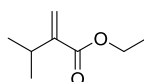
Ethyl 2-benzylacrylate (4.52b)¹⁸



General procedure A was followed employing ethyl 2-benzyl-3-oxobutanoate as starting material. Purification by flash chromatography eluting with hexane/EtOAc (20:1) afforded **4.52b** (3.0 g, 93%) as colorless oil.

¹H NMR (400 MHz, CDCl₃) δ : 1.22 (t, $J_{\text{H,H}} = 7.2$ Hz, 3H), 3.59 (s, 2H), 4.14 (q, $J_{\text{H,H}} = 7.2$ Hz, 2H), 5.41 (bs, 1H), 6.19 (bs, 1H), 7.15-7.27 (m, 5H, Ar). ¹³C NMR (100.6 MHz, CDCl₃) δ : 14.2 (1C), 38.1 (1C), 60.8 (1C), 126.0 (1C), 126.3-138.8 (6C, Ar), 140.4 (1C), 167.0 (1C). These signals are in agreement with those reported in the literature.

Ethyl 3-methyl-2-methylenebutanoate (4.52c)¹⁸

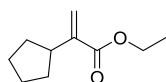


General procedure A was followed employing ethyl 2-acetyl-3-methylbutanoate as starting material. Purification by flash

chromatography eluting with hexane/EtOAc (20:1) afforded **4.52c** (2.2 g, 54%) as colorless oil.

$^1\text{H NMR}$ (400 MHz, CDCl_3) δ : 1.07 (d, $J_{\text{H,H}} = 8$ Hz, 6H), 1.30 (t, $J_{\text{H,H}} = 8$ Hz, 3H), 2.80 (m, 1H), 4.21 (q, $J_{\text{H,H}} = 8$ Hz, 2H), 5.50 (bs, 1H), 6.11 (bs, 1H). $^{13}\text{C NMR}$ (100.6 MHz, CDCl_3) δ : 14.3 (1C), 21.9 (2C), 29.4 (1C), 60.6 (1C), 121.6 (1C), 147.5 (1C), 167.6 (1C). Peaks in agreement with those reported in the literature.

Ethyl 2-cyclopentylacrylate (**4.52d**)

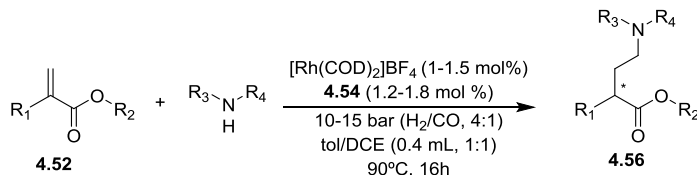


General procedure A was followed employing ethyl 2-cyclopentyl-3-oxobutanoate (10 mmol) as starting material. Purification by flash chromatography eluting with hexane/EtOAc (30:1) afforded **4.52d** (850 mg, 51%) as colorless oil.

$^1\text{H NMR}$ (400 MHz, CDCl_3) δ : 1.26 (t, $J_{\text{H,H}} = 8$ Hz, 3H), 1.58 (m, 2H), 1.64 (m, 5H), 1.70 (m, 1H), 2.84 (m, 1H), 4.20 (q, $J_{\text{H,H}} = 8$ Hz, 2H), 5.51 (bs, 1H), 6.10 (bs, 1H). $^{13}\text{C NMR}$ (100.6 MHz, CDCl_3) δ : 14.3 (1C), 25.0 (2C), 31.2 (2C), 41.5 (1C), 60.5 (1C), 121.6 (1C), 144.8 (1C), 167.7 (1C). **ESI-HRMS**: Calculated for $\text{C}_{10}\text{H}_{16}\text{O}_2$. Exact: (M: 168.1150, M+H: 169.1229); Experimental: (M+H: 169.1221).

4.5.3. Rh-catalyzed asymmetric hydroaminomethylation of α -alkyl acrylates **4.52**

General procedure B: rhodium catalyzed asymmetric hydroaminomethylation of α -alkyl acrylates **4.52 with secondary amines.**

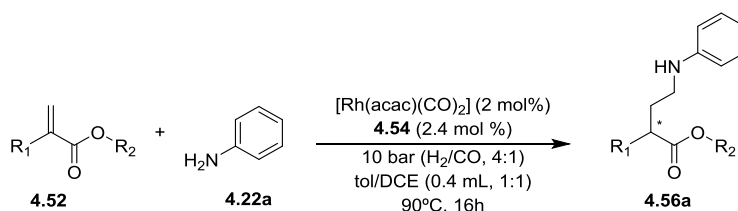


A 2 mL glassware reactor tube was charged with α -alkyl acrylate **4.52** (0.5 mmol), amine (0.5 mmol), bis(1,5-cyclooctadiene)rhodium (I) tetrafluoroborate (2 mg,

Rhodium catalyzed asymmetric HAM of α -alkyl acrylates

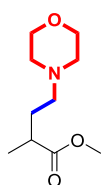
0.005 mmol) in DCE (0.2 mL) and chiral ligand (*R,R*)-QuinoxP* **4.54** (2 mg, 0.006 mmol) in toluene (0.2 mL). The reaction tube was placed in the reactor which was pressurized at the desired pressure, heated to 90°C and left stirring at 900 rpm. The reaction was stopped after 16 h by cooling the reactor in an ice bath for 20 min followed by venting of the system. The mixture was purified by chromatographic column and the enantiomeric excess of the resulting α -alkyl- γ -aminobutyric esters **4.56** analyzed by chiral HPLC or ^1H NMR using $\text{Eu}(\text{hcf})_3$.

General procedure C: rhodium catalyzed asymmetric HAM of α -alkyl acrylates **4.52 with aniline **4.22a**.**



A 2 mL glassware reactor tube was charged with α -alkyl acrylate **4.52** (0.5 mmol), aniline **4.22a** (0.5 mmol), dicarbonyl(acetylacetonato)rhodium (I) (2.6 mg, 0.01 mmol) in DCE (0.2 mL) and chiral ligand (*R,R*)-QuinoxP* **4.54** (4 mg, 0.012 mmol) in toluene (0.2 mL). The reaction tube was placed in the reactor which was pressurized with 10 bar of H_2/CO (4:1), heated to 90°C and left stirring at 900 rpm. The reaction was stopped after 16 h by cooling the reactor in an ice bath for 20 min followed by venting of the system. The mixture was purified by chromatographic column and the enantiomeric excess of the resulting α -alkyl- γ -aminobutyric esters **4.56** analyzed by chiral HPLC.

Methyl 2-methyl-4-morpholinobutanoate (4.56a)

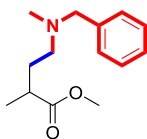


General procedure B was followed employing methyl methacrylate **4.52a** (53.5 μL , 0.5 mmol) and morpholine (44 μL , 0.5 mmol). Purification by flash chromatography eluting with pentane/ Et_2O (2:1)

afforded **4.56a** (60 mg, 60%) as colorless oil. The enantiomeric excess was determined to be 73% by UPC² analysis on a Acquity Trefoil Cel2 column with a gradient 90:10 CO₂/Acetonitrile with 0.1% of diethylamine as additive, flow rate 2mL/min, $\lambda = 230$ nm: $t_{r\text{ minor}} = 2.0$ min, $t_{r\text{ major}} = 1.5$ min.

¹H NMR (400 MHz, CDCl₃) δ : 1.15 (d, $J_{\text{H,H}} = 7.2$ Hz, 3H), 1.55 (m, 1H), 1.90 (m, 1H), 2.31 (dt, $J_{\text{H,H}} = 2, 8$ Hz, 2H), 2.49 (bs, 4H), 2.52 (m, 1H), 3.66 (s, 3H), 3.69 (t, $J_{\text{H,H}} = 4.4$, 4H). ¹³C NMR (100.6 MHz, CDCl₃) δ : 17.4 (1C), 30.5 (1C), 37.9 (1C), 51.7 (1C), 53.8 (2C), 56.8 (1C), 67.1 (2C), 177.1 (1C). **ESI-HRMS**: Calculated for C₁₀H₁₉NO. Exact: (M: 201.1365, M+H: 202.1443); Experimental: (M+H: 202.1435).

Methyl 4-(benzyl(methyl)amino)-2-methylbutanoate (**4.56b**)

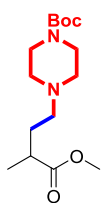


General procedure B was followed employing **4.52a** (53.5 μ L, 0.5 mmol) and N-Benzylmethylamine (66.5 μ L, 0.5 mmol). Purification by flash chromatography eluting with pentane/Et₂O

(3:1) afforded **4.56b** (57 mg, 50%) as colorless oil.

¹H NMR (400 MHz, CDCl₃) δ : 1.12 (d, $J_{\text{H,H}} = 7.2$ Hz, 3H), 1.59 (m, 1H), 1.94 (m, 1H), 2.17 (s, 3H), 2.37 (t, $J_{\text{H,H}} = 6.8$ Hz, 2H), 2.55 (m, 1H), 3.47 (bs, 2H), 3.64 (s, 3H), 7.24-7.31 (m, 5H, Ar). ¹³C NMR (100.6 MHz, CDCl₃) δ : 17.3 (1C), 31.4 (1C), 37.5 (1C), 42.2 (1C), 51.7 (1C), 55.0 (1C), 62.6 (1C), 112.7-148.1 (6C, Ar) 177.4 (1C). **ESI-HRMS**: Calculated for C₁₄H₂₁NO₂. Exact: (M: 235.1572, M+H: 236.1651); Experimental: (M+H: 236.1647).

Methyl 4-(tert-butyl piperazine-1-carboxylate)-2-methylbutanoate (**4.56c**)

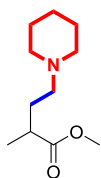


General procedure B was followed employing **4.52a** (53.5 μ L, 0.5 mmol) and N-Boc-piperazine (93.1 mg, 0.5 mmol). Purification by flash chromatography eluting with pentane/Et₂O (2:1) afforded **4.56c** (75.1 mg, 50%) as colorless oil. The enantiomeric excess was determined to be 69 % by UPC² analysis on a Daicel Chiralpak IG column with a

Rhodium catalyzed asymmetric HAM of α -alkyl acrylates

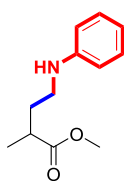
gradient 90:10 CO₂/MeOH with 0.1% of diethylamine as additive, flow rate 2mL/min, $\lambda = 230$ nm: $t_{r\text{ minor}} = 2.2$ min, $t_{r\text{ major}} = 2.3$ min.

¹H NMR (400 MHz, CDCl₃) δ : 1.16 (d, $J_{\text{H,H}} = 7.2$ Hz, 3H), 1.45 (s, 9H), 1.57 (m, 1H), 1.91 (m, 1H), 2.33 (m, 6H), 2.50 (m, 1H), 3.40 (t, $J_{\text{H,H}} = 4.8$ Hz, 4H), 3.66 (s, 3H). ¹³C NMR (100.6 MHz, CDCl₃) δ : 17.3 (1C), 28.4 (3C), 30.6 (1C), 37.8 (1C), 43.0 (2C), 51.6 (1C), 52.9 (2C), 56.2 (1C), 79.6 (1C), 154.7(1C), 176.9 (1C). **ESI-HRMS**: Calculated for C₁₅H₂₈N₂O₄. Exact: (M: 300.2049, M+H: 301.2127); Experimental: (M+H: 301.2126).

Methyl 2-methyl-4-(piperidin-1-yl)butanoate (4.56d)

General procedure B was followed employing **4.52a** (53.5 μ L, 0.5 mmol) and piperidine (49.5 μ L, 0.5 mmol). Purification by flash chromatography eluting with Et₂O afforded **4.56d** (50 mg, 50%) as colorless oil.

¹H NMR (400 MHz, CDCl₃) δ : 1.15 (d, $J_{\text{H,H}} = 7.2$ Hz, 3H), 1.44 (bs, 2H), 1.56 (m, 5H), 1.90 (m, 1H), 2.25 (m, 2H), 2.34 (bs, 4H), 2.45 (m, 1H), 3.66 (s, 3H). ¹³C NMR (100.6 MHz, CDCl₃) δ : 17.2 (1C), 24.4 (1C), 25.9 (2C), 30.9 (1C), 37.9 (1C), 51.5 (1C), 54.6 (1C), 57.0 (2C), 177.1 (1C). **ESI-HRMS**: Calculated for C₂₁H₂₁NO₂. Exact: (M: 199.1572, M+H: 200.1651); Experimental: (M+H: 200.1660).

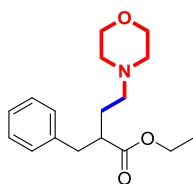
Methyl 2-methyl-4-(phenylamino)butanoate (4.56e)

General procedure C was followed employing **4.52a** (53.5 μ L, 0.5 mmol) and aniline (46 μ L, 0.5 mmol). Purification by flash chromatography eluting with pentane/Et₂O (2:1) afforded **4.56e** (19 mg, 19%) as colorless oil. The enantiomeric excess was determined to

be 60% by UPC² analysis on a Daicel Chiralpak IA column with a gradient 95:05 CO₂/EtOH with 0.1% of diethylamine as additive, flow rate 3mL/min, $\lambda = 240$ nm: $t_{r\text{ minor}} = 1.2$ min, $t_{r\text{ major}} = 1.1$ min.

¹H NMR (400 MHz, CDCl₃) δ: 1.21 (d, $J_{H,H} = 7.2$ Hz, 3H), 1.76 (m, 1H), 1.99 (m, 1H), 2.61 (m, 1H), 3.16 (t, $J_{H,H} = 7.2$ Hz, 2H), 3.68 (s, 3H), 6.59 (m, 2H, Ar), 6.7 (tt, $J_{H,H} = 7.2, 1.2$ Hz, 1H, Ar), 7.18 (m, 2H, Ar). **¹³C NMR** (100.6 MHz, CDCl₃) δ: 17.3 (1C), 33.3 (1C), 37.4 (1C), 41.8 (1C), 51.7 (1C), 112.7-148.1 (6C, Ar), 176.9 (1C). **ESI-HRMS**: Calculated for C₁₂H₁₇NO₂. Exact: (M: 207.1259, M+H: 208.1338); Experimental: (M+H: 208.1331).

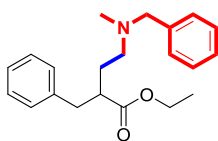
Ethyl 2-benzyl-4-morpholinobutanoate (4.56f)



General procedure B was followed employing **4.52b** (95 mg, 0.5 mmol) and morpholine (44 μL, 0.5 mmol). Purification by flash chromatography eluting with pentane/Et₂O (1:2) afforded **4.56f** (70 mg, 48%) as colorless oil. The enantiomeric excess was determined to be 75 % by UPC² analysis on a Daicel Chiralpak IG column with a gradient 95:05 CO₂/Methanol with 0.1% of diethylamine as additive, flow rate 2mL/min, λ = 210 nm: $t_{r\text{ minor}} = 4.7$ min, $t_{r\text{ major}} = 3.9$ min.

¹H NMR (400 MHz, CDCl₃) δ: 1.08 (t, $J_{H,H} = 7.2$ Hz, 3H), 1.56 (m, 1H), 1.80 (m, 1H), 2.27 (m, 6H), 2.65 (m, 2H), 2.87 (m, 1H), 3.59 (m, 4H), 4.0 (m, 2H), 7.08-7.22 (m, 5H, Ar). **¹³C NMR** (100.6 MHz, CDCl₃) δ: 14.2 (1C), 28.5 (1C), 38.7 (1C), 45.9 (1C), 53.7 (2C), 56.8 (1C), 60.3 (1C), 67.0 (2C), 126.4-139.4 (6C, Ar), 175.4 (1C). **ESI-HRMS**: Calculated for C₁₇H₂₅NO₃. Exact: (M: 291.1834, M+H: 292.1913); Experimental: (M+H: 292.1907).

Ethyl 2-benzyl-4-(benzyl(methyl)amino)butanoate (4.56g)

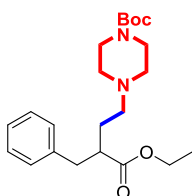


General procedure B was followed employing **4.52b** (95 mg, 0.5 mmol) and N-benzylmethylamine (66.5 μL, 0.5 mmol). Purification by flash chromatography eluting with pentane/Et₂O (4:1) afforded **4.56g** (58 mg, 37%) as colorless oil. The enantiomeric excess was determined to be 69 % by UPC² analysis on a CEL2 column with a

Rhodium catalyzed asymmetric HAM of α -alkyl acrylates

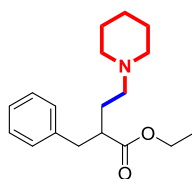
gradient 98:02 CO₂/Methanol with 0.1% of diethylamine as additive, flow rate 2mL/min, $\lambda = 210$ nm: $t_{r\text{ minor}} = 5.7$ min, $t_{r\text{ major}} = 4.9$ min.

¹H NMR (400 MHz, CDCl₃) δ : 1.04 (t, $J_{\text{H,H}} = 7.2$ Hz, 3H), 1.61 (m, 1H), 1.81 (m, 1H), 2.05 (s, 3H), 2.29 (m, 2H), 2.68 (m, 2H), 2.84 (m, 1H), 3.36 (bs, 2H), 3.94 (q, $J_{\text{H,H}} = 7.2$ Hz, 2H), 7.07-7.23 (m, 10H, Ar). ¹³C NMR (100.6 MHz, CDCl₃) δ : 14.2 (1C), 29.4 (1C), 38.6 (1C), 42.0 (1C), 45.5 (1C), 55.0 (1C), 60.2 (1C), 62.5 (1C), 126.3-139.3 (12C, Ar), 175.5 (1C). **ESI-HRMS**: Calculated for C₂₁H₂₇NO₂. Exact: (M: 325.2042, M+H: 326.2120); Experimental: (M+H: 326.2116).

Tert-butyl 4-(3-benzyl-4-ethoxy-4-oxobutyl)piperazine-1-carboxylate (4.56h)

General procedure B was followed employing **4.52b** (95 mg, 0.5 mmol) and N-Boc-piperazine (94 mg, 0.5 mmol). Purification by flash chromatography eluting with pentane/Et₂O (1:1) afforded **4.56h** (97 mg, 50%) as colorless oil. The enantiomeric excess was determined to be 71 % by UPC² analysis on a Daicel Chiralpak IG column with a gradient 85:15 CO₂/Methanol, flow rate 2mL/min, $\lambda = 205$ nm: $t_{r\text{ minor}} = 2.5$ min, $t_{r\text{ major}} = 2.7$ min.

¹H NMR (400 MHz, CDCl₃) δ : 1.07 (t, $J_{\text{H,H}} = 7.2$ Hz, 3H), 1.38 (s, 9H), 1.60 (m, 1H), 1.80 (m, 1H), 2.24 (m, 6H), 2.64 (m, 2H), 2.88 (dd, $J_{\text{H,H}} = 13.2, 7.6$ Hz, 1H), 3.30 (m, 4H), 3.99 (m, 2H), 7.08-7.20 (m, 5H, Ar). ¹³C NMR (100.6 MHz, CDCl₃) δ : 14.2 (1C), 28.4 (3C), 28.7 (1C), 38.7 (1C), 45.9 (2C), 52.9 (2C), 56.4 (1C), 60.3 (1C), 79.6 (1C), 126.4-139.1 (6C, Ar), 154.8 (1C), 175.4 (1C). **ESI-HRMS**: Calculated for C₂₂H₃₄NO₂. Exact: (M: 390.2519, M+H: 391.2597); Experimental: (M+H: 391.2596).

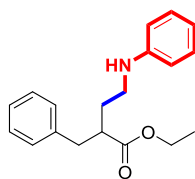
Ethyl 2-benzyl-4-(piperidin-1-yl)butanoate (4.56i)

General procedure B was followed employing **4.52b** (95 mg, 0.5 mmol) and piperidine (49.5 μ L, 0.5 mmol). Purification by flash chromatography with Al₂O₃ eluting with pentane/Et₂O (20:1)

afforded **4.56i** (40 mg, 28%) as colorless oil.

$^1\text{H NMR}$ (400 MHz, CDCl_3) δ : 1.07 (t, $J_{\text{H,H}} = 7.2$ Hz, 3H), 1.33 (m, 2H), 1.47 (m, 4H), 1.67 (m, 1H), 1.82 (m, 1H), 2.21 (m, 6H), 2.59 (m, 1H), 2.68 (dd, $J_{\text{H,H}} = 13.2, 6.8$ Hz, 1H), 2.68 (dd, $J_{\text{H,H}} = 13.6, 8.4$ Hz, 1H), 3.98 (q, $J_{\text{H,H}} = 7.2$ Hz, 2H), 7.08-7.21 (m, 5H, Ar). $^{13}\text{C NMR}$ (100.6 MHz, CDCl_3) δ : 14.2 (1C), 24.4 (1C), 25.9 (2C), 29.0 (1C), 38.7 (1C), 46.1 (1C), 54.6 (2C), 57.1 (1C), 60.2 (1C), 126.2-139.2 (6C, Ar), 175.4 (1C). **ESI-HRMS**: Calculated for $\text{C}_{18}\text{H}_{27}\text{NO}_2$. Exact: (M: 289.2042, M+H: 290.2120); Experimental: (M+H: 290.2119).

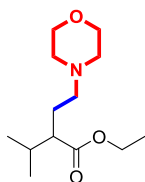
Ethyl 2-benzyl-4-(phenylamino)butanoate (**4.56j**)



General procedure C was followed employing **4.52b** (95 mg, 0.5 mmol) and aniline (46.0 μL , 0.5 mmol). Purification by flash chromatography eluting with pentane/ Et_2O (4:1) afforded **4.56j** (26 mg, 18%) as colorless oil. The enantiomeric excess was determined to be 66 % by UPC² analysis on a Daicel Chiralpak IA column with a gradient 90:10 CO_2 /Methanol, flow rate 3mL/min, $\lambda = 241$ nm: $t_{r \text{ minor}} = 1.5$ min, $t_{r \text{ major}} = 1.7$ min.

$^1\text{H NMR}$ (400 MHz, CDCl_3) δ : 1.14 (t, $J_{\text{H,H}} = 7.2$ Hz, 3H), 1.81 (m, 1H), 1.97 (m, 1H), 2.77 (m, 2H), 3.01 (m, 1H), 3.15 (m, 2H), 4.06 (q, $J_{\text{H,H}} = 7.2$ Hz, 3H), 6.55 (d, $J_{\text{H,H}} = 8.4$ Hz, 2H, Ar), 6.67 (t, $J_{\text{H,H}} = 7.2$ Hz, 1H, Ar), 7.14-7.30 (m, 7H, Ar). $^{13}\text{C NMR}$ (100.6 MHz, CDCl_3) δ : 14.2 (1C), 31.4 (1C), 38.6 (1C), 42.0 (1C), 45.5 (1C), 60.5 (1C), 112.7-148.0 (12C, Ar), 175.3 (1C). **ESI-HRMS**: Calculated for $\text{C}_{19}\text{H}_{23}\text{NO}_2$. Exact: (M: 297.1729, M+H: 298.1807); Experimental (M+H: 298.1802).

Ethyl 2-isopropyl-4-morpholinobutanoate (**4.56k**)

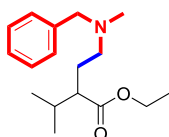


General procedure B was followed employing **4.52c** (71 mg, 0.5 mmol) and morpholine (44 μL , 0.5 mmol). Purification by flash chromatography eluting with pentane/ Et_2O (1:1) afforded **4.56k**

Rhodium catalyzed asymmetric HAM of α -alkyl acrylates

(117 mg, 96%) as colorless oil. The enantiomeric excess was determined to be 84% by UPC² analysis on a Daicel Chiralpak IG column with a gradient 95:5 CO₂/Acetonitrile with 0.1% of diethylamine as additive, flow rate 2mL/min, $\lambda = 230$ nm: $t_{r\text{ minor}} = 1.8$ min, : $t_{r\text{ major}} = 1.7$ min.

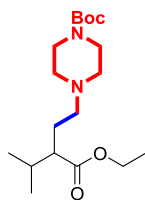
¹H NMR (400 MHz, CDCl₃) δ : 0.92 (t, $J_{\text{H,H}} = 6.8$ Hz, 6H), 1.26 (t, $J_{\text{H,H}} = 7.2$ Hz, 3H), 1.65 (m, 1H), 1.82 (m, 2H), 2.11 (m, 1H) 2.26 (m, 2H), 2.41 (bs, 4H), 3.68 (t, $J_{\text{H,H}} = 4.8$ Hz, 4H), 4.14 (m, 2H). ¹³C NMR (100.6 MHz, CDCl₃) δ : 14.5 (1C), 20.3 (1C), 20.5 (1C), 26.4 (1C), 30.9 (1C), 51.0 (1C), 53.9 (2C), 57.6 (1C), 60.1 (1C), 67.1 (2C), 175.6 (1C). **ESI-HRMS**: Calculated for C₁₃H₂₅NO₃. Exact: (M: 243.1834, M+H: 244.1913); Experimental: (M+H: 244.1907).

Ethyl 4-(benzyl(methyl)amino)-2-isopropylbutanoate (4.56I)

General procedure B was followed employing **4.52c** (71 mg, 0.5 mmol) and N-benzylmethylamine (66.5 μ L, 0.5 mmol). Purification by flash chromatography eluting with pentane/Et₂O (1:3) afforded **4.56I** (98 mg, 70%) as colorless oil. The enantiomeric excess was determined to be >80% by ¹H NMR using Eu(hfc)₃.

¹H NMR (400 MHz, CDCl₃) δ : 0.92 (t, $J_{\text{H,H}} = 7.2$ Hz, 6H), 1.23 (t, $J_{\text{H,H}} = 7.2$ Hz, 3H), 1.69 (m, 1H), 1.81 (m, 1H), 1.86 (m, 1H), 2.15 (s, 3H), 2.19 (m, 1H), 2.29 (m, 1H), 2.37 (m, 1H), 3.40 (d, $J_{\text{H,H}} = 12.8$ Hz, 1H), 3.50 (d, $J_{\text{H,H}} = 12.8$ Hz, 1H), 4.09 (m, 2H), 7.26-7.30 (m, 5H, Ar). ¹³C NMR (100.6 MHz, CDCl₃) δ : 14.3 (1C), 20.1 (1C), 20.4 (1C), 27.1 (1C), 30.7 (1C), 42.0 (1C) 50.4 (1C), 55.7 (1C), 59.9 (1C), 62.5 (1C), 126.8-139.1 (6C, Ar), 175.5 (1C). **ESI-HRMS**: Calculated for C₁₇H₂₇NO₂. Exact: (M: 277.2042, M+H: 278.2120); Experimental: (M+H: 278.2115).

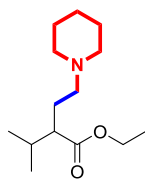
Tert-butyl 4-(3-(ethoxycarbonyl)-4-methylpentyl)piperazine-1-carboxylate (4.56m)



General procedure B was followed employing **4.52c** (71 mg, 0.5 mmol) and N-Boc-piperazine (93.1 mg, 0.5 mmol). Purification by flash chromatography eluting with pentane/Et₂O (1:1) afforded **4.56m** (94 mg, 55%) as colorless oil. The enantiomeric excess was determined to be >90% by ¹H NMR using Eu(hfc)₃.

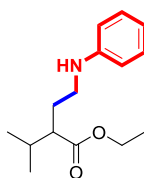
¹H NMR (400 MHz, CDCl₃) δ: 0.91 (t, *J*_{H,H} = 7.2 Hz, 6H), 1.25 (t, *J*_{H,H} = 7.2 Hz, 3H), 1.44 (s, 9H), 1.63 (m, 1H), 1.83 (m, 1H), 2.12 (m, 1H), 2.23 (m, 1H), 2.30 (m, 1H), 2.34 (bs, 4H), 3.39 (t, *J*_{H,H} = 4.8 Hz, 4H), 4.13 (m, 2H). ¹³C NMR (100.6 MHz, CDCl₃) δ: 14.5 (1C), 20.2 (1C), 20.5 (1C), 26.5 (1C), 28.4 (3C), 30.7 (1C), 43.1 (1C), 43.8 (1C), 50.9 (1C), 53.0 (2C), 57.0 (1C), 59.9 (1C), 79.5 (1C), 154.7 (1C), 175.4 (1C). **ESI-HRMS**: Calculated for C₁₈H₃₄N₂O₄. Exact: (M: 342.2519, M+H: 343.2597); Experimental: (M+H: 343.2595).

Ethyl 2-isopropyl-4-(piperidin-1-yl)butanoate (4.56n)



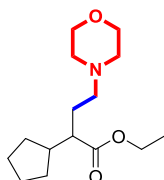
General procedure B was followed employing **4.52c** (71 mg, 0.5 mmol) and piperidine (49.5 μL, 0.5 mmol). Purification by flash chromatography eluting with Et₂O afforded the **4.56n** (111 mg, 92%) as colorless oil.

¹H NMR (400 MHz, CDCl₃) δ: 0.92 (dd, *J*_{H,H} = 8, 6.8 Hz, 6H), 1.26 (t, *J*_{H,H} = 6.8 Hz, 3H), 1.41 (m, 2H), 1.55 (m, 4H), 1.68 (m, 2H), 1.84 (m, 1H), 2.09 (m, 1H), 2.18 (m, 1H), 2.30 (m, 1H), 2.34 (bs, 4H), 4.13 (m, 2H). ¹³C NMR (100.6 MHz, CDCl₃) δ: 14.4 (1C), 20.1 (1C), 20.5 (1C), 24.4 (1C), 26.0 (2C), 26.8 (1C), 30.8 (1C), 51.2 (1C), 54.7 (2C), 57.8 (1C), 59.9 (1C), 175.6 (1C). **ESI-HRMS**: Calculated for C₁₄H₂₇NO₂. Exact: (M: 241.2042, M+H: 242.2120); Experimental: (M+H: 242.2109).

Ethyl 2-isopropyl-4-(phenylamino)butanoate (4.56o)

General procedure C was followed employing **4.52c** (71 mg, 0.5 mmol) and aniline (46 μ L, 0.5 mmol). Purification by flash chromatography eluting with pentane/Et₂O (1:1) afforded **4.56o** (68.7 mg, 55%) as colorless oil. The enantiomeric excess was determined to be 77% by UPC² analysis on a Daicel Chiralpak IG column with a gradient 85:15 CO₂/Acetonitrile with 0.1% of diethylamine as additive, flow rate 3 mL/min, λ = 243 nm: $t_{r\text{ minor}}$ = 2.3 min, $t_{r\text{ major}}$ = 1.8 min.

¹H NMR (400 MHz, CDCl₃) δ : 0.93 (dd, $J_{\text{H,H}}$ = 6.6, 2.4, 6H), 1.25 (t, $J_{\text{H,H}}$ = 7.2 Hz, 3H), 1.81 (m, 1H), 1.93 (m, 2H), 2.23 (m, 1H), 3.10 (m, 2H), 4.14 (m, 2H), 6.58 (m, 2H, Ar), 6.59 (tt, $J_{\text{H,H}}$ = 7.2, 1.2 Hz, 1H, Ar), 7.16 (m, 2H, Ar). ¹³C NMR (100.6 MHz, CDCl₃) δ : 14.5 (1C), 20.2 (1C), 20.5 (1C), 29.2 (1C), 30.9 (1C), 42.7 (1C), 50.6 (1C), 60.4 (1C), 112.8-148.2 (6C, Ar), 175.6 (1C). **ESI-HRMS**: Calculated for C₁₅H₂₃NO₂. Exact: (M: 249.1729, M+H: 250.1807); Experimental: (M+H: 250.1796).

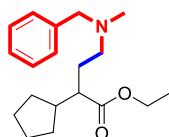
Ethyl 2-cyclopentyl-4-morpholinobutanoate (4.56p)

General procedure B was followed employing **4.52d** (84.1 mg, 0.5 mmol) and morpholine (44 μ L, 0.5 mmol). Purification by flash chromatography eluting with pentane/Et₂O (1:1) afforded **4.56p** (101 mg, 75%) as colorless oil. The enantiomeric excess was determined to be 85% by UPC² analysis on a Daicel Chiralpak IG column with a gradient 96:4 CO₂/MeOH with 0.1% of diethylamine as additive, flow rate 2 mL/min, λ = 230 nm: $t_{r\text{ minor}}$ = 3.7 min, $t_{r\text{ major}}$ = 3.5 min.

¹H NMR (400 MHz, CDCl₃) δ : 1.14 (tt, $J_{\text{H,H}}$ = 6.8, 2Hz, 1H), 1.22 (t, $J_{\text{H,H}}$ = 7.2 Hz, 1H), 1.26 (t, $J_{\text{H,H}}$ = 7.2 Hz, 3H), 1.50-1.69 (m, 6H), 1.82 (m, 2H), 1.96 (m, 1H), 2.12 (m, 1H), 2.22 (m, 1H), 2.31 (m, 1H), 2.40 (bs, 4H), 3.68 (bs, 4H), 4.13 (m, 2H). ¹³C NMR (100.6 MHz, CDCl₃) δ : 14.5 (1C), 25.1 (1C), 28.6 (1C), 30.8 (1C), 31.0 (1C), 43.0 (1C), 50.0 (1C), 53.9 (2C), 54.1 (1C), 57.4 (1C), 60.1 (1C), 67.1 (2C), 176.0 (1C). **ESI-HRMS**:

Calculated for $C_{15}H_{27}NO_3$. Exact: (M: 269.1991, M+H: 270.2069); Experimental: (M+H: 270.2065).

Ethyl 4-(benzyl(methyl)amino)-2-cyclopentylbutanoate (4.56q)

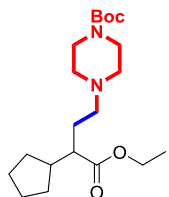


General procedure B was followed employing **4.52d** (84.1 mg, 0.5 mmol) and morpholine N-benzylmethylamine (66.5 μ L, 0.5 mmol).

Purification by flash chromatography eluting with pentane/Et₂O (1:1) afforded **4.56q** (82 mg, 55%) as colorless oil.

¹H NMR (400 MHz, CDCl₃) δ : 1.14 (m, 2H), 1.22 (t, $J_{H,H}$ = 7.2 Hz, 3H), 1.50-1.83 (m, 8H), 1.97 (m, 1H), 2.14 (s, 3H), 2.25 (m, 2H), 2.39 (m, 1H), 3.41 (d, $J_{H,H}$ = 12.8 Hz, 1H), 3.50 (d, $J_{H,H}$ = 12.8 Hz, 1H), 4.10 (m, 2H), 7.22-7.31 (m, 5H, Ar). ¹³C NMR (100.6 MHz, CDCl₃) δ : 14.4 (1C), 25.1 (2C), 29.4 (1C), 30.7 (1C), 31.0 (1C), 42.1 (1C), 43.0 (1C), 49.5 (1C), 55.7 (1C), 60.0 (1C), 62.6 (1C), 127.0-139.3 (6C, Ar), 176.0 (1C). **ESI-MS**: Calculated for $C_{19}H_{29}NO_3$. Exact: (M: 303.2198, M+H: 304.2277); Experimental: (M+H: 304.2280).

Tert-butyl 4-(3-cyclopentyl-4-ethoxy-4-oxobutyl)piperazine-1-carboxylate (4.56r)



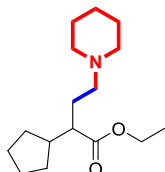
General procedure B was followed employing **4.52d** (84.1 mg, 0.5 mmol) and 1-Boc-piperazine (93.1 mg, 0.5 mmol). Purification by flash chromatography eluting with pentane/Et₂O (4:1) afforded

4.56r (136.4 mg, 74%) as colorless oil. The enantiomeric excess was determined to be 84% by UPC² analysis on a Daicel Chiralpak IG column with a gradient 90:10 CO₂/MeOH with 0.1% of diethylamine as additive, flow rate 2 mL/min, λ = 230 nm: $t_{r\text{ minor}}$ = 3.2 min, $t_{r\text{ major}}$ = 3.7 min.

¹H NMR (400 MHz, CD₂Cl₂) δ : 1.03 (m, 1H), 1.15 (t, $J_{H,H}$ = 7.2 Hz, 3H), 1.15 (m, 1H), 1.35 (s, 9H), 1.43 (m, 6H), 1.51 (m, 2H), 1.85 (m, 1H), 2.14 (m, 1H), 2.25 (m, 2H), 2.33 (m, 4H), 2.45 (m, 1H), 3.39 (m, 4H), 4.10 (m, 2H). ¹³C NMR (100.6 MHz, CD₂Cl₂) δ : 14.2 (1C), 15.9 (1C), 25.0 (1C), 28.1 (3C), 28.6 (1C), 30.5 (1C), 30.8 (1C), 42.9 (2C), 49.9 (1C), 53.0 (2C), 56.8 (1C), 60.0 (1C), 64.7 (1C), 79.7 (1C), 154.5 (1C), 175.6

(1C). **ESI-HRMS**: Calculated for $C_{20}H_{37}N_2O_4$. Exact: (M: 368.2675, M+H: 369.2753); Experimental: (M+H: 369.2696).

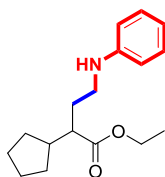
Ethyl 2-cyclopentyl-4-(piperidin-1-yl)butanoate (4.56s)



General procedure B was followed employing **4.52d** (84.1 mg, 0.5 mmol) and piperidine (49.5 μ L, 0.5 mmol). Purification by flash chromatography eluting with pentane/Et₂O (1:1) afforded **4.56s** (67 mg, 50%) as colorless oil. The enantiomeric excess was determined to be 84% by UPC² analysis on a Daicel Chiralpak IC column with a gradient 90:10 CO₂/EtOH, with 0.1% of diethylamine as additive, flow rate 2 mL/min, $\lambda = 230$ nm: $t_{r\text{ minor}} = 3.5$ min, $t_{r\text{ major}} = 3.8$ min.

¹H NMR (400 MHz, CDCl₃) δ : 1.15 (m, 2H), 1.24 (m, 1H), 1.25 (t, $J_{H,H} = 7.2$ Hz, 3H), 1.43 (bs, 2H), 1.51 (m, 2H), 1.60 (bs, 7H), 1.84 (m, 3H), 1.96 (m, 1H), 2.13 (td, $J_{H,H} = 10, 3.6$ Hz, 1H), 2.24 (m, 1H), 2.40 (bs, 4H), 4.13 (m, 2H). ¹³C NMR (100.6 MHz, CDCl₃) δ : 14.5 (1C), 24.5 (1C), 25.1 (1C), 25.9 (2C), 28.8 (1C), 30.8 (1C), 30.9 (1C), 43.0 (2C), 50.1 (1C), 54.7 (2C), 57.6 (1C), 60.0 (1C), 175.8 (1C). **ESI-HRMS**: Calculated for C₁₆H₂₉NO₂. Exact: (M: 267.2198, M+H: 268.2277); Experimental: (M+H: 268.2285).

Ethyl 2-cyclopentyl-4-(piperidin-1-yl) butanoate (4.56t)



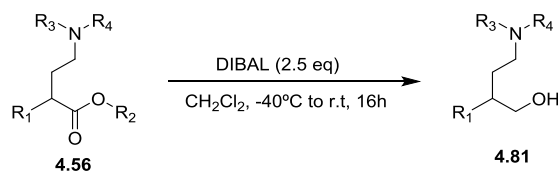
General procedure C was followed employing **4.52d** (84.1 mg, 0.5 mmol) and aniline (46.0 μ L, 0.5 mmol). Purification by flash chromatography eluting with pentane/Et₂O (1:1) afforded **4.56t** (68.9 mg, 50%) as colorless oil. The enantiomeric excess was determined to be 84% by UPC² analysis on a Daicel Chiralpak IG column with a gradient 80:20 CO₂/MeOH, with 0.1% of diethylamine as additive, flow rate 3 mL/min, $\lambda = 243$ nm: $t_{r\text{ minor}} = 3.4$ min, $t_{r\text{ major}} = 2.8$ min.

¹H NMR (400 MHz, CDCl₃) δ : 1.11 (m, 1H), 1.20 (m, 1H), 1.24 (t, $J_{H,H} = 7.2$ Hz, 3H), 1.56 (m, 6H), 1.84 (m, 3H), 2.01 (m, 1H), 2.26 (m, 1H), 3.11 (m, 2H), 4.14 (q, $J_{H,H} =$

7.2 Hz, 2H), 6.59 (m, 2H, Ar), 6.69 (t, $J_{H,H} = 7.6$ Hz, 1H, Ar), 7.16 (m, 2H, Ar). ^{13}C
NMR (100.6 MHz, CDCl_3) δ : 14.3 (1C), 25.0 (2C), 30.7 (1C), 30.8 (1C), 31.2 (1C), 42.4
 (1C), 42.8 (1C), 49.5 (1C), 60.3 (1C), 112.8-148.1 (6C, Ar), 175.9 (1C). **ESI-HRMS**:
 Calculated for $\text{C}_{17}\text{H}_{25}\text{NO}_2$. Exact: (M: 275.1885, M+H: 276.1964); Experimental:
 (M+H: 276.1962).

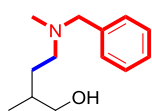
4.5.4. Reduction of α -alkyl- γ -aminobutyric esters

**General procedure D: reduction of α -alkyl- γ -aminobutyric esters 4.56 into the
 corresponding aminoalcohols 4.81**



Diisobutylaluminum hydride (DIBAL) solution 1.0 M in DCM (2.5 eq) was added dropwise to a solution of the corresponding amino ester **4.56** (1 eq) in CH_2Cl_2 (2.0 mL) at -40°C . The reaction was left stirring at -40°C for 1h, then allowed to reach room temperature and left stirring overnight. The reaction was quenched by addition of NH_4Cl sat. solution (2 mL) at 0°C and the mixture was left stirring for 2h. Then, the aqueous phase was extracted with CH_2Cl_2 (3 x 2 mL), the organic phases were dried with MgSO_4 , filtrated and concentrated under vacuum. The residue was finally purified by chromatographic column using Al_2O_3 to afford the corresponding **4.81**.

4-(benzyl(methyl)amino)-2-methylbutan-1-ol (**4.81a**)

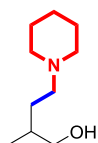


General procedure D was followed employing **4.56c** (31 mg, 0.13 mmol) and DIBAL (325 μL , 0.33 mmol). Purification by flash chromatography eluting with CH_2Cl_2 and 1% of MeOH afforded **4.81a** (26 mg, 95 %) as colorless oil. The enantiomeric excess was determined to be 62%

by HPLC analysis on a Chiralpack IG column with a gradient 95:05 CO₂/MeOH, with 0.1% of diethylamine as additive, flow rate 2 mL/min, $\lambda = 210$ nm: $t_{r\ minor} = 7.4$ min, $t_{r\ major} = 7.7$ min.

¹H NMR (400 MHz, CDCl₃) δ : 0.86 (d, $J_{H,H} = 6.8$ Hz, 3H), 1.55 (m, 1H), 1.64 (m, 1H), 1.75 (m, 1H), 2.13 (s, 3H), 2.43 (m, 1H), 2.52 (m, 1H), 3.29 (dd, $J_{H,H} = 11.4, 8.4$ Hz, 1H), 3.47 (d, $J_{H,H} = 12.4$ Hz, 1H), 3.51 (dd, $J_{H,H} = 11.6, 1.2$ Hz, 2H), 3.56 (d, $J_{H,H} = 12.4$ Hz, 1H), 7.27 (m, 5H, Ar). ¹³C NMR (100.6 MHz, CDCl₃) δ : 18.3 (1C), 34.0 (1C), 36.9 (1C), 41.1 (1C), 56.5 (1C), 62.7 (1C), 68.7 (1C), 127.5-137.4 (6C, Ar). **ESI-HRMS**: Calculated for C₁₃H₂₂NO. Exact: (M: 207.1623, M+H: 208.1701); Experimental: (M+H: 208.1698).

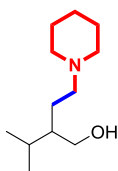
2-methyl-4-(piperidin-1-yl) butan-1-ol (**4.81b**)



General procedure D was followed employing **4.56d** (59.8 mg, 0.3 mmol) and DIBAL (750 μ L, 0.75 mmol). Purification by flash chromatography eluting with CH₂Cl₂ and 1% of MeOH afforded **4.81b** (15 mg, 30 %) as colorless oil.

¹H NMR (400 MHz, CDCl₃) δ : 0.81 (d, $J_{H,H} = 7.2$ Hz, 3H), 1.33-1.57 (m, 10H), 1.69 (m, 1H), 2.30 (m, 4H), 2.47 (bs, 1H), 3.18 (dd, $J_{H,H} = 11.2, 8.8$ Hz, 1H), 3.43 (dd, $J_{H,H} = 10.4, 3.6$ Hz, 1H). ¹³C NMR (100.6 MHz, CDCl₃) δ : 18.3 (1C), 24.4 (1C), 25.5 (2C), 33.6 (1C), 37.3 (1C), 54.3 (1C), 57.5 (2C), 68.6 (1C). **ESI-HRMS**: Calculated for C₁₀H₂₂NO. Exact: (M: 171.1623, M+H: 172.1701); Experimental: (M+H: 172.1697).

2-isopropyl-4-(piperidin-1-yl) butan-1-ol (**4.81c**)

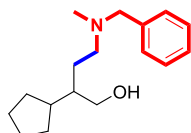


General procedure D was followed employing **4.56n** (73 mg, 0.31 mmol) and DIBAL (780 μ L, 0.78 mmol). Purification by flash chromatography eluting with CH₂Cl₂ and 1% of MeOH afforded **4.81c** (33 mg, 53 %) as colorless oil.

¹H NMR (400 MHz, CDCl₃) δ : 0.88 (t, $J_{H,H} = 6.8$ Hz, 6 H), 1.49 (m, 2H), 1.66 (m, 4H), 1.82 (q, $J_{H,H} = 6.4$ Hz, 2H), 1.91 (bs, 4H), 2.90 (bs, 4H), 3.52 (dd, $J_{H,H} = 11.2, 8.4$ Hz, 1

H), 3.71 (dd, $J_{H,H} = 11.2, 3.6$ Hz, 1H). ^{13}C NMR (100.6 MHz, CDCl_3) δ : 19.6 (1C), 19.9 (1C), 23.3 (2C), 24.2 (1C), 26.4 (1C), 29.8 (1C), 46.6 (1C), 53.8 (1C), 57.3 (2C), 64.6 (1C). **ESI-HRMS**: Calculated for $\text{C}_{12}\text{H}_{26}\text{NO}$. Exact: (M: 199.1936, M+H: 200.2014); Experimental: (M+H: 200.2013).

4-(benzyl(methyl)amino)-2-cyclopentylbutan-1-ol (4.81d)



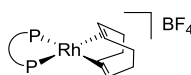
General procedure D was followed employing **4.56q** (91 mg, 0.3 mmol) and DIBAL (750 μL , 0.75 mmol). Purification by flash chromatography eluting with CH_2Cl_2 and 1% of MeOH afforded

4.81d (33 mg, 55 %) as colorless oil. The enantiomeric excess was determined to be 48% by UPC² analysis on a Daicel Chiralpak IG column with a gradient 90:10 CO_2/MeOH with 0.1% of diethylamine as additive, flow rate 2 mL/min, $\lambda = 210$ nm: $t_{r\text{ minor}} = 5.0$ min, $t_{r\text{ major}} = 5.6$ min.

^1H NMR (400 MHz, CDCl_3) δ : 1.10 (m, 2H), 1.40-1.50 (m, 10H), 2.15 (s, 3H), 2.44 (m, 1H), 2.55 (m, 1H), 3.44 (dd, $J_{H,H} = 11.6, 7.6$ Hz, 1H), 3.52 (d, $J_{H,H} = 12.8$ Hz, 1H), 3.56 (d, $J_{H,H} = 12.8$ Hz, 1H), 3.64 (dd, $J_{H,H} = 11.6, 2.4$ Hz, 1H), 7.26-7.35 (m, 5H, Ar). ^{13}C NMR (100.6 MHz, CDCl_3) δ : 25.1 (1C), 25.3 (1C), 30.5 (1C), 30.9 (1C), 31.0 (1C), 41.1 (1C), 41.4 (1C), 47.4 (1C), 56.0 (1C), 62.7 (1C), 66.0 (1C), 127.5-131.2 (6C, Ar). **ESI-HRMS**: Calculated for $\text{C}_{17}\text{H}_{27}\text{NO}$. Exact: (M: 261.2093, M+H: 262.2171); Experimental: (M+H: 262.2179).

4.5.5. Synthesis of Rhodium complexes 4.63, 4.64 and 4.65

[Rh(COD)(4.54)]BF₄ (4.63)



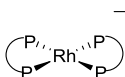
Bis(1,5-cyclooctadiene)rhodium(I) tetrafluoroborate (40 mg, 0.1 mmol) was dissolved in anhydrous dichloromethane (5 mL) and cooled to -20°C . Then, (*R,R*)-QuinoxP* **4.54** (33.4 mg, 0.1 mmol) in anhydrous dichloromethane (5 mL) was added dropwise for 30 min. The reaction was left stirring at -20°C for 1h and then left stirring at room temperature for another 1h. After that, the crude was concentrated under vacuum, and the complex was

Rhodium catalyzed asymmetric HAM of α -alkyl acrylates

precipitated with anhydrous diethyl ether at 0°C. The precipitated was filtrated, and washed with anhydrous hexane to afford the desired complex **4.63** (49 mg, 78 %) as orange solid.

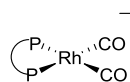
$^1\text{H NMR}$ (400 MHz, CD_2Cl_2) δ : 1.10 (d, $J_{\text{P,H}} = 15.2$ Hz, 18H), 1.86 (d, $J_{\text{P,H}} = 8.0$ Hz, 6H), 2.23 (m, 4H), 2.56 (m, 2H), 2.67 (m, 2H), 5.03 (m, 2H), 6.12 (m, 2H), 7.99 (dd, $J_{\text{H,H}} = 6.4, 3.2$ Hz, 2H, *Ar*), 8.29 (dd, $J_{\text{H,H}} = 6.4, 3.2$ Hz, 2H, *Ar*). $^{13}\text{C NMR}$ (100.6 MHz, CD_2Cl_2) δ : 4.0 (t, $J_{\text{P,C}} = 10.3$ Hz, 2C), 26.2 (2C), 28.4 (6C), 35.8 (2C), 38.4 (t, $J_{\text{P,C}} = 12.8$ Hz, 2C), 92.4 (m, 2C), 107.2 (dt, $J_{\text{Rh,C}} = 7.8$ Hz, $J_{\text{P,C}} = 2.2$ Hz, 2C), 130.2-142.8 (6C, *Ar*), 154.4 (td, $J_{\text{P,C}} = 53.3$ Hz, $J_{\text{Rh,C}} = 2.4$ Hz, 2C, *Ar*). $^{31}\text{P NMR}$ (161.97 MHz, CD_2Cl_2) δ : 41.6 (d, $J_{\text{Rh,P}} = 148.2$ Hz, 2P). **ESI-HRMS**: Calculated for $\text{C}_{26}\text{H}_{40}\text{N}_2\text{P}_2\text{Rh}$. Exact: (M+: 545.1716); Experimental: (M+: 545.1715).

[Rh(4.54)₂]BF₄ (4.64)

 Bis(1,5-cyclooctadiene)rhodium(I) tetrafluoroborate (40 mg, 0.1 mmol) was dissolved in anhydrous CH_2Cl_2 (2 mL). Then, (*R,R*)-QuinoxP* **4.54** (100 mg, 0.3 mmol) in anhydrous dichloromethane (2 mL) was added dropwise, and the reaction was left stirring for 1h. After that, the crude was concentrated under vacuum, and the complex was precipitated with anhydrous diethyl ether at 0°C. The precipitated was filtrated, and washed with anhydrous hexane to afford the desired complex **4.64** (73 mg, 85 %) as orange solid.

$^1\text{H NMR}$ (400 MHz, CD_2Cl_2) δ : 1.07 (t, $J_{\text{P,H}} = 7.2$ Hz, 36H), 2.23 (s, 12H), 7.99 (dd, $J_{\text{H,H}} = 6.4, 3.2$ Hz, 4H, *Ar*), 8.32 (dd, $J_{\text{H,H}} = 6.4, 3.2$ Hz, 4H, *Ar*). $^{13}\text{C NMR}$ (100.6 MHz, CD_2Cl_2) δ : 9.5 (t, $J_{\text{P,C}} = 6.9$ Hz, 4C), 28.4 (12C), 38.3 (t, $J_{\text{P,C}} = 6.4$ Hz, 4C), 130.0-142.5 (12C, *Ar*), 155.8 (td, $J_{\text{P,C}} = 26.8$ Hz, $J_{\text{Rh,C}} = 1.4$ Hz, 4C, *Ar*). $^{31}\text{P NMR}$ (161.97 MHz, CD_2Cl_2) δ : 38.9 (d, $J_{\text{Rh,P}} = 130.4$ Hz, 2P). **ESI-HRMS**: Calculated for $\text{C}_{36}\text{H}_{56}\text{N}_4\text{P}_4\text{Rh}$. Exact: (M+: 771.2505); Experimental: (M+: 771.2539).

[Rh(4.54)(CO)₂]BF₄ (4.65)



Complex [Rh(COD)(4.54)]BF₄ **4.63** (20 mg, 0.035 mmol) was dissolved in anhydrous CH₂Cl₂ (5 mL). Then, CO was bubbled into the previous solution for 1h. After that, the solvent was evaporated under vacuum, and the residue was washed with Et₂O (3 x 1 mL) to afford the desired complex **4.65** (20 mg, 97 %) as yellow solid.

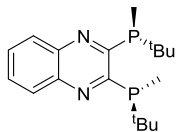
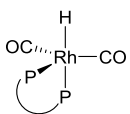
¹H NMR (400 MHz, CD₂Cl₂) δ: 1.24 (d, *J*_{P,H} = 17.2 Hz, 18H), 2.13 (dd, *J*_{P,H} = 10.0 Hz, *J*_{Rh,H} = 1.2 Hz, 6H), 8.12 (dd, *J*_{H,H} = 6.4, 3.6 Hz, 2H, *Ar*), 8.38 (dd, *J*_{H,H} = 6.4, 3.6 Hz, 2H, *Ar*). ¹³C NMR (100.6 MHz, CD₂Cl₂) δ: 7.5 (t, *J*_{P,C} = 13.5 Hz, 2C), 27.8 (6C), 36.5 (t, *J*_{P,C} = 13.8 Hz, 2C), 130.0-142.7 (6C, *Ar*), 152.3 (td, *J*_{P,C} = 57.8 Hz, *J*_{Rh,C} = 2.6 Hz, 2C, *Ar*), 184.6 (m, 2C, CO). ³¹P NMR (161.97 MHz, CD₂Cl₂) δ: 47.2 (d, *J*_{Rh,P} = 114.7 Hz, 2P). IR (neat): ν (CO) = 2097, 2051 cm⁻¹

4.5.6. In situ HP-NMR experiments

In a typical experiment, a sapphire tube (∅ = 5 mm) was filled under nitrogen atmosphere with a solution of the rhodium precursor, and a solution of (*R,R*)-QuinoxP* **4.54** in a ratio Rh/L = 1:1.2 in a total volume of 0.4 mL. The HP-NMR tube was purged with vacuum/CO, pressurized to the appropriate pressure of H₂/CO, heated if required, and left shaking. After that, the solution was analyzed by NMR spectroscopy, and finally the solution was analyzed by IR and GC-MS after depressurizing if required.

4.5.7. Synthesis of [RhH(CO)₂(L)] complexe 4.61

[RhH(CO)₂(4.54)] 4.61



A solution of [Rh(acac)(CO)₂] (3.9 mg, 0.015 mmol) and (*R,R*)-QuinoxP* ligand **4.54** (6 mg, 0.018 mmol) in tol-*d*₈ (0.4 mL) was introduced in the HP-NMR tube under inert

atmosphere. After that, the HP-NMR tube was then pressurized at 10 bar (H_2/CO , 4:1) and left shaking for 96h at room temperature.

1H NMR (400 MHz, $C_6D_5CD_3$) δ : - 8.5 (td, $J_{Rh,H} = 10.4$ Hz, $J_{P,H} = 57.6$ Hz), 1.05 (m, 18H), 1.79 (bs, 6H), 7.3 (m, 2H), 7.9 (m, 2H). ^{13}C NMR (100.6 MHz, $C_6D_5CD_3$) δ : 14.9 (2C), 28.0 (6C), 31.9 (t, $J_{P,C} = 9.4$ Hz, 2C), 129.9-141.2 (6C, Ar), 162.5 (t, $J_{P,C} = 47.9$ Hz, 2C, Ar), 199.1 (dt, $J_{P,C} = 10.8$ Hz, $J_{Rh,C} = 68.8$ Hz, 2C, CO). ^{31}P NMR (161.97 MHz, $C_6D_5CD_3$) δ : 51.6 (d, $J_{Rh,P} = 114.7$ Hz).

4.6. References

- ¹ Kalck, P.; Urrutigoity, M. *Chem. Rev.* **2018**, *118*, 3833-3861.
- ² Crozet, D.; Kefalidis, C. E.; Urrutigoity, M.; Maron, L.; Kalck, P. *ACS Catal.* **2014**, *4*, 435-447.
- ³ Hoffmann, S.; Nicoletti, M.; List, B. *J. Am. Chem. Soc.* **2006**, *128*, 13074-13075.
- ⁴ Villa-Marcos, B.; Xiao, J. *Chin. J. Catal.* **2015**, *36*, 106-112.
- ⁵ Meng, J.; Li, X.-H.; Han, Z.-Y. *Org. Lett.* **2017**, *19*, 1076-1079.
- ⁶ Chen, C.; Jin, S.; Zhang, Z.; Wei, B.; Wang, H.; Zhang, K.; Lv, H.; Dong, X.-Q.; Zhang, X. *J. Am. Chem. Soc.* **2016**, *138*, 9017-9020.
- ⁷ Limanto, J.; Ashley, E. R.; Yin, J.; Beutner, G. L.; Grau, B. T.; Kassim, A. M.; Kim, M. M.; Klapars, A.; Liu, Z.; Strotman, H. R.; Truppo, M. D. *Org. Lett.* **2014**, *16*, 2716-2719.
- ⁸ Cross, P. E.; MacKenzie, A. R., U.S. Patent 005096890A, **1992**.
- ⁹ a) Wu, G. *Amino Acids* **2009**, *37*, 1-17. b) Wagner, I.; Musso, H. *Angew. Chem. Int. Ed.* **1983**, *22*, 816-828.
- ¹⁰ Brown, K. M.; Roy, K. K.; Hockerman, G. H.; Doerksen, R. J.; Colby, D. A. *J. Med. Chem.* **2015**, *58*, 6336-6347.
- ¹¹ Abdel-Halim, H.; Hanrahan, J. R.; Hibbs, D. E.; Johnston, G. A. R.; Chebib, M. *Chem. Biol. Drug Des.* **2008**, *71*, 306-327.

¹² a) Mann, A.; Boulanger, T.; Brandau, B.; Durant, F.; Evrard, G.; Heaulme, M.; Desaulles, E.; Wermuth, C. G. *J. Med. Chem.* **1991**, *34*, 1307-1313. b) Fromm, G. H.; Terrence, C. F.; Chattha, A. S.; Glass, J. D. *Archives of Neurology* **1980**, *37*, 768-771.

¹³ a) Hoekstra, M. S.; Sobieray, D. M.; Schwindt, M. A.; Mulhern, T. A.; Grote, T. M.; Huckabee, B. K.; Hendrickson, V. S.; Franklin, L. C.; Granger, E. J.; Karrick, G. L. *Org. Process Res. Dev.* **1997**, *1*, 26-38. b) Chandrasekhar, S.; Mohapatra, S. *Tetrahedron Lett.* **1998**, *39*, 6415-6418.

¹⁴ Lippert, B.; Metcalf, B. W.; Jung, M. J.; Casara, P. *Eur. J. Biochem.* **1977**, *74*, 441-445.

¹⁵ Lapin, I. *CNS Drug Rev.* **2001**, *7*, 471-481.

¹⁶ a) Ordóñez, M.; Cativiela, C. *Tetrahedron: Asymmetry* **2007**, *18*, 3-99. b) Ordóñez, M.; Cativiela, C.; Romero-Estudillo, I. *Tetrahedron: Asymmetry* **2016**, *27*, 999-1055.

¹⁷ a) Strunz, A. K.; Zweemer, A. J. M.; Weiss, C.; Schepmann, D.; Junker, A.; Heitman, L. H.; Koch, M.; Wünsch, B. *Bioorg. Med. Chem.* **2015**, *23*, 4034-4049. b) Butora, G.; Morriello, G. J.; Kothandaraman, S.; Guiadeen, D.; Pasternak, A.; Parsons, W. H.; MacCoss, M.; Vicario, P. P.; Cascieri, M. A.; Yang, L. *Bioorg. Med. Chem. Lett.* **2006**, *16*, 4715-4722. c) Nair, P. C.; Srikanth, K.; Sobhia, M. E. *Bioorg. Med. Chem. Lett.* **2008**, *18*, 1323-1330.

¹⁸ Wang, X.; Buchwald, S. L. *J. Am. Chem. Soc.* **2011**, *133*, 19080-19083.

¹⁹ Imamoto, T.; Tamura, K.; Zhang, Z.; Horiuchi, Y.; Sugiya, M.; Yoshida, K.; Yanagisawa, A.; Gridnev, I. D. *J. Am. Chem. Soc.* **2012**, *134*, 1754-1769.

²⁰ Fuentes, J. A.; Wawrzyniak, P.; Roff, G. J.; Buhl, M.; Clarke, M. L. *Catal. Sci. Technol.* **2011**, *1*, 431-436.

²¹ Crozet, D.; Gual, A.; McKay, D.; Dinoi, C.; Godard, C.; Urrutigoity, M.; Daran, J.-C.; Maron, L.; Claver, C.; Kalck, P. *Chem. Eur. J.* **2012**, *18*, 7128-7140.

²² Noonan, G. M.; Fuentes, J. A.; Cogley, C. J.; Clarke, M. L. *Angew. Chem. Int. Ed.* **2012**, *51*, 2477-2480.

²³ Scheetz, P. M.; Blank, N. F.; Gibbons, S. K.; Glueck, D. S.; Rheingold, A. L. *Inorg. Chim. Acta* **2018**, *483*, 111-115.

²⁴ Gridnev, I. D.; Higashi, N.; Asakura, K.; Imamoto, T. *J. Am. Chem. Soc.* **2000**, *122*, 7183-7194.

Rhodium catalyzed asymmetric HAM of α -alkyl acrylates

- ²⁵ a) Ingleson, M. J.; Brayshaw, S. K.; Mahon, M. F.; Ruggiero, G. D.; Weller, A. S. *Inorg. Chem.* **2005**, *44*, 3162-3171. b) Kubas, G. J. *Chem. Rev.* **2007**, *107*, 4152-4205.
- ²⁶ Shen, Z.; Dornan, P. K.; Khan, H. A.; Woo, T. K.; Dong, V. M. *J. Am. Chem. Soc.* **2009**, *131*, 1077-1091.
- ²⁷ *Mechanisms in Homogeneous Catalysis*, Eds. Heaton, B. Wiley-VCH, Darmstadt, Germany, **2005**.
- ²⁸ Matsubara, T.; Saito, Y. *J. Mol. Catal.* **1994**, *92*, 1-8.
- ²⁹ a) Gridnev, I. D.; Imamoto, T. *ACS Catal.* **2015**, *5*, 2911-2915. b) Landis, C. R.; Halpern, J. *J. Am. Chem. Soc.* **1987**, *109*, 1746-1754.
- ³⁰ Scheuermann née Taylor, C. J.; Jaekel, C. *Adv. Synth. Catal.* **2008**, *350*, 2708-2714.
- ³¹ Gridnev, I. D.; Imamoto, T.; Hoge, G.; Kouchi, M.; Takahashi, H. *J. Am. Chem. Soc.* **2008**, *130*, 2560-2572.

UNIVERSITAT ROVIRA I VIRGILI
RH-CATALYZED CARBOXYLATION OF DISUBSTITUTED OLEFINS: ASYMMETRIC CATALYSIS, CONTINUOUS
FLOW AND TANDEM HYDROAMINOMETHYLATION REACTION
Anton Cunillera Martin

Chapter 5

Synthesis of $\beta^{2,2}$ -amino esters via Rh-catalyzed regioselective HAM

UNIVERSITAT ROVIRA I VIRGILI
RH-CATALYZED CARBONYLATION OF DISUBSTITUTED OLEFINS: ASYMMETRIC CATALYSIS, CONTINUOUS
FLOW AND TANDEM HYDROAMINOMETHYLATION REACTION
Anton Cunillera Martin

5.1 Introduction

5.1.1. Rh-catalyzed regioselective hydroformylation for the production of quaternary carbon

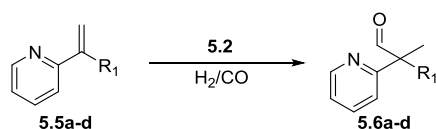
The selective hydroformylation of disubstituted olefins is a challenging process for two main reasons: the difficulty to control the regioselectivity, and the inherent low reactivity of these olefins.¹ While the hydroformylation of 1,2-disubstituted olefins has been explored in more details, the transformation of 1,1-disubstituted alkenes remains less studied. In the regioselective hydroformylation of 1,1-disubstituted olefins, the linear product is the preferential product (Scheme 5.1). Indeed, the branched product is disfavored according to Keuleman's rule, which states that "in hydroformylation, formyl groups are not produced at quaternary centers".² However, the formation of quaternary carbons is of great importance due to its presence in a large number of natural products and biologically active molecules (Scheme 5.1).³ Moreover, the formation of a quaternary carbon center with an adjacent aldehyde group offers the possibility to further functionalize the molecule.

In this reaction, the formation of quaternary carbons is possible under the appropriate reaction conditions.

The selectivity to the branched product depends on 3 factors (Scheme 5.1):

- 1) Substrate substituents: if R_1 and/or R_2 are electron-withdrawing (EWG), the branched product can be favored, while if they are alkyl groups, the linear product will be preferentially produced. Moreover, if the R groups contain a directing group, the branched hydroformylation can be facilitated.⁴
- 2) Reaction conditions: when high pressures and low temperatures are used, the formation of the branched product is favored.⁵

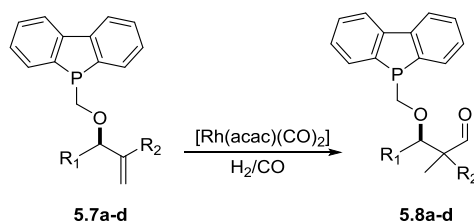
excellent, the use of none or minimally modified catalyst usually requires harsh reaction conditions.



5.6	iso (%)
a R ₁ = Me	>99
b R ₂ = ^t Bu	-
c R ₁ = Ph	>99
d R ₁ = 4-Br-C ₆ H ₄	>99

Scheme 5.3: Rh-catalyzed hydroformylation of **5.5** using complex **5.2**.

Leighton *et al.* reported the regioselective hydroformylation of the allylic ethers **5.7** containing a phosphorus moiety in the backbone (Scheme 5.4).⁹ The presence of the phosphorus resulted in the reaction taking place at the internal position, and although most of the substrates are monosubstituted olefins, there is one example containing a 1,1-disubstituted olefin with excellent regioselectivity.

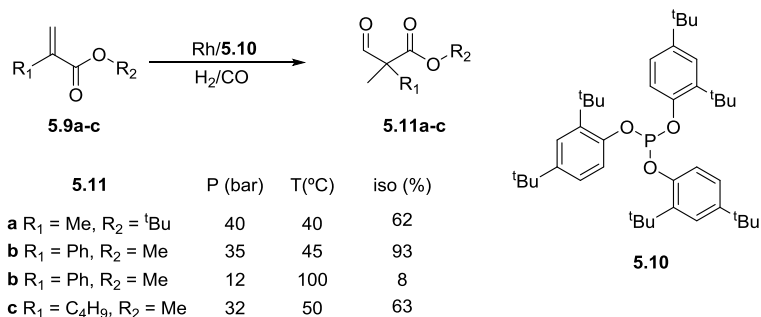


5.8	iso (%)
a R ₁ = Me, R ₂ = H	>98
b R ₁ = Ph, R ₂ = H	>98
c R ₁ = ⁱ Pr, R ₂ = H	>98
d R ₁ = H, R ₂ = Me	92

Scheme 5.4: Rh-catalyzed hydroformylation of **5.7** using a phosphorus moiety as directing group.

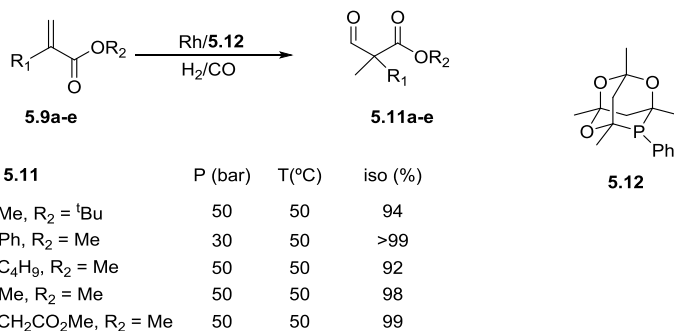
Promising results were obtained by Clarke and co-workers in the Rh-catalyzed regioselective hydroformylation of α -alkyl acrylates **5.9** using the bulky phosphite **5.10** (Scheme 5.5).¹⁰ The presence of the ester group favors the formation of the iso product; however when alkyl substituents were used, moderate regioselectivity

was afforded (up to 63%). In contrast, the phenyl group favored the regioselectivity up to 93% at the internal position. The effect of the reaction parameters on the regioselectivity was clear in this case, since an increase of the temperature and reduction of the total pressure led to an inversion of the regioselectivity.



Scheme 5.5: Rh-catalyzed regioselective hydroformylation of **5.9** using bulky phosphite **5.10**.

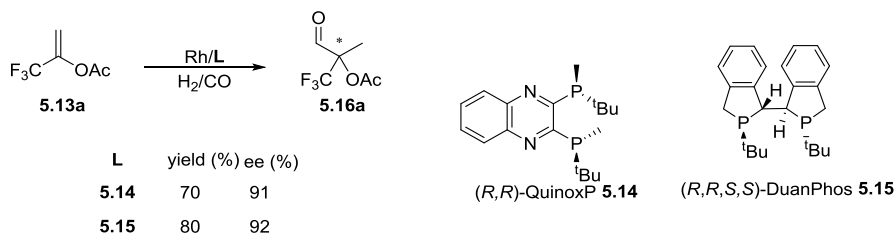
Later, the same group reported the regioselective hydroformylation of α -substituted acrylates **5.9** using the monodentate phosphine ligand **5.12** with excellent regioselectivities (Scheme 5.6).¹¹



Scheme 5.6: Rh-catalyzed regioselective hydroformylation of **5.9** using ligand **5.12**.

The isomerization into more stable trisubstituted olefins was observed in the hydroformylation of long carbon chain acrylates such as **5.9c**. Nonetheless, the catalytic system used was able to hydroformylate trisubstituted olefins and maintain the regioselectivity to the branched product.

Later, Buchwald and co-workers reported the asymmetric hydroformylation of 3,3,3-trifluoroprop-1-en-2-yl acetate **5.13** using the (*R,R*)-QuinoxP* ligand **5.14** and the (*R,R,S,S*)-DuanPhos ligand **5.15** (Scheme 5.7).¹² This constituted the first example of successful asymmetric hydroformylation of 1,1-disubstituted olefins with high yields for the branched product (up to 80%) and excellent enantioselectivity (up to 92%).

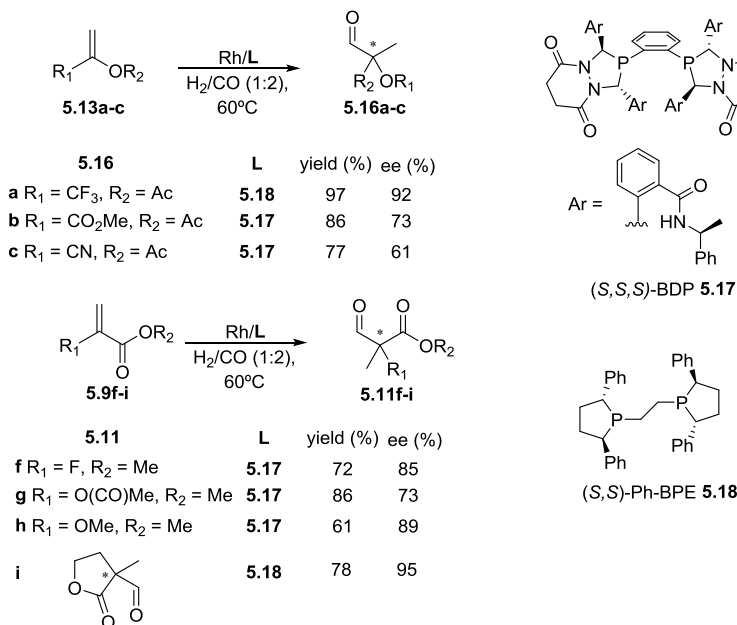


Scheme 5.7: Rh-catalyzed asymmetric hydroformylation of **5.13** using ligands **5.14** and **5.15**.

Interestingly, the reaction was carried out at high temperatures (80-100°C) and relatively low pressures (10-31 bar). It was demonstrated that this preference was due to the highly electron-withdrawing trifluoromethyl group. When the trifluoromethyl group was replaced for a methyl group, the regioselectivity was in favor of the linear aldehyde under the same reaction conditions. Increasing the temperature resulted in the production of more linear aldehyde and alkene hydrogenation product, while increasing the total pressure favored the formation of the branched product.

Recently, Landis *et al.* reported the AHF of 1,1-disubstituted alkenes and attempted the AHF of 1,1,2-trisubstituted olefins for the branched product using (*S,S,S*)-BDP ligand **5.17** and (*S,S*)-Ph-BPE ligand **5.18** (Scheme 5.8).¹³ Up to 97% yield for the branched aldehyde and up to 95% ee were obtained in the case of α,β -unsaturated enol esters **5.13** and α -substituted acrylates **5.9** (Scheme 5.8). In most of the cases, a temperature of 60°C was required to afford a good compromise between yield, regioselectivity and enantioselectivity. The CO partial

pressure was also crucial to obtain good regioselectivities towards the branched aldehydes, and finally 10.3 bar (H_2/CO , 1:2) were used.



Scheme 5.8: Rh-catalyzed asymmetric hydroformylation of α,β -unsaturated enol esters **5.13** and esters **5.9** using ligands **5.17** and **5.18**.

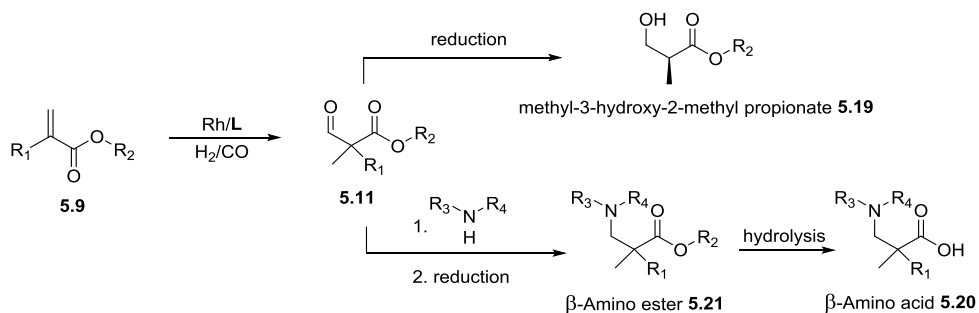
In the same report, the AHF of 1,1,2-trisubstituted olefins was attempted with unsuccessful results in terms of Rh for the yield for the branched product (up to 7%), and no enantiomeric excess was afforded.

Despite the successful results recently reported, the regioselective hydroformylation of 1,1-disubstituted alkenes for the production of quaternary centers remains a challenging reaction to date. Moreover, the asymmetric version to produce tetrasubstituted stereogenic centers is underdeveloped.

5.1.2. Rhodium catalyzed hydroaminovinylolation of acrylates

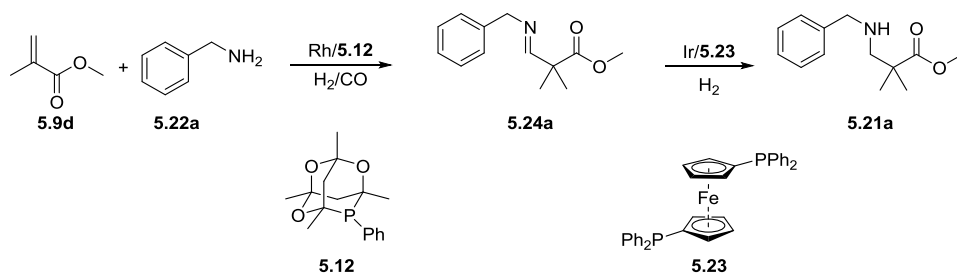
The hydroformylation of acrylates has been largely studied, since the corresponding aldehyde is used as starting material for the synthesis of the versatile enantiopure building block methyl-3-hydroxy-2-methyl propionate **5.19**,¹⁴

or β -amino acids **5.20** (Scheme 5.9).¹⁵ In the particular case of β -amino acids, the introduction of an amine in the reaction media provides the corresponding imine or enamine via condensation with the aldehyde. Subsequent reduction of the imine or enamine would provide the β -amino ester **5.21**. Finally, the hydrolysis of the ester would provide β -amino acids **5.20** (Scheme 5.9).



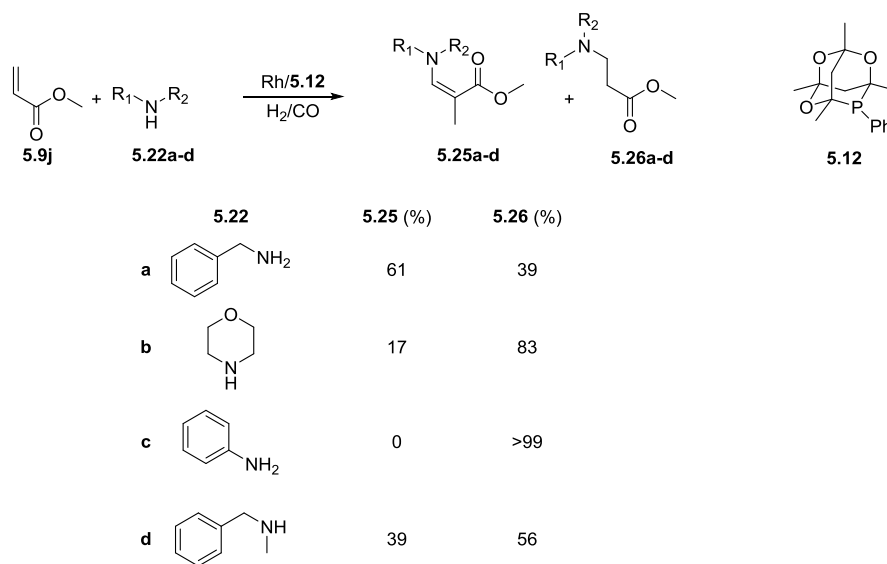
Scheme 5.9: Rh-catalyzed hydroformylation of **5.9** followed by functionalization of **5.11** into molecules of interest.

Despite that the rhodium catalyzed hydroaminomethylation has been studied for the synthesis of a large number of nitrogen containing molecules (Chapter 1), to the best of our knowledge, the rhodium catalyzed regioselective HAM of acrylates for the production of β -amino ester **5.21** has not been successfully reported in an auto tandem process. Indeed, Clarke and co-workers attempted the Rh-catalyzed hydroaminomethylation of methyl methacrylate **5.9d** with benzyl amine **5.22a** after developing a successful Rh-catalyzed hydroformylation system to obtain the branched aldehyde **5.11d**.¹¹ However, an extra step using an iridium catalyst with dppf ligand **5.23** was necessary to reduce the corresponding imine **5.24a** produced via the Rh-catalyzed hydroformylation of methyl methacrylate **5.9d** in the presence of benzyl amine **5.22a** in an orthogonal tandem process (Scheme 5.10).



Scheme 5.10: Rh-catalyzed hydroaminovinylation of **5.9a** with **5.22a** followed by reduction of **5.24a** into **5.21a**.

The same group later reported the formation of various enamines **5.25** in poor to good yields via the rhodium catalyzed hydroaminovinylation of methyl acrylate **5.9j** using the ligand **5.12** (Scheme 5.11). Through this study, it was observed that depending on the amine, the Michael products **5.26** can be generated as non-desired reaction products (up to >99%).



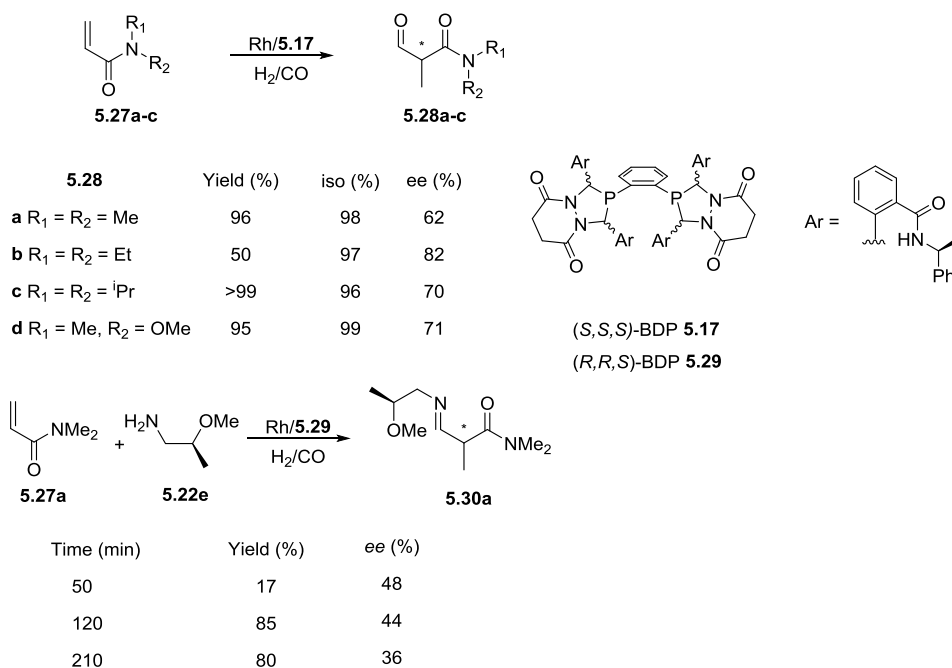
Scheme 5.11: Rh-catalyzed hydroaminovinylation of methyl acrylate **5.9j** with amines **5.22** using ligand **5.12**.

The system maintains the selectivity for the branched product. Nevertheless, it was not possible to hydrogenate the enamine **5.25**, even at high pressures (up to

Synthesis of $\beta^{2,2}$ -amino esters via Rh-catalyzed regioselective HAM

60 bar), which proves how challenging is the development of a system able to hydroformylate the alkene and hydrogenate the corresponding imine or enamine in the Rh-catalyzed hydroaminomethylation reaction.

According to Clarke and co-workers, the enantioselective hydroformylation of α,β -unsaturated esters is very complex due to the rapid enol equilibrium of the formyl ester product. In this context, the same group reported the asymmetric hydroformylation of α,β -unsaturated amides **5.27** using the ligand BDP **5.17** since the corresponding product of hydroformylation does not suffer from this equilibrium, and are interesting precursors for the synthesis of β -amino acids, hydroxyl esters, or γ -aminoalcohols (Scheme 5.12).¹⁶



Scheme 5.12: Rh-catalyzed asymmetric hydroformylation and hydroaminovinilation of **5.27** using ligands **5.17** and **5.29**.

The aldehyde **5.28** was produced in excellent yield, and good to high enantioselectivity (up to 82%). With an efficient system for the production of chiral aldehydes **5.28** in hand, the asymmetric hydroaminomethylation reaction was

attempted in order to create chiral amines. However, only the chiral imine **5.30a** was obtained using the BDP ligand **5.29** (Scheme 5.12). Moreover, it was observed that the imine-enamine equilibrium affects the enantioselectivity over time.

5.1.3. β -amino acids

The β -amino acids are incorporated into secondary metabolites in bacteria, plants, fungi and cyanobacteria, and have potential biological and physical activities.¹⁷ Moreover, they are precursors for the synthesis of β -lactams, which are important class of antibiotics.¹⁸ In this context, over the last years, significant efforts have been devoted to the synthesis of these building blocks as pharmaceutical intermediates and peptidomedics.¹⁵ Most of these approaches are based on asymmetric hydrogenation¹⁹, Mannich reaction²⁰ or conjugated additions²¹.

As mentioned before, various molecules possessing quaternary carbon centers display biological activity, and the case of $\beta^{2,2}$ -amino acids is one example. The $\beta^{2,2}$ -amino acids and derivatives contain a quaternary carbon center at the α -position to the carbonyl. Molecules such as HY-2901 **5.31** and H₁/5-HT_{2A} **5.32** antagonist are potential sleeping disorder drugs for the insomnia treatment (Figure 5.1).²²

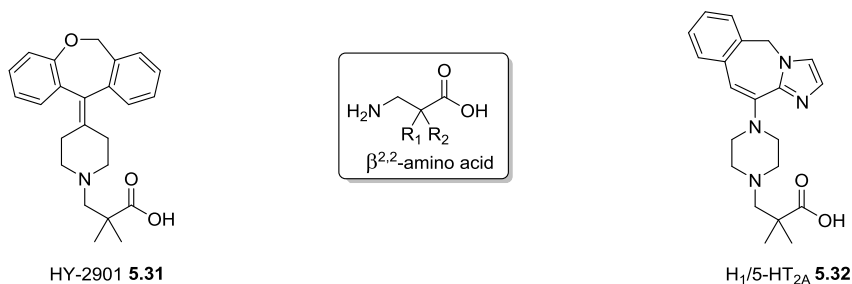
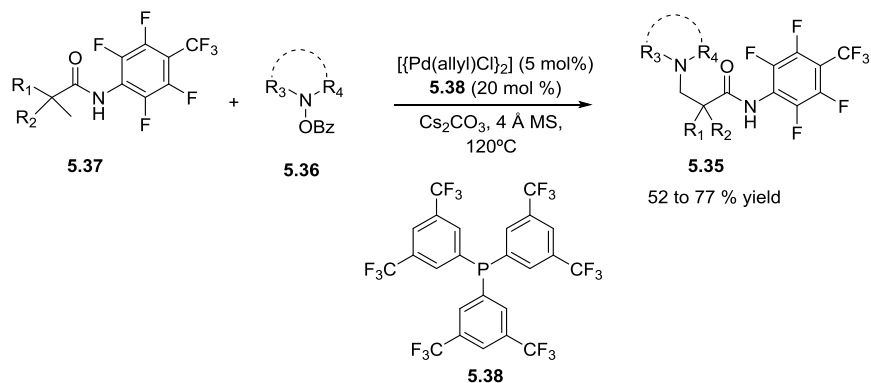


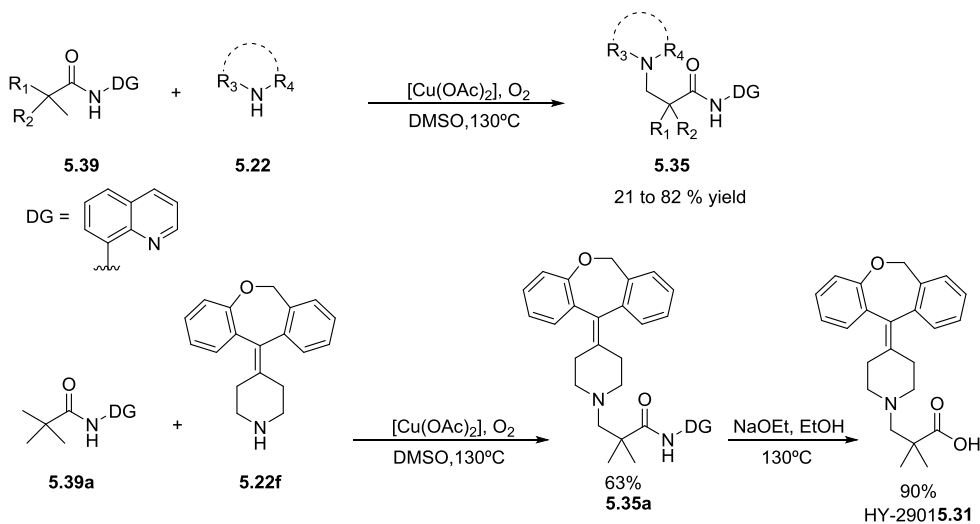
Figure 5.1: Two examples of $\beta^{2,2}$ -amino acid molecules with biological activity.

The high steric hindrance at the α -position to the carbonyl is one of the issues to overcome in order to access $\beta^{2,2}$ -amino acid and derivatives. In view of the interest for these target molecules, various strategies have been reported for their synthesis.



Scheme 5.14: Pd-catalyzed C-H amination process used for the synthesis of $\beta^{2,2}$ -amino amides **5.35**.

Later, Qin *et al.* used a similar system based on Cu-catalyzed C-H amination of amides **5.39** to access $\beta^{2,2}$ -amino amides **5.35** in poor to high yield (Scheme 5.15).²⁵



Scheme 5.15: Synthesis of $\beta^{2,2}$ -amino acid derivatives via metal catalyzed C-H amination.

The system allowed the use of unprotected secondary amines **5.22**, although an excess was required. Furthermore, a directing group at the amide **5.39** was necessary to address the reaction at the desired α -position. Oxygen was used to oxidize Cu^{I} to Cu^{II} in the catalytic cycle. To demonstrate the applicability of the system, the $\beta^{2,2}$ -amino amide **5.35a** was synthesized in 63% yield using this methodology followed by amide hydrolysis to afford HY-2901 **5.31**.

In this context, the development of efficient synthetic methods for β -amino acids and derivatives via metal catalyzed processes using readily available reagents without using sacrificial reagents is of high interest. As such, the rhodium catalyzed hydroaminomethylation of α -alkyl acrylates at the internal position is an elegant strategy that provides access to this scaffold via a tandem catalytic process.

5.2 Objectives of this chapter

This chapter deals with the development of an efficient catalytic system for the synthesis of $\beta^{2,2}$ -amino acid or derivatives.

The specific objectives of this chapter are:

- The screening of phosphorus ligands for the regioselective hydroaminomethylation of methyl methacrylate **5.9d** to afford the branched product.
- The synthesis of $\beta^{2,2}$ -amino esters **5.21** via rhodium catalysed hydroaminomethylation of methyl methacrylate **5.9d** with secondary amines.
- The synthesis of $\beta^{2,2}$ -amino esters **5.21** via rhodium catalysed hydroaminomethylation of methyl methacrylate **5.9d** with aniline and derivatives.
- The synthesis of $\beta^{2,2}$ -amino esters **5.21** via rhodium catalysed hydroaminomethylation of methyl methacrylate **5.9d** with primary alkyl amines.
- The test of various chiral phosphorus ligands for the synthesis of chiral $\beta^{2,2}$ -amino esters **5.21** via rhodium catalysed asymmetric hydroaminomethylation of α -alkyl acrylates **5.9**.

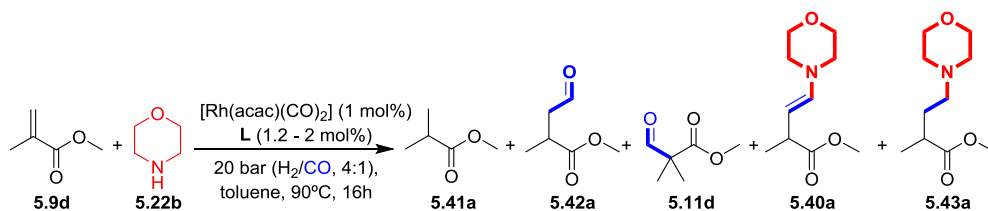
5.3 Results and discussion

5.3.1 Optimization of the reaction conditions for the regioselective HAM of methyl methacrylate

To conduct the rhodium catalyzed regioselective HAM of α -alkyl acrylates **5.9** with the amines **5.22**, a brief screening of phosphorus ligands was carried out using methyl methacrylate **5.9d** as substrate in the presence of morpholine **5.22b** under 20 bar of syngas (H_2/CO , 4:1), in toluene, at 90°C, for 16h (Table 5.1).

Screening of phosphorus ligands

Using the dppf ligand **5.23**, 88% conversion of the alkene was obtained. Good yields for the branched aldehyde **5.11d** (65%) was achieved, along with 23% of the linear enamine **5.40a** (entry 1, Table 5.1). The alkene hydrogenation product **5.41a** was not detected, nor was the linear aldehyde **5.42a**, and the linear amino ester **5.43a** under these conditions. When the Xantphos ligand **5.44** was applied, the linear enamine **5.40a** was afforded in 46% yield, the alkene hydrogenation product **5.41a** in 26%, and the branched aldehyde **5.11d** in 2% (entry 2, Table 5.1). Next, monodentate phosphines were tested (entries 3-6, Table 5.1). The use of monodentate phosphine **5.45** provided low conversion (33%) and full chemoselectivity towards the hydrogenation of the alkene (entry 3, Table 5.1). Interestingly, the monodentate phosphine **5.46** bearing two tertbutyl groups provided full conversion, the linear amine **5.43a** in high yield (75%), and the hydrogenated alkene **5.41a** in 25% yield (entry 4, Table 5.1).

Synthesis of $\beta^{2,2}$ -amino esters via Rh-catalyzed regioselective HAM**Table 5.1:** Screening of phosphorus ligands for the regioselective HAM of **5.9a** with **5.22b**.

Entry ^a	L	Conv. (%) ^b	5.41a ^a	5.42a ^b	5.11d ^b	5.40a ^b	5.43a ^b
1		88	-	-	65	23	-
2		83	26	9	2	46	-
3		33	33	-	-	-	-
4		>99	25	-	-	-	75
5		80	49	4	8	19	-
6		>99	9	-	82	-	9

^a Reaction conditions: **5.9d** (0.5 mmol), **5.22b** (0.5 mmol), $[\text{Rh}(\text{acac})(\text{CO})_2]$ (1 mol%), **L** = bidentate (1.2 mol %), **L** = monodentate (2.0 mol %), P = 20 bar (H_2/CO , 4:1), toluene (0.4 m), T = 90°C , t = 16 h. ^b % conversion and yields determined by ^1H NMR using naphthalene as internal standard.

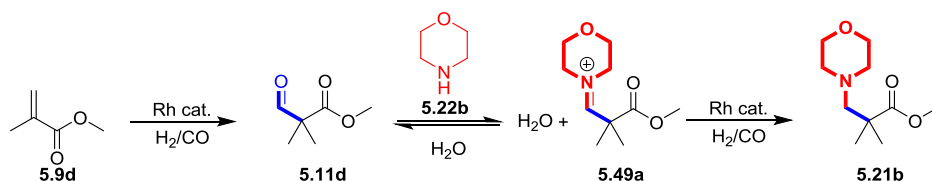
When the ligand **5.47** was applied, the alkene was hydrogenated in 49% yield and the hydroformylation products were obtained in poor yield (entry 5, Table 5.1). Finally, the use of diphenylmethyl phosphine ligand **5.48** afforded full conversion,

and high regioselectivity towards the branched aldehyde **5.11d** (82%), and the hydrogenated alkene **5.41a** and linear amine **5.43a** only in poor yield (9%) (entry 6, Table 5.1). Despite the high regioselectivity obtained towards the branched aldehyde **5.11d** using ligand **5.48**, no traces of the $\beta^{2,2}$ -amino ester **5.21b** were detected in any case.

If the hydroformylation takes place at internal position of the alkene, the branched aldehyde **5.11d** is generated (Scheme 5.16). Then, the condensation of the secondary amine **5.22b** takes place to produce the iminium cation **5.49a**, which is expected to be highly reactive, and water as byproduct. Thus, if the water generated is not removed from the media, it will react with the iminium **5.49a** to provide the branched aldehyde **5.11d** again. Therefore, it is necessary to remove the water during the reaction. At this point, an optimization was carried out in order to promote the formation of $\beta^{2,2}$ -amino ester **5.21b**.

Effect of the molecular sieve and catalyst loading

First, the pressure was regulated to 10 bar (H_2/CO , 1:1) since higher CO partial pressure can favor the formation of the branched aldehyde **5.11d**, and 50 mg of 4 Å MS were added in order to capture the water (entry 1, Table 5.2).



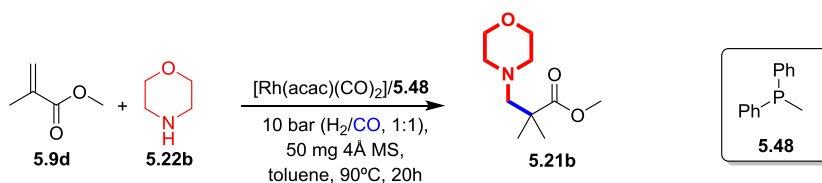
Scheme 5.16: Rh-catalyzed hydroaminomethylation pathway of **5.9d** with **5.22b**.

To our delight, under these reaction conditions the amino ester **5.21b** was detected in 31% yield by GC-MS (entry 1, Table 5.2). Nonetheless, alkene hydrogenation product **5.43a** was observed by GC when the crude was analyzed. Next, various amounts of the rhodium precursor and ligand were tested (entry 2-5, Table 5.2). The use of a higher rhodium/ligand ratio ($Rh/L = 1$) decreased the yield

Synthesis of $\beta^{2,2}$ -amino esters via Rh-catalyzed regioselective HAM

of **5.21b** to 11% (entry 2, Table 5.2). When the catalyst loading was increased to 2 mol%, the amino ester **5.21b** was afforded in 26% yield (entry 3, Table 5.2). Using again a ratio Rh/L of 0.5 with a catalyst loading of 2 mol %, the yield of amino ester **5.21b** increased up to 36% (entry 4, Table 5.2). Finally, lower rhodium/ligand ratio was used (Rh/L = 0.4), but no significant changes were observed (entry 5, Table 5.2).

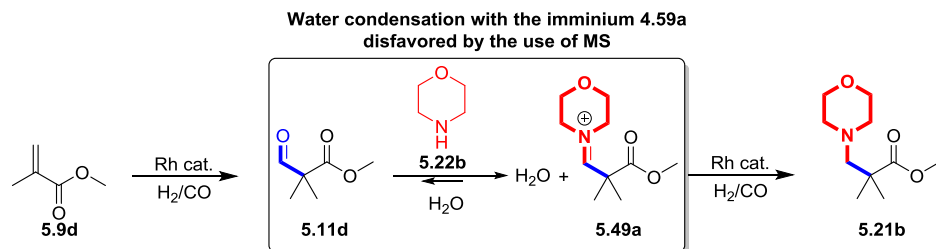
Table 5.2: Rh-catalyzed HAM of **5.9d** with **5.22a** using various catalyst loadings.



Entry ^a	Rh (mol %)	5.48 (mol %)	Conv. % ^b	5.21b ^b
1	1	2	>99	31
2	1	1	>99	11
3	2	2	>99	26
4	2	4	>99	36
5	2	5	>99	33

^a Reaction conditions: **5.9d** (0.5 mmol), **5.22b** (0.5 mmol), 50 mg 4 Å MS, P = 10 bar (H₂/CO, 1:1), toluene (0.4 ml), T = 90°C, t = 20 h. ^b % determined by GC using naphthalene as internal standard.

It was therefore concluded that the use of molecular was beneficial (Scheme 5.17). Encouraged by these results, a study on the influence of the different reaction parameters was studied.

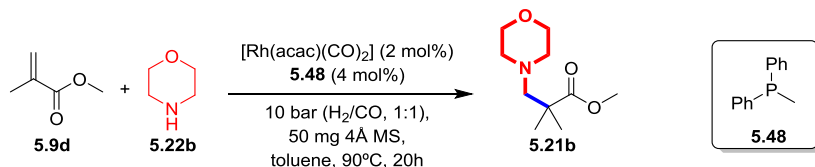


Scheme 5.17: Effect of the molecular sieves observed in the Rh-catalyzed regioselective HAM of **5.9d** with **5.22b**.

Effect of the amount of amine

As described in Scheme 5.16, the condensation of morpholine **5.22b** is challenging due to the steric hindrance of the branched aldehyde **5.11d**. Moreover, the reaction of iminium **5.49a** with water to displace the equilibrium back to the aldehyde **5.11d** is also an issue to overcome. In order to favor the equilibrium towards the iminium **5.49a**, various equivalents of morpholine **5.22b** were tested (Table 5.3).

Table 5.3: Rh-catalyzed HAM of **5.9d** with various equivalents of morpholine **5.22b**.

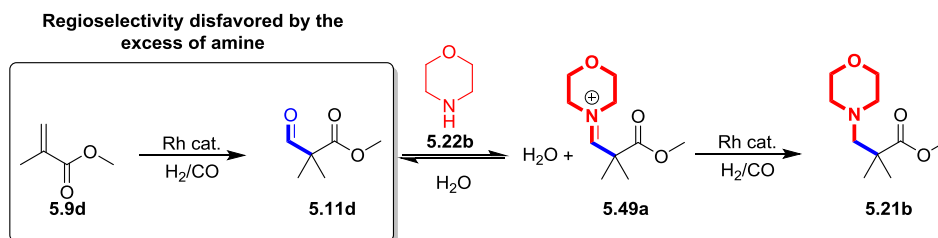


Entry ^a	5.22 b (equiv.)	Conv. % ^b	5.21b ^b
1	0.5 mmol (1 equiv.)	>99	36
2 ^c	0.6 mmol (1.2 equiv.)	>99	27
3 ^c	0.75 mmol (1.5 equiv.)	>99	21

^a Reaction conditions: **5.9d** (0.5 mmol), 50 mg 4 Å MS, P = 10 bar (H₂/CO, 1:1), toluene (0.4 ml), T = 90°C, t = 20 h. ^b % yield determined by GC using naphthalene as internal standard. ^c Products **5.40a** and **5.43a** were detected by GC-MS.

When 1.2 and 1.5 equivalents of morpholine **5.22b** were used, a decrease of the amino ester **5.21b** yield was observed (27% and 21% respectively) (entry 2-3, Table 5.3). The linear enamine **5.40a** and the linear amine **5.43a** were qualitatively

detected by GC-MS. These products were not previously observed by GC-MS under these pressure (10 bar (H_2/CO , 1:1)) and temperature (90°C) (Table 5.2). Therefore, it was concluded that the use of amine in excess changes the regioselectivity in the hydroformylation towards the linear products, but did not help to favor the formation of amino ester **5.21b** (Scheme 5.18).



Effect of the temperature, time and amount of molecular sieves

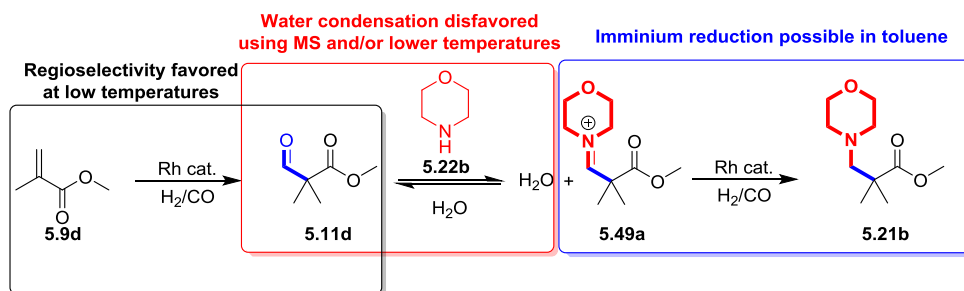
As previously observed, low temperatures favor the formation of the branched product in the Rh-catalyzed hydroformylation of α -alkyl acrylates **5.9**.¹¹ Thus, the reaction was performed at lower temperature (70°C) (entry 1, Table 5.4). Although the yield of amino ester **5.21b** did not increase, lower degree of hydrogenation of the alkene was observed by GC. When a higher temperature (120°C) was applied, the yield decreased and linear products were detected by GC (entry 3, Table 5.4). Next, the effect of the molecular sieve was tested by increasing the amount to 100 mg, and amino ester **5.21b** was afforded in 42% yield (entry 4, Table 5.4). At this point, it was decided to increase the reaction time to 72 h, and to our delight the yield of **5.21b** was improved to a 67% (62% isolated yield) (entry 5, Table 5.4). Interestingly, when the temperature was reduced to 50°C, amino ester **5.21b** was afforded in 82% yield (79% isolated yield) (entry 7, Table 5.4). Therefore, it was concluded that lower temperatures were necessary in order to favor the formation of amino ester **5.21b** (Scheme 5.19).

Table 5.4: Rh-catalyzed HAM of **5.9d** with **5.22b** at variable temperature, time and amount of 4 Å MS.

Entry ^a	T (°C)	4 Å MS (mg)	t (h)	Conv. % ^b	5.21b [Y] ^b
1	70	50	20	>99	36
2	90	50	20	>99	36
3 ^c	120	50	20	>99	20
4	70	100	20	>99	42
5	70	100	72	>99	67 [62]
6	50	50	72	>99	56
7	50	100	72	>99	82 [79]

^a Reaction conditions: **5.9d** (0.5 mmol), **5.22b** (0.5 mmol), Rh (2 mol %), **5.48** (4 mol %), P = 10 bar (H₂/CO, 1:1), toluene (0.4 ml). ^b % determined by GC using naphthalene as internal standard, values in bracket refer to isolated yield. ^c Linear enamine **5.40a** and linear amine **5.43a** detected by GC.

It is expected that lower temperatures minimize rate of the reaction of water with the iminium **5.49a**. Moreover, a positive effect of the molecular sieves was observed (Scheme 5.19). In contrast to our previous results in Chapter 4 and the reported results reported by Clarke and co-workers,¹¹⁻²⁶ the hydroaminomethylation reaction was performed using the neutral [Rh(acac)(CO)₂] precursor in toluene without the use of other polar solvents such as DCE (Scheme 5.19). Since the iminium **5.49a** is the expected intermediate, this result suggests that monohydride species are capable to reduce this species, while they cannot hydrogenate imines or enamines, as proposed in Chapter 4.



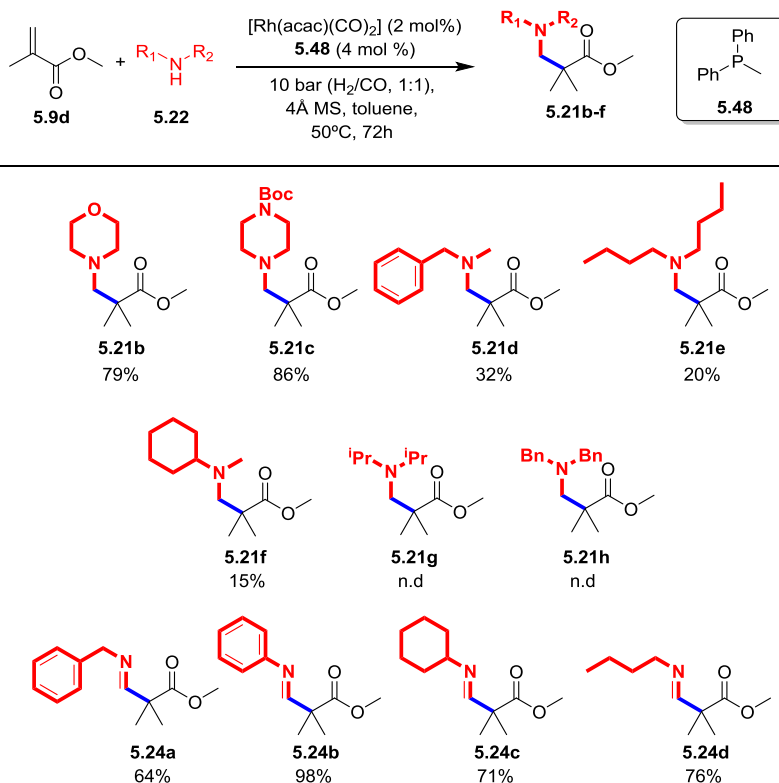
Scheme 5.19: Effects observed in the Rh-catalyzed regioselective HAM of **5.9d** with **5.22b**.

5.3.2 Rh-catalyzed regioselective HAM of methyl methacrylate with various amines

With these optimized conditions in hand (entry 7, Table 5.4), the scope of $\beta^{2,2}$ -amino esters **5.21** was expanded using various amines (Table 5.5).

The $\beta^{2,2}$ -amino esters **5.21b-c** bearing secondary cyclic amines such as morpholine and N-boc piperazine **5.22g** were afforded in high yields (up to 86%). Nonetheless, when non cyclic secondary amines such as N-methylbenzyl amine **5.22d**, N-dibutyl amine **5.22h**, and N-methylcyclohexyl amine **5.22i** were applied, the yields obtained were from poor to moderate (up 32%). The use of diisopropyl amine **5.22j** and dibenzyl amine **5.22k** did not yield the desired amino esters **5.21g** and **5.21h**; respectively; instead, only the branched aldehyde **5.11d** was observed. This could be due the higher steric hindrance and thus lower nucleophilicity of these amine that inhibit the condensation with the aldehyde. A different outcome was observed when primary amines were used. Instead of the expected amino ester **5.21**, the corresponding imines **5.24** were afforded in good to excellent yield (up to 98%). Similar results were obtained by Clarke and co-workers when the HAM of methyl methacrylate **5.9d** with benzyl amine **5.22a** was attempted using ligand **5.12** (Scheme 5.10). These results indicated that under these reaction conditions, the hydrogenation of the imines did not take place.

Table 5.5: Scope of amines in the Rh-catalyzed regioselective HAM of methyl methacrylate **5.9d**.



^a Reaction conditions: methyl methacrylate **5.9d** (0.5 mmol), amine **5.22** (0.5 mmol), [Rh(acac)(CO)₂] (2 mol %), **5.48** (4 mol %), P = 10 bar (H₂/CO, 1:1), toluene (0.4 ml), 100 mg 4Å MS, T = 50°C, t = 72h. ^b % isolated yields.

The steric hindrance of the amine revealed an important factor since cyclic secondary amines provided good results, but non-cyclic secondary amines afforded the amino ester **5.21** in lower yields. Moreover, when primary amines were used, the reaction stops at the imine **5.24**. Thus, it was concluded under these reaction conditions, it is possible to reduce the iminium **5.49** obtained with secondary amines but not the imines **5.24** afforded with primary amines.

To improve the yield for non-cyclic secondary amines, a brief optimization was attempted using methyl methacrylate **5.9d** and dibutylamine **5.22f** as substrates (Table 5.6). First, it was decided to use mixture of toluene with polar solvents to

study whether the condensation of the amine **5.22** and/or reduction of the iminium **5.49** could be favored (entry 2-3, Table 5.6). It was observed that when 2-methyl tetrahydrofuran (2-MeTHF) was used, lower conversions were obtained (up to 60%) compared to those obtained in Table 5.5, where full conversion was obtained, and no signals of the amino ester **5.21e** were detected (entry 2, Table 5.6). Interestingly, when DCE was used as solvent, a slight increase in the yield of **5.21e** was observed (up to 30%) (entry 3, Table 5.6). The use of dimethylformamide (DMF) provided high degree of hydrogenation of the alkene (up to 87%), and poor yield for the branched aldehyde **5.11d** (entry 4, Table 5.6). Furthermore, the amino ester **5.21e** was not detected.

Table 5.6: Optimization for the Rh-catalyzed HAM of methyl methacrylate **5.9d** with dibutylamine **5.22h**.

Entry ^a	L	Solvent	Conv. % ^b	5.41a ^b	5.11d ^b	5.21e ^b
1	5.48	Toluene	>99	-	74	26
2	5.48	Toluene/2-MeTHF (1:1)	60	-	60	-
3	5.48	Toluene/DCE (1:1)	>99	-	70	30
4	5.48	Toluene/DMF (1:3)	>99	87	13	-
5 ^c	5.12	Toluene	>99	-	57	37

^a Reaction conditions: **5.9d** (0.5 mmol), **5.22f** (0.5 mmol), Rh (2 mol %), **L** (4 mol %), P = 10 bar (H₂/CO, 1:1), solvent (0.4 ml), 100 mg 4Å MS, T = 50°C, t = 72h. ^b % determined by ¹H NMR using naphthalene as internal standard. ^c linear aldehyde **5.42a** = 6% yield.

Finally, it was decided to test the ligand **5.12** used by Clarke and co-workers in the regioselective hydroformylation of α -alkyl acrylates (entry 5, Table 5.6). However, the ligand **5.12** improved the yield of amino ester **521.e** up to 37%, the increase was moderate. It was concluded that the optimization of reaction parameters such as the pressure would be necessary. However, due to lack of time, this optimization was not carried out in this project and will be studied in the future.

5.3.3 Optimization of the reaction conditions for the Rh-catalyzed regioselective HAM of methyl methacrylate with aniline

All the reported systems to directly access $\beta^{2,2}$ -amino esters involve the use of secondary amines, probably due to issues related to reactivity or selectivity using primary amines.

In view of the results obtained in Table 5.5, an optimization was necessary in order to afford the desired amine using primary amines. The following optimization was carried out using the ligands **5.48** and **5.12** under variable reaction conditions.

Effect of the rhodium precursor and ligand

The optimization was initiated using the ligand **5.48**, the neutral rhodium precursor $[\text{Rh}(\text{acac})(\text{CO})_2]$, and toluene as solvent (entry 1, Table 5.7). It was confirmed that the imine **5.24b** can be afforded in yield >99% under these reaction conditions. When the ligand **5.12** was tested under the same reaction conditions, the imine **5.23b** was afforded in 40% yield and the branched aldehyde **5.11d** in 60% yield (entry 2, Table 5.7). Interestingly, the use of the cationic rhodium precursor $[\text{Rh}(\text{COD})_2]\text{BF}_4$ with ligand **5.48** in a mixture of toluene/DCE, provided the alkene hydrogenation product **5.41a** in 75% yield, and the desired amino ester **5.21i** was afforded in 25% yield (entry 3, Table 5.7).

Synthesis of $\beta^{2,2}$ -amino esters via Rh-catalyzed regioselective HAM**Table 5.7:** Rh-catalyzed HAM of **5.9d** with **5.22c** using various rhodium precursors and ligands **5.48** and **5.12**.

Entry ^a	L	Rh	Conv. (%) ^b	5.41a ^b	5.11d ^b	5.24b ^b	5.21i ^b
1	5.48	[Rh(acac)(CO) ₂]	>99	-	-	>99	-
2	5.12	[Rh(acac)(CO) ₂]	>99	-	60	40	-
3 ^c	5.48	[Rh(COD) ₂] ₂ BF ₄	>99	75	-	-	25
4 ^c	5.12	[Rh(COD) ₂] ₂ BF ₄	>99	6	29	34	31

^a Reaction conditions: **5.9d** (0.5 mmol), **5.22c** (0.5 mmol), Rh (2 mol %), L (4 mol %), P = 10 bar (H₂/CO, 1:1), toluene (0.4 ml), T = 50°C, t = 20h. ^b % determined by ¹H NMR using naphthalene as internal standard. ^c solvent = toluene/DCE (1:1).

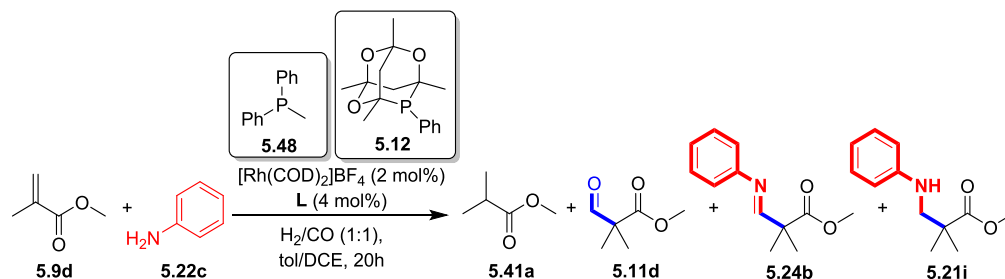
At this stage, the ligand **5.12** was tested under the same reaction conditions (entry 4, Table 5.7), and to our delight the amino ester **5.21i** was afforded in 31% yield, the imine **5.24d** in 34% yield, and the branched aldehyde **5.11d** in 29% yield.

Therefore, it was concluded that the cationic precursor [Rh(COD)₂]₂BF₄ and the mixture of toluene/DCE as solvent was necessary to hydrogenate the imine **5.24b** as previously observed in the systems described in Chapter 4. Differences in chemoselectivity were observed when ligand **5.48** and **5.12** were tested under the same reaction conditions (entry 3-4, Table 5.7). The use of ligand **5.48** provided more hydrogenation of the alkene, while the use of ligand **5.12** afforded more hydroformylation products.

Effect of the pressure and temperature

The effect of the pressure and temperature is crucial in this reaction, not on the activity, but also on the chemo and regioselectivity. In these tests, the cationic rhodium precursor was used based on the previous results obtained (Table 5.7). First, the ligand **5.48** was tested under 30 bar of syngas (H_2/CO , 1:1) (entry 1, Table 5.8). The amino ester **5.21i** was afforded in 40% yield, and the alkene hydrogenation product **5.41a** was reduced to 60 % yield. Although this result constituted an improvement compared with the reaction under 10 bar of syngas (H_2/CO , 1:1) (entry 2, Table 5.8), the alkene hydrogenation compound **5.41a** was still the major product.

Table 5.8: Rh-catalyzed HAM of **5.9d** with **5.22c** at variable temperature and pressure.



Entry ^a	L	P	T	Conv. (%) ^b	5.41a ^a	5.11d ^b	5.24b ^b	5.21i [Y] ^b
1	5.48	30	50	>99	60	-	-	40 [36]
2	5.48	10	50	>99	75	-	-	25
3	5.12	10	70	>99	17	4	11	67
4	5.12	30	70	>99	10	<1	<1	90
5 ^c	5.12	30	70	>99	6	<1	<1	94 [87]

^a Reaction conditions: **5.9a** (0.5 mmol), **5.22c** (0.5 mmol), $[Rh(COD)_2]BF_4$ (2 mol %), **L** (4 mol %), toluene/DCE (0.4 ml, 1:1), $t = 20h$. ^b % yield determined by 1H NMR using naphthalene as internal standard, values in brackets refer to isolated yields. ^c $[Rh(COD)_2]BF_4$ (1 mol %), **5.12** (2 mol %).

For this reason, the optimization was carried out using ligand **5.12** (entry 3-5, Table 5.8). When the temperature was increased up to 70°C, the amino ester **5.21i** was afforded in 67% yield along with the alkene hydrogenation product **5.41a** in 17% yield (entry 3, Table 5.8). The increase of the pressure to 30 bar at 70°C provided the amino ester **5.21i** in excellent yield (up to 90%) (entry 4, Table 5.8). In view of this promising result, it was decided to decrease the catalyst loading to 1 mol % (entry 5, Table 5.8). To our delight, the amino ester **5.21i** was detected in excellent yield (up to 94%) by ^1H NMR spectroscopy, and after purification via column, the product was isolated in 87% yield.

It was therefore concluded that the use of a cationic rhodium precursor in a mixture of toluene/DCE is necessary to afford the amino ester **5.21** using aniline **5.22c** as amine. The catalytic system using ligand **5.48** mainly provided the alkene hydrogenation compound **5.41a**, while the catalytic system using ligand **5.12** provided the desired products in high yield. Finally, the use of 1 mol% of rhodium with ligand **5.12** under 30 bar of syngas at 70°C provided the amino ester **5.21i** in high yield.

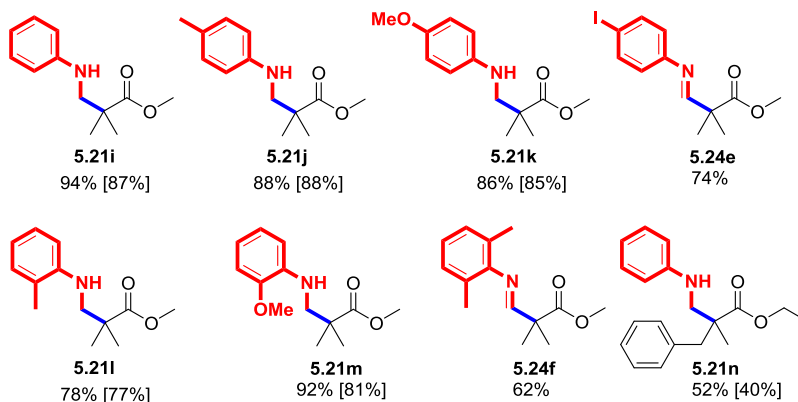
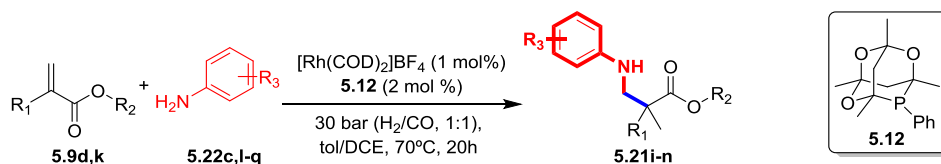
5.3.4 Rh-catalyzed regioselective HAM of α -alkyl acrylates with aniline derivatives

At this stage, the scope of $\beta^{2,2}$ -amino esters **5.21** was extended using aniline derivatives using the optimized reaction conditions (entry 5, Table 5.8).

First, the electronic effect was studied using *para*-substituted anilines. No significant effect was observed when *para*-substituted anilines bearing electron-donating methyl and methoxy group, respectively, were used. In both cases, the corresponding amino esters **5.21j** and **5.21k** were afforded in high yields (up to 88%). On the other hand, when the aniline derivative bearing electron-withdrawing iodide group in *para*-position was tested, only the imine **5.24e** was detected in high yields by ^1H NMR spectroscopy, and no traces of the corresponding amino

ester were observed; moreover the aldehyde **5.11d** was detected (19% yield by ^1H NMR).

Table 5.9: Rh-catalyzed HAM of α -alkyl acrylates **5.9** with different aniline derivatives.



^a Reaction conditions: **5.9** (0.5 mmol), **5.22** (0.5 mmol), $[\text{Rh}(\text{COD})_2]\text{BF}_4$ (1 mol %), **5.12** (2 mol %), P = 30 bar (H_2/CO , 1:1), toluene/DCE (0.4 ml, 1:1), T = 70°C , t = 20h ^b % yield determined by ^1H NMR using naphthalene as internal standard, values in brackets refer to isolated yields.

The steric effect was then studied using *ortho*-substituted anilines bearing methyl and methoxy groups respectively. When the aniline derivatives bearing methyl and methoxy groups in the *ortho* position, respectively, were applied, the amino esters **5.21l** and **5.21m** were afforded in high yield (up to 81%). However, when the steric hindrance was increased using 2,6-dimethyl aniline, only the imine **5.24f** was detected in 62% yield by ^1H NMR, and the branched aldehyde **5.11d** in 38% yield. Finally, when the α -alkyl acrylate **5.9k** bearing a benzyl substituent in α -position was used with the aniline **5.22c**, the corresponding amino ester **5.21n** was afforded in 40% isolated yield. In this specific case, the alkene isomerization

product was detected in 42% yield and the alkene hydrogenation product in 6% yield by ^1H NMR.

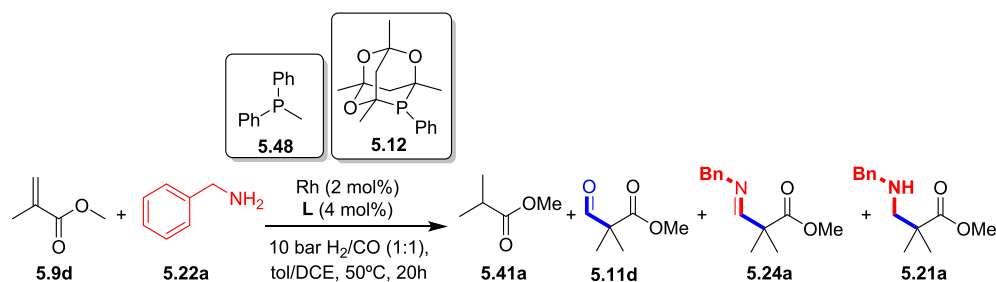
In conclusion, several $\beta^{2,2}$ -amino esters **5.21** bearing aniline and derivatives were produced in high yield using aniline and derivatives under optimized reaction conditions. It was observed that both electronic and steric effects are important in the outcome of the reaction. The system is able to afford $\beta^{2,2}$ -amino esters **5.21** bearing aniline with electron-donating groups in *para* position in high yields, but with electron-withdrawing groups are in *para* position, the reaction stops at the imine **5.24**. A more electron-poor imine **5.24** seems to be more challenging to hydrogenate than an electron-rich. This effect might be due to difficulties in the coordination of the imine to the rhodium center, or due to problems in the migratory insertion step of the hydrogenation. The steric effect was minimal for 2-substituted anilines, but when a 2,6-disubstituted aniline was tested, the reaction was blocked at the imine **5.24**, due to problems in the coordination of the imine to the rhodium catalyst. Finally, the substituent in α -position of the acrylate was also important, and the isomerization of the alkene is an important side reaction if a benzyl group is present. The formation of a more stable tri-substituted olefin conjugated to an aromatic ring favors this reaction.

5.3.5 Rh-catalyzed regioselective HAM of methyl methacrylate with benzyl amine

Our previous results demonstrated that under appropriate conditions, it is possible to afford $\beta^{2,2}$ -amino esters can be obtained using secondary amines and aniline derivatives. Motivated by these results, the hydroaminomethylation of methyl methacrylate **5.9d** with benzyl amine **5.22a** was performed. It is noteworthy that for this reaction Clarke and co-workers did not obtain the desired product using ligand **5.12** and the neutral precursor $[\text{Rh}(\text{acac})(\text{CO})_2]$ (Scheme 5.10).¹¹

The use of neutral precursor $[\text{Rh}(\text{acac})(\text{CO})_2]$ with ligand **5.48** only provided the imine **5.24a** in excellent yield (entry 1, Table 5.10). To our surprise, when the cationic $[\text{Rh}(\text{COD})_2]\text{BF}_4$ was tested with ligand **5.48** in the mixture of toluene/DCE, the imine **5.24a** was obtained in excellent yield (entry 2, Table 5.10).

Table 5.10: Rh-catalyzed HAM of methyl methacrylate **5.9d** with benzyl amine **5.21a** using various reaction conditions.



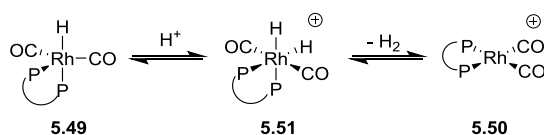
Entry ^a	Rh	Conv. (%) ^b	5.41a ^a	5.11d ^b	5.24a ^b	5.21a ^b
1	$[\text{Rh}(\text{acac})(\text{CO})_2]$	90	-	-	90	-
2	$[\text{Rh}(\text{COD})_2]\text{BF}_4$	95	5	-	90	-
3	$[\text{Rh}(\text{COD})(\mu\text{-Cl})_2]$	>99	2	3	94	-
4 ^c	$[\text{Rh}(\text{COD})_2]\text{BF}_4$	>99	-	-	>99	-
5 ^d	$[\text{Rh}(\text{COD})_2]\text{BF}_4$	>99	15	-	85	-

^a Reaction conditions: **5.9d** (0.5 mmol), **5.22a** (0.5 mmol), Rh (2 mol %), **5.48** (4 mol %), P = 10 bar (H_2/CO , 1:1), toluene/DCE (0.4 ml, 1:1), T = 50°C, t = 20 h. ^b % yield determined by ^1H NMR using naphthalene as internal standard. ^c P = 30 bar (H_2/CO , 1:1). ^d L = **5.12** (4 mol %), P = 30 bar (H_2/CO , 1:1).

The use of the dimeric precursor $[\text{Rh}(\text{COD})(\mu\text{-Cl})_2]$, provided similar results than the other precursors (entry 3, Table 5.10). To force the hydrogenation of the imine, the total pressure was increased up to 30 bar of syngas using the cationic precursor $[\text{Rh}(\text{COD})_2]\text{BF}_4$. Nevertheless, the result was similar than those afforded at 10 bar (entry 4, Table 5.10). The ligand **5.12** was also tested at 30 bar of syngas

pressure with the cationic precursor $[\text{Rh}(\text{COD})_2]\text{BF}_4$ in the mixture of toluene/DCE, however, the imine **5.24a** was afforded in 85% yield, and the alkene hydrogenation product **5.41a** was detected in 15% yield and no signals of the amino ester **5.21a** were detected (entry 5, Table 5.10).

It was concluded that the previous modifications in the reaction conditions seem to be inefficient for the hydrogenation of the imine **5.24a**. Since the problem lies in the hydrogenation step, a different approach was attempted. According to Kalck and co-workers, the neutral monohydride species **5.49** in charge of the hydroformylation is in equilibrium with the cationic species **5.50** in charge of the hydrogenation via the species **5.51** (Scheme 5.20).²⁷



Scheme 5.20: Equilibrium between species in hydroaminomethylation described by Kalck et. al.

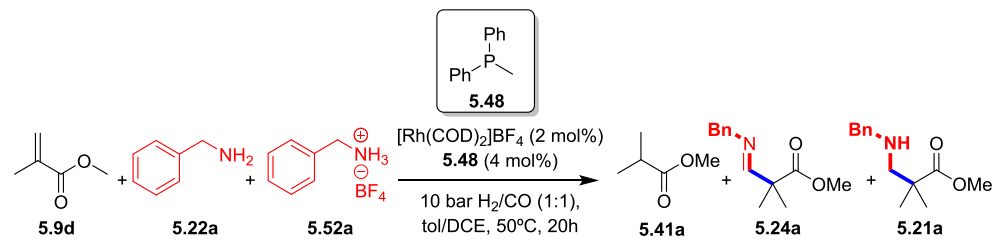
According to the equilibrium, a proton source is necessary to move from the neutral rhodium monohydride species **5.49** to the cationic rhodium species **5.50** through a cationic rhodium dihydride species **5.51** (Scheme 5.20). For this reason, the addition of various acids was tested in the reaction (Table 5.11). Moreover, Beller and co-workers reported that the use of tetrafluoroboric acid (HBF_4) facilitated the formation of amines in the HAM of vinylarenes.²⁸

First, tetrafluoroboric acid (HBF_4) was used in 2 mol% under the previous reaction conditions (entry 2, Table 5.11), but no signals of amino ester **5.21a** were detected (entry 1, Table 5.11). Then, the neutral precursor $[\text{Rh}(\text{acac})(\text{CO})_2]$ was used but the imine **5.24a** remained as major product (entry 2, Table 5.11).

At this stage, the ammonium salt **5.52a** was synthesized, and used as proton source in the reaction at different ratios with benzylamine **5.22a** in DCE as solvent (entry 3-5, Table 5.11). Nevertheless, it was observed that the use of this salt only

promoted the hydrogenation of the methyl methacrylate **5.9d** into the alkane **5.41a**.

Table 5.11: Rh-catalyzed HAM of **5.9d** with **5.22a** using various proton sources.



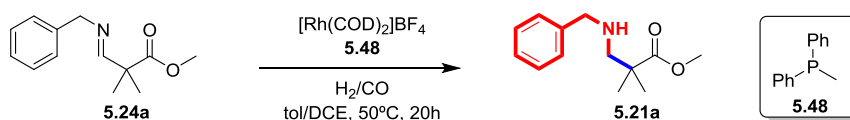
Entry ^a	Acid	5.22a / 5.52a	Conv. (%) ^b	5.41a ^a	5.11d ^b	5.24a ^b	5.21a ^b
1	HBFB ₄	1:0	95	7	6	82	-
2 ^c	HBFB ₄	1:0	82	5	2	75	-
3 ^d	-	1:1	>99	95	-	5	-
4 ^e	-	4:1	>99	73	9	18	-

^a Reaction conditions: **5.9d** (0.5 mmol), **5.22a** (0.5 mmol), [Rh(COD)₂]BF₄ (2 mol %), **5.48** (4 mol %), P = 10 bar (H₂/CO, 1:1), toluene/DCE (0.4 ml, 1:1), T = 50°C, t = 20h. ^b % yield determined by ¹H NMR using naphthalene as internal standard. ^c [Rh(acac)(CO)₂] (2 mol %). ^d solvent = DCE, **5.52a** (0.25 mmol). ^e solvent = DCE, **5.52a** (0.1 mmol).

Since several attempts to conduct the rhodium catalyzed HAM of methyl methacrylate **5.9d** with benzyl amine **5.22a** only provided the imine **5.24a**, the ability of the catalytic system containing ligand **5.48** to hydrogenate the imine **5.24a** was questioned. To confirm whether the catalytic system using a cationic rhodium precursor and the ligand **5.48** was capable to hydrogenate the imine **5.24a** under HAM reaction conditions, two control experiments were carried out (Table 5.12). First, the imine **5.24a** was submitted to hydrogen pressure (5 bar) in the presence of the cationic precursor [Rh(COD)₂]BF₄ and ligand **5.48** in toluene/DCE as solvent (entries 1-2, Table 5.12). Interestingly, the amino ester **5.21a** was afforded in moderate to high yield (up to 67%) under these reaction conditions. In the second experiment, the imine **5.24a** was submitted to hydrogen

pressure (5 bar) and CO pressure (5 bar) in the presence of the cationic precursor $[\text{Rh}(\text{COD})_2]\text{BF}_4$ with ligand **5.48** (entry 3, Table 5.12). However, under these reaction conditions, no conversion of the imine **5.24a** was observed.

Table 5.12: Rh-hydrogenation of **5.24a** using ligand **5.48** under H_2 and H_2/CO pressure.



Entry ^a	Rh (mol%)	H_2 (bar)	CO (bar)	Conv. (%) ^b	5.21a ^b
1	1.8	5	-	67	67[48]
2	1.2	5	-	32	32
3	2	5	5	0	-

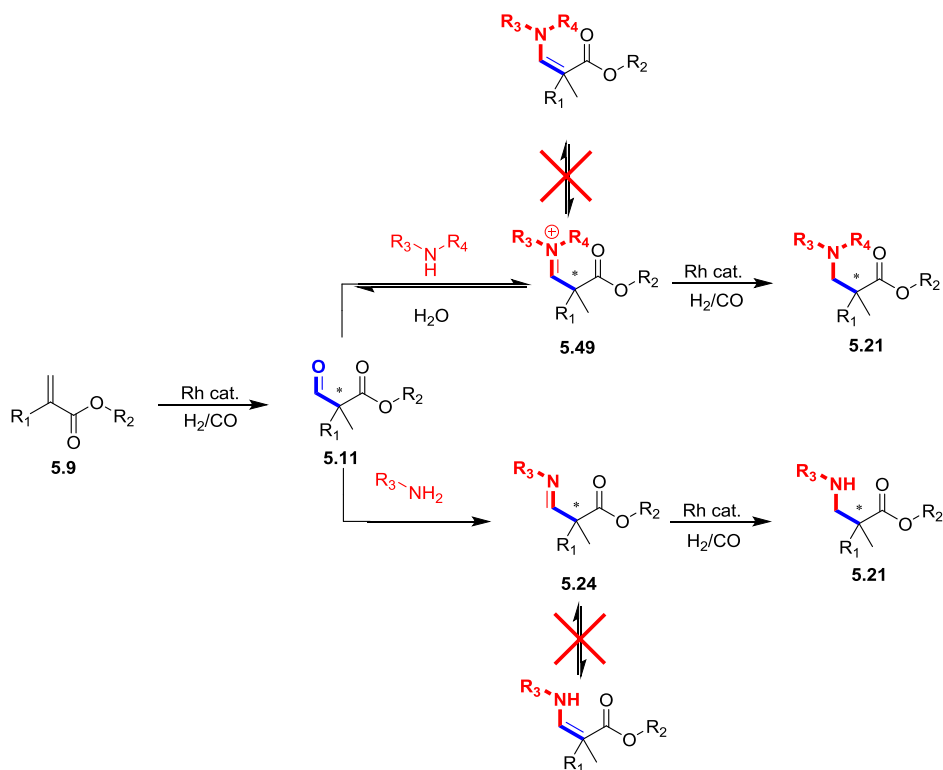
^a Reaction conditions: **5.24a** (0.5 mmol), L/Rh = 2, toluene/DCE (0.4 ml, 1:1), T = 50°C, t = 20h. ^b % yield determined by ^1H NMR using naphthalene as internal standard, values in bracket refer to isolated yields.

Therefore, it was concluded that under hydrogenation reaction conditions (5 bar of H_2), the catalytic system containing the ligand **5.48** and the cationic precursor $[\text{Rh}(\text{COD})_2]\text{BF}_4$ in toluene/DCE as solvent is able to hydrogenate the imine **5.24a** into the amino ester **5.21a**. Furthermore, since the presence of CO stopped the reaction, it was concluded that CO is acting as poison for the hydrogenation of this specific imine **5.24a**, probably by preventing the coordination of the imine to the rhodium center.

5.3.6 Rh-catalyzed AHF of ethyl benzylacrylate

We have successfully reported the Rh-catalyzed regioselective HAM of methyl methacrylate **5.9d** for the synthesis of $\beta^{2,2}$ -amino esters **5.21**. Furthermore, it was possible to access the racemic $\beta^{2,2}$ -amino esters **5.21n** via Rh-catalyzed HAM of ethyl benzylacrylate **5.9k** and aniline **5.22c** using ligand **5.12**. Thus, the development of an asymmetric version of this procedure would be of interest for

the production of enantioenriched $\beta^{2,2}$ -amino esters **5.21**. In this context, following the same approach described in Chapter 4, the regioselective asymmetric HAM of α -alkyl acrylates **5.9** at the branched position was attempted. The chirality could be induced in the AHF step (Scheme 5.21), and the final hydrogenation of the unsaturated compound would provide chiral amino esters **5.21**.

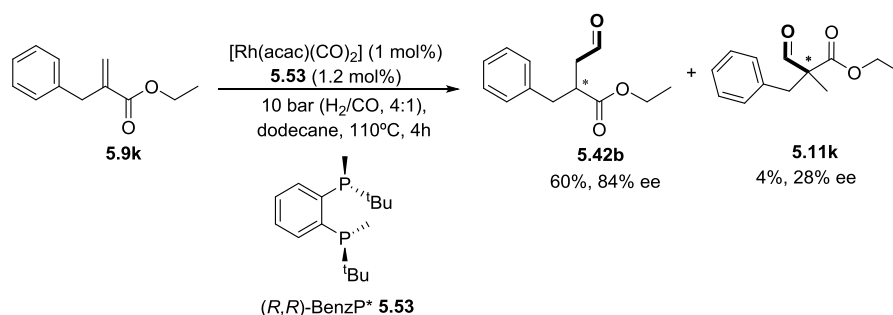


Scheme 5.21: Rh-catalyzed asymmetric HAM of α -alkyl acrylates **5.9** for the production of enantioenriched $\beta^{2,2}$ -amino esters **5.21**.

However, as mentioned in the introduction of this chapter, there are only two reports of Rh-catalyzed asymmetric hydroformylation for the production of chiral quaternary centers, and the most recent has been reported during the development of this work.¹²⁻¹³

Buchwald and co-worker reported that in the asymmetric hydroformylation of α -alkyl acrylates **5.9** for the production of chiral linear aldehyde **5.42b**, the use of

(*R,R*)-BenzP* **5.53** as ligand provided the branched aldehyde **5.11k** in 4% yield and 28% enantiomeric excess (Scheme 5.17).²⁹ This result suggests that the asymmetric hydroformylation of ethyl benzylacrylate **5.9k** is possible using chiral phosphorus ligands, and opens the possibility for the asymmetric HAM of ethyl benzylacrylate **5.9k**. In order to conduct the Rh-catalyzed asymmetric HAM of ethyl benzylacrylate **5.9k**, it is first necessary to establish an efficient system for the Rh-catalyzed AHF of ethyl benzylacrylate **5.9k**, not only with high enantioselectivity, but also with high regioselectivity for the branched product.



Scheme 5.17: Rh-catalyzed asymmetric hydroformylation of **5.9k** using ligand **5.53**.

Based on our previous experience and the reported procedures, the rhodium catalyzed asymmetric hydroformylation of ethyl benzylacrylate **5.9k** was performed using with various chiral phosphorus ligands at 50°C, and 10 bar (H_2/CO , 1:1), since these reaction conditions previously favored the formation of branched aldehyde **5.11** (Table 5.13). The screening begun with the (*R,R*)-Et-BPE ligand **5.54**, which provided low activity under these reaction conditions, but afforded the aldehyde **5.11k** in 28% yield (entry 1, Table 5.13). However, the enantioselectivity afforded was only 2%. Then, the monodentate (*S*)-Neomenthyl diphenylphosphine (NMDPP) **5.55** and monodentate ligand **5.56** were tested (entry 2-3, Table 5.13), and the branched aldehyde **5.11k** was afforded in 16% and 30% yield respectively. Nevertheless, the enantioselectivities obtained were poor in both cases (up to 6%).

Table 5.13: Screening of phosphorus ligand for the Rh-catalyzed AHF of **5.9k**.

Entry ^a	L	Conv. (%) ^b	5.41b ^a	5.58a ^b	5.42b ^b	5.11k ^b	ee (%) ^c
1	 (<i>R,R</i>)-Et-BPE 5.54	45	14	-	3	28	2
2	 (<i>S</i>)-NMDPP 5.55	>99	12	65	7	16	6
3	 5.56	>99	29	34	7	30	1
4	 (-)-DIOP 5.3	>99	41	39	10	10	4
5	 (<i>R,R</i>)-QuinoxP* 5.14	>99	52	26	2	20	30

^a Reaction conditions: **5.9k** (0.5 mmol), [Rh(acac)(CO)₂] (2 mol%), L = bidentate (1.2 mol %), L = monodentate (4 mol%), P = 10 bar (H₂/CO, 1:1), toluene (0.4 ml), T = 50°C, t = 18 h. ^b % yield determined by ¹H NMR using naphthalene as internal standard. ^c % enantiomeric excess determined by GC.

When (-)-DIOP **5.3** was used as ligand, the major products obtained were those of alkene hydrogenation **5.41b** and alkene isomerization **5.58a** (41% and 39% yield respectively), and the branched aldehyde **5.11k** was afforded in only 10% yield with poor enantioselectivity (up to 4%). Finally, (*R,R*)-QuinoxP* **5.14** was tested

and the branched aldehyde **5.11k** was obtained in 20% yield, and 30% ee, which is the best result obtained so far.

It was concluded that the rhodium catalyzed AHF of ethyl benzylacrylate **5.9k** for the production of chiral quaternary carbon centers is very challenging. Various chiral ligands were tested, and ee's up to 30% ee were obtained using (*R,R*)-QuinoxP* **5.14** as ligand. Apart from the low ee's obtained, poor to moderate yields were afforded for the branched aldehyde **5.11k**. The alkene isomerization was identified as one of the major problems to overcome when using this substrate.

5.4 Conclusions

From the study described in this chapter, the following conclusions can be extracted:

- i) The first synthesis of $\beta^{2,2}$ -amino esters **5.21** via regioselective Rh-catalyzed HAM of methyl methacrylate **5.9d** with secondary amines was achieved.
- ii) The presence of molecular sieves was crucial to afford $\beta^{2,2}$ -amino esters **5.21** bearing secondary amines.
- iii) The steric hindrance in the secondary amines had a negative effect on the condensation step and therefore in the final yields.
- iv) When primary amines were used under the same reaction conditions, only imines **5.24** were afforded in high to excellent yields.
- v) The synthesis of $\beta^{2,2}$ -amino esters **5.21** in high yields via Rh-catalyzed HAM of methyl methacrylate **5.9d** with aniline and derivatives was achieved using the cationic rhodium precursor $[\text{Rh}(\text{COD})_2]\text{BF}_4$ with ligand **5.12**, in the mixture of toluene/DCE as solvent, under 30 bar (H_2/CO , 1:1) of pressure, and at 70°C.

- vi) The steric hindrance has only a significant negative effect when *diortho*-substituted anilines are used.
- vii) The electronic effect was studied and it was concluded that electron-donating substituents have no significant effect while electron-withdrawing have negative effect on the condensation step and hydrogenation of the branched imine **5.24**.
- viii) When benzyl amine **5.22a** was used under HAM reaction conditions, the imine **5.24a** was obtained. Various rhodium precursors, pressures, and ligands **5.48** and **5.12** were tested but in all the cases, the branched imine **5.24a** was obtained in high to excellent yields.
- ix) The use of external proton sources such as HBF_4 or ammonium salt **5.52a** did not provide amino ester **5.21a**. Instead, the ammonium salt **5.52a** favored the hydrogenation of the methyl methacrylate **5.9d**.
- x) The direct hydrogenation of the imine **5.24a** in the presence of $[\text{Rh}(\text{COD})_2]\text{BF}_4$ and ligand **5.48** under 5 bar of hydrogen proved that the system is able to hydrogenate the imine and afford the $\beta^{2,2}$ -amino ester **5.21a**. However, in the presence of syngas pressure (H_2/CO , 1:1), no hydrogenation of the imine **5.24a** was observed, which suggests that CO is inhibiting the hydrogenation step.
- xi) Preliminary studies in the asymmetric HAM of ethyl benzylacrylate **5.9k** to access chiral $\beta^{2,2}$ -amino esters **5.21** were conducted via the rhodium catalyzed asymmetric hydroformylation of ethyl benzylacrylate **5.9k**. It was observed that under regioselective hydroformylation conditions, the branched aldehyde **5.11k** can be obtained in poor to moderate yield, along with the alkene isomerization product **5.58a** as main byproduct. Ee up to 30% was obtained using the ligand (*R,R*)-QuinoxP* **5.14** (Table 5.13).

5.5 Experimental

5.5.1 General considerations

All the reactions were carried out using Schlenk-line or glovebox techniques. Anhydrous solvents were collected from the system Braun MB SPS-800 except except from 1,2-dichloroethane, which was dried over CaH_2 , and stored under inert atmosphere.

^1H , $^{13}\text{C}\{^1\text{H}\}$ and $^{31}\text{P}\{^1\text{H}\}$ NMR spectra were recorded using a Varian Mercury VX 400 spectrometer (400, 100.6, and 161.97 MHz respectively). Chemical shift values (δ) are reported in ppm relative to TMS (^1H and $^{13}\text{C}\{^1\text{H}\}$) or H_3PO_4 ($^{31}\text{P}\{^1\text{H}\}$), and coupling constants are reported in Hertz. The following abbreviations are used to indicate the multiplicity: s, singlet; d, doublet; t, triplet; q, quartet; m, multiplet; bs, broad signal. High-resolution mass spectra (HRMS) were recorded on an Agilent Time-of-Flight 6210 using ESI-TOF (electrospray ionization-time of flight). Samples were introduced in the mass spectrometer ion source by direct injection using a syringe pump and were externally calibrated using sodium formate. The instrument was operating in the positive ion mode. Reactions were monitored by TLC carried out on 0.25 mm E. Merck silica gel 60 F_{254} glass or aluminum plates. Developed TLC plates were visualized under a short-wave UV lamp (254 nm) or heating plates that were dipped in potassium permanganate. Flash column chromatography was carried out using forced flow of the indicated solvent on Merck silica gel 60 (230-400 mesh).

The Rh-catalyzed HAM reaction and Rh-catalyzed AHF reaction were set up in a CAT24 autoclave from HEL Inc. and were stirred with a teflon-coated magnetic stir bar.

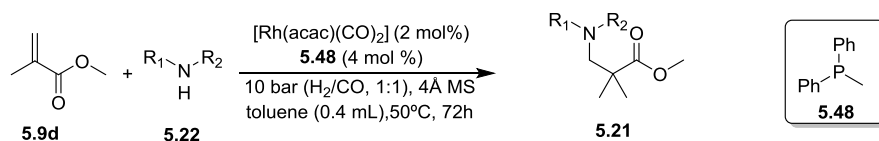
The enantiomeric excess of branched aldehyde **5.11f** was determined by GC analysis on chiral stationary phase employing CP Chiralsi-Dex CD, 25 m x 0.25 mm x 0.25 mm using the conditions reported in the literature.²⁹

Commercial reagents and solvents were purchased at the highest commercial quality from Sigma-Aldrich, Fluka, Alfa Aesar, Fluorochem, Strem and used as received, without further purification, unless otherwise stated.

The ethyl benzylacrylate **5.9k** was synthesized according to the procedure described in Chapter 4.²⁹

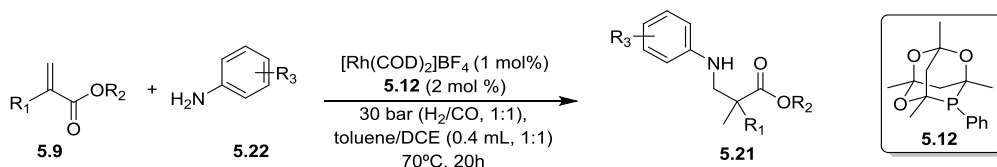
5.5.2 Rh-catalyzed regioselective HAM of α -alkyl acrylates 5.9

General procedure A: rhodium catalysed regioselective HAM of methyl methacrylate for the synthesis of $\beta^{2,2}$ -amino esters using secondary amines



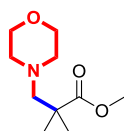
A 2 mL glassware reactor tube was charged with methyl methacrylate **5.9d** (0.5 mmol), secondary amine **5.22** (0.5 mmol), 100 mg of 4Å MS, ligand **5.48** (3.7 μL , 0.02 mmol), dicarbonyl(acetylacetonato)rhodium(I) (2.6 mg, 0.01 mmol) in toluene (0.4 mL). The reaction tube was placed in the reactor which was pressurized with 10 bar of H_2/CO (1:1), heated at 50°C and left stirring at 800 rpm. The reaction was stopped after 72 h by cooling the reactor in an ice bath for 20 min followed by venting the system. The mixture was purified by chromatographic column with Al_2O_3 to afford the resulting $\beta^{2,2}$ -amino esters **5.21**.

General procedure B: rhodium catalysed regioselective HAM of α -alkyl acrylates for the synthesis of $\beta^{2,2}$ -amino esters using aniline and derivatives



A 2 mL glassware reactor tube was charged with α -alkyl acrylate **5.9** (0.5 mmol), aniline derivative **5.22** (0.5 mmol), bis(1,5-cyclooctadiene)rhodium (I) tetrafluoroborate (2 mg, 0.005 mmol) in DCE (0.2 mL), and ligand **5.12** (2.9 mg, 0.01mmol) in toluene (0.2 mL). The reaction tube was placed in the reactor which was pressurized with 30 bars of H_2/CO (1:1), heated to 70°C and left stirring at 800 rpm. The reaction was stopped after 20 h by cooling the reactor in an ice bath for 20 min followed by venting the system. The mixture was purified by chromatographic column with SiO_2 to afford the resulting $\beta^{2,2}$ -amino esters **5.21**.

Methyl 2,2-dimethyl-3-morpholinopropanoate (5.21b):



General procedure A was followed employing methyl methacrylate **5.9d** (53.5 μ L, 0.5 mmol) and morpholine (44 μ L, 0.5 mmol).

Purification by flash chromatography eluting with pentane/ Et_2O (2:1)

afforded **5.21b** (79.2 mg, 79%) as colorless oil.

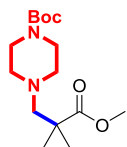
1H NMR (400 MHz, $CDCl_3$) δ : 1.16 (s, 6H), 2.46 (bs, 6H), 3.63 (bs, 4H), 3.65 (s, 3H).

^{13}C NMR (100.6 MHz, $CDCl_3$) δ : 23.9 (2C), 44.0 (1C), 51.8 (1C), 55.4 (2C), 67.3 (2C),

67.4 (1C), 178.2 (1C). **ESI-HRMS**: Calculated for $C_{10}H_{20}NO_3$. Exact: (M: 201.1365, M+H: 202.1443); Experimental (M+H: 202.1437).

Tert-butyl 4-(3-methoxy-2,2-dimethyl-3-oxopropyl)piperazine-1-carboxylate

(5.21c):



General procedure A was followed employing methyl methacrylate

5.9d (53.5 μL , 0.5 mmol) and N-Bocpiperazine (93.1 mg, 0.5 mmol).

Purification by flash chromatography eluting with pentane/ Et_2O (2:1)

afforded **5.21c** (129 mg, 86%) as colorless oil.

$^1\text{H NMR}$ (400 MHz, CDCl_3) δ : 1.16 (s, 6H), 1.44 (s, 9H), 2.41 (bs, 4H), 2.48 (bs, 2H),

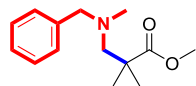
3.34 (bs, 4H), 3.65 (s, 3H). $^{13}\text{C NMR}$ (100.6 MHz, CDCl_3) δ : 23.9 (2C), 28.7 (3C), 43.5

(1C), 44.1 (1C), 44.6 (1C), 51.8 (1C), 54.8 (2C), 66.8 (1C), 79.7 (1C), 154.9 (1C), 178.2

(1C). **ESI-HRMS**: Calculated for $\text{C}_{15}\text{H}_{28}\text{N}_2\text{O}_4$. Exact: (M: 300.2049, M+H: 301.2127);

Experimental (M+H: 301.2132).

Methyl 3-(benzyl(methyl)amino)-2,2-dimethylpropanoate (5.21e):



General procedure A was followed employing methyl

methacrylate **5.9d** (53.5 μL , 0.5 mmol) and N-methylbenzyl

amine (66.5 μL , 0.5 mmol). Purification by flash chromatography eluting with

pentane/ Et_2O (8:1) afforded **5.21e** (38 mg, 32%) as colorless oil.

$^1\text{H NMR}$ (400 MHz, CDCl_3) δ : 1.20 (s, 6H), 2.15 (bs, 3H), 2.63 (bs, 2H), 3.54 (bs, 2H),

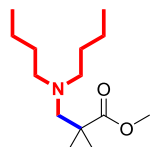
3.66 (s, 3H), 7.30 (m, 5H, Ar). $^{13}\text{C NMR}$ (100.6 MHz, CDCl_3) δ : 24.0 (2C), 43.9 (1C),

44.3 (1C), 51.8 (1C), 64.2 (1C), 66.9 (1C), 126.9-140 (6C, Ar), 178.4 (1C). **ESI-HRMS**:

Calculated for $\text{C}_{14}\text{H}_{21}\text{NO}_3$. Exact: (M: 235.1572, M+H: 236.1651); Experimental

(M+H: 236.1657).

Methyl 3-(dibutylamino)-2,2-dimethylpropanoate (5.21d):



General procedure A was followed employing methyl methacrylate

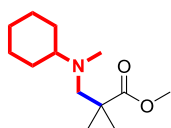
5.9d (53.5 μL , 0.5 mmol) and dibutyl amine (85 μL , 0.5 mmol).

Purification by flash chromatography eluting with pentane/ Et_2O

(40:1) afforded **5.21f** (59 mg, 24%) as colorless oil.

^1H NMR (400 MHz, CDCl_3) δ : 0.89 (t, $J_{\text{H,H}} = 7.2$ Hz, 6H), 1.14 (s, 6H), 1.24-1.36 (m, 10H), 2.37 (t, $J_{\text{H,H}} = 6.8$ Hz, 4H), 2.54 (s, 2H), 3.64 (s, 3H). **^{13}C NMR** (100.6 MHz, CDCl_3) δ : 14.3 (2C), 20.7 (2C), 24.0 (2C), 29.4 (2C), 44.3 (1C), 51.6 (1C), 55.4 (2C), 64.7 (1C), 178.5 (1C). **ESI-HRMS**: Calculated for $\text{C}_{14}\text{H}_{29}\text{NO}_2$. Exact: (M: 243.2198, M+H: 244.2277); Experimental (M+H: 244.2271).

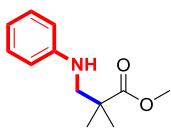
Methyl 3-(cyclohexyl(methyl)amino)-2,2-dimethylpropanoate (5.21g):



General procedure A was followed employing methyl methacrylate **5.9d** (53.5 μL , 0.5 mmol) and N-methylcyclohexyl (65.5 μL , 0.5 mmol). Purification by flash chromatography eluting with pentane/ Et_2O (2:1) afforded **5.21g** (18 mg, 15%) as colorless oil.

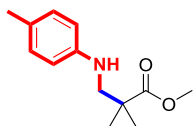
^1H NMR (400 MHz, CDCl_3) δ : 1.14 (s, 6H), 1.17 (bs, 4H), 1.51-1.70 (m, 7H), 2.21 (s, 3H), 2.55 (s, 2H), 3.58 (s, 3H). **^{13}C NMR** (100.6 MHz, CDCl_3) δ : 23.9 (2C), 26.4 (1C), 26.5 (1C), 28.8 (2C), 39.5 (1C), 44.3 (2C), 51.7 (1C), 64.1 (1C), 64.9 (1C), 178.5 (1C). **ESI-HRMS**: Calculated for $\text{C}_{13}\text{H}_{25}\text{NO}_2$. Exact: (M: 227.1885, M+H: 228.1964); Experimental (M+H: 228.1961).

Methyl 2,2-dimethyl-3-(phenylamino)propanoate (5.21i):



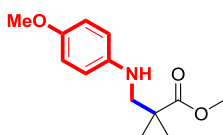
General procedure B was followed employing methyl methacrylate **5.9d** (53.5 μL , 0.5 mmol) and aniline (46 μL , 0.5 mmol). Purification by flash chromatography eluting with pentane/ Et_2O (3:1) afforded **5.21i** (90.2 mg, 88%) as colorless oil.

^1H NMR (400 MHz, CDCl_3) δ : 1.27 (s, 6H), 1.58 (1H, NH), 3.23 (s, 2H), 3.68 (s, 3H), 6.61 (d, $J_{\text{H,H}} = 7.6$ Hz, 2H, Ar), 6.68 (t, $J_{\text{H,H}} = 7.2$ Hz, 1H, Ar), 7.16 (m, 2H, Ar). **^{13}C NMR** (100.6 MHz, CDCl_3) δ : 23.7 (2C), 43.8 (1C), 52.2 (1C), 52.8 (1C), 113.1-148.6 (6C, Ar), 177.7 (1C). **ESI-HRMS**: Calculated for $\text{C}_{12}\text{H}_{17}\text{NO}_2$. Exact: (M: 207.1259, M+H: 208.1338); Experimental (M+H: 208.1328).

Methyl 2,2-dimethyl-3-(p-tolylamino)propanoate (5.21j):

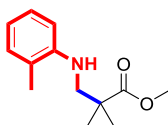
General procedure B was followed employing methyl methacrylate **5.9d** (53.5 μL , 0.5 mmol) and *para*-toluidine (53.6 mg, 0.5 mmol). Purification by flash chromatography eluting with pentane/ Et_2O (6:1) afforded **5.21j** (97.4 mg, 88%) as white solid.

$^1\text{H NMR}$ (400 MHz, CDCl_3) δ : 1.24 (s, 6H), 1.60 (1H, NH), 2.23 (s, 3H), 3.21 (s, 2H), 3.67 (s, 3H), 6.54 (d, $J_{\text{H,H}} = 8.4$ Hz, 2H, *Ar*), 6.96 (d, $J_{\text{H,H}} = 8$ Hz, 2H, *Ar*). $^{13}\text{C NMR}$ (100.6 MHz, CDCl_3) δ : 20.4 (1C), 23.7 (2C), 43.8 (1C), 52.1 (1C), 53.3 (1C), 113.2-146.4 (6C, *Ar*), 177.7 (1C). **ESI-HRMS**: Calculated for $\text{C}_{13}\text{H}_{20}\text{NO}_2$. Exact: (M: 221.1416, M+H: 222.1494); Experimental (M+H: 222.1486).

Methyl 2,2-dimethyl-3-(p-tolylamino)propanoate (5.21k):

General procedure B was followed employing methyl methacrylate **5.9d** (53.5 μL , 0.5 mmol) and *para*-anisidine (53.6 mg, 0.5 mmol). Purification by flash chromatography eluting with pentane/ Et_2O (5:1) afforded **5.21k** (100.9mg, 85%) as colourless oil

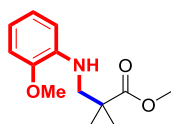
$^1\text{H NMR}$ (400 MHz, CDCl_3) δ : 1.27 (s, 6H), 3.18 (s, 2H), 3.67 (s, 3H), 3.74 (s, 3H), 6.60 (d, $J_{\text{H,H}} = 8.8$ Hz, 2H, *Ar*), 6.77 (d, $J_{\text{H,H}} = 9.2$ Hz, 2H, *Ar*). $^{13}\text{C NMR}$ (100.6 MHz, CDCl_3) δ : 23.7 (2C), 43.7 (1C), 52.1 (1C), 54.2 (1C), 55.9 (1C), 114.5-152.2 (*Ar*, 6C), 177.6 (1C). **ESI-HRMS**: Calculated for $\text{C}_{13}\text{H}_{19}\text{NO}_3$. Exact: (M: 237.1365, M+H: 238.1443); Experimental (M+H: 238.1438).

Methyl 2,2-dimethyl-3-(o-tolylamino)propanoate (5.21l):

General procedure B was followed employing methyl methacrylate **5.9d** (53.5 μL , 0.5 mmol) and *ortho*-toluidine (53.5 μL , 0.5 mmol). Purification by flash chromatography eluting with pentane/ Et_2O (3:1) afforded **5.21l** (85.2 mg, 77%) as colorless oil.

$^1\text{H NMR}$ (400 MHz, CDCl_3) δ : 1.31 (s, 6H), 2.14 (s, 3H), 3.25 (s, 2H), 3.69 (s, 3H), 6.64 (t, $J_{\text{H,H}} = 7.8$ Hz, 2H, Ar), 7.05 (d, $J_{\text{H,H}} = 6.8$ Hz, 1H, Ar), 7.11 (t, $J_{\text{H,H}} = 8$ Hz, 1H, Ar). $^{13}\text{C NMR}$ (100.6 MHz, CDCl_3) δ : 17.5 (1C), 23.8 (2C), 43.5 (1C), 52.2 (1C), 52.7 (1C), 109.9-146.5 (6C, Ar), 177.7 (1C). **ESI-HRMS**: Calculated for $\text{C}_{13}\text{H}_{19}\text{NO}_2$. Exact: (M: 221.1416, M+H: 222.1494); Experimental (M+H: 222.1491).

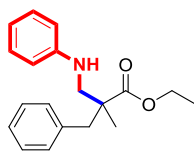
Methyl 3-((2-methoxyphenyl)amino)-2,2-dimethylpropanoate (**5.21m**):



General procedure B was followed employing methyl methacrylate **5.9d** (53.5 μL , 0.5 mmol) and *ortho*-anisidine (56.5 μL , 0.5 mmol). Purification by flash chromatography eluting with pentane/ Et_2O (4:1) afforded **5.21m** (96.1 mg, 81%) as colorless oil.

$^1\text{H NMR}$ (400 MHz, CDCl_3) δ : 1.29 (s, 6H), 3.26 (s, 2H), 3.67 (s, 3H), 3.84 (s, 3H), 6.64 (m, 2H, Ar), 6.76 (dd, $J_{\text{H,H}} = 8.4, 1.6$ Hz, 1H, Ar), 6.85 (m, 1H, Ar). $^{13}\text{C NMR}$ (100.6 MHz, CDCl_3) δ : 23.7 (2C), 43.9 (1C), 52.1 (1C), 52.6 (1C), 55.6 (1C), 109.7-146.9 (6C, Ar), 177.6 (1C). **ESI-HRMS**: $\text{C}_{13}\text{H}_{19}\text{NO}_3$. Exact: (M: 237.1365, M+H: 238.1443); Experimental (M+H: 238.1441).

Ethyl 2-benzyl-2-methyl-3-(phenylamino)propanoate (**5.21n**):

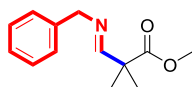


General procedure B was followed employing ethyl benzylacrylate **5.9k** (95 mg, 0.5 mmol) and aniline (46 μL , 0.5 mmol). Purification by flash chromatography eluting with pentane/ Et_2O (12:1) afforded **5.21n** (60 mg, 40%) as colorless oil.

$^1\text{H NMR}$ (400 MHz, CDCl_3) δ : 1.22 (s, 3H), 1.23 (t, $J_{\text{H,H}} = 7.2$ Hz, 3H), 2.93 (d, $J_{\text{H,H}} = 13.2$ Hz, 1H), 3.02 (d, $J_{\text{H,H}} = 13.6$ Hz, 1H), 3.13 (d, $J_{\text{H,H}} = 12.4$ Hz, 1H), 3.35 (d, $J_{\text{H,H}} = 12.4$ Hz, 1H), 4.14 (t, $J_{\text{H,H}} = 7.2$ Hz, 2H), 6.62 (d, $J_{\text{H,H}} = 8.4$ Hz, 2H, Ar), 6.70 (t, $J_{\text{H,H}} = 7.2$ Hz, 1H, Ar), 7.13-7.28 (m, 7H, Ar). $^{13}\text{C NMR}$ (100.6 MHz, CDCl_3) δ : 14.7 (1C), 20.5 (1C), 42.5 (1C), 48.1 (1C), 50.8 (1C), 60.9 (1C), 113.1-148.4 (12C, Ar), 176.1

(1C). **ESI-HRMS:** Calculated for $C_{19}H_{23}NO_2$. Exact: (M: 297.1729, M+H: 298.1807); Experimental (M+H: 298.1809).

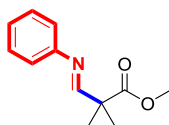
Methyl-3-(benzylimino)-2,2-dimethylpropanoate (5.24a):



General procedure A was followed employing methyl methacrylate **5.9d** (53.5 μ L, 0.5 mmol) and benzyl amine (55 μ L, 0.5 mmol). Purification by flash chromatography eluting with pentane/Et₂O (3:1) afforded **5.24a** (70 mg, 64%) as colorless oil.

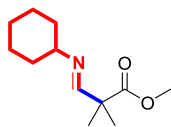
¹H NMR (400 MHz, CD₂Cl₂) δ : 1.35 (s, 6H), 3.67 (s, 3H), 4.57 (s, 2H), 7.21 (m, 3H, Ar), 7.30 (m, 2H, Ar), 7.84 (s, 1H). ¹³C NMR (100.6 MHz, CD₂Cl₂) δ : 22.6 (2C), 47.7 (1C), 51.9 (1C), 64.2 (1C), 126.8-139.5 (6C, Ar), 166.7 (1C), 175.3 (1C). **ESI-HRMS:** Calculated for $C_{13}H_{17}NO_2$. Exact: (M: 219.1259, M+H: 220.1338); Experimental (M+H: 220.1331).

Methyl -2,2-dimethyl-3-(phenylimino)propanoate (5.24b):



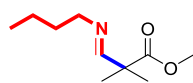
General procedure A was followed employing methyl methacrylate **5.9d** (53.5 μ L, 0.5 mmol) and aniline (46 μ L, 0.5 mmol). Purification by flash chromatography eluting with pentane/Et₂O (5:1) afforded **5.24b** (100 mg, 98%) as colorless oil.

¹H NMR (400 MHz, CD₂Cl₂) δ : 1.43 (s, 6H), 3.70 (s, 3H), 6.99 (m, 2H, Ar), 7.21 (m, 1H, Ar), 7.34 (m, 2H, Ar), 7.89 (s, 1H). ¹³C NMR (100.6 MHz, CD₂Cl₂) δ : 22.8 (2C), 48.5 (1C), 52.6 (1C), 120.9-152.2 (6C, Ar), 166.9 (1C), 175.5 (1C). **ESI-HRMS:** Calculated for $C_{12}H_{15}NO_2$. Exact: (M: 205.1103, M+H: 206.1181); Experimental (M+H: 206.1170).

Methyl-3-(cyclohexylimino)-2,2-dimethylpropanoate (5.24c):

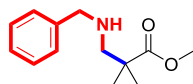
General procedure A was followed employing methyl methacrylate **5.9d** (53.5 μ L, 0.5 mmol) and cyclohexyl amine (57.5 μ L, 0.5 mmol). Purification by flash chromatography eluting with pentane/Et₂O (6:1) afforded **5.24c** (75 mg, 71%) as colorless oil.

¹H NMR (400 MHz, CD₂Cl₂) δ : 1.27 (s, 6H), 1.37 (m, 4H), 1.58 (m, 4H), 1.74 (m, 2H), 2.97 (m, 1H), 3.64 (s, 3H), 7.68 (s, 1H). ¹³C NMR (100.6 MHz, CD₂Cl₂) δ : 22.7 (2C), 24.6 (2C), 25.6 (2C), 34.2 (1C), 47.3 (1C), 51.8 (1C), 69.0 (1C), 162.8 (1C), 175.6 (1C). **ESI-HRMS**: Calculated for C₁₂H₂₁NO₂. Exact: (M: 211.1572, M+H: 212.1651); Experimental (M+H: 212.1638).

Methyl-3-(butylimino)-2,2-dimethylpropanoate (5.24d):

General procedure A was followed employing methyl methacrylate **5.9d** (53.5 μ L, 0.5 mmol) and butyl amine (49.5 μ L, 0.5 mmol). Purification by flash chromatography eluting with pentane/Et₂O (8:1) afforded the **5.24d** (70 mg, 76%) as colorless oil.

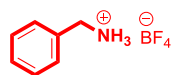
¹H NMR (400 MHz, CD₂Cl₂) δ : 0.82 (t, $J_{H,H}$ = 7.2 Hz, 3H), 1.22 (m, 8H), 1.45 (m, 2H), 3.29 (t, $J_{H,H}$ = 6.8 Hz, 2H), 3.58 (s, 3H), 7.58 (bs, 1H). ¹³C NMR (100.6 MHz, CD₂Cl₂) δ : 13.6 (1C), 20.2 (1C), 22.6 (2C), 32.7 (1C), 47.7 (1C), 51.9 (1C), 64.2 (1C), 164.9 (1C), 175.5 (1C). **ESI-HRMS**: Calculated for C₁₀H₁₉NO₂. Exact: (M: 185.1416, M+H: 186.1494); Experimental (M+H: 184.1486).

Methyl 3-(benzylamino)-2,2-dimethylpropanoate (5.21a):

Modified general procedure B was followed employing imine **5.24a** (62 mg, 0.28 mmol), ligand **5.48** (1.7 μ L, 0.01 mmol) and 5 bar of H₂. Purification by flash chromatography eluting with pentane/Et₂O (2:1) afforded **5.21a** (30 mg, 48%) as colorless oil.

$^1\text{H NMR}$ (400 MHz, CDCl_3) δ : 1.14 (s, 6H), 2.61 (s, 2H), 3.62 (s, 3H), 3.74 (s, 2H), 7.21-7.27 (bs, 5H, Ar). $^{13}\text{C NMR}$ (100.6 MHz, CDCl_3) δ : 23.8 (2C), 43.7 (1C), 51.9 (1C), 54.4 (1C), 58.0 (1C), 126.9-140.8 (6C, Ar), 178.1 (1C). **ESI-HRMS**: Calculated for $\text{C}_{13}\text{H}_{19}\text{NO}_2$. Exact: (M: 221.1416, M+H: 222.1494); Experimental (M+H: 222.1495).

Benzyl ammonium tetrafluoroborate (5.52a):



Tetrafluoroboric acid 48% in H_2O (914 mg, 5 mmol) was added to a solution of benzyl amine (0.456 mL, 5 mmol) in a solution of acetonitrile/dichloromethane (1:1), and the reaction was left stirring at room temperature overnight. Then, the solvent was evaporated under vacuum and the precipitated washed with dichloromethane (3 x 5 mL) to afford **5.52a** (810 mg, 83%) as white solid.

$^1\text{H NMR}$ (400 MHz, $(\text{CD}_3)_2\text{SO}$) δ : 4.01 (s, 2H), 7.37-7.45 (m, 5H, Ar). $^{13}\text{C NMR}$ (100.6 MHz, $(\text{CD}_3)_2\text{CO}$) δ : 43.0 (1C), 128.9-135.0 (6C, Ar). **ESI-HRMS**: Calculated for $\text{C}_7\text{H}_{10}\text{BF}_4\text{N}$. Exact: (M+: 108,0808); Experimental (M+: 108,0810).

5.6 References

¹ Cunillera, A.; Godard, C.; Ruiz, A. *Asymmetric Hydroformylation Using Rhodium*. In *Rhodium Catalysis*, Springer Nature, Cham, Switzerland, **2018**, pp. 99-143.

² Keulemans, A. I. M.; Kwantes, A.; van Bavel, T. *Rec. Trav. Chim. Pays Bas*. **1948**, *67*, 298-308.

³ a) Corey, E. J.; Guzman-Perez, A. *Angew. Chem. Int. Ed.* **1998**, *37*, 388-401. b) Fujii, K. *Chem. Rev.* **1993**, *93*, 2037-2066.

⁴ Breit, B.; Seiche, W. *Synthesis* **2001**, *2001*, 0001-0036.

⁵ Clarke, M. L. *Curr. Org. Chem.* **2005**, *9*, 701-718.

⁶ Freixa, Z.; van Leeuwen, P. W. N. M. *Dalton Transactions* **2003**, 1890-1901.

- ⁷ Gladiali, S.; Pinna, L. *Tetrahedron: Asymmetry* **1990**, *1*, 693-696.
- ⁸ a) Botteghi, C.; Paganelli, S.; Bigini, L.; Marchetti, M. *J. Mol. Catal.* **1994**, *93*, 279-287. b) Botteghi, C.; Marchetti, M.; Paganelli, S.; Sechi, B. *J. Mol. Catal. A: Chem.* **1997**, *118*, 173-179. c) Botteghi, C.; Chelucci, G.; Del Ponte, G.; Marchetti, M.; Paganelli, S. *J. Org. Chem.* **1994**, *59*, 7125-7127.
- ⁹ Krauss, I. J.; Wang, C. C. Y.; Leighton, J. L. *J. Am. Chem. Soc.* **2001**, *123*, 11514-11515.
- ¹⁰ Clarke, M. L. *Tetrahedron Lett.* **2004**, *45*, 4043-4045.
- ¹¹ Clarke, M. L.; Roff, G. J. *Chem. Eur. J.* **2006**, *12*, 7978-7986.
- ¹² Wang, X.; Buchwald, S. L. *J. Org. Chem.* **2013**, *78*, 3429-3433.
- ¹³ Eshon, J.; Foarta, F.; Landis, C. R.; Schomaker, J. M. *J. Org. Chem.* **2018**, *83*, 10207-10220.
- ¹⁴ Kawabata, T.; Kimura, Y.; Ito, Y.; Terashima, S.; Sasaki, A.; Sunagawa, M. *Tetrahedron Lett.* **1986**, *27*, 6241-6244.
- ¹⁵ Weiner, B.; Szymański, W.; Janssen, D. B.; Minnaard, A. J.; Feringa, B. L. *Chem. Soc. Rev.* **2010**, *39*, 1656-1691.
- ¹⁶ Noonan, G. M.; Newton, D.; Cobley, C. J.; Suárez, A.; Pizzano, A.; Clarke, M. L. *Adv. Synth. Catal.* **2010**, *352*, 1047-1054.
- ¹⁷ *Enantioselective Synthesis of β -Amino Acids*, Eds. Juaristi, E.; Soloshonok, V. A. Wiley-VCH, New Jersey, **2005**.
- ¹⁸ Magriotis, P. A. *Angew. Chem. Int. Ed.* **2001**, *40*, 4377-4379.
- ¹⁹ Bruneau, C.; Renaud, J.-L.; Jerphagnon, T. *Coord. Chem. Rev.* **2008**, *252*, 532-544.
- ²⁰ Córdova, A. *Acc. Chem. Res.* **2004**, *37*, 102-112.
- ²¹ Kobayashi, S.; Ishitani, H. *Chem. Rev.* **1999**, *99*, 1069-1094.
- ²² a) Gianotti, M.; Corti, C.; Fratte, S. D.; Di Fabio, R.; Leslie, C. P.; Pavone, F.; Piccoli, L.; Stasi, L.; Wigglesworth, M. *J. Bioorg. Med. Chem. Lett.* **2010**, *20*, 5069-5073. b) Edgar, D. M.; Hangauer, D. G.; Leighton, H. J.; E. J. M. Mignot, WO 03032912, **2003**. c) Edgar, D. M.; Hangauer, D. G.; White, J. F.; M. Solomon, WO

2005058880, **2005**.^{d)} Palomer, A.; Princep, M.; Guglietta, A. *Chapter 5 Recent Advances in the Treatment of Insomnia*. In *Annual Reports in Medicinal Chemistry*, Academic Press, Vol. 42, **2007**, pp. 63-80.

²³ Romanens, A.; Bélanger, G. *Org. Lett.* **2015**, *17*, 322-325.

²⁴ He, J.; Shigenari, T.; Yu, J.-Q. *Angew. Chem. Int. Ed.* **2015**, *54*, 6545-6549.

²⁵ Gou, Q.; Yang, Y.-W.; Liu, Z.-N.; Qin, J. *Chem. Eur. J.* **2016**, *22*, 16057-16061.

²⁶ Fuentes, J. A.; Wawrzyniak, P.; Roff, G. J.; Buhl, M.; Clarke, M. L. *Catal. Sci. Technol.* **2011**, *1*, 431-436.

²⁷ Crozet, D.; Gual, A.; McKay, D.; Dinoi, C.; Godard, C.; Urrutigoity, M.; Daran, J.-C.; Maron, L.; Claver, C.; Kalck, P. *Chem. Eur. J.* **2012**, *18*, 7128-7140.

²⁸ Routaboul, L.; Buch, C.; Klein, H.; Jackstell, R.; Beller, M. *Tetrahedron Lett.* **2005**, *46*, 7401-7405.

²⁹ Wang, X.; Buchwald, S. L. *J. Am. Chem. Soc.* **2011**, *133*, 19080-19083.

Chapter 6

General conclusions

UNIVERSITAT ROVIRA I VIRGILI
RH-CATALYZED CARBONYLATION OF DISUBSTITUTED OLEFINS: ASYMMETRIC CATALYSIS, CONTINUOUS
FLOW AND TANDEM HYDROAMINOMETHYLATION REACTION
Anton Cunillera Martin

From the study of chiral Rh-complexes immobilized onto carbon supports carried out in [Chapter 3](#), the following conclusions were extracted:

- The synthesis of the chiral pyrene tagged diphosphite ligands **3.27** and **3.28** was successfully completed.
- The corresponding cationic complexes $[\text{Rh}(\text{COD})(\mathbf{3.27})]\text{BF}_4$ **3.40** and $[\text{Rh}(\text{COD})(\mathbf{3.28})]\text{BF}_4$ **3.41** were synthesized in excellent yields.
- Systems containing pyrene tagged diphosphite ligands were successfully applied in the rhodium catalyzed AHF of norbornene **3.2** with similar results to analogous systems bearing alkyl groups. Thus, the pyrene moiety has no effect in the performance of the catalyst.
- HP-NMR experiments confirmed a fluxional **eq-eq** coordination mode of the ligand **3.27** in the $[\text{Rh}(\text{CO})_2(\mathbf{3.27})]$ complex. Moreover, NOESY experiments confirmed that the pyrene moiety remains far from the active center.
- The pyrene tagged Rh complexes **3.40** and **3.41** were successfully immobilized onto various carbon supports (MWCNTs, rGO, and CBs) to provide **Rh@support** heterogenized catalysts using ethyl acetate as solvent.

With the new heterogenized catalysts in hand, they were applied in the Rh-catalyzed AHF of norbornene **3.2** in batch and flow modes with the following conclusions:

- The Rh-catalyzed AHF norbornene **3.2** in batch using heterogenized catalysts provided lower activity and enantioselectivity compared to the homogeneous catalysts. Furthermore, recycling experiments in batch were not successful due to catalyst leaching.

- The heterogenized catalysts were successfully applied in the Rh-catalyzed AHF of norbornene **3.2** under flow conditions, obtaining higher enantioselectivities than those obtained with the homogeneous system in batch.
- The **3.41@CBs** provided the best performance among the heterogenized catalysts tested. Moreover, the robustness of the system was demonstrated.

From the study on the Rh-catalyzed asymmetric hydroaminomethylation of α -alkyl acrylates for the synthesis of chiral γ -aminobutyric esters described in [Chapter 4](#), the following conclusions can be extracted:

- The synthesis of chiral γ -aminobutyric esters **4.56** via Rh-catalyzed asymmetric hydroaminomethylation of α -alkyl acrylates **4.52** was successfully achieved using one single rhodium precursor, (*R,R*)-QuinoxP* **4.54** as ligand, and a mixture of toluene/DCE as solvent.
- The reaction proved to be tolerant to various protecting groups, secondary amines and aniline, and using various acrylates with alkyl substituents as substrates.
- This constitutes the first example in the literature of Rh-catalyzed asymmetric HAM of alkenes using one single catalyst.

In view of the successful system developed, HP-NMR studies were conducted, and the following conclusions can be extracted:

- The reaction of the cationic precursor $[\text{Rh}(\text{COD})_2]\text{BF}_4$ with (*R,R*)-QuinoxP* **4.54** in toluene/DCE provided species $[\text{Rh}(\text{COD})(\mathbf{4.54})]\text{BF}_4$ **4.63** and $[\text{Rh}(\mathbf{4.54})_2]\text{BF}_4$ **4.64**. The X-Ray structures of complexes **4.63** and **4.64** were elucidated.

- The reaction of complexes **4.63** and **4.64** under CO provided the dicarbonyl Rh species $[\text{Rh}(\text{CO})_2(\mathbf{4.54})]\text{BF}_4$ **4.65** at room temperature, and tricarbonyl Rh species $[\text{Rh}(\text{CO})_3(\mathbf{4.54})]\text{BF}_4$ **4.66** at 90°C.
- The reaction of complexes **4.63** and **4.64** in the presence of hydrogen provides the rhodium species $[\text{Rh}(\text{Solvent})_2(\mathbf{4.54})]\text{BF}_4$ **4.67**.
- The reaction of complexes **4.63** and **4.64** under syngas pressure at 90°C provided the Rh species $[\text{Rh}(\text{CO})_3(\mathbf{4.54})]\text{BF}_4$ **4.66**.
- The presence of a strong base such as morpholine is necessary to promote the heterolytic cleavage of hydrogen, and facilitate the formation of rhodium monohydride species from the mixture of the cationic precursor $[\text{Rh}(\text{COD})_2]\text{BF}_4$ with (*R,R*)-QuinoxP* **4.54** in toluene/DCE. Moreover, aniline is capable to induce the heterolytic cleavage of the hydrogen.
- Two rhodium monohydride $[\text{RhH}(\text{CO})_2(\text{PP})]$ species were identified, one (**4.68**) bearing the quinaxoline backbone intact, and another one (**4.69**) where the quinaxoline backbone is partially reduced.

Finally, the HAM reaction was monitored via HP-NMR spectroscopy, and the following conclusions were extracted:

- The presence of neutral and cationic species was crucial to complete the HAM reaction.
- The species **4.76** was identified as a cationic complex bearing the linear enamine **4.51a** coordinated; such species is expected to be involved in the hydrogenation step.
- The use of a polar solvent as DCE was necessary to solubilize both neutral and cationic species in the solution.
- The rate determining step of the reaction was the hydrogenation of the enamine.

Chapter 6

From the study in the Rh-catalyzed regioselective hydroaminomethylation of α -alkyl acrylates for the synthesis of $\beta^{2,2}$ -amino esters described in [Chapter 5](#), the following conclusions can be extracted:

- The synthesis of $\beta^{2,2}$ -amino esters **5.21** via Rh-catalyzed regioselective hydroaminomethylation of α -alkyl acrylates **5.9** was successfully achieved with secondary amines and aniline derivatives.
- The Catalytic systems using diphenylmethylphosphine **5.48** and monophosphine cage **5.12** ligand provided excellent regioselectivity for the branched products.

When secondary amines were used, the following conclusions were extracted:

- The use of molecular sieves was crucial to remove water from the media and allow the reduction of the iminium intermediate.
- Neutral rhodium species are capable to reduce the iminium intermediates, even using toluene as solvent.
- The steric hindrance at the secondary amine has a negative effect on the condensation step and therefore on the final yields.

When aniline and derivatives were used, the following conclusions were extracted:

- The use of a cationic $[\text{Rh}(\text{COD})_2]\text{BF}_4$ precursor together with ligand **5.12** in a mixture of toluene/DCE was necessary to reduce the imine intermediate and afford the desired amino ester.
- The steric effect at the aniline was only significant when di-*ortho*-substituted anilines are used.

- The electronic effect had no significant effect for electron-donating substituents in *para*-position of the aniline, while electron-withdrawing groups block the reaction at the imine.

Finally, the Rh-catalyzed asymmetric hydroformylation of α -alkyl acrylates **5.9** for the production of chiral quaternary carbon centers was conducted, and the following conclusions were extracted:

- The Rh-catalyzed asymmetric hydroformylation of ethyl benzylacrylate **5.9k** was successfully conducted to afford the branched aldehyde in poor to moderate yield, and enantioselectivities up to 30%.
- The system containing (*R,R*)-QuinoxP* **5.14** ligand provided the best results in terms of enantioselectivity.
- The challenge in this reaction does not only lie on the enantioinduction but also in the chemoselectivity. The alkene hydrogenation and the alkene isomerization were observed as major reaction product in many cases.

UNIVERSITAT ROVIRA I VIRGILI
RH-CATALYZED CARBONYLATION OF DISUBSTITUTED OLEFINS: ASYMMETRIC CATALYSIS, CONTINUOUS
FLOW AND TANDEM HYDROAMINOMETHYLATION REACTION
Anton Cunillera Martin

APPENDIX

UNIVERSITAT ROVIRA I VIRGILI
RH-CATALYZED CARBOXYLATION OF DISUBSTITUTED OLEFINS: ASYMMETRIC CATALYSIS, CONTINUOUS
FLOW AND TANDEM HYDROAMINOMETHYLATION REACTION
Anton Cunillera Martin

Publications

“Asymmetric Hydroformylation Using Rhodium ” [Cunillera, A.](#); Ruiz, A.; Godard, C.
in *Rhodium Catalysis*, Springer Nature, Cham, Switzerland, **2018**, pp. 99-143.

“Highly efficient Rh-catalysts immobilised by π - π stacking for the asymmetric hydroformylation of norbornene under continuous flow conditions” [Cunillera, A.](#);
Blanco C.; Gual, A.; Marinkovic J. M.; Garcia-Suarez E. J.; Riisager, A.; Claver, C.;
Ruiz, A.; Godard, C. *Manuscript submitted*.

“Rhodium catalyzed asymmetric hydroaminomethylation of α -alkyl acrylates for the synthesis of chiral γ -aminobutyric esters.” [Cunillera, A.](#); Díaz de los Bernardos, M.; Urrutigoity, M.; Claver, C.; Ruiz, A.; Godard, C. *Manuscript under preparation*.

“Rhodium catalyzed regioselective hydroaminomethylation of α -alkyl acrylates for the synthesis of $\beta^{2,2}$ -amino esters.” [Cunillera, A.](#); Claver, C.; Ruiz, A.; Godard, C. *Manuscript under preparation*.

Conferences and Scientific Meetings

[Cunillera, A.](#); Godard, C.; Ruiz, A. **“Synthesis, characterization and application of pyrene tagged chiral diphosphites for rhodium catalyzed asymmetric hydroformylation”** 18th Organometallic Chemistry Directed Towards Organic Synthesis, Sitges, Spain, June **2015**. Poster communication.

Cunillera, A.; Godard, C.; Ruiz, A.; Claver, C. **“New pyrene tagged chiral Rh-catalysts anchored onto carbon nanotubes for asymmetric hydroformylation of bicyclic alkenes”** 20th International Conference on Homogeneous Catalysis, Kyoto, Japan, July **2016**. Poster communication.

Cunillera, A.; Godard, C.; Ruiz, A. **“Novel chiral Rh catalysts for asymmetric hydroformylation heterogenised via π - π stacking interactions”** XXXIV Congress of the Organometallic Chemistry Specialized Group of the Real Sociedad Española de Química, Girona, Spain, September **2016**. Poster communication.

Cunillera, A.; Godard, C.; Ruiz, A.; Claver, C. **“Synthesis of γ -aminobutyric esters via rhodium catalysed hydroaminomethylation of acrylates”** 1st Trans Pyrenean Meeting in Catalysis, Toulouse, France, October **2016**. Poster communication.

Cunillera, A.; Godard, C.; Ruiz, A.; Claver, C. **“Rhodium catalyzed hydroaminomethylation of acrylates for the synthesis of β - and γ -amino esters”** 10th CarLa Winter School, Heidelber, Germany, February **2017**. Flash and Poster communication.

Cunillera, A.; Godard, C.; Ruiz, A.; Claver, C. **“Rhodium catalysed asymmetric hydroaminomethylation of acrylates for the synthesis of γ -amino esters”** 2nd GDRI-HC3A Meeting, Toulouse, France, January **2018**. Poster communication.

Cunillera, A.; Godard, C.; Ruiz, A. **“Synthesis of chiral γ -aminobutyric esters via Rhodium catalysed asymmetric hydroaminomethylation of α -alkyl acrylates”** 2nd Trans Pyrenean Meeting in Catalysis, Tarragona, Spain, October **2018**. Oral communication.

UNIVERSITAT ROVIRA I VIRGILI
RH-CATALYZED CARBONYLATION OF DISUBSTITUTED OLEFINS: ASYMMETRIC CATALYSIS, CONTINUOUS
FLOW AND TANDEM HYDROAMINOMETHYLATION REACTION
Anton Cunillera Martin



UNIVERSITAT
ROVIRA i VIRGILI